Review for *Comprehensive Inorganic Chemistry III*

Solution NMR of Transition Metal Complexes

Zi-Ling Xue, *Department of Chemistry, University of Tennessee, Knoxville, TN, United States*

Tabitha M. Cook, *Department of Chemistry and Biochemistry, Berry College, Mount Berry, GA, United States*

Emails: xue@utk.edu; ORCID No.: 0000-0001-7401-9933

tcook@berry.edu; ORCID No.: 0000-0001-6572-2539

Abstract

This review covers the literature between 1990 and 2019. NMR of transition metal nuclides, such as ^{45}Sc and ^{199}Hg, and α-atoms of ligands is discussed, with the exception of ^{1}H, ^{13}C, ^{19}F and ^{31}P. Complexes of the 32 transition metals, including La, Lu and Ac, are arranged into ten sections based on the groups in the periodic table. Later, properties (and features) shared by complexes of three or more transition metals are summarized. At the end, an overview is given about advanced NMR techniques and methods.

Table of Contents

1. Introduction

Solution NMR, especially ^{1}H, ^{13}C, ^{19}F and ^{31}P NMR of ligands, is now among the most widely used spectroscopies to characterize transition metal complexes - their structures and reaction mechanisms. Many methods, including those to obtain NMR of metal nuclides, became fairly mature before 1990, leading to their extensive uses over the past 30 years.

NMR of transition metal nuclides can provide direct information about physical and chemical environments of the metal centers, and it was the subject of a 1991 book edited by Pregosin and completed in 1990.[1] Earlier, Harris and Mann edited the 1978 book "NMR and the Periodic Table",[2] and Mason edited the 1987 book "Multinuclear NMR",[3] summarizing the achievements on NMR of transition metal compounds to the times. Since 1991, there have been books[4-8] and reviews[9-11] on fundamentals of NMR as well as selected subjects, including a 2016 book on NMR of paramagnetic molecules[5] and a 1993 review on paramagnetic metalloproteins[9] by Bertini and coworkers, a 2013 book on NMR in organometallic chemistry by Pregosin,[6] a 2011 review on NMR applications in inorganic chemistry,[11] a 2004 book about how to conduct >200 NMR experiments by Berger and Braun,[8] a 1997 book on NMR of non-metallic elements,[12] a 1996 book on applications of NMR to organometallic chemistry,[13] a 1996 article on NMR of metallic nuclei in clusters,[14] and a 1991 review on transition metal NMR of organometallic compounds.[10] A special 2008 issue of *Coord. Chem. Rev.* edited by Pregosin was published on the applications of NMR to inorganic and organometallic chemistry, covering some 15 topics.[15]

Solution NMR of transition metal complexes was not covered in Comprehensive Inorganic Chemistry II published in 2013.[16] The first edition, Comprehensive Inorganic Chemistry, was published in 1973.[17] Given that the 1991 book on the NMR of transition metal nuclides reviewed the literature till early 1990,[1] we decided to cover the literature on the solution NMR of transition metal complexes between 1990 to 2019. Publications on the subject in SciFinder over the 30-year period were selected for consideration here. For each transition

metal, nuclear properties of NMR-active nuclide(s) are briefly reviewed, followed by discussion of main papers on the NMR of the metal nuclide(s). Given the large number of papers on the solution NMR of complexes of 32 transition metals (including La, Lu[18-19] and Ac) over the 30 years, we were able to review only part of the literature on the subject. In other words, this is not a comprehensive review. Our goal is to give an overview of the solution NMR of transition metal compounds reported in 1990-2019, providing the reader a general understanding of the developments during the period.

For the 4th-row transition metals including Lr (lawrencium), other than one paper on the ^{31}P NMR spectrum of a ligand in an Ac complex,[20] we did not find papers on NMR of these elements.

For the ligands in metal complexes, the focus of the current review is on NMR of α-atoms on the ligands bound to the metal atom. Since ^{1}H, ^{13}C, ^{19}F and ^{31}P NMR is extensively used, these nuclides are generally not discussed in this review, except when they are part of special techniques or rarely used for the transition metals. The reader may find more detailed discussion of NMR of the non-metallic elements in the 1997 book by Berger, Braun, and Kalinowski,[12] and a 1996 article on the ^{29}Si NMR in organometallic compounds.[21]

Unless noted, the chemical shifts cited in this review are at room temperature.

Quadrupolar nuclides [nuclear spin >1/2;[22-23] quadrupole moment Q (or more precisely the geometrical part of the quadrupole moment eQ) ≠ 0] in non-cubic (i.e., non-T_d or non-O_h) complexes usually give relatively broad NMR peaks of the nuclides, as a result of short T_1 and T_2 (relaxation times) from efficient quadrupolar relaxation processes.[22] Among the 43 NMR-active, transition metal nuclides, 32 have a quadrupole moment.[24] NMR properties of complexes with these quadrupolar nuclides were a subject of a 2007 review.[24]

Peak widths and errors in the chemical shifts and other properties, including natural abundances of nuclides[25] and kinetic and thermodynamic parameters of chemical reactions, are not listed in the current review. Certain details, such as solvents used to make the NMR

solutions and coupling constants are generally not provided. The author may find the information in the references. For coupling constants J_{A-B} listed in the current review, the mass numbers of the element A or B are not listed (as in $^{1}J_{Nb-F}$), unless there is more than one NMR-active nuclide for A or B (as in $^{1}J^{51}{}_{V-C}$ or $^{1}J^{51}{}_{V-}{}^{15}{}_{N}$).

After NMR of each transition metal is discussed, a section is devoted to the properties (and features) shared by complexes of three or more transition metals. Afterwards, advanced NMR techniques and methods are summarized.

IUPAC (International Union of Pure and Applied Chemistry) made recommendations in 2001 (IUPAC Recommendations 2001) about a unified scale to report the NMR chemical shifts of all nuclides relative to the ^{1}H resonance of $SiMe_4$ (tetramethylsilane or TMS).[26] Additional recommendations for NMR shielding and chemical shifts (IUPAC Recommendations 2008) were published in 2008.[27] The unified scale is based on a precise ratio (in %), Ξ, of the resonance frequency of a given nuclide to that of the ^{1}H resonance of TMS in dilute solution (volume fraction < 1%) in chloroform. In essence, Ξ is the frequency (MHz) of the nuclide relative to that of ^{1}H at 100.000000 MHz. Advantage of the unified scale that its use avoids direct handling of any secondary references.[26] For example, this unified scale for ^{103}Rh NMR [Ξ = 3.186447% for $Rh(acac)_3$ in saturated $CDCl_3$][27] has been used in reporting shifts of Rh complexes.[28-31] Here, 3.186447 MHz is the frequency of the ^{103}Rh resonance of $Rh(acac)_3$ at 0 ppm in the same magnetic field where the ^{1}H resonance of $SiMe_4$ occurs at 100.000000 MHz.

2. Group 3 (Sc, Y, La, Lu and Ac)

For Sc, Y and La, NMR of both the metals (^{45}Sc, ^{89}Y, ^{139}La) and ligands have been reported. For Lu and Ac, we found only papers on NMR of ligands. Nuclear and NMR properties of the nuclides, including recommended and commonly used references, are given in Table 1.

Table 1.[26] Nuclear and NMR properties of ^{45}Sc, ^{89}Y, ^{139}La, ^{175}Lu and ^{227}Ac

Nuclide	Natural abun-dance (%)[a]	Spin	Relative receptivity[b]		Gyromagnetic ratio (10^7) (rad s^{-1} T^{-1})	Quadrupole moment Q (fm^2)	Ξ (and frequency MHz; ^1H = 100 MHz, 2.3488 T)[c]	Reference sample
			D^H (^1H = 1.00)	D^C (^{13}C = 1.00)				
^{45}Sc	100	7/2	0.302	1.78×10^3	6.5087973	-22.0	24.291747	$Sc(NO_4)_3$ (aq)
^{89}Y	100	1/2	1.19×10^{-4}	0.700	-1.3162791	—	4.900198	$Y(NO_3)_3$ (aq)
^{138}La	0.08881	5	8.46×10^{-5}	0.497	3.557239	45.0	13.194300	$LaCl_3$ (aq)
^{139}La	99.91119	7/2	6.05×10^{-2}	356	3.8083318	20.0	14.125641	
^{175}Lu[d]	97.401	7/2	3.12×10^{-2} [e]	156[e]	3.0552	349.0	(11.404)[e]	—
^{227}Ac ($t_{1/2}$ = 21.772 year)[32]	—	3/2	—	—	3.5	170	13.1	—

[a] Unless noted, the isotopes are stable. The natural abundances are based on the data by the US National Institute of Standards and Technology (NIST).[25]

[b] D^H and D^C are receptivities relative to those of ^1H and ^{13}C, respectively.[26]

[c] Ξ is the ratio of the secondary (isotope-specific) frequency to that of ^1H in $SiMe_4$ (TMS) in dilute solution (volume fraction, ϕ < 1%) in chloroform in the same magnetic field.[26] It is used for a recommended unified scale for reporting the NMR chemical shifts of all nuclei relative to the ^1H resonance of TMS.

[d] Although we did not find reports of ^{175}Lu and ^{227}Ac NMR, they are listed here for comparison.

[e] Values in brackets are approximate (calculated from the gyromagnetic ratios).

2.1. *Scandium complexes*

^{45}Sc NMR is feasible because of 100% natural abundance of ^{45}Sc nuclide, its NMR frequency (close to that of ^{13}C NMR), and high relative sensitivity (Table 1). In addition to $Sc(ClO_4)_3$ (aq), aqueous solutions of $Sc(NO_3)_3$ and $ScCl_3$ (including in D_2O) were used as

standards or external standards.[1,33] In low pH, dilute (≤ 0.1 M) solution of $Sc(H_2O)_6^{3+}$, the nearly ideal O_h symmetry of the cation minimizes ^{45}Sc peak broadening by quadrupole relaxation. For diamagnetic compounds, ^{45}Sc shifts of diamagnetic complexes typically range from 396 ppm for $Sc[N(SiMe_3)_2]_3$ to -50 ppm for $Sc[(Me_2N)_2C{=}O]_6^{3+}$.[34] Line widths of ^{45}Sc peaks are often reported mostly because of quadrupole-dominated relaxation.[1]

^{45}Sc NMR of scandium salts, including halides, nitrate, sulfate, and phosphate, was discussed in a 2017 review.[35] Periodate $[Sc(H_2O)_3][IO_4(OH)_2]$ in aqueous periodic acid showed a broad ^{45}Sc peak (δ 22) at 77 °C.[36]

^{45}Sc NMR was used to characterize halide and nitrate complexes with additional ligands listed below: (a) Phosphines, phosphine oxides and arsine oxides, including $Sc(dmpe)_2I_3$ (δ 361; dmpe = $Me_2PCH_2CH_2PMe_2$),[37] $Sc(O{=}PPh_3)_3Cl_3$ (δ 121),[38] $Sc(O{=}PPh_3)_2(NO_3)_3$ (δ -7.5),[39] and $[Sc(O{=}AsMe_3)_6](NO_3)_3$ (δ 58.0);[40] (b) Oxo-,[41-42] thio-,[43] seleno-[43] and aza-crowns,[41] including $[Sc(15\text{-crown-}5)Cl_2]SbCl_6$ (δ 127.6),[41] $[Sc(18\text{-crown-}6)Cl_2]FeCl_4$ (δ 132),[42] and its S- and Se-analogs $[Sc([18]aneO_4E_2)Cl_2]FeCl_4$ [E = S, δ 204; Se, δ 205; $[18]aneO_4E_2$ (**1**)];[43] (c) N,N,N ligands, including $Sc(terpyridine)Cl_3$ (δ 254)[44] and R_3-tacn [1,4,7-trisubstituted-1,4,7-triazacyclononane (**2**)] such as $Sc(R_3\text{-tacn})F_3$ [R_3 = Me_3 or $Me_2(CH_2Ph)$, both δ 104],[44] $Sc(Me_3\text{-tacn})Cl_3$ (δ 300),[44] and $Sc(Me_3\text{-tacn})Me_3$ (δ 626) as an organometallic derivative.[45]

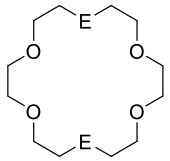

$[18]aneO_4E_2$ (E = S, Se)

(**1**)

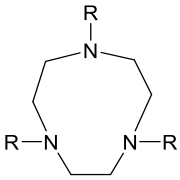

(**2**)

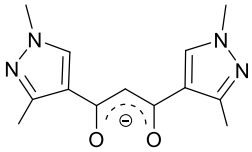

(**3**)

^{45}Sc NMR properties of several new organometallic complexes, including $ScMe_3(THF)_x$ (δ 601.7) and $Sc(CH_2SiMe_3)_3(THF)_2$ (δ 745.0), were summarized and compared with those

reported before 1990.[34] ScX_3 [X = 1,3-bis(1,3-dimethyl-1H-pyrazol-4-yl)-1,3-propanedionate (**3**); ^{45}Sc δ = 96.9] with dipyrazole-substituted 1,3-diketonate ligands was found to have unusual electroluminescent properties for organic light-emitting diode (OLED) applications.[46]

Endofullerenes, i.e., fullerenes containing atoms, ions or clusters enclosed within their inner spheres, are one major focus of research using ^{45}Sc NMR.[47-48] Sc-containing endofullerenes, include those with Sc-carbide,[47] -nitride (such as $Sc_3N@I_h$-C_{80}[49]),[47] -oxide,[47] -sulfide,[50-51] and -cyanide[52] clusters. These endofullerenes were the focus of a 2014[47] and a 2015[48] monograph, including a review on NMR properties,[48] and a 2014 review on redox properties.[53] Several publications on the subject have been published since 2014.[54-59] Both size and symmetry of the fullerene cages significantly affect ^{45}Sc shifts of encapsulated clusters.[55,58] Often the Sc clusters rotate inside the cages, leading to broad ^{45}Sc NMR peaks.[59] Motion of the cluster in $Sc_3N@I_h$-C_{80} was probed by variable-temperature (VT) ^{45}Sc NMR and compared with dynamics of other endofullerenes.[54]

^{45}Sc and ^{13}C NMR studies of $MSc_2N@I_h$-C_{80} (M = Y, lanthanide) were performed to study the effect of unpaired *f* electrons on the NMR properties.[60] Here, the endofullerenes, some with paramagnetic cages, were classified into three groups: (a) Diamagnetic M^{III} (Y, La, Lu); (b) M^{III} with oblate-shape 4*f* density (Ce, Pr, Nd, Tb, Dy, Ho); (c) M^{III} with prolate-shape 4*f* density (Er, Tm). For lanthanide M(III) ions with oblate and prolate 4*f* electron densities, see Reference [61]. While ^{45}Sc NMR shifts of diamagnetic $MSc_2N@I_h$-C_{80} are in the range noted earlier in this section, paramagnetic $DySc_2N@I_h$-C_{80} and $ErSc_2N@I_h$-C_{80} are at δ 1892 and δ -233, respectively.[60] In addition, for paramagnetic $MSc_2N@I_h$-C_{80} containing M^{III} ions with oblate and prolate *f* electron densities, ^{45}Sc peaks are more deshielded and shielded, respectively, than those of the diamagnetic analogs.[60] The paramagnetic NMR data were interpreted by ligand field calculations.

The cage complex $Sc_3N@I_h$-C_{80} was synthesized in another study and the complex was investigated via ^{45}Sc and ^{14}N NMR.[62] The ^{14}N NMR spectroscopy was utilized to probe the

dynamic motional processes inside the cage at room temperature. $M_3N@I_h$-C_{80} (M = Y and Lu) were synthesized and studied as well.[62] The ^{14}N signals for the Sc(III), Y(III), and Lu(III) complexes were observed at δ 292.0, 381.7 and 395.9, respectively.[62] In variable-temperature (VT) NMR studies of the Sc(III) complex, the ^{14}N signal became slightly more shielded (δ 394.1-397.7) and narrower.[62]

Radionuclides ^{44}Sc (β^+, $t_{1/2}$ = 3.97 h) and ^{47}Sc (β^-, $t_{1/2}$ = 3.35 day) are of interest for therapeutic and medical imaging applications.[63] Thermodynamics and kinetics of coordination between Sc(III) ion and a variety of ligands, such as tetraaza-12-crown-4-tetraacetic acid [dota (**4**)],[33] its monophosphorus acid derivatives[63] and diethylenetriamine pentaacetic acid [dtpa (**5**)],[33] was studied, including by ^{45}Sc NMR, for the potential applications of the Sc complexes as radiopharmaceuticals.

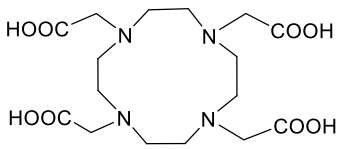

(**4**)

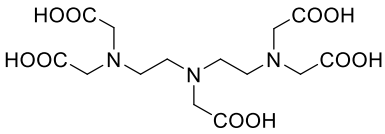

(**5**)

In two 1994 papers, studies of Sc^{3+} binding to ovotransferrin, which are proteins with two high-affinity Fe^{3+}-binding sites, using ^{45}Sc[64-65] and ^{13}C[64] NMR were reported. Sc^{3+} with ionic radius slightly larger than that of Fe^{3+} was found to be a good probe for the Fe^{3+}-binding sites.

For NMR of ligands, ^{11}B NMR was used to characterize the new half-sandwich scandium boryl complex $Me_2Si(C_5Me_4)(NPh)Sc[B(NDippCH)_2](\mu\text{-}Cl)Li(thf)_3$ (**6**, Dipp = 2,6-Pr^i_2-C_6H_3, δ 37.0).[66] Reaction of **6** with CO led to CO insertion into the Sc-B bond in **6** (**Figure 1**) yielding the Sc(III) boryl oxycarbene complex $Me_2Si(C_5Me_4)(NPh)Sc[\eta^2\text{-}OCB(NDippCH)_2](thf)$ (**7**, δ 16.9).[67]

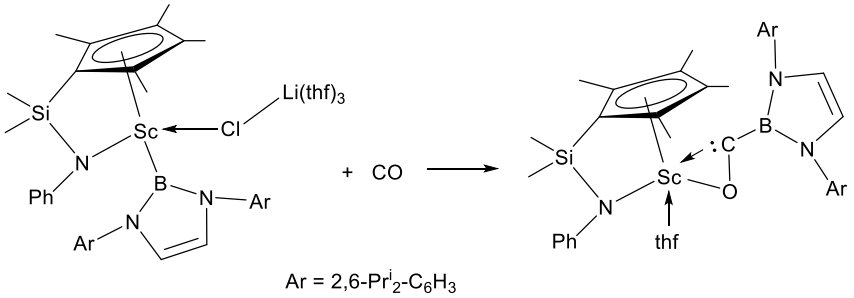

(**6**) (**7**)

Figure 1. Formation of **7** from **6**.

2.2. *Yttrium complexes*

^{89}Y NMR is attractive, as ^{89}Y is a spin 1/2 nuclide at 100% natural abundance, leading to sharp peaks and observations of small couplings with other nuclides.[1] In addition, large nuclear Overhauser enhancement factor (NOEF) values are possible,[68] when ^{89}Y is relaxed by dipolar interactions with other nuclei. However, a few properties of the nuclide (Table 1) make ^{89}Y NMR challenging, including slow spin-lattice relaxation, a low magnetic moment, low receptivity, and low measuring frequency.[69] ^{89}Y shifts of diamagnetic organometallic complexes mostly fall within δ 895.0[70-81] and δ -169.5 for $Cp_2Y[N(PPh_2S)_2]$ [with a chelating ligand $N(PPh_2S)_2^-$ (**8**)].[79]

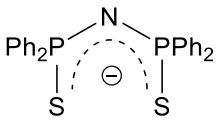

(**8**)

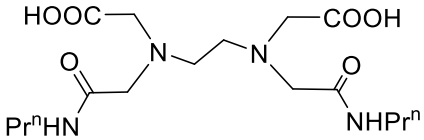

(**9**)

^{89}Y NMR has been used to probe coordination of Y(III) ions to N- and O-containing ligands, including macrocyclic ligands[82-83] [such as *N,N′*-bis(propylamide)ethylenediamine-*N,N′*-diacetic acid (**9**)],[84] NCS^-,[85] and solvent mixtures of dimethylformamide (dmf), as well as dimethylacetamide,[86] and $Y(thd)_3$ [^{89}Y δ 163; thd = $Bu^tC(=O)CHC(=O)Bu^t$-].[87] ^{89}Y shifts of

complexes with phosphine oxide ($O=PR_3$),[39] arsine oxide ($O=AsR_3$)[40] and derivative[88] ligands were reported. ^{31}P-^{89}Y shift correlation was used to probe speciation of $Y(NO_3)_3 \cdot 6H_2O$ with $O=PPh_3$.[89] Shifts of Y alkoxide[90-91] and siloxide[92] complexes were also reported. These ^{89}Y shifts are within the δ 895.0 to -169.5 range noted above.

$[Y(H_2O)_3][IO_4(OH)_2]$ dissolved in excess hot aqueous H_5IO_6 and recorded at 350 K gave the ^{89}Y resonance at δ 10.[36]

Organometallic complexes comprise a large of number of papers.[70-81] ^{89}Y NMR was found to be a potentially useful diagnostic probe of the ligand environment.[70] The ^{89}Y shifts of a series complexes such as $Cp^*_2Y(OAr)$ (δ -129.3; Cp* = η^5-$C_5Me_5^-$; Ar = 2,6-Bu^t_2-C_6H_3), $Cp^*Y(OAr)_2$ (δ 21.0), $Cp^*_2YCH(SiMe_3)_2$ (δ 78.9), $Y[N(SiMe_3)_2]_3$ (δ 570.0), $Y(OAr)_3$ (δ 168.4), and $Y[CH(SiMe_3)_2]_3$ (δ 895.0) led to calculated group contributions to the ^{89}Y shift of, e.g., -100 ppm for Cp*, 56 ppm for OAr, 190 ppm for $N(SiMe_3)_2$, and 298 ppm for $CH(SiMe_3)_2$.[70] Application of Y complexes with metallocene, linked Cp-amide, methyl or their analog ligands as olefin polymerization catalysts was a driving force.[71-74] DFT methods were used to calculated ^{89}Y NMR shifts in organometallic complexes containing Cp, alkyl, hydride, and aryloxide ligands with agreement between predicted and experimental shifts typically within ±70 ppm (~5% of ca. 1300 ppm range).[93]

^{89}Y NMR was one of techniques to probe speciation of $[Y_2(bet)_6(H_2O)_4](NTf_2)_6$ ($Hbet^+$ = betainium) in ionic liquid betainium bis(trifluoromethylsulfonyl)imide [(Hbet)(NTf_2) (**10**)] at 363 K with one ^{89}Y peak at δ 37.7.[94]

$[Y_6O(OH)_8(NO_3)_6(H_2O)_{12}]^{2+}$ stabilized as nanoaggregates in ethylene glycol (EG) showed liquid-state of ^{89}Y resonance at δ 78 at 50 °C, comparing to δ -22 for $Y(NO_3)_3 \cdot 6H_2O$ in EG.[95]

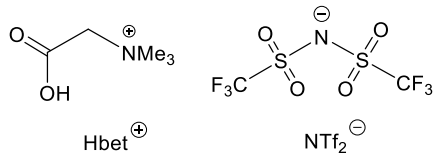

(**10**)

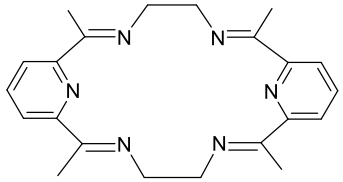

(**11**)

^{89}Y data on carboxylate and aminocarboxylate complexes in aqueous solution, such as Y(edta)$^{-}$ (δ 129.6), Y(dtpa)$^{2-}$ (δ 82.2) and Y^{3+}:malonate (δ 7.9), were summarized.[96] Adding to 4*f*^{7} Gd(ham)$^{3+}$ [ham = hexaazamacrocycle (**11**)] or Gd(dtpa)$^{2-}$ as a paramagnetic relaxation agent to Y(dtpa)$^{2-}$ solution in D_2O led to shortening of the spin-lattice relaxation time T_1 and signal/noise (S/N) enhancement of the ^{89}Y peak.[97] ^{89}Y NMR was used to probe Y^{3+} binding to parvalbumin, a calcium-binding protein involved in calcium signaling, with the assistance of Gd(dtpa)$^{2-}$.[96] ^{89}Y and ^{13}C T_1 relaxation times in a mixed Gd^{III}/Y^{III} complex ligand containing two monophosphinate triacetate dota-like units provided useful structural information.[98]

Dynamic nuclear polarization NMR (DNP NMR) was developed to significantly increase ^{89}Y sensitivity by creating nuclear spin polarization levels much higher than Boltzmann levels at ambient temperature.[99-100] DNP was based on the transfer of electron spin polarization from a stable free organic radical, which had been irradiated by microwave near the EPR frequency, to coupled ^{89}Y nuclei in a frozen glass matrix at ~1 K. The radical included TEMPO [(2,2,6,6-tetramethylpiperidin-1-yl)oxyl (**12**)][100-101] and hydroxyethyl tetrathiatriarylmethyl radical OX063 (**13**).[100] In the so-called "dissolution-DNP" process, the frozen sample was then rapidly dissolved and warmed up to room temperature before collecting NMR data, while retaining much of the polarization built up in the solid state.[100-101] DNP NMR may lead to >60,000-fold enhancement of ^{89}Y NMR signal.[100] Such hyperpolarized Y complexes were pH-sensitive NMR probes[99] and used to probe kinetics of Y-ligand complexation[101] with potential for direct imaging of metal ions in biological systems by magnetic resonance.[100]

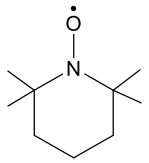

(**12**)

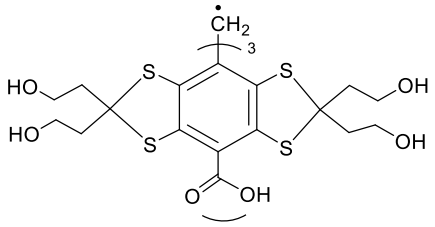

(**13**)

For NMR of ligands, the dissociation of dimer $(Cp^*_2YH)_2$ to the monomer was studied via VT ^{1}H NMR.[102] Below -40 °C, the hydride ligand was coupled to two ^{89}Y nuclei making a sharp triplet. As the temperature was raised, the hydride resonance shifted and broadened. This was attributed to the increasing rate of dissociation and the loss of the hydride coupling to the ^{89}Y nuclei.[102]

2.3. *Lanthanum complexes*

^{139}La is one of two NMR-active nuclides and the only one used in studies of La complexes that we found in 1990-2019, as indicated in Table 1. The other nuclide, ^{138}La (spin 5)[32] with low (0.08881%) natural abundance and a fairly large quadrupole moment, is not practical for NMR studies.[1] ^{139}La shifts of diamagnetic complexes are typically between δ 1090 for $(Bu^n_4N)_3(LaBr_6)$ and δ -772 as one of two peaks for Cp_4La^- anion.[1] Line widths of ^{139}La peaks were often reported mostly because of quadrupole-dominated relaxation.[1]

^{139}La NMR was used to probe coordination of La(III) ions to N- and O-containing ligands, including macrocyclic ligands,[82] D-ribose with $LaCl_3$ in aqueous solution,[103] acetohydroxamic acid [MeC(=O)NHOH] with $La(ClO_4)_3$,[104] and *p*-sulfonatocalix[4]arene with $LaCl_3$.[105] ^{139}La NMR was also used to study MeOH-substituted lanthanum halides, including $[La(H_2O)_7(MeOH)_2]Br_3$ (δ -32.7), $LaBr_3(MeOH)_5$ (δ -34.7), $[(MeOH)_4Cl_2La(\mu\text{-}Cl)]_2$ (δ -31.2), and $[La(MeOH)_9]I_3$•MeOH (δ -35.1).[106] Interactions of $ZnCl_2$ with La(dtpa) and other La(III) complexes containing dtpa

derivative ligands have been probed by ^{139}La NMR.[107] Multinuclear NMR study, including the use of ^{139}La NMR, was performed to study the La(III)-catalyzed alkylation of ethylene glycol with maleate.[108]

Addition of H_5IO_6 to aqueous solution of $La(NO_3)_3$ gave a ^{139}La resonance at δ 11.[36]

Organometallic complexes studied by ^{139}La NMR include those with allyl ligands $La(\eta^3\text{-}C_3H_5)_2X\cdot 2THF$ (X = Cl^-, δ 520; Br^-, δ 550; I^-, 585),[109] $La(\eta^3\text{-}C_3H_5)_3$•L [L = $MeOCH_2CH_2OMe$ (dme), δ 440;[110] $Me_2NCH_2CH_2NMe_2$ (tmed), δ 475;[110] $2O{=}P(NMe_2)_3$, δ 285;[110] 1,5-dioxan, δ 440[109]], and Cp and Cp* allyl complexes, $CpLa(\eta^3\text{-}C_3H_5)_2(1,5\text{-dioxan})_{0.2}$ (δ 13), $Cp^*La(\eta^3\text{-}C_3H_5)_2$ (δ 95), $Cp_2La(\eta^3\text{-}C_3H_5)$ (δ -214), and $Cp^*_2La(\eta^3\text{-}C_3H_5)$ (δ -167).[111] ^{139}La shift of Cp_3La•L are δ -560 for L = thf[111] and δ -558 for triindenyl complex $(C_7H_9)_3La$•thf.[112] ^{139}La NMR was used to study Schlenk-type equilibria for cyclopentadienyl complexes Cp_3La, $CpLaI_2$, and $[(\eta^5\text{-}1,3\text{-}R_2C_5H_3)_2La(\mu\text{-}Cl)]_2$ (R = $SiMe_3$) as well as with bimetallic complexes $X_2La\text{-}Ru(CO)_2Cp$ (X = Cp^-, $\eta^5\text{-}1,3\text{-}R_2C_5H_3^-$).[113]

^{139}La NMR of endofullerenes was reported, including $La_2@C_{72}$ (δ -575.6),[114] $La_2@C_s(17490)\text{-}C_{76}$ (δ -617.8),[115] $La_2@C_{80}$ (δ -402.6)[114] and silylated[116] and pyrrolidine[117] derivatives as well as the anion of $La@C_{82}$ (δ -470) and derivatives.[118]

Binding of La(III) ions in $La(NO_3)_3$ to aqualysin I, a heat-stable protease with two Ca^{2+}-binding sites, was probed by ^{139}La NMR.[119]

For NMR of ligands, La(III) was added to a solution containing dcf [dcf = methyl dicarboxy-α-D-fructofuranoside (**14**)] and the product was studied via ^{17}O NMR in order to seek evidence of a fourth donor cite in this ligand in the complex $La(dcf)_2^-$.[120] The dihedral angles of the protons were estimated from the coupling constants *J*. From the *J* values, it was determined that the arrangement of the ligand around the metal ion effectively allowed for a fourth coordination site for the La(dcf) moiety in $La(dcf)_2^-$ as shown in **15**.[120]

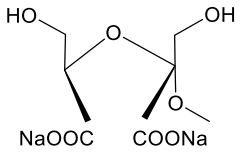

(**14**)

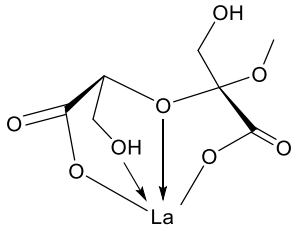

(**15**)

2.4. *Lutetium complexes*

We did not find reports of ^{175}Lu NMR which was also not discussed in the 1991 book edited by Pregosin[1] or the 1987 book on multinuclear NMR edited by Mason.[3]

For NMR of ligands, ^{15}N and ^{13}C NMR was used to characterize Lu isocyanate complexes $[(H_2O)_5Lu(NCS)]^{2+}$ through $[(H_2O)Lu(NCS)_5]^{2-}$.[121] The ^{13}C and ^{15}N signals showed a noticeable concentration dependence, which was used to identify the signals of the five complexes. The ^{13}C and ^{15}N shifts of the mono- to penta-isothiocyanato complexes were all more shielded than that of free NCS^- (δ -165 referenced to $^{15}NO_3^-$).[121]

2.5. *Actinium complex*

We did not find reports of ^{227}Ac NMR which was also not discussed in the 1987 and 1991 books edited by Mason[3] and Pregosin,[1] respectively. Among Ac isotopes which are all radioactive, ^{227}Ac has the longest half-life of $t_{1/2}$ = 21.772 years[20] and is found in traces in uranium and thorium ores along with traces of ^{228}Ac ($t_{1/2}$ = 6.15 hours[122]).

Reaction of Ac(III) in nitric acid with 1,4,7,10-tetraazacyclododecane-1,4,7,10-tetra(methylene)phosphonic acid [H_8dotp (**16**)] gave $Ac(dotp)^{5-}$ which showed a sharp ^{31}P NMR resonance at δ 20.2. This peak was 3 ppm deshielded from that of its La(III) analog $La(dotp)^{5-}$.[20] The NMR spectrum was collected with microscopic reagent quantities (27.8 μg of Ac^{3+} and 67 μg $dotp^{8-}$ in 25 μL), giving reasonable S/N within 12 hours.[20]

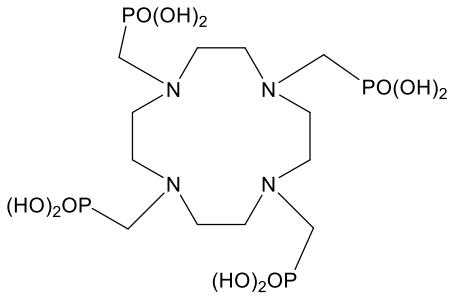

H_8dotp

(**16**)

3. Group 4 (Ti, Zr and Hf)

For Ti and Zr, NMR of both the metals (twinned ^{47}Ti and ^{49}Ti, ^{91}Zr) and ligands have been reported. For Hf, we have found only papers on NMR of ligands. Nuclear and NMR properties of the nuclides, including recommended and commonly used references, are given in Table 2.

Table 2.[26] Nuclear and NMR properties of ^{47}Ti, ^{49}Ti, ^{91}Zr, ^{177}Hf and ^{179}Hf

Nuclide	Natural abun-dance (%)[a]	Spin	Relative receptivity		Gyromagnetic ratio (10^7) (rad s^{-1} T^{-1})	Quadrupole moment Q (fm^2)	Ξ (and frequency, MHz; ^{1}H = 100 MHz, 2.3488 T)	Reference sample
			D^H (^{1}H = 1.00)	D^C (^{13}C = 1.00)				
^{47}Ti	7.44	5/2	1.56×10^{-4}	0.918	-1.5105	30.2	5.637534	$TiCl_4$ (neat)
^{49}Ti	5.41	7/2	2.05×10^{-4}	1.20	-1.51095	24.7	5.639037	
^{91}Zr	11.22	5/2	1.07×10^{-3}	6.26	-2.49743	-17.6	9.296298	Cp_2ZrCl_2 (CH_2Cl_2)
^{177}Hf[b]	18.60	7/2	2.61×10^{-4}	1.54	1.086	336.5	(4.007)[c]	—
^{179}Hf[b]	13.62	9/2	7.45×10^{-5}	0.438	-0.6821	379.3	(2.517)[c]	

[a] Unless noted, the isotopes are stable. The natural abundances are based on the NIST data.[25]

[b] Although we did not find reports of ^{177}Hf and ^{179}Hf NMR, they are listed here for comparison.

[c] Value in parenthesis was calculated from literature data on nuclear magnetic moments.[26]

3.1. *Titanium complexes*

Ti NMR spectra show both ^{47}Ti and ^{49}Ti peaks with the ^{49}Ti peak more deshielded by 266 ppm from the ^{47}Ti peak.[1] The twinning is a result of very similar gyromagnetic ratios and thus NMR frequencies. The ^{49}Ti peak has a better S/N ratio even though the ^{49}Ti natural abundance is smaller. The sharper ^{49}Ti signal is a consequence of the larger ^{49}Ti nuclear spin and its slightly smaller quadrupole moment. Because of the quadrupole moments, sharp ^{47}Ti and ^{49}Ti signals with well-resolved multiplets were only observed for complexes with cubic O_h or T_d symmetry such as TiF_6^{2-}.[1] Line widths of ^{47,49}Ti peaks were often reported mostly because of quadrupole-dominated relaxation.[1] The range of ^{47,49}Ti shifts for diamagnetic complexes spans δ 1375 for $Ti(CH_2CMe_2Ph)_4$[123] to δ -1389 for Ti(-II) $Ti(^{13}CO)_6^{2-}$ [with K(2.2.2-cryptand)$^+$ cation].[1] Selected complexes with reported ^{47,49}Ti shifts are listed in Table 3. ^{47,49}Ti and ^{13}C NMR spectra of Ti-containing catalysts were reported, many of which were in Table 3.[123] It should be noted that shifts of same Ti complexes in different papers may be slightly different.[124-128]

Table 3. ^{47,49}Ti chemical shifts of selected Ti complexes

Complexes	**^{47,49}Ti shifts (δ)**
$TiCl_4$[123]	0.0
$TiBr_4$[123]	471.3
$(NH_4)_2TiF_6$[123]	-1160.9
$Ti(NMe_2)_4$[123]	-230
$Ti(NEt_2)_4$[123]	-216

$Ti(OEt)_4$[129]	-825 (CH_2Cl_2)
$Ti(OPr^i)_4$[123]	-856
$Ti(OPr^i)_3Cl$[123]	-749
$Ti(OPr^i)_2Cl_2$[123]	-598
$Ti(OPr^i)Cl_3$[123]	-358
$Ti(OBu^t)_4$[123]	-896
$Ti(OCH_2Bu^t)_4$[123]	-851
$Ti(CH_2CMe_2Ph)_4$[123]	1375
$CpTiCl_3$[127]	-396.5
$(\eta^5\text{-}C_5H_4Me)TiCl_3$[124]	-332
$(\eta^5\text{-}C_5H_4SiMe_3)TiCl_3$[124]	-361
Cp^*TiCl_3[124]	-85
Cp^*TiMe_3[126]	551
Tp^*TiCl_3 [Tp* = tris(3,5-dimethyl-1-pyrazolyl)borate][129]	-406
Cp_2TiCl_2[123]	-769
$Cp^*_2TiCl_2$[123]	-439
$Cp_2Ti^{II}(CO)_2$[129]	-1156
$[K(2.2.2\text{-cryptand})]_2[Ti(^{13}CO)_6]$[1]	-1389

^{49}Ti shifts of half-sandwich complexes, including those listed above, were reported in several papers.[124-128] $^{47,49}Ti$ shifts of $(\eta^5\text{-}C_5H_4X)TiCl_3$ with a silyl-substituted cyclopentadienyl ligand (X = SiR_3; R_3 = Me_3, Me_2Cl, $MeCl_2$, Cl_3, Me_2F, MeF_2, F_3) showed a nearly linear relationship with λ_{max} (wavelength of the first charge-transfer band in the UV-visible spectra) of the complexes, revealing that both ^{49}Ti NMR shifts and λ_{max} demonstrated the electron-releasing

and -withdrawing nature of the X substituents.[128] These (η^5-C_5H_4X)$TiCl_3$[128] and Cp*TiMeX'$_2$ [X'$_2$ = (Me)$C_6F_5^{2-}$, (Me)$OC_6F_5^{2-}$, $(OC_6F_5)_2^{2-}$][126] were initiators for olefin polymerization. Half-sandwich complexes with allyl and enantiomeric alkoxide ligands were used in the enantioselective allyltitanation of aldehydes.[124]

^{49}Ti shift of $TiCl_4$ in ambient-temperature ionic liquid (also known as molten salt), $AlCl_3$-1-ethyl-3-methylimidazolium chloride (ImCl), was δ -4, while in basic (chloride-rich) liquids, ^{49}Ti shift of $TiCl_6^{2-}$ was δ -237.[130]

^{47,49}Ti shifts of electron donor-acceptor complexes between 9-methylanthracene and $TiCl_4$ were reported.[131]

Spin-lattice relaxation times T_1 for several complexes were reported: $TiCl_4$ (^{47}Ti: 86.1 ms; ^{49}Ti: 265 ms), $TiBr_4$ (^{47}Ti: 90.4 ms; ^{49}Ti: 303 ms), $Ti(OBu^t)_4$ (^{47}Ti: 9.74 ms) and $Ti(OPr^i)_4$ (^{47}Ti: 3.67 ms).[123] Spin-spin relaxation times T_2 have also been reported for $TiCl_4$ (^{47}Ti: 72 ms; ^{49}Ti: 191 ms).[123]

^{49}Ti shifts of TiX_4 (X = Cl^-, Br^-, F^-), $TiCl_nMe_{4-n}$ (n = 0–3), Cp_2TiX_2 (X = F^-, Cl^-, Br^-) and $Ti(CO)_6^{2-}$ were calculated by a DFT method.[132]

For NMR of ligands, dmf exchange on $[Ti(dmf)_6]^{3+}$ was studied as a function of temperature and pressure by ^{1}H and ^{17}O NMR in order to expand upon the trend in exchange in hexa-solvated, trivalent, first-row transition metal cations.[133] Along this row of metal ions and Ga(III), the mechanism changed from an associative activation mode for the earlier elements, such as Ta(III), to a dissociative activation mode for the later elements and Ga(III).[133] ^{17}O NMR was used to analyze Ti(IV) tartrates and alkoxides, such as $[Ti(dipt)(OPr^i)_2]_2$ [δ 293, 268, 180 and 177; dipt = (+)-diisopropyl tartrate (**17**) enriched with ^{17}O at the hydroxyl positions] and $Ti(OPr^i)_4$ (δ 295).[134]

In order to gain an understanding about the reactivity of metal peroxo complexes, such as those containing Ti(IV), V(V), Mo(VI), and W(VI), several complexes were studied via ^{17}O NMR the electronic charge transfer band, the O-O vibrational frequency, and the length of the

oxygen-oxygen bond in the peroxo ligand.[135] The peroxo ligands of $Ti(O_2)(C_2O_4)_2^{2-}$ and $Ti(O_2)(dipic)(H_2O)_2$ (dipic = pyridine-2,6-dicarboxylate) had ^{17}O shifts of δ 591[135] and 585,[136] respectively. The other metalloperoxide complexes will be discussed in sections of other transition metals in the current review.

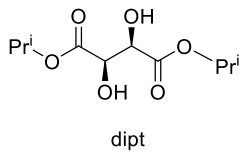

(**17**)

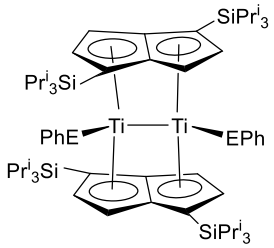

(**18**)

^{17}O shifts of Ti(IV) oxo porphyrin complexes, such as Ti(TMP)(=O) (δ 1010 referenced to H_2O; H_2TMP = 5,10,15,20-tetramesitylporphyrin, also known as tetramesitylporphyrin), were probed.[137] Diphenylchalcogenoate complexes $(\mu,\eta^5{:}\eta^5\text{-Pn})_2[Ti(EPh)]_2$ [**18**, Pn = 1,4-$(SiPr^i_3)_2$-C_8H_4, E = S, Se, Te] were analyzed via ^{29}Si NMR (δ in the 2.74-5.20 range).[138] The Se and Te complexes were also studied via ^{77}Se and ^{125}Te NMR, respectively. The resonances at δ_{Se} 511 and δ_{Te} 418 were both more shielded compared to those of most other Ti(IV) selenolate and tellurolate complexes such as $Cp_2Ti(SePh)_2$ (δ_{Se} 847) and $Cp_2Ti(TeSiPh_3)_2$ (δ_{Te} 709).[138]

The NMR studies of several Ti σ-borane complexes were discussed in a 2008 review.[139]

3.2. *Zirconium complexes*

^{91}Zr NMR is more favorable than ^{49}Ti, as the ^{91}Zr nuclide (Table 2) has higher natural abundance, larger relative sensitivity and receptivity, and smaller quadrupole moment with a larger resonance frequency (closer to that of ^1H NMR).[1] Line widths of ^{91}Zr peaks were often reported mostly because of quadrupole-dominated relaxation.[1] ^{91}Zr shifts of diamagnetic

complexes are typically in the range of δ 893 for $Zr(NMe_2)_4$[140] to δ -348 for $Cp_2Zr(\eta^4$-butadiene).[1]

Hydrolysis of Cs_2ZrF_6 (δ -191) in aqueous solution and in 30% H_2O_2 solution was probed using ^{91}Zr and ^{19}F NMR.[141] In aqueous solutions, only ZrF_6^{2-} and F^- ions were observed. However, in the water-peroxide medium, a peroxo intermediate (dimer F_5Zr-OO-ZrF_5^{4-}) was detected.[141]

^{91}Zr shifts and line widths were used as indicators of coordination geometry distortions in 32 zirconocene complexes,[140] including Cp_2ZrCl_2 (δ -112), $Cp_2Zr(Cl)Me$ (δ 126), Cp_2ZrMe_2 (δ 386), $(\eta^5\text{-}C_5H_4Me)_2ZrCl_2$ (δ -69), $(\eta^5\text{-}C_5H_4Me)_2ZrMe_2$ (δ 401), $Cp^*_2ZrCl_2$ (δ 85), $Cp^*_2ZrMe_2$ (δ 443) and a number of other ring-substituted and -bridged zirconocene complexes. They were compared with those of $Zr(NMe_2)_4$ listed above and $ZrCl_4$•2THF (δ 628).[140] For Cp'_2ZrX_2 (Cp' = substituted and -bridged cyclopentadienyl; X = Br^-, Cl^-, Me^-), a*b initio* computations suggested that the magnitude of the electric field gradient (EFG) at the Zr atom dominated line widths when the ligands X were varied, while substituents at Cp' rings affected much less the computed EFGs.[140] ^{91}Zr shifts of additional non-ansa alkyl-substituted cyclopentadienyl and phospholyl complexes, which were used in the ethylene polymerization, were reported.[142-143]

Reactions of Cp_2ZrMe_2 with fluorocarbon acids such as $H_2C(SO_2CF_3)_2$ were studied, giving, e.g., $Cp_2ZrMe[HC(SO_2CF_3)_2]$ (δ 20) and $Cp_2Zr[HC(SO_2CF_3)_2]_2$ (δ -331).[144] ^{91}Zr shifts of a series of zirconocene products were given.[144] The newly compounds from the reactions with fluorocarbon acids were compared with those of Cp_2ZrCl_2, $Cp_2Zr(Cl)Me$, and Cp_2ZrMe_2.[144]

^{91}Zr shifts of $CpTpZrCl_2$ [Tp = hydrotris(pyrazolyl)borate, $HB(C_3H_3N_2)_3^-$; δ 22] and $Cp[H_2B(C_3H_3N_2)_2]ZrCl_2$ (δ 53) were studied.[145] The complexes, when activated by methylalumoxane (MAO), became catalysts for olefin polymerization.[145]

^{91}Zr shifts of acetylacetonate (acac) complexes, $(acac)_3ZrCl$ (δ 77) and $Zr(acac)_4$ (δ -46), were also reported in the study of their potentials, when activated by MAO, as catalysts for olefin polymerization.[145] After reacting with MAO, ^{91}Zr shifts are as follows: $(acac)_2ZrCl_2$/MAO (δ 9.2), $(acac)_3ZrCl$/MAO (δ 156.6), and $(acac)_4Zr$/MAO (δ 147.5) in toluene solution at the Al:Zr

ratio of 1000:1.[145] In comparison, $(dbm)_3ZrCl$/MAO [δ 35.7; dbm = dibenzoylmethanate = 1,3-diphenylpropanedionate (**19**)].[145]

DFT calculations predicted δ -1500 for $Zr@C_{28}$ endohedral compound, after it was detected by mass spectrometry.[146]

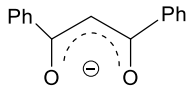

(**19**)

For NMR of ligands, the tetrameric Zr(IV) cation $[Zr_4(OH)_8(H_2O)_8(H_2O)_8]^{8+}$ was studied via several spectral methods including ^{17}O NMR (δ ~180).[147] In this cation, there are two labile and two inert water molecules per Zr atom.[147] ^{11}B and ^{31}P NMR were used to analyze Zr and Hf polyhydride complexes $M_3H_6(BH_4)_6(PMe_3)_4$ and $M_2H_4(BH_4)(dmpe)_2$ (M = Zr, Hf).[148] B-containing diamide complexes $(Bu^tN\text{-}BPh\text{-}NBu^t)_2M(THF)$ and $Li_2[M(Bu^tN\text{-}BPh\text{-}NBu^t)_3]$ (M= Zr, Hf) were synthesized from the reacitons of $PhB(Bu^tNLi)_2$ with the metal halides.[149] These complexes were analyzed via ^1H and ^{11}B NMR and X-ray crystallography.[149] A large series of zirconocene and hafnocene silyl complexes were synthesized and analyzed via ^1H, ^{13}C, and ^{29}Si NMR.[150]

The *in-situ* polymerization of hyperpolarized 1-hexene with either $[(EBI)ZrMe]B(C_6F_5)_4$ [EBI = *rac*-C_2H_4(1-indenyl)$_2$] or $(Cp_2ZrMe)B(C_6F_5)_4$ was analyzed via dissolution DNP NMR.[151] With this technique, several aspects of the reaction such as stereochemistry, measurement of kinetic rate constants, and identification of deactivation processes could be studied simultaneously.[151] Stop-flow NMR was also used to directly observe the kinetics of 1-hexene polymerization with either $[(EBI)ZrMe]B(C_6F_5)_4$.[151] Diffusion NMR was used to study the individual components and combinations of a ternary system containing Cp_2ZrMe_2/MAO (DMAO) in 2,6-Bu^t_2-phenol (MAO = methylaluminoxane, DMAO = $AlMe_3$-depleted MAO).[152] Variable-pressure 2-D (2-dimensional) ^1H Exchange Spectroscopy (EXSY) was used in the

assignment for the *cis*/*trans*-isomerization of $ZrCl_4[O=P(OMe)_3]_2$.[153] For an overview of EXSY, see Section 13.1.

Heptacoordinated Zr and Hf complexes $M[MeC(NPr^i)_2]_3Cl$ (M = Zr, Hf) and $M[MeC(NPr^i)_2]_3R$ (M = Zr, Hf; R = Me, Et) were analyzed via several methods including ^1H-^{15}N *g*HMBC NMR.[154] The average bond lengths of M-N in the $M[MeC(NPr^i)_2]_3Cl$ were shorter than those in the $M[MeC(NPr^i)_2]_3Et$ as observed in their crystal structures. Since fast exchange was needed to detect the HMBC cross peaks, the 2-D NMR experiments for $M[MeC(NPr^i)_2]_3Cl$ were performed at an elevated temperature (60 °C).[154] The ^1H-^{15}N *g*HMBC NMR of $M[MeC(N^iPr)_2]_3Me$ was also obtained at elevated temperatures (45 °C).[154]

The ^{11}B NMR spectrum was obtained for the complex $[(Zr_6BI_{12})(H_2O)_6]^+$ (δ 215.2) which was formed from the dissolution of KZr_6BI_{14} in deoxygenated water.[155]

3.3. *Hafnium complexes*

We did not find reports of ^{177}Hf or ^{179}Hf NMR which were also not discussed in the 1991 book edited by Pregosin[1] or a 1987 book on multinuclear NMR edited by Mason.[3]

For NMR of ligands, the silyene complex $(\eta\text{-}C_5H_4\text{-}Et)_2(PMe_3)Hf{=}Si(SiMeBu^t_2)_2$ was analyzed via ^1H, ^{13}C, ^{31}P, and ^{29}Si NMR.[156] This was the first example of a stable Schrock-type silyene complex and the first complex with a Hf=Si double bond.[156]

For the discussion of polyhydride complexes $Hf_3H_6(BH_4)_6(PMe_3)_4$,[148] $Hf_2H_4(BH_4)(dmpe)_2$,[148] B-containing diamide complexes $(Bu^tN\text{-}BPh\text{-}NBu^t)_2Hf(thf)$ and $Li_2[Hf(Bu^tN\text{-}BPh\text{-}NBu^t)_3]$,[149] and heptacoordinated $Hf[MeC(NPr^i)_2]_3Cl$,[154] see previous Section 3.2 on their Zr analogs.

4. Group 5 (V, Nb and Ta)

For V and Nb, NMR of both the metals (^{51}V, ^{93}Nb) and ligands have been reported. For Ta, we found only papers on NMR of ligands in 1990-2019. It should be pointed out that solution

^{181}Ta NMR of the TaF_6^- anion prepared by dissolving Ta metal in HF/HNO_3 was reported in 1973 in order to determine the ^{181}Ta nuclear gyromagnetic ratio and its magnetic moment.[157] Later, ^{181}Ta NMR spectra of $(Et_4N)(TaCl_6)$, $(Et_4N)[Ta(CO)_6]$, and $K_2(TaF_7)$ in solution were published in 1986.[158]

Nuclear and NMR properties of the nuclides, including recommended and commonly used references, are given in Table 4.

Table 4.[26] Nuclear and NMR properties of ^{51}V, ^{93}Nb, and ^{181}Ta

Nuclide	Natural abun-dance (%)[a]	Spin	Relative receptivity		Gyromagnetic ratio (10^7) (rad s^{-1} T^{-1})	Quadrupole moment Q (fm^2)	Ξ (and frequency, MHz; ^{1}H = 100 MHz, 2.3488 T)	Reference sample
			D^H (^{1}H = 1.00)	D^C (^{13}C = 1.00)				
(^{50}V)[b,c]	0.250	6	1.39×10^{-4}	0.818	2.6706490	21.0	9.970309	$VOCl_3$ (neat/C_6D_6)
^{51}V	99.750	7/2	0.383	2.25×10^3	7.0455117	-5.2	26.302948	
^{93}Nb	100	9/2	0.488	2.87×10^3	6.5674	-32.0	24.476170	$KNbCl_6$ (MeCN) or $NEt_4(NbCl_6)$[159-160] (MeCN or CD_3CN)
^{181}Ta	99.98799	7/2	3.74×10^{-2}	220	3.2438	317.0	11.989600	$KTaCl_6$ (MeCN) or $NEt_4(TaCl_6)$ (1:1 MeCN:Me_2CO[158])

[a] Unless noted, the isotopes are stable. The natural abundances are based on the NIST data.[25]

[b] ^{50}V is radioactive with $t_{1/2}$ >3.9 x 10^{17} years.[32]

[c] ^{50}V in parenthesis is considered to be the less favorable of the element for NMR.[26]

4.1. *Vanadium complexes*

We did not find papers published in 1990-2019 on ^{50}V NMR. The reader may find a summary of ^{50}V NMR work published by 1990 in Reference 1.

^{51}V NMR is one of mostly used metal NMR spectroscopies with many papers. In fact, ^{51}V nuclear properties in Table 4 make its NMR among the easiest in transition metals even for compounds with nearly no symmetry.[1] Solution ^{51}V shifts of diamagnetic complexes are typically in the range of δ 2375 for $Cp^*_2V_2(\mu,\eta^2\text{-}Se_2)(\mu\text{-}Te)_2$[1] to -2054 for $(NEt_4)[CpV(CO)_3(SnPh_3)]$.[161] ^{51}V NMR studies of V^V, V^{III}, V^I and V^{-I} complexes up to 1990 were reviewed in detail in References 1 and [162]. Biological applications of ^{51}V NMR were discussed in another 1990 review.[163] In addition, ^{51}V NMR of organometallic complexes at V^V, V^{IV} (in V-V bonded dimers), V^{III}, V^I, and V^{-I} oxidation states was surveyed in depth in a 2008 review.[164] ^{51}V NMR developments during 1997-2008 were reviewed in 2008.[165]

Complexes with V-O bonds, including vanadate (VO_4^{3-}) derivatives, polyoxometalates, and peroxo derivatives, continue to be a focus of ^{51}V NMR studies driven in large part to find insulin-mimetic V compounds in diabetic treatments.

Vanadate derivatives typically contain N,O,[166-167] O,O,[168-170] O,N,O[171-173] and O,N,N[174] ligands. Reported complexes with N,O ligands included those with NH_2OH,[166] MeNHOH,[166] and 8-hydroxyquinoline-5-sulfonic acid [H(8-HQS) (**20**)],[167] suggesting, e.g., that 5- (δ -527) and 6-coordinated (δ -537 and -540 from isomers) V centers were present in the 8-HQS complexes.[167] The equilibria of vanadate with β-alaninehydroxamic acid ($H_2NCH_2CH_2CONHOH$),[168] aldaric acids (*D*-saccharic acid and mucic acid),[169] 1,2-dimethyl-3-hydroxy-4-pyridinone[175] in aqueous solution, giving O,O complexes, were studied by ^{51}V NMR, showing, e.g., δ -520 and -450 for 1:1 and 1:2 V:ligand (ligand = β-alaninehydroxamate) complexes, respectively.[168] Interactions of vanadate with adenosine, and imidazoles in aqueous solution were probed by potentiometry and ^{51}V NMR.[176]

O,N,O complexes included those from vanadate reactions with iminodiacetic acid $[HN(CH_2CO_2H)_2]$, *N*-(2-hydroxyethyl)iminodiacetic acid $[HOCH_2CH_2N(CH_2CO_2H)_2]$,[171] *N,N*-bis(2-

hydroxyethyl)glycine [$(HOCH_2CH_2)_2NCH_2CO_2H$],[171] 2,6-pyridinedicarboxylate,[173] and 4-hydroxypyridine-2,6-dicarboxylic acid (H_2-dipic-OH),[172] forming products with tridentate ligands such as Na[VO_2(dipic-OH)] (δ -529.0).[172] Tridentate O,N,O complexes **21** with (*E*)-*N*'-[1-(5-acetyl-2,4-dihydroxyphenyl)ethylidene] hydrazide-type ligands were synthesized and characterized, including by single-crystal diffraction for a few complexes.[177] Their ^{51}V NMR showed resonances in the δ -534.0 to -547.8 range.[177] O,N,N complexes include those from the reactions of vanadate(V) with dipeptides (Val-Gln, Ala-Gln, Gly-Gln, Gly-Glu, and Ala-Gly), which were characterized by multinuclear (^{51}V, ^{14}N, ^{13}C) NMR.[174]

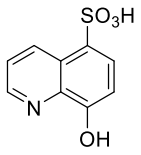

(**20**)

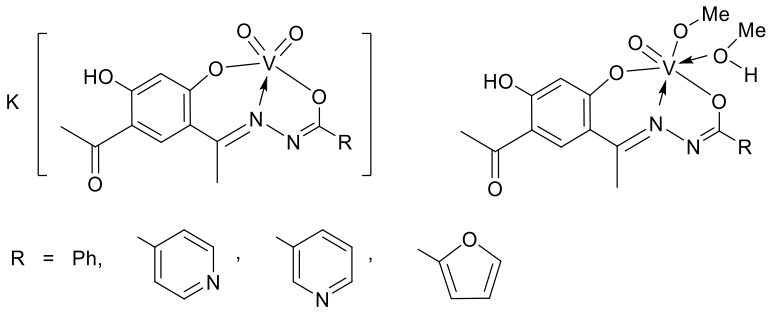

(**21**)

^{51}V NMR was used as a pH-dependent probe for acidification of reverse micellar nanodroplets by CO_2 in the confined space.[178] Multinuclear NMR approaches, in particular ^{51}V, were employed to elucidate the nature of vanadates and peroxovanadates in hydrophilic ionic liquids, (bmim)BF_4 and (bmim)(OTf) [$bmim^+$ = 1-n-butyl-3-methylimidazolium (**22**)], indicating that ionic liquids had a strong influence on the vanadate chemistry both for the formation of the aggregates (with and without H_2O_2) and the rate of peroxide consumption catalyzed by vanadium.[179] V_2O_5 was dissolved at >70 °C in, e.g., (bmim)$AlCl_4$ ionic liquid, giving different species as a function of melt acidity.[180] ^{51}V, ^{1}H, and ^{13}C NMR and IR indicated that, in basic and neutral melts, $VO_2Cl_2^-$ and a metavanadate species, $[(VO_3)_n]^{n-}$ were the products. While $VO_2Cl_2^-$

was prominent in basic melts, but as the melt became neutral or as the concentration of V_2O_5 was increased, the concentration of $[(VO_3)_n]^{n-}$ increased.[180]

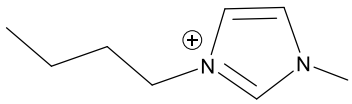

(**22**)

Vanadate (VO_4^{3-}), stable in the highly alkaline region (pH >13) oligomerized as basicity was reduced and at pH 2-6, the main species was polyoxovanadate $V_{10}O_{28}^{6-}$, which could exist in several protonated forms.[181] Structural studies of polyoxometalates by ^{51}V and ^{17}O NMR were reviewed in 2006.[182] Time-resolved ^{51}V NMR EXSY was used to probe kinetics of the oligomerization of vanadate into dimer, tetramer, and pentamer in aqueous solutions, giving rate constants.[183] The existence of linear tri- and tetra-vanadate anions, $V_3O_{10}^{5-}$ [^{51}V δ -554.3 ($V_{terminal}$), -586.6 ($V_{central}$); 273 K] and $V_4O_{13}^{6-}$ [^{51}V δ -554.3 ($V_{terminal}$), -585.4 ($V_{central}$)], in aqueous solution were confirmed by ^{51}V and ^{17}O NMR and potentiometry, yielding constants of their formation from H^+ and HVO_4^{2-} (δ -537.2) through dimer intermediates $V_2O_7^{4-}$ (δ -558.8) and $HV_2O_7^{3-}$ (δ -559.9) in 5% ^{17}O-riched solution.[184] ^{17}O NMR resonances were in the δ 920-360 range. ^{17}O magnetization-transfer experiments indicated that the O atoms in $V_3O_{10}^{5-}$ and $V_4O_{13}^{6-}$ underwent exchanges likely through intramolecular processes.[184] When a neutral, 3% ^{17}O-riched aqueous vanadate solution in NaCl was rapidly acidified at room temperature to pH 1.5, transient tridecavanadate $H_{12}V_{13}O_{40}^{3-}$, containing 12 V atoms (δ -538.0) around a central, tetrahedrally coordinated V atom (δ -523.3) in a Keggin structure, was identified by ^{51}V and ^{17}O NMR.[185] ^{17}O NMR peaks at δ 981, 853, and 575 from solvent O atoms were observed. The tridecavanadate had a half-life of 80 min at 298 K.[185] Dodecavanadate, $V_{12}O_{32}^{4-}$, is a bowl-type host with a 4.4-Å-diameter cavity entrance that reacted with guest anion X^- (X^- = CN^-, OCN^-, NO_2^-, NO_3^-, HCO_2^-, and $CH_3CO_2^-$) to form host–guest complexes, $V_{12}O_{32}(X)^{5-}$, as ^{51}V NMR and

X-ray crystallographic analyses showed.[186]

Vanadate could also form mixed-metal polyoxometalates such as α-$H_2W_{11}VO_{40}^{7-}$ (δ -543)[187] and heteropolymetalates with main group oxyanions such as the Keggin-type α-$SiVW_{11}O_{40}^{5-}$ (Na^+ salt; ^{51}V δ -551.3; ^{29}Si δ -81.87).[188] Two tungstovanadates, $WV_9O_{29}^{5-}$ and *mer*-$W_3V_3O_{19}^{5-}$, were identified in equilibrated aqueous solution of WO_4^{2-} and VO_3^- using ^{51}V NMR and ^{51}V-^{51}V COSY (Correlation Spectroscopy) which supported structures analogous to known molybdovanadates.[189] ^{51}V and ^{17}O NMR showed that silicate anions reacted with HVO_4^{2-} in aqueous alkaline solution, forming $H_2VSiO_7^{3-}$, $H_3VSiO_7^{2-}$ and related monovanadooligosilicates.[190] Molybdovanadates with high Mo:V ratios in aqueous solution, such as *cis*-$Mo_4V_2O_{19}^{4-}$, *cis*-$HMo_4V_2O_{19}^{3-}$, $Mo_5VO_{19}^{3-}$, $Mo_4V_5O_{27}^{5-}$, $HMo_4V_5O_{27}^{4-}$, and β-$Mo_7VO_{26}^{5-}$, were characterized by ^{51}V and ^{17}O NMR as well as ^{95}Mo NMR for some species.[191] Reaction of $NaVO_3$ with Na_2WO_4 in NaCl-containing aqueous solution yielded several tungstovanadates, such as *cis*-$W_4V_2O_{19}^{4-}$ (^{51}V δ -511.3), $WV_9O_{28}^{5-}$ (^{51}V δ in the range of -428.2 to -525.7), and α-$H_2W_{11}VO_{40}^{7-}$ (^{51}V δ -544.3) in equilibrium with $H_2V_{10}O_{28}^{4-}$ and VO_4^{3-}.[192] ^{51}V, ^{183}W and ^{17}O NMR and potentiometry were used to characterize the mixtures.[192] Mixing of Na_2HVO_4 with varying proportions of Na_2WO_4 and Na_2MoO_4 in NaCl-containing water, followed by acidification with HCl, yielded the complete series of hexametalate anions $V_2Mo_nW_{4-n}O_{19}^{4-}$ (n = 0-4) in the Lindqvist structure with two *cis* V atoms.[193] ^{51}V shifts of the species in the δ -497.9 to -513.7 range and their monoprotonated tetraanions in the δ -511 to -541 range were assigned.[193] Reaction of hydrous niobium oxide with V_2O_5, H_3PO_4 and NMe_4OH in water at 130 °C gave a Keggin-type polyoxoniobate $(NMe_4)_9[PV_2Nb_{12}O_{42}]$ (^{51}V δ -540; ^{31}P δ 2.4; pH 7.3) containing a central P site and two capping V sites.[194] ^{51}V NMR (for V^V component), EPR (for V^{IV} component) and voltammetry were used to study the initial reduction of 1- and 4-$[S_2VW_{17}O_{62}]^{5-}$ forming V^{IV} products.[195] When a mixture of $Na_7H(Nb_6O_{19})$, $NaVO_3$, and $NaHCO_3$ in water was heated at 220 °C in an autoclave, the reaction gave a bicapped α-Keggin vanadododecaniobate, $Na_9H_4[VNb_{12}O_{40}[NbO(CO_3)]_2]$.[196] ^{51}V NMR and ESI-MS data indicated that this anion in solution

was in equilibrium with $VNb_{12}O_{40}^{15-}$ and oligomeric species from dissociation of the $NbO(CO_3)^+$ fragments.[196] In the presence of K^+, the same reaction gave $V_xNb_{24}O_{76}^{n-}$ (x = 4, n = 12; x = 3, n = 17).[196] A V-Co cluster, $[Co_4(tacn)_4V_4O_{12}(OH)_4](OTf)_4$ [tacn = 1,4,7-triazacyclononane (**2**, R_3 = H_3)], was prepared from the reaction of Na_3VO_4 with $[Co(tacn)(H_2O)_3](OTf)_3$ (whose ^{59}Co NMR was given below) in aqueous triflic acid solution.[197] The triflate product could be converted to Cl^-, Br^- or ClO_4^- derivatives. ^{51}V and ^{59}Co NMR of the cation solution show δ -380 and 9,650, respectively.[197]

For the use of electron-electron double resonance (ELDOR)-detected NMR (EDNMR), hyperfine sub-level correlation (HYSCORE), and electron-nuclear double resonance (ENDOR) to study hyperfine interactions in polyoxometalate $PV_2Mo_{10}O_{40}^{6-}$ with one reduced V(IV) ion,[198] see Section 13.3.

Vanadium peroxo compounds were of interest mainly due to their role in biological systems and their application in oxidation reactions.[199] Vanadium peroxo compounds were identified as a new class of powerful insulin mimetic agents.[200] Vanadium peroxo materials were also found to be in haloperoxidases that likely play a key role in the production of biogenic organohalogens in the environment.[201] Addition of H_2O_2 to NH_4VO_3 in acid aqueous solutions gave monoperoxo $VO(O_2)^+$ (δ_V -540.5) or diperoxo $VO(O_2)_2^-$ (δ_V -693.1) complexes.[202] In the presence of bidentate ligands L, e.g., picolinic or pyrazinic acid (HL), complexed peroxo vanadium species such as $VO(O_2)L$, $VO(O_2)L_2^-$, and $VO(O_2)_2L^{2-}$ were identified by ^{51}V NMR,[202] and their shifts in twelve solvents were also studied.[203] In MeCN, the picolinate complex, $VO(O_2)(picolinate)(H_2O)_2$•MeCN was found to oxidize hydrocarbons and the spin trap 3,3,5,5-tetramethyl-pyrroline-N-oxide (TMPO), forming V(IV) species, as ^{51}V NMR and EPR studies showed.[204]

^{51}V NMR revealed that reactions of aqueous monoperoxo $VO(O_2)^+$ with amino acids such as glycine or proline gave two types of bis(amino acid) products, in which the two amino acid ligands were either bidentate or one bidentate and one monodentate through the amino

group.[201] No reaction of $VO(O_2)^+$ with imidazole or the imidazole ring of histidine was observed. In contrast, reactions of aqueous diperoxo $VO(O_2)_2^-$ with amino acids give monodentate products either the carboxyl or the amino groups, with bonding by the amines favored. Imidazole, as the free ligand or as the side chain in histidine, complexed strongly to diperoxovanadate, as did N-methylimidazole and also pyridine.[201] Quantitative ^{51}V NMR and potentiometric studies of the speciation in the vanadate-peroxide-imidazole systems also showed that imidazole binds strongly to diperoxovanadate.[205] When *L*-lactic acid [$CH_3CH(OH)COOH$] and H_2O_2 at pH 1-7 was added ammonium vanadate(V), the reaction gave three dimers - Two are 2:2:1 (metal:ligand:peroxo) isomers and the third is a 2:2:2 species.[199] At pH < 2, an additional 1:1:1 complex was formed.[199] Similar reactions with glycolic acid[206] and *L*-malic acid[207] were studied. The speciation of $H_2VO_4^-$ and H_2O_2 with *L*-α-alanyl-L-histidine (**23**) in acidic aqueous solution was studied by quantitative ^{51}V NMR and potentiometry, showing the formation of four 1:1:1 (metal:ligand:peroxo) and four 1:1:2 products.[208] Reaction of $K_3[VO(O_2)_2(oxalate)]$ or $VO(O_2)_2(D_2O)^-/VO(O_2)_2(HOD)^-$ with glycyl-histidine (**24**) in aqueous (H_2O or D_2O) solution gave two $VO(O_2)_2(glycyl\text{-}histidine)^-$ isomers with V-N bonds to either the ε-N or δ-N atom in the imidazole ring, as VT NMR, Diffusion-Ordered Spectroscopy (DOSY), HMQC and DFT calculations showed.[209] Additional discussion of HMQC[4] and DOSY[4] is given in Section 13.1 below. NMR studies (including ^1H, ^{13}C, ^{14}N, ^{51}V and DOSY) of the reaction between $K_3[VO(O_2)_2(oxalate)]$ with ethylenediamine ($H_2NCH_2CH_2NH_2$ = en) in aqueous solution indicated the formation of 6-coordinated $[OV(O_2)_2(en)]^-$ with one V-N bond.[210] In contrast, a similar mixture with $HNEt_2$ instead did not lead to the formation of a new complex.[210] Reaction of siloxy $VO_2(OSiPh_3)_2^-$ with H_2O_2 gave oxoperoxo complex $VO(O_2)(OSiPh_3)_2^-$ (δ -596.8).[211] ^{51}V NMR, ESI-MS, and *ab initio* calculations techniques were used to study vanadium triperoxo complexes such as $V(O_2)_3^-$ in protic solvents, showing a step-by-step decomposition process.[212] When $Na[V(O_2)_3]\bullet 3H_2O$ was dissolved in strongly basic water (pH 14), its decomposition from the blue-violet (triperoxo vanadte; δ -847) to yellow (diperoxo vanadate) was slowed down,

allowing the characterization by ^{51}V NMR.[212]

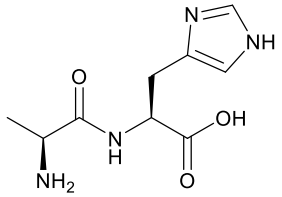

(**23**)

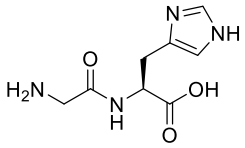

(**24**)

Cysteine oxidation to cystine by oxo diperoxo complexes $[VO(O_2)_2(L)]^{n-}$ (L = oxalate, n = 3; L = picolinate, n = 2; L = bipyridil, phenanthroline, n = 1) with insulin-mimetic activity was studied by ^{51}V NMR, UV, and stopped-flow techniques.[200] The oxalate ligand underwent a total ligand dissociation during the reaction, while the other three complexes held their ligands in solution.[200] DNA-photocleavage by peroxo V(V) complexes irradiated at 365 nm in aqueous solution was studied by ^{51}V NMR, showing VO_3^- as the vanadium product.[213] Photolysis-EPR spin-trapping experiments supported the notion that singlet oxygen was the reactive species.[213]

Nuclease activity of $VO(acac)_2$ and its derivatives was studied by several techniques including ^{51}V NMR, showing that the mechanism was oxidative and associated with the formation of reactive oxygen species (ROS).[214] Interactions of vanadate with bovine Cu,Zn-superoxide dismutase was probed by ^{51}V NMR, suggesting that the vanadate tetramer bound to the two lysine residues in the solvent channel of Cu,Zn-SOD.[215]

^{51}V NMR of organometallic complexes was discussed in a 2008 review, as indicated earlier.[164] ^{51}V shifts of selected complexes are listed in Table 5.[164] ^{51}V NMR was used to characterize $[VO(\mu\text{-}OCH_2CF_3)(OCH_2CF_3)(C_6F_5)]_2$ (δ -481), $[VO(\mu\text{-}OCH_2CF_3)(OCH_2CF_3)_2]_2$ (δ -570), $O{=}V(NEt_2)_3$ (δ -205), and $(F_5C_6)_3B{\leftarrow}O{=}V(NEt_2)_3$ (δ 57).[216]

Table 5. ^{51}V chemical shifts of selected V organometallic complexes from Reference [164]

Complexes	^{51}V shifts (δ)
Bu^t-N=V(CH_2Bu^t)$_3$	879
Bu^t-N=V(CH_2SiMe_3)$_3$	877, $^1J_{V-N}$ = 86 Hz
Bu^t-N=V(OBu^t)$_3$	-751
O=V(CH_2SiMe_3)$_3$	1205
O=V($OSiPh_3$)$_3$[164]	-723
(Bu^tCH_2)$_3$V=N-N=V(CH_2Bu^t)$_3$	1237, $^1J^{51}_{V-}{}^{14}_{N}$ = 48 Hz, $^1J^{51}_{V-}{}^{15}_{N}$ = 76 Hz
CpV(CO)$_4$	-1534, $^1J^{51}_{V-C}$ = 107 Hz

Catalytic activities of vanadium complexes were studied by ^{51}V NMR.[217-219] Cyclohexene oxidation by cumyl or t-butyl hydroperoxides to cyclohexene oxide, catalyzed by VO(acac)$_2$(OR) (R = Bu^t, δ -477; CMe_2Ph, δ -475), was probed by ^{51}V NMR.[217] The alkoxides were converted to peroxide complexes VO(acac)$_2$(OOR) (R = Bu^t, δ -351; CMe_2Ph, δ -365) which then transferred an O atom to cyclohexene. In acid isopropanol/water solution under aerobic conditions, $Bu^n{}_4NVO_3$ catalyzed autoxidation of Pr^iOH to acetone and O_2 reduction to H_2O_2.[218] The V-substituted, Lindqvist-type polyoxotungstate $VW_5O_{19}^{3-}$ in MeCN promoted cyclooctene epoxidation by H_2O_2 into cyclooctene oxide.[219] Oxidative carbonylation of toluene to *p*-toluic acid by CO and O_2 using Rh(CO)$_2$(CF_3COO)$_3$ as catalyst and [V(μ-O)O(CF_3COO)]$_2$ (δ -634 in toluene; -545 in D_2O) as co-catalyst were studied by ^{103}Rh, ^{51}V and ^{13}C NMR.[220] In the catalytic cycle, [V^V(μ-O)O(CF_3COO)]$_2$ reoxidized Rh(I) to Rh(III), forming V^{IV}O(CF_3COO)$_2$, and the dimer structure of the former was based on DFT calculations.

DFT calculations were performed to obtain the geometry and electronic structures and solution ^{51}V and ^{17}O NMR shifts of a series of 7 oxo-peroxo V(V) complexes with tetradentate

tripodal amine ligands, which mimicked the active site of vanadium bromoperoxidase.[221] The more reactive complexes for bromide oxidation contained weakly electron donating amine ligands and more deshielded ^{51}V and ^{17}O resonances.

For ligands, ^{17}O NMR of oxo complexes was discussed earlier. In addition, ^{17}O NMR of peroxide ligands in monomer V(V) complexes[135-136] and diperoxyo vanadium complexes were obtained to probe the complexes.[135-136] ^{17}O and $^{35/37}Cl$ NMR spectroscopies were used to study the hexa-aqua V(III) cation structure in various mixed acid-based electrolyte solutions used in vanadium redox flow batteries.[222]

4.2. *Niobium complexes*

^{93}Nb NMR was used to characterize $[NbF_4(diphosphine)_2](NbF_6)$ [diphosphine = *o*-$(PMe_2)_2$-C_6H_4, $Me_2P(CH_2)_2PMe_2$ (dimethylphosphinoethane or dmpe)] produced from the reactions of NbF_5 with diphosphine in MeCN, showing the binomial septet at δ -1553 for the anion NbF_6^- and a broad peak at δ -1110 and -1062 for the cations, respectively (Table 6).[160] ^{93}Nb shifts of $NbF_5(SMe_2)$ and $NbF_5(SeMe_2)$ (^{77}Se) were also reported (Table 6).[223] In $[NbF_4(dithioether)_2](NbF_6)$ [dithioether = $RS(CH_2)_2SR$ (R = Me, Et or Pr^i)], the anion NbF_6^- was observed as a binomial septet at δ -1551 to -1554 (J_{Nb-F} = 335 Hz) at 220 or 243 K (Table 6).[223] The ^{93}Nb shifts of the cations $[NbF_4(SMe_2)_4]^+$ and $[NbF_4(dithioether)_2]^+$ at 295 K are listed in Table 6.[223] Chalcogenoether complexes $NbCl_5(SBu^n_2)$ and $NbCl_5(SeBu^n_2)$ and dinuclear $(NbCl_5)_2[\mu$-*o*-$(CH_2SEt)_2$-$C_6H_4]$ were prepared from the reactions of $NbCl_5$ with respective chalcogenoethers, and they were characterized by ^{93}Nb and ^{77}Se NMR (Table 6).[224] These complexes were tested as potential single source precursors for chemical vapor deposition of NbS_2 or $NbSe_2$ films. $NbCl_3(S_2CNEt_2)_2$ and $[Nb(S_2CNEt_2)_4](NbCl_6)$ were prepared from the reaction of $NbCl_5$ with dithiocarbamate $Me_3SiSC(=S)NEt_2$.[225] ^{93}Nb shifts of $NbCl_3(S_2CNEt_2)_2$,[225] $NbCl_2(S_2CNEt_2)_3$,[226] $NbBr_2(S_2CNEt_2)_3$,[226] and $[Nb(S_2CNEt_2)_4](NbCl_6)$[225] are given in Table 6. $[NbCl_3(thf)_2]_2(\mu\text{-}N_2)$ was prepared from $NbCl_5$ and $(Me_3Si)_2NN(SiMe_3)_2$, and its ^{93}Nb resonance is

listed in Table 6.[226]

Table 6. ^{93}Nb chemical shifts of selected Nb compounds

Complexes	^{93}Nb shifts (δ)		^{77}Se shifts (δ)
	Cation	Anion[a]	
$[NbF_4[o\text{-}(PMe_2)_2\text{-}C_6H_4]_2](NbF_6)$[160]	-1110	-1553	-
$[NbF_4(dmpe)_2](NbF_6)$[160]	-1062	-1553	-
$[NbF_4(dithioether)_2](NbF_6)$ [dithioether = $RS(CH_2)_2SR$ (R = Me, Et or Pr^i)][223]	-1540 to -1550	-1551 to -1554	-
$[Nb(S_2CNEt_2)_4](NbCl_6)$[225]	-325	0	
$NbF_5(SMe_2)$[223]	-1440		-
$NbF_5(SeMe_2)$[223]	-1509		247.2
$NbCl_5(SBu^n{}_2)$[224]	97		-
$NbCl_5(SeBu^n{}_2)$[224]	123		273.6
$(NbCl_5)_2[\mu\text{-}o\text{-}(CH_2SEt)_2\text{-}C_6H_4]$[224]	94		
$NbCl_3(S_2CNEt_2)_2$[225]	-418		
$NbCl_2(S_2CNEt_2)_3$[226]	-315		
$NbBr_2(S_2CNEt_2)_3$[226]	-545		
$[NbCl_3(thf)_2]_2(\mu\text{-}N_2)$[226]	-532		

[a] The anion NbF_6^- appeared as a binomial septet with $^1J_{Nb\text{-}F}$ = 335 Hz.

Alcoholysis of $NbCl_5$ (δ 2.6) by MeOH was probed by ^{93}Nb NMR in benzene, showing formation of $NbCl_{5\text{-}x}(OMe)_x$ (x = 1, δ -497; 3, δ -810; 4, δ -1010; 5, δ -1160) with increasing shielding of the Nb atom with replacement of Cl^- by OMe^- ligands.[227] Similar NMR properties were also observed in MeOD solution.[228] In a mixture of $NbCl_5(CD_3CN)$, MeOH and H_2O, ^{93}Nb resonances of $NbCl_4(OMe)(MeCN)$ and $NbCl_4(OH)(MeCN)$ were found to be at δ -560 and -495,

respectively.[229] Quinolinol derivatives $Nb_4(\mu\text{-}O)_4(\mu\text{-}OEt)_2(ONC_{10}H_8)_2(OEt)_8$ and $Nb_4(\mu\text{-}O)_4(\mu\text{-}OEt)_2(ONC_9H_5Cl)_2(OEt)_8$, prepared from the reaction of $Nb(OEt)_5$ with 8-hydroxy-2-methylquinoline ($HONC_{10}H_8$) and 5-chloro-8-hydroxyquinoline ($HONC_9H_5Cl$), showed ^{93}Nb resonances at δ 206, 131 for the former and 197, 122 for the latter.[230] Both peroxo complexes $K[Nb(OH)(O_2)_2(8\text{-quinolinolate})]$ and $K[Nb(O_2)_2(8\text{-quinolinolate})_2]$ in D_2O give ^{93}Nb resonances at δ -739.[159] Polyoxoanion complex $(Bu^n{}_4N)_4(NbW_5O_{18})_2O$ with a Nb-O-Nb oxo bridge gave a broad ^{93}Nb resonance at δ -975.[231] ^{17}O-enriched sample $(Bu^n{}_4N)_3[Nb(^{17}O)W_5O_{18}]$ showed the ^{17}O resonance at δ 795.[231]

A 1991 review summarized ^{93}Nb NMR of organometallic compounds by then,[10] showing its chemical shift range of ca. 3,000 ppm. The subject was discussed in a 1996 article.[232]

^{93}Nb NMR showed increasing shielding on the Nb atom in d^4 $NbX(CO)_2(EtC{\equiv}CEt)(PEt_3)_2$ when the halide ligand X changed from Cl^- (δ -799.4) to Br^- (δ -834.3) and I^- (δ -931.4), the least electronegative of the three halogen elements.[233] d^2 $(\eta^5\text{-}MeC_5H_4)_2Nb(\eta^3\text{-allyl})$ gave a ^{93}Nb resonance at δ -1738.[234] ^{93}Nb shifts were reported for a series of d^0 $(silox)_3NbX_2$ and d^2 $(silox)_3NbL$ complexes (silox = $Bu^t{}_3SiO$).[235] A few (referenced to saturated $NbCl_5$ in acetonitrile) are selected here: X_2 = =NN=CHSiMe$_3$ (δ -965), =O (δ -947), Cl_2 (δ -755), ½(μ:η^1,η^1-N_2) (as a dimer with N_2 bridging ligand, δ -570), =CH_2 (δ 11.1), =PMe (δ 660). For d^2 $(silox)_3Nb(CH_2{=}CH_2)$ with both olefin and metalacyclopropane character, δ 296.[235] DFT-calculated ^{93}Nb shifts correlated with the experimental values, and indicated that, in the $(silox)_3NbX_2$ complexes, δ was generally proportional to $1/\chi$ (χ = Pauling electronegativity of the atoms bonded to Nb), with most electronegative more shielded from the shifts of other complexes. This trend was derived from the paramagnetic contribution.[235]

^{93}Nb shifts in 19 Nb complexes, $NbX_{6\text{-}n}Y_n^-$ (n = 0-6; X, Y = F^-, Cl^-, and Br^-) were calculated by the *ab initio* Hartree-Fock method, giving calculated values in very good agreement with the experimental data.[236] ^{93}Nb shifts were found to be dominated by the paramagnetic contributions and were due to the d-d* transition and excitation energy Δ*E*. The

computations also showed that the ^{93}Nb shift was related to the electronegativity of the ligand atom, net charge, and the d-electron population of the Nb atom.[236] DFT computations of ^{93}Nb shifts of a series of complexes, such as NbF_6^-, $NbCl_6^-$, $Nb(CO)_6^-$, $Nb_2(OMe)_{10}$, $CpNb(CO)_4$, and Cp_2NbH_3, were performed and the calculated shifts were compared with experimental shifts.[237] Trends in the ^{93}Nb peak line widths for anionic $Nb(CO)_5^{3-}$, $Nb(CO)_5H^{2-}$, and $Nb(CO)_5(NH_3)^-$ were rationalized in terms of computed electric field gradients at the Nb atom.

Nb oxoclusters stabilized by ionic liquid (Bu_4^nN)(lactate) were probed by ^{93}Nb NMR, showing three resonances at δ -849, -1108, and -1036 in D_2O.[238] The stabilized oxoclusters catalyzed epoxidation of olefins and allylic alcohols by H_2O_2, and catalytic cycle was followed by ^{93}Nb NMR, including the identification of a peroxo intermediate.

For NMR of ligands, reactions of $(Me_4N)_6Nb_{10}O_{28}$ with bases such as KOH, NaOH and Me_4NOH formed several polyniobates, including hexaniobate anion $Nb_6O_{19}^{8-}$, that were monitored via ^{17}O NMR over the course of weeks.[239] For $Nb_6O_{19}^{8-}$ formed by different bases, such as KOH or Me_4OH, ranges of the ^{17}O shifts of the ONb, ONb_2, and ONb_6 were found to be at δ 612-648, 378-393, and 29-41, respectively.[239]

NMR studies of several Nb σ-borane were discussed in a 2008 review.[139]

^{1}H-^{15}N HMBC (Heteronuclear Multiple Bond Correlation) was also used to obtain ^{15}N (spin 1/2) NMR shifts of Nb complexes with Nb-N bonds at the ^{15}N natural abundance of 0.364%.[240-243] The discussion of the inverse detection method is given in Sections 7 and 13.1.

4.3. *Tantalum complexes*

As noted earlier, for tantalum complexes, we have found only papers on NMR of ligands in 1990-2019. However, solution ^{181}Ta NMR of complexes were reported before 1990, including TaF_6^-,[157] $(Et_4N)(TaCl_6)$, $(Et_4N)[Ta(CO)_6]$, and $K_2(TaF_7)$.[158,232]

Parahydrogen-induced polarization (PHIP) was used to observe the kinetic, unsymmetric isomer of $Cp^*_2TaH_2Cl$, where the hydride ligands were next each other in the complex.[244] Since

PHIP requires that H_2 add pairwise in nonequivalent proton sites, this unsymmetric isomer would be the only isomer exhibiting polarization in PHIP.[244] For NMR techniques that are based on parahydrogen (*p*-H_2), see Section 13.6.

^{1}H-^{15}N HMBC was also used to obtain ^{15}N (spin 1/2) NMR shifts of Ta complexes with Ta-N bonds at the ^{15}N natural abundance of 0.364%.[240-243]

DOSY studies of *cis*- and *trans*-[Ta(μ-OMe)Me(=NSiMe$_3$)[N(SiMe$_3$)$_2$]]$_2$ in equilibrium demonstrated that they exist as dimers in solution.[245] For an overview of DOSY, see Section 13.2.

5. Group 6 (Cr, Mo and W)

For Cr, Mo and W, NMR of both the metals (^{53}Cr, ^{95}Mo, ^{183}W) and ligands have been reported. In addition to Reference 1, NMR of the three metals was reviewed in 1996.[246] Nuclear and NMR properties of the nuclides, including recommended and commonly used references, are given in Table 7.

Table 7.[26] Nuclear and NMR properties of ^{53}Cr, ^{95}Mo, ^{97}Mo and ^{183}W

Nuclide	**Natural abun-dance (%)[a]**	**Spin**	**Relative receptivity**		**Gyromagnetic ratio (10^7) (rad s^{-1} T^{-1})**	**Quadrupole moment *Q* (fm^2)**	**Ξ (and frequency, MHz; ^{1}H = 100 MHz, 2.3488 T)**	**Reference sample**
			***D*^{H} (^{1}H = 1.00)**	***D*^{C} (^{13}C = 1.00)**				
^{53}Cr	9.501	3/2	8.63 x 10^{-5}	0.507	-1.5152	-15.0	5.652496	K_2CrO_4 (aq) or $Cr(CO)_6$ (δ -1795 in THF[1])
^{95}Mo	15.84	5/2	5.21 x 10^{-4}	3.06	-1.751	-2.2	6.516926	Na_2MoO_4 (aq) or $Mo(CO)_6$ (δ -1856 in THF[1])
(^{97}Mo)[c,d]	9.60	5/2	3.33 x 10^{-4}	1.95	-1.788	25.5	6.653695	

^{183}W	14.31	1/2	1.07×10^{-5}	0.0631	1.1282403	-	4.166387	Na_2WO_4 (aq) or $W(CO)_6$ (δ -3483 in THF[1])

[a] Unless noted, the isotopes are stable. The natural abundances are based on the NIST data.[25]

[b] The data are from Reference [32].

[c] We only found publications in 1990-2019 on solution ^{95}Mo NMR of inorganic compounds and did not find a paper on ^{97}Mo NMR in 1990-2019. However, ^{97}Mo properties are listed here for comparison. Additional discussions about this issue are given below.

[d] ^{97}Mo in parenthesis is considered to be the less favorable of the element for NMR.[26]

MO_4^{2-} (aqueous solution, K^+ or Na^+ salt) in alkaline D_2O solution (pD 11) are references.[1] $M(CO)_6$ in THF solution are used as secondary standards, particularly in organometallic chemistry (Table 7).[1]

The ratio of the chemical shift ranges for ^{183}W and ^{95}Mo is ca. 1.6, which relates empirically the δ values of both nuclides in isostructural compounds.[1] Although the ratio has no theoretical support, it was used to predict, e.g., ^{183}W resonance regions of W compounds when ^{95}Mo shifts of their Mo analogs were known.[1]

Isotropic NMR shielding constants were obtained using DFT with gauge-including-atomic-orbitals (GIAO) in a spin-free formalism for the metal nuclides in MO_4^{2-} and $M(CO)_6$ (M = Cr, Mo, W).[247] Relativistic effects for NMR shielding constants were calculated using the zero-order-regular-approximation (ZORA) for relativistic effects.

5.1. *Chromium complexes*

The number of ^{53}Cr NMR data is small due to several factors.[1,246] ^{53}Cr is a quadrupolar nuclide (Table 7), leading to NMR peak broadening in complexes of low symmetry. Its natural abundance and the overall receptivity are insufficient to offset a rather small magnetic moment

resulting in a low Larmor frequency (5.653 MHz at 2.3488 T) which, in turn, leads to a low sensitivity.

Carbonate-containing capsule $(NBu^n_4)_2L_2(CO_3)$ [L = tris(2-aminoethyl)amine-based 3-cyanophenyl-substituted tripodal urea (**25**), a urea-based anion receptor] dissolved in CH_2Cl_2 was found to extract chromate CrO_4^{2-} from water, forming $(NBu^n_4)_2L_2(CrO_4)$ with ^{53}Cr shift at δ -99.98 (vs. δ 0 for CrO_4^{2-} in water as reference).[248] The chromate-containing capsule was structurally characterized by single-crystal X-ray diffraction and ^1H and ^{13}C NMR.[248]

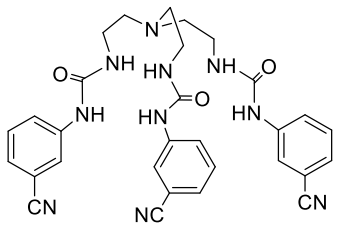

(**25**)

For ^{53}Cr and ^{14}N NMR of $Cr(CO)_5(CNBu^t)$ and $Cr(CO)_4(CNBu^t)_2$ in ambient acetone-d_6, pressurized liquid CO_2 or supercritical CO_2, see Section 12.1.[249]

^{53}Cr shifts of CrO_4^{2-}, $Cr_2O_7^{2-}$, CrO_3X^-, CrO_2X_2 (X = F^-, Cl^-), and $Cr(CO)_5L$ (L = CO, PF_3, $=CHNH_2$, $=CMeNMe_2$) were computed by the DFT methods, and the computed shifts were compared with experimental values.[250] Also, ^{53}Cr shifts were predicted for CrO_3, $(\eta^6\text{-}C_6H_6)_2Cr$, $(\eta^6\text{-}C_6H_6)Cr(CO)_3$, and, with reduced reliability, for $Cr_2(\mu\text{-}O_2CH)_4$.

In NMR studies of α atoms of ligands, ^{17}O NMR shifts of Cr diperoxo complexes were found to be between δ 726 and 818, which were more deshielded than those of other metal diperoxo complexes at δ 350-460.[135] Along with the anomalous ^{17}O shifts, the diperoxo Cr complexes show other features, including lower energy λ_{max} values for ligand-to-metal charge transfer (LMCT) transitions in UV-visible spectra, higher O-O bond vibrational frequencies, and shorter O-O bond lengths than the other diperoxo complexes studied.[135] The ^{17}O shift of Cr(IV)

oxo porphyrin complexes, such as Cr(TMP)(=O) (δ 1247 referenced to H_2O; H_2TMP = tetramesitylporphyrin) were studied.[137]

Nitride complexes, including $[N{\equiv}Cr(N^iPr_2)_2(PMe_2Ph)]^+$ and $[N{\equiv}Cr(N^iPr_2)_2(PMe_3)]^+$ with several counter anions such as PF_6^- and $BArF_{20}^-$, were studied via ^{14}N NMR.[251] The linewidths in the ^{14}N NMR spectra in several paramagnetic Cr(III) amine and diamine complexes such as $[Cr(NH_3)_6]^{3+}$, $[Cr(en)_3]^{3+}$, *cis*-$[CrF_2(en)_2]^+$, *trans*-$[CrF_2(en)_2]^+$ were investigated and compared with those of similar diamagnetic Co(III) complexes.[252] The peaks of the Cr complexes range from δ -322.7 to -345.9.[252] The ^{11}B NMR signal for the borylene complex $(OC)_5Cr{=}BSi(SiMe_3)_3$ was found to be at δ 204.3 which was more deshielded than δ 92.3 in $(OC)_5Cr{=}B{=}N(SiMe_3)_2$.[253]

5.2. *Molybdenum complexes*

^{95}Mo NMR is preferred to ^{97}Mo NMR, even though the two nuclides have the same spin quantum number and resonate at very similar frequencies. This is because ^{95}Mo has a significantly higher natural abundance, smaller quadrupole moment, and a greater sensitivity, as listed in Table 7.

^{95}Mo NMR of inorganic compounds was extensively used in inorganic chemistry.[1,246] In addition to a 1990 book chapter[1] and a comprehensive review covering the literature in 1985-1995, structural studies of polyoxometalates by ^{95}Mo and ^{17}O NMR were reviewed in 2006.[182] Thus, for polyoxometalates, the current review covers the literature since 2006 and, for other inorganic complexes, the literature since 1996 is surveyed.

^{95}Mo shifts cover the range of δ 4199 for quadruple-bonded $Mo^{II}_2(\mu\text{-}O_2CCF_3)_4(py)_2$ to δ -2953 for $(Cp_2Mo^{VI}H_3)Cl$ based on the publications that we found.[254]

Analysis of ^{95}Mo shifts of eleven Mo^{VI} oxo and peroxo complexes with mono- (N) and poly-dentate (N,N, N,O, or N,N,N) ligands showed a correlation of electronic densities on the metal atoms with the ^{95}Mo shifts. The correlation was used to indicate whether a complex was hexa- or hepta-coordinated.[255] ^{95}Mo NMR was employed, along with other spectroscopies and

DFT calculations, to study reactions of Na_2MoO_4 with 8-hydroxyquinoline-5-sulfonic acid [H(8-HQS) (**20**)] in water, forming one dimeric $[Mo_2O_4(8\text{-}HQS)_2(\mu\text{-}O)]^{2-}$ (δ 36) and two monomeric $MoO_2(8\text{-}HQS)_2^{2-}$ (δ 88 and 109) complexes.[256] Reactions of Na_2MoO_4 with 2-phospho-*D*-glyceric acid and 3-phospho-*D*-glyceric acid, gave one and four products containing 2-phospho-*D*-glycerate and 3-phospho-*D*-glycerate ligands, respectively.[257] Multinuclear NMR and DFT studies were used to identify the complexes. ^{95}Mo shifts were in the ranges of δ 99 and -55. ^{17}O shifts were in the ranges of δ 867-760 for terminal oxo ligands and δ 399-300 for bridging oxo ligands.[257] ^{1}H, ^{13}C, ^{14}N, ^{17}O and ^{95}Mo NMR showed that the complex of MoO_4^{2-} with triethanolamine in dmso or dmso-d_6 contained one free and two bound hydroxyethyl arms, and three arms of the ligand readily exchange.[258] The ^{95}Mo shift was found at δ 129.7, and the ^{14}N signal was at δ -323, while two ^{17}O resonances at δ 876.4, 841.4 were assigned for the two terminal Mo=O ligands.[258] ^{95}Mo shifts of several Mo(V) dithiocarbamate complexes such as $[MoO(S_2CNMe_2)]_2(\mu\text{-}O)(\mu^2\text{-}OC_2H_4S)$ (δ 329), in which both the S and O atoms of 2-mercaptoethanolate ligand bridged the Mo atoms, were obtained.[259] When the Me groups on the dithiocarbamate $S_2CNMe_2^-$ ligands were replaced by bulkier groups such as Ph (δ 345), the line width of the ^{95}Mo peak increased (270 Hz for Me; 470 Hz for Ph).[259] $(Et_4N)_2[MoS(edt)](\mu\text{-}S)_2$ (δ 1465, edt = ethane-1,2-dithiolate) was used to react with 1 equiv of $M(PPh_3)_3^+$ (M = Cu, Ag) to give incomplete cubane-like clusters $(Et_4N)[Mo_2(edt)_2M(PPh_3)(\mu\text{-}S)_3(\mu_3\text{-}S)]$ (**26**, M = Cu, δ 1800; Ag, δ 1656).[260] When 2 equiv of $Cu(PPh_3)_3^+$ was used, the reaction yielded cubane-like $Mo_2(edt)_2Cu_2(PPh_3)_2(\mu_3\text{-}S)_4$ (**27**, δ 2002).[260]

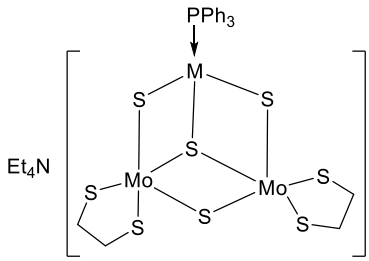

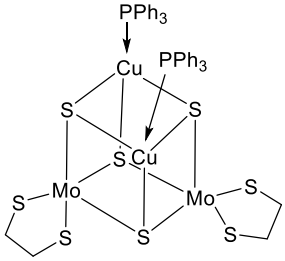

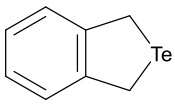

(**26**) (**27**) (**28**)

^{95}Mo shifts of octahedral Mo(II) halide clusters $(Bu^n{}_4N)_2(Mo_6X_{14})$ (X = Cl^-, δ 2937; X = Br^-, δ 3203; X = I^-, δ 3256) were used to compare with those from quantum chemical calculations to study the influences of different factors on the quality of the calculated shifts.[261] ^{95}Mo shifts of their mixed halide analogs $(Bu^n{}_4N)_2[(Mo_6X_8)Y_6]$ (X, Y = Cl^-, Br^-, I^-) were found to correlate with first- and second-order spin−orbit coupling constants (in the ranges of 620-870 and 50-99 cm^{-1}, respectively) of the clusters.[262]

^{95}Mo and ^{17}O NMR studies of polyoxomolybdate $Mo_7O_{24}{}^{6-}$ at pH 7-1 in 0.3-6 M $HClO_4$ showed that shifts of Mo atoms with terminal oxo ligands are in the δ ~20-34 range, while those of central Mo atoms with no terminal oxo ligands were δ ~200-210.[263] ^{17}O shifts of terminal and bridging oxo ligands were δ 745-837 (terminal =O), 354-784 (μ-O), 293-339 (μ_3-O), and 121-122 (μ_4-O).[263]

For the use of electron-electron double resonance (ELDOR)-detected NMR (EDNMR), hyperfine sub-level correlation (HYSCORE), and electron-nuclear double resonance (ENDOR) to study hyperfine interactions in polyoxometalate $PV_2Mo_{10}O_{40}{}^{6-}$ with one reduced V(IV) ion,[198] see Section 13.3.

Organometallic Mo(IV) complex $[[(\eta^5\text{-}C_5H_4Me)_2Mo(\mu\text{-}H)_2]_2Ag]PF_6$ gave a very broad ^{95}Mo peak at δ 3953.[264] *cis*-$Mo(CO)_4$(bdmsa) [bdmsa = bis(2-dimethylstibanylbenzyl)methylamine, $MeN(CH_2\text{-}o\text{-}SbMe_2\text{-}C_6H_4)_2$] containing a chelating bis-stibine ligand was synthesized, giving a ^{95}Mo resonance at δ -1729.[265] ^{95}Mo and ^{77}Se NMR were used to characterize *cis*-$Mo(CO)_4[o\text{-}(CH_2SeMe)_2\text{-}C_6H_4]$ with a chelating bis-seleno-ether ligand, giving resonances at ^{95}Mo δ -1393 and ^{77}Se δ 157.6.[266] Analogous complexes were also prepared and characterized. NMR studies of $Mo(CO)_5L$ with a tellurophene ligand [L = 1,3-dihydro-benzo[c]tellurophene (**28**)] gave ^{95}Mo δ -1731 and ^{125}Te δ 418.[267] ^{95}Mo and ^{77}Se NMR were used to characterize di- and tri-substituted complexes *cis*-$Mo(CO)_4L_2$ (^{95}Mo δ -1550; ^{77}Se δ 468) and *fac*-$Mo(CO)_3L_3$ (^{95}Mo δ -1320; ^{77}Se δ

532).[267]

Studies of ^{95}Mo spin-lattice relaxation times T_1 for $Mo(CO)_6$ encapsulated in dried 13-Å Na-Y zeolite at 223-323 K showed that $Mo(CO)_6$ experienced significant rotational freedom in the zeolite supercages.[268] The activation energy for rotation was about 40(4) kJ mol^{-1} and rotational correlation time, τ_c, at ambient temperature was approximately 3 orders of magnitude longer than that in solution.

Molecular topology was used to show that there was a positive correlation between experimental ^{95}Mo shifts in potassium oxothiomolybdenates [MoO_4^{2-} (δ 0), MoO_3S^{2-} (δ 497), $MoO_2S_2^{2-}$ (δ 1066), $MoOS_3^{2-}$ (δ 1654), MoS_4^{2-} (δ 2258)] and bond-parameterized topological indexes.[269] Randic earlier developed the Randic connectivity indices to characterize molecular branching of, e.g., hydrocarbons.[270] Extended Randic index developed later by Zhang and Xin was used for inorganic compounds, and expanded further here by Li and You to correlate with the ^{95}Mo shifts.[271] Semi-empirical, CNDO and *ab initio* MO methods were used to calculate ^{95}Mo shifts of the oxothiomolybdenates.[272] The work showed that shift was mainly determined by the increasing *d,p*-orbital electron populations on the Mo atom from the softer S atom and better overlap between the 3*s*,3*p* orbitals of the S atoms with the Mo valence orbitals. Large electron populations increased the paramagnetic contribution to the ^{95}Mo shift.[272]

In NMR studies of α atoms of ligands, the peroxide ^{17}O shifts of monoperoxyo Mo complexes were found to be at δ 487-536.[135-136] ^{17}O shifts of the diperoxyo Mo(VI) complexes were more shielded at δ 412-468 than those of the monoperoxo complexes.[135-136] Other ^{17}O studies were performed on Mo complexes derived from desferrioxamine B,[273] acetohydroxamic acid,[273] and hydroxypyridinonate systems.[274]

$(Bu^tO)_3Mo{\equiv}^{15}N$ was synthesized via the heated reaction of $MeC{\equiv}^{15}N$ with $(Bu^tO)_3Mo{\equiv}N$, which was monitored via ^{15}N NMR. The ^{15}N signal for the $(Bu^tO)_3Mo{\equiv}^{15}N$ was found at δ 828.8.[275] When $(Bu^tO)_3Mo{\equiv}N$ reacted with its W(VI) analog $(Bu^tO)_3W{\equiv}^{15}N$, both $(Bu^tO)_3Mo{\equiv}^{15}N$ and $(Bu^tO)_3W{\equiv}^{15}N$ were found via ^{15}N NMR,[275-276] indicating a rapid metathesis process. VT ^{1}H,

^{15}N, and 2-D ^{1}H-^{1}H ROESY (ROESY = Rotating Frame Overhauser Effect Spectroscopy) spectra indicated a rapid exchange of the proton on one N atom and the hydride ligand on [CpMo(H)(CO)($P^{R}_{2}N^{R'}_{2}H$)](BAr^{F}_{4}) complexes (**29**, $P^{R}_{2}N^{R'}_{2}$ = 1,5-diaza-3,7-diphosphacyclooctane diphosphine with R groups on N and P atoms; R = Ph, Bu^{t}, R′ = Ph, Bu^{t}, CH_2Ph).[277] For additional discussion of ROESY, see Section 13.1.

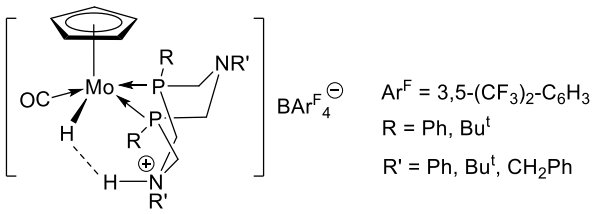

(**29**)

5.3. *Tungsten complexes*

^{183}W is a spin 1/2 nuclide with 14.31% natural abundance. However, both its gyromagnetic ratio and sensitivity (relative to ^{13}C) are low. In addition, there are technical difficulties in ^{183}W NMR spectroscopy, including relatively slow relaxation requiring long delays between NMR pulses for data collection and low NMR frequency near the lower limit of many commercial instruments. Thus, ^{183}W NMR studies had been limited for several years even though its chemical shift range is >11,000 ppm.[69,246]

^{183}W NMR of inorganic compounds reported before 1996 was reviewed.[246] Thus, the current review focuses on the publications since then.

Polyoxometalates were a focus in the studies using ^{183}W NMR. As discussed in the section on vanadium complexes, ^{51}V, ^{183}W and ^{17}O NMR was used to characterize the mixtures of tungstovanadates from the reaction of $NaVO_3$ with Na_2WO_4, such as *cis*-$W_4V_2O_{19}^{4-}$ (^{183}W δ 69.0) and $WV_9O_{28}^{5-}$ (^{183}W δ 74.5).[192] ^{17}O NMR shifts in the range of δ 1191 to -68.2 were assigned to different O ligands in the complexes. For α-$H_2W_{11}VO_{40}^{7-}$, six ^{183}W resonances,

centered around δ -123, were observed.[192] For Preyssler heteropolyoxoanions $M^{n+}P_5W_{30}O_{110}^{n-15}$ (M^{n+} = Na^+, Ca^{2+}, Sr^{2+}, Y^{3+}, La^{3+} and Th^{4+}), their ^{183}W NMR spectra (shifts in the range of δ -196 to -291) were used to identify the atomic origin of the LUMO states, which were composed primarily of orbitals from the ring of five W atoms near the M^{n+} ion.[278] Reaction of $H_3PW_{12}O_{40}$ with K_2CrO_4 led to the formation of $K_{13}(KP_2W_{20}O_{72})$ which was characterized by ^{183}W NMR and other spectroscopies.[279] The reaction of $Na_{10}(\alpha\text{-}SiW_9O_{34})$ with Ce^{4+} and Hf^{4+} in CH_3COONa buffer solution leads to the formation of sandwich polyoxometalates $Ce_4(\mu_3\text{-}O)_2(SiW_9O_{34})_2(CH_3COO)_2^{10-}$ and $Hf_3(\mu\text{-}OH)_3(SiW_9O_{34})_2^{11-}$, respectively.[280] The compounds with a polynuclear cluster fragment stabilized by two $\alpha\text{-}SiW_9O_{34}^{10-}$ polyanions were characterized by ^{183}W NMR, giving several resonances (δ -147.9 to -180.2) for the former and two resonances (δ -145 and -175) for the latter. ^{29}Si NMR of the two compounds showed one sharp resonance at δ -84 and -85, respectively, consistent with two equivalent $SiW_9O_{34}^{10-}$ units in the molecules.[280] $(Et_2NH_2)_8[\alpha\text{-}PW_{11}O_{39}M(\mu\text{-}OH)(H_2O)]_2$ (M = Zr, Hf), containing dinuclear Zr and Hf fragments sandwiched between 2 mono-lacunary α-Keggin polyoxometalates, were prepared and characterized by ^{183}W and ^{31}P NMR.[281] The ^{183}W spectra showed six resonances for each compound in the range of δ -107.6 to -155.5 in aqueous solution.[281] Equilibrium of the proton cryptate polyoxometalate, $\alpha\text{-}H_2W_{12}O_{40}^{6-} + H^+ \rightleftharpoons H_3W_{12}O_{40}^{5-}$ (as $Bu^n{}_4N^+$ salt) in CD_3CN was characterized by ^1H and ^{183}W NMR and other techniques.[282] The studies show that, in nonaqueous media, the internal cryptand cavity of $\alpha\text{-}H_2W_{12}O_{40}^{6-}$ (^1H δ 6.01; ^{183}W δ -99) reversibly accommodated only one H^+ ion to yield $H_3W_{12}O_{40}^{5-}$ (^1H δ 6.81; ^{183}W δ -88). Speciation and equilibria during base decomposition of $\alpha\text{-}PW_{12}O_{40}^{3-}$ (^{183}W δ -96.7) were probed using ^{31}P and ^{183}W NMR at pH 0.7-13.5.[283] ^{183}W resonances of chiral polyoxotungstats $\alpha\text{-}P_2W_{17}O_{61}^{10-}$ (17 peaks each in the range of δ -108.5 to -226.1) was assigned to the W atoms in the clusters using selective ^{31}P-^{183}W decoupling and ^{183}W-^{183}W COSY NMR.[284]

^{183}W NMR was used, along with other spectroscopies and DFT calculations, to study reactions of Na_2WO_4 with 8-hydroxyquinoline-5-sulfonic acid [H(8-HQS) (**20**)] in water, forming

one dimeric $[W_2O_4(8\text{-HQS})_2(\mu\text{-O})]^{2-}$ (δ -74.5) and two monomeric $WO_2(8\text{-HQS})_2^{2-}$ (δ 20.7 and 63.3) complexes.[256] Reactions of Na_2WO_4 with 3-phospho-D-glyceric acid, giving five products,[257] which were identified by multinuclear NMR and DFT studies.[257] ^{183}W shifts were in the ranges of δ 48.0 and -241.8. ^{17}O shifts were in the ranges of δ 647-526 for terminal oxo ligands and δ 342 for bridging oxo ligands.[257] The ^{17}O shifts of the tungsten 3-phospho-D-glycerate complexes (δ 554, 526 for terminal W=^{17}O; 342 for bridging W-^{17}O-W)[257] were more shielded than the Mo analogs (δ 867, 842, 833 for terminal Mo=^{17}O; 381 for bridging Mo-^{17}O-Mo),[257] which followed a trend for multiple-bonded ligands.[285] Reaction of peroxotungstates, prepared from H_2WO_4 and H_2O_2, with H_2SeO_4 gave Se-containing dinuclear complex, $(Bu^n{}_4N)_2[(\mu\text{-}SeO_4)W_2O_2(O_2)_4]$, which was characterized by ^{77}Se (δ 1046) and ^{183}W (δ -569.2) NMR and other techniques.[286] This complex was a catalyst for the epoxidation of homoallylic and allylic alcohols with H_2O_2. $(Bu^n{}_4N)_2WO_4$ catalyzed fixation of CO_2 with *o*-phenylenediamine into 2-benzimidazolone.[287] Reaction of $(Bu^n{}_4N)_2WO_4$ with *o*-phenylenediamine gave an adduct through hydrogen bonds between the N-H groups and the oxo ligands, shifting ^{183}W resonance in WO_4^{2-} to δ 16.4 which is more shielded by 14.7 ppm.[287] Reaction of $(Bu^n{}_4N)_2WO_4$ with CO_2 gave $(Bu^n{}_4N)_2[WO_4(CO_2)]$ (^{183}W δ 57.8) and $(Bu^n{}_4N)_2[WO_4(CO_2)_2]$ (^{183}W δ 22.6), in which the oxo ligands were believed to bind to the C atom in CO_2.[287]

^{183}W NMR was also used to characterize organometallic complexes. ^{183}W-^{31}P HMQC spectra were used to obtain indirectly ^{183}W shifts of *cis* and *trans* isomers of diphosphines $W(CO)_4(PPh_3)(PR_3)$ [R_3 = $Bu^n{}_3$, Me_3, Me_2Ph, $MePh_2$, Ph_3, $(4\text{-OMe-}C_6H_4)_3$, $(4\text{-Me-}C_6H_4)_3$, $(4\text{-F-}C_6H_4)_3$] and phosphine phosphites $W(CO)_4(PPh_3)[P(OR)_3]$ [R_3 = $(OMe)_3$, $(OEt)_3$, $(OPh)_3$].[288] ^{183}W shifts of *trans*-$W(CO)_4(PPh_3)(PCy_3)$ (δ 797) and *trans*-$W(CO)_4(PPh_3)[P(NMe_2)_3]$ (δ 824) were similarly measured. The ^{183}W shift range of the complexes was δ 964 for *cis*-$W(CO)_4(PPh_3)[P(4\text{-F-}C_6H_4)_3]$ to 722 for *trans*-$W(CO)_4(PPh_3)[P(OMe)_3]$ with, e.g., δ 842 and 849 for *trans*-$W(CO)_4(PPh_3)(PMe_3)$ and *cis*-$W(CO)_4(PPh_3)(PMe_3)$, respectively.[288] How the shifts were correlated with Tolman electronic factors and cone angles of the PR_3 and $P(OR)_3$ ligands was

discussed.[288] Spectroscopic, structural and computational studies of the starting complex (**30**) in **Figure 2** indicated that it was a heterocyclic ylide complex (δ_W -3303).[289] The product of the reaction (**31**) (δ_W -3221) may be formally considered to be a phosphanylcarbene complex.

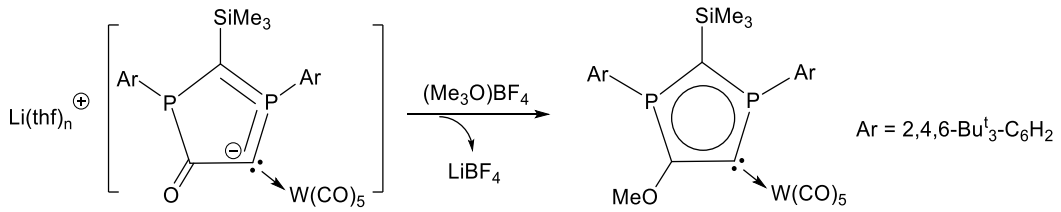

(**30**) (**31**)

Figure 2. Reaction of **30** with $(Me_3O)BF_4$ to give **31.**

Calculations of ^{183}W shifts were reported in several publications, including the use of DFT methods for polyoxometalates[290] and to optimize structures of the four isomers of $SiW_{11}O_{39}^{8-}$, calculating their ^{183}W NMR spectra, which were compared with experimental shifts.[291] Relativistic DFT methods were used calculate ^{183}W shifts of polyoxometalates,[292] polyoxotungstates,[293] counterion effects on the ^{183}W NMR spectra of the lacunary Keggin polyoxotungstate $PW_{11}O_{39}^{7-}$,[294] and ^{183}W and ^{17}O NMR shifts for large polyoxotungstates such as $W_6O_{19}^{2-}$.[295] Extended Hückel MO calculations were employed to analyze ^{183}W and ^{17}O NMR shifts in polyoxometalates.[296]

In NMR studies of α atoms of ligands, the ^{17}O shifts of the peroxide ligand in diperoxyo W complexes were found at δ 346-400.[135-136] Several peroxotungstate species, such as $[WO(OH)(O_2)_2]^-$ and $W_4O_{12}(O_2)_2]^{4-}$, prepared from the reaction of $Na_2(WO_4)$ with H_2O_2, were identified by ^{17}O NMR using the ratio of the shift of the O atom in the W anion to the shift of the O atom in the known Mo anion.[297] This ratio was consistently around 79%. Many of these signals in the NMR were pH dependent.[297]

$(Bu^tO)_3W{\equiv}^{15}N$ was synthesized via the reaction of $MeC{\equiv}^{15}N$ with $(Bu^tO)_3W{\equiv}N$, which

was monitored via ^{15}N NMR. The ^{15}N signal for the $(Bu^tO)_3W{\equiv}^{15}N$ was at δ 791.8.[275] Several metathesis reactions of organic and inorganic complexes containing the nitride ≡N group were carried out with $(Bu^tO)_3W{\equiv}^{15}N$ in order to study the degree of ^{15}N scrambling.[275-276]

Several techniques such as ^{15}N, ^{13}C INEPT, and ^{19}F NMR were used to analyze $WOF_4(aph)^-$ (aph = acetone phenylhydrazonate, $Me_2C{=}N{-}(Ph)N^-$).[298] It was found that the aph acted as an N,N donor ligand, and stereoisomeric interconversion occurred in $WOF_4(aph)^-$ at elevated temperatures with activation parameters of $\Delta H^{\neq}$ = 78.5 kJ/mol, $\Delta S^{\neq}$ = 56.78 J/mol·K, $\Delta G^{\neq}_{313}$ = 60.71 kJ/mol.[298] ^{119}Sn NMR was used to monitor the conversion of $(\mu\text{-}Cl)_3W_2(SnCl_3)(CO)$ to $(\mu\text{-}Cl)_3[W(SnCl_3)(CO)_3]_2^-$ over time in $CDCl_3$ or CD_2Cl_2 solution.[299]

6. Group 7 (Mn, Tc and Re)

For the three elements, NMR of both the metals (^{55}Mn, ^{99}Tc, ^{187}Re) and ligands have been reported. Nuclear and NMR properties of the nuclides, including recommended and commonly used references, are given in Table 8. The receptivities (relative to ^{13}C) of the nuclides are fairly large, and their resonance frequencies (with ^1H = 100 MHz) are relatively high. However, all are quadrupole nuclides with modest to large quadrupole moments. Thus, line widths sometimes lead to sensitivity losses.

Table 8.[26] Nuclear and NMR properties of ^{55}Mn, ^{99}Tc and ^{187}Re

Nuclide	Natural abun-dance (%)[a]	Spin	Relative receptivity		Gyromagnetic ratio (10^7) (rad s^{-1} T^{-1})	Quadrupole moment Q (fm^2)	Ξ (and frequency, MHz; ^1H = 100 MHz, 2.3488 T)	Reference sample
			D^H (^1H = 1.00)	D^C (^{13}C = 1.00)				
^{55}Mn	100	5/2	0.179	1.05×10^3	6.6452546	33.0	24.789218	$KMnO_4$ (aq)
^{99}Tc	- (β	9/2	-	2134[1]	6.046	-12.9	22.508326	NH_4TcO_4

	decay)							(aq)
(^{185}Re)[b,c]	37.40	5/2	5.19 × 10^{-2}	305	6.1057	218.0	22.524600	$KReO_4$ (aq)
^{187}Re[b]	62.60	5/2	8.95 × 10^{-2}	526	6.1682	207.0	22.751600	

[a] Unless noted, the isotopes are stable. The natural abundances are based on the NIST data.[25]

[b] We did not find a publication in 1990-2019 on the ^{185}Re or ^{187}Re NMR of a metal complex.

[c] ^{185}Re in parenthesis is considered to be the less favorable of the element for NMR.[26]

6.1. *Manganese complexes*

Publications using ^{55}Mn NMR that we found were mostly on manganese carbonyl derivatives,[265-267,300-313] many of which were published in the 1990s and early 2000s.[267,300-313] Selected complexes are discussed here, and their ^{55}Mn shifts may be compared with δ -2353 in $Mn_2(CO)_{10}$.[1,303] *C*-Glycosyl compounds function as nucleoside surrogates and they served as biochemical probes.[311] $RMn(CO)_5$ (e.g., R = glycosyl) were studied as starting materials to make carbonyl derivatives through migratory insertion. ^{55}Mn NMR shifts of methylether derivatives of, e.g., β-glucosyl-$Mn(CO)_5$ (**32**, δ -2059) were found to be in a narrow range (±10 ppm), typical for alkyl-$Mn(CO)_5$ complexes.[311]

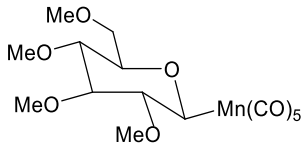

(**32**)

$(4\text{-}X\text{-}C_6H_4)_3Sn\text{-}Mn(CO)_5$ (X = H, Me, OMe, SMe, F, Cl) were characterized by ^{55}Mn, ^{119}Sn and ^{13}C NMR, giving, e.g., ^{55}Mn δ -2502 and ^{119}Sn δ -11.93 for $Ph_3Sn\text{-}Mn(CO)_5$ (X = H).[313] The ^{55}Mn and ^{119}Sn shift ranges are δ -2479 to -2526 and δ 1.13 to -11.93, respectively, for the complexes.[313] $[(OC)_5Mn]_3(\mu_3\text{-}E)$ (E = As, Sb, Bi), containing one E atom bonded to three $Mn(CO)_5$ groups in trigonal pyramid structures, were characterized by ^{55}Mn NMR.[302] The shifts

(δ) of the three pnictogen compounds, E = As (-2020), Sb (-2230), Bi (-2320), show an increase of shielding on the Mn atom in the order E = As, Sb, Bi.[302] Stibine complexes $Mn_2(CO)_9(SbPh_3)$ and $(Ph_3Sb)(OC)_4Mn\text{-}Mn(CO)_4(SbPh_3)$ [with the $SbPh_3$ ligand(s) in the axial position(s)] show two ^{55}Mn resonances for the former (δ -2389 and -2394) and one resonance (δ -2070) for the latter.[304] Distibine complexes $Mn_2(CO)_8(\mu\text{-}R_2SbCH_2SbR_2)$ (R = Me, Ph) give ^{55}Mn shifts at δ -2317 and -2195, respectively.[303] ^{55}Mn resonance for $Mn(CO)_3[MeN(CH_2\text{-}o\text{-}SbMe_2\text{-}C_6H_4)_2](OTf)$ containing a chelating bis-stibine ligand is δ -850.[265] Multinuclear NMR, including ^{55}Mn, was used to study a series of Mn(I) phosphine, arsine, and stibine carbonyl halide complexes, such as *fac*-$MnX(CO)_3(Ph_2PCH_2CH_2CH_2PPh_2)$ (δ X = Cl^-, -916; Br^-, -1005), showing that the less electronegative Br^- ligand led to more shielding on the Mn(I) ion.[309] ^{55}Mn shifts of the stibine analogs, such as $MnX(CO)_3(Ph_2SbCH_2CH_2CH_2SbPh_2)$ (δ X = Cl^-, -880; Br^-, -1006) and As compounds, such as $MnX(CO)_3(Ph_2AsCH_2CH_2AsPh_2)$ (δ X = Cl^-, -932; Br^-, -1046), were also reported.[309]

^{55}Mn and ^{77}Se NMR were used to characterize $Mn(CO)_3Cl[o\text{-}(CH_2SeMe)_2\text{-}C_6H_4]$ with a chelating bis-selenoether ligand, giving ^{55}Mn and ^{77}Se resonances (Table 9) for different invertomers of the complex.[266] Invertomers are isomers interconverted by inversion of an atom with a lone pair of electrons. NMR studies of the di-tellurophene complex *fac*-$MnCl(CO)_3L_2$ [L = 1,3-dihydro-benzo[c]tellurophene (**28**)] showed ^{55}Mn and ^{125}Te resonances (Table 9).[267] The NMR shifts of telluroether complexes *fac*-$MnCl(CO)_3(TeMe_2)_2$ and its *mer,trans* isomer were studied (Table 9),[307] and compared with thioether and selenoether analogs $MnCl(CO)_3(EMe_2)_2$ (E = S, Se, Table 9),[307] showing increasing shielding of the Mn(I) ion in the order S, Se and Te. This order is consistent with the electronegativity decrease from S, Se to Te, thus placing most electron density on the Mn(I) ion in the Te compound.

Table 9. NMR chemical shifts of selected Mn carbonyl complexes with thio-, seleno- or telluroether ligands

Complexes	^{55}Mn shifts (δ)	^{77}Se shifts (δ)	^{125}Te shifts (δ)
$MnCl(CO)_3(SMe_2)_2$[307]	-57	-	-
$MnCl(CO)_3(SeMe_2)_2$[307]	-205	66	-
fac-$MnCl(CO)_3(TeMe_2)_2$[307]	-637	-	161
mer,trans-$MnCl(CO)_3(TeMe_2)_2$[307]	-920	-	271
$Mn(CO)_3Cl[o\text{-}(CH_2SeMe)_2\text{-}C_6H_4]$[266] (different invertomers)	-42, -77, -113	147.8, 124.1, 122.5, 120.5	-
fac-$MnCl(CO)_3L_2$ [L = (**28**)][267]	-600	-	472

For Mn organometallic complexes without CO ligand, ^{55}Mn NMR of $CpMn(\eta^6\text{-}C_6H_6)$ and derivatives with substituents on either the Cp^- or benzene ligand as well as on both ligands was studied, showing, e.g., δ -180 for $CpMn(\eta^6\text{-}C_6H_6)$.[314]

Calculations and electronic analyses of NMR chemical shifts for $Mn(CO)_5X$ (X = F^-, Cl^-, Br^-, I^-, and Me^-) showed that the origin of the chemical shifts was the paramagnetic effects from d-d transitions on the Mn ions.[315]

In NMR studies of α atoms of ligands, reaction dynamics of water exchange on Mn(II) polyoxometalate $[Mn_4(H_2O)_2(P_2W_{15}O_{56})_2]^{16-}$ has been determined as a function of pH using VT ^{17}O NMR.[316] The NMR signals were compared with monomeric $[Mn(H_2O)_6]^{2+}$. While the water exchange rate of $[Mn(H_2O)_6]^{2+}$ was affected by pH in the 3.2-6.0 range, the rate of exchange of the polyoxometalate ion varied greatly.[316] Water exchange dynamics in Mn porphyrin[317] and salen[318] complexes was also studied via ^{17}O NMR.

^{15}N-enriched guanine (G) was incorporated into self-complementary oligodeoxynucleotides containing the GG doublet and GGG triplet in order to study the reactivity differences in the G runs.[319] The line broadening in the ^{15}N NMR showed that site-selective binding of Mn(II) and Co(II) ions to G runs was correlated with with HOMO distribution obtained

by MO calculations.[319] In other words, the binding of electron-deficient metal ions to the N atom of electron-rich G is likely a HOMO-controlled process.[319]

Several silane complexes and σ-borane Mn complexes, which were studied by ^{29}Si and ^{11}B NMR, respectively, were discussed in a 2008 review.[139]

6.2. *Technetium complexes*

Technetium is the only transition metal in the 3d, 4d and 5d series (and the lightest element in the periodic table) whose isotopes are all radioactive. ^{99}Tc (used in NMR) decays to stable ^{99}Ru as a weak beta emitter with a half-life of 2.111 x 10^5 years.[320] It is the most significant long-lived fission product of U fission.

Tc chemistry was inspired to a large degree by applications of the short-lived metastable nuclear isomer ^{99m}Tc in molecular imaging and radiopharmacy.[320] ^{99m}Tc decays by isomeric transition to ^{99}Tc with a half-life of only 6 h, making it difficult to characterize ^{99m}Tc complexes directly. Thus, the long-lived ^{99}Tc analogues are often used. Binding of TcO_4^- to uranyl ion was also studied, as TcO_4^- was co-extracted with UO_2^{2+}, Pu^{IV} and Zr^{IV} from irradiated nuclear fuel dissolved in HNO_3.[321-322]

Solution ^{99}Tc NMR of inorganic compounds reported up to 2004 was reviewed.[323] A figure showing the correlation between ^{99}Tc chemical shifts and Tc oxidation states in reported complexes was given in a 2017 paper.[324] We focus on the publications since 2004 in the current review.

Speciation of Tc(VII) pertechnetate in concentrated $HClO_4$ and HNO_3 was studied by several techniques, including ^{99}Tc NMR, showing that pertechnetic acid, $HTcO_4$, formed in >8 M $HClO_4$ while in concentrated HNO_3, TcO_4^- was still the predominant species.[325] In 12 M H_2SO_4, experiments and DFT calculations showed the formation of yellow $TcO_3(OH)(H_2O)_2$ (δ 300).[326] When $HTcO_4$ solution concentrated, likely products with different colors, such as H_5TcO_6, $HTcO_4 \cdot H_2O$, and Tc_2O_5, were probed by ^{99}Tc NMR among others.[327] Reaction of $HTcO_4$ with

MeOH and 12 M H_2SO_4 studied by spectroscopies (e.g., ^{99}Tc NMR) and *ab initio* calculations showed the formation of reduced Tc(V) oxo sulfate species that lack ^{99}Tc NMR signals in the δ 0-800 region.[328]

The ^{99}Tc NMR spectrum of the aqueous pertechnetate ion with natural abundance of ^{17}O (0.038%, spin 5/2) and ^{18}O (0.205%, spin 0) isotopes[25] was sensitive to the O isotopes and temperature of the solution.[329] Since ^{17}O and ^{18}O atoms have one and two more neutrons, respectively, than an ^{16}O atom (99.757% natural abundance, spin 0), the ^{99}Tc ion in $Tc(^{16}O)_3(^{17}O)^-$ and $Tc(^{16}O)_3(^{18}O)^-$ was more shielded than that in $Tc(^{16}O)_4^-$. This is a result of the isotope effects in nuclear shielding.[330] Since the Ta=^{17}O and Ta=^{18}O bonds with the heavier O isotopes are the shorter than the Ta=^{16}O bond, the shorter bonds in the heavier isotopomers lead to larger shielding of the ^{99}Tc nuclei and thus isotope shifts of the ^{99}Tc resonance to become more shielded. The shift of the $Tc(^{16}O)_3(^{18}O)^-$ resonance [$\delta_{Tc(^{16}O)_3(^{18}O)^-} - \delta_{Tc(^{16}O)_4^-}$ = -0.428 ppm] is well resolved from the peak of $Tc(^{16}O)_4^-$ at 10 °C.[329] Coupling by the ^{17}O atom in $Tc(^{16}O)_3(^{17}O)^-$ gave a sextet with the ^{99}Tc resonance (extracted by averaging the six lines) showing an isotope shift of $Tc(^{16}O)_3(^{17}O)^-$ [$\delta_{Tc(^{16}O)_3(^{17}O)^-} - \delta_{Tc(^{16}O)_4^-}$ = -0.241 ppm] at 10 °C.[329] Isotopomers with more ^{18}O atoms, such as $Tc(^{16}O)_2(^{18}O)_2^-$, $Tc(^{16}O)(^{18}O)_3^-$ and $Tc(^{18}O)_4^-$, showed additional isotope shifts to be more shielded.[331]

TcO_4^- ions coordinated directly to actinides in the presence of $O{=}PR_3$ ligands, yielding $[O_3Tc(\mu\text{-}O)]_2UO_2(O{=}PPh_3)_3$ and $[O_3Tc(\mu\text{-}O)]_4Th(O{=}PBu^n{}_3)_4$, both giving broad ^{99}Tc resonances.[322] When chelating bis(diphenylphosphino)methane dioxide ligand $[Ph_2(O{=})PCH_2P({=}O)Ph_2]$ was used, a similar reaction yielded $[O_3Tc(\mu\text{-}O)UO_2[Ph_2(O{=})PCH_2P({=}O)Ph_2]_2](TcO_4)$ with two ^{99}Tc resonances (δ 2.0 and 16.9 for coordinated and uncoordinated TcO_4^-, respectively.[321]

^{99}Tc shifts of Ph_3EOTcO_3 (E = C, δ 67.3; Si, δ 68.3; Ge, δ 25.2; Pb, δ 7.0) and $(THF)Ph_3SnOTcO_3$ (δ -5.1) and related Tc(VII) complexes were reported.[332] ^{99}Tc NMR was used

to characterize Ta(VII) complexes with the TcO_3^+ core and multi-dentate ligands such as TcO_3(bpza) [δ 220; Hbpza = di-1H-pyrazol-1-ylacetic acid (**33**)] with the N,O,N ligand.[333]

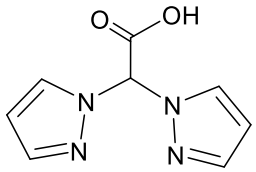

(**33**)

Organometallic Tc complexes characterized by ^{99}Tc NMR are mainly Tc(I) carbonyl compounds, especially those with *fac*-$Tc(CO)_3^+$ fragment for its high stability.[334] Kinetics of water exchange processes in *fac*-$Tc(CO)_3(H_2O)_3^+$ was investigated by ^{17}O (δ -52) and ^{99}Tc (δ -868, $^1J_{Tc\text{-}O}$ = 80 Hz) NMR.[334] Conversion of *fac*-$Tc(CO)_3(H_2O)_3^+$ in 10 M NaOH and 5 M NaOH caustic solution was studied by ^{99}Tc NMR, showing that *fac*-$Tc(CO)_3(H_2O)_3^+$ (δ -869) was deprotonated stepwise to form *fac*-$Tc(CO)_3(H_2O)_2(OH)$ (δ -1069), *fac*-$Tc(CO)_3(H_2O)(OH)_2^-$ (δ -1146), and *fac*-$Tc(CO)_3(OH)_3^{2-}$ (δ -1204) based on DFT calculations, as the Tc(I) ions were increasingly shielded with deprotonation.[335] Theoretical modeling of ^{99}Tc NMR shifts was developed based on DFT calculations and the calculated shifts were compared with the experimental values of *fac*-$Tc(CO)_3(H_2O)_3^+$ and *fac*-$Tc(CO)_3(H_2O)_{3\text{-}n}(OH)_n^{(n\text{-}1)\text{-}}$.[335] When *fac*-$Tc(CO)_3(H_2O)_3^+$ was exposed to ^{13}CO (49 atm) in water in a sapphire NMR tube (^{99}Tc δ -866.7), stepwise replacement of CO ligands to form *fac*-$Tc(^{13}CO)_3(H_2O)_3^+$ at 4 °C in several days was probed by ^{99}Tc NMR.[336-337] The ^{99}Tc NMR spectrum of *fac*-$Tc(^{13}CO)_3(H_2O)_3^+$ (**Figure 3**)[337] showed an isotope shift as well as the coupling by three ^{13}CO ligands, giving a 1:3:3:1 quartet at δ -869.7 ($^1J_{Tc\text{-}C}$ = 354 Hz).[336] In three weeks at room temperature, substitution of water ligands by ^{13}CO, yielding *fac*-$Tc(^{13}CO)_6^+$ (δ -1961 as a septet, $^1J_{Tc\text{-}C}$ = 261 Hz), was used to follow the reaction.[336-337] Since ^{99m}Tc was a precursor to radiopharmaceutical agents,[334] the kinetic properties, which were important to the preparation, uptake and clearance of the ^{99m}Tc agents, were reviewed in

2008.[337] Properties of *fac*-$Tc(CO)_3(OH_2)_{3-n}(OH)_n^{1-n}$ (n = 0-3) in aqueous solutions with high ionic strength, including ^{99}Tc NMR, were studied to help identify and treat Tc speciation in nuclear waste.[338]

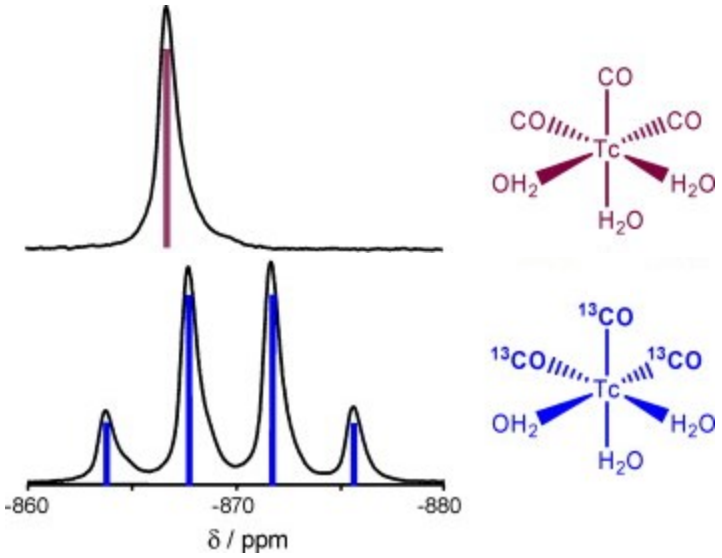

Figure 3. ^{99}Tc NMR spectra of *fac*-$Tc(CO)_3(H_2O)_3^+$ and *fac*-$Tc(^{13}CO)_3(H_2O)_3^+$ under ^{13}CO (49 atm), demonstrating ^{13}C-isotope shifts and the $^1J_{Tc\text{-}C}$ coupling.[337]

$Tc(CO)_5X$ (X = Cl^-, Br^-, I^-) gave ^{99}Tc resonances at δ -1745, -1802 and -2034, respectively, showing the most shielded Tc(I) ion in $Tc(CO)_5I$ with the least electronegative iodine in the halide series.[339] The perchlorate analog $Tc(CO)_5(ClO_4)$ containing a Tc-O bond showed the ^{99}Tc resonance at δ -1353.[340]

Nitrosyl complex $(NEt_4)_2[Tc(CO)_2(NO)Cl_3]$ (δ -460) and a dimer $[TcCl(\mu\text{-}Cl)(CO)_2(NO)]_2$ (δ -389) were prepared and characterized by ^{99}Tc NMR among others.[341] ^{99}Tc resonances of several cyclopentadienyl nitrosyl complexes $CpTc(NO)(PPh_3)X$ (X = OTf^-, δ 242; $O_2CCF_3^-$, δ 19; SCN^-, -820; I^-, -668; I_3^-, -679) were measured.[342] ^{99}Tc shifts of other Tc(I) complexes, such as $Cs[Tc(NO)(PPh_3)_2(OOCCF_3)_2F]$ (δ 952) and $[Tc(NO)(dppe)_2(OOCCF_3)](PF_6)$ (δ -627; dppe = $Ph_2PCH_2CH_2PPh_2$), as well as those at Tc(III), Ta(V) and Tc(VII) oxidation states were

summarized in a figure in Reference [324].

^{99}Tc shifts of several Tc(VII), Tc(I) and Tc(0) species were computed by DFT methods.[343] Complexation to aqueous uranyl, UO_2^{2+}, was predicted to only slightly affect the ^{99}Tc shift of TcO_4^-.[343] DFT calculations were also performed to obtain ^{99}Tc NMR parameters for $Tc(CO)_3$(N,N,O) (**34**) containing a tridentate N,N,O ligand, as its ^{99m}Tc isomer is a potential breast cancer radiopharmaceutical.[344]

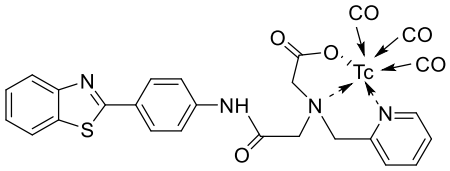

(**34**)

For the NMR studies of α atoms of ligands, see the previous discussion in this section on the use of ^{17}O and ^{13}C NMR of Tc complexes.

6.3. *Rhenium complexes*

We did not find a publication in 1990-2019 on either ^{185}Re or ^{187}Re NMR of metal complexes, as indicated in Table 8. Very few solution ^{185}Re or ^{187}Re NMR spectra have been reported. Thus, the following reports before 1990 are briefly discussed.

Solution NMR spectrum of $NaReO_4$, showing both ^{185}Re and ^{187}Re resonances, was reported in 1970,[345] 1986,[346] and 1987.[347] In 1981, ^{185,187}Re resonance of the Re(I) complex $[Re(CO)_6]Cl{\cdot}HCl$ in THF at 295 K was found to be δ -3400 relative to aqueous $NaReO_4$.[348] ^{185,187}Re resonances of $(Ph_4P)(ReO_4)$ in $HCONMe_2$/toluene (δ ~0) and $(Et_4N)(ReS_4)$ in $MeCN/CH_2Cl_2/Me_2S{=}O$ at 305 K [δ(^{185}Re/^{187}Re) 3200/3435] were reported in 1986.[346]

In NMR studies of α atoms of ligands, the diperoxo complex $ReO(O_2)_2Me(H_2O)$ was synthesized and characterized by ^{17}O NMR and X-ray crystallography.[135,349] The ^{17}O shifts of the

peroxide ligands were found to be at δ 363 and 422.[135] Several silane complexes and σ-borane Mn complexes, which were studied by ^{29}Si and ^{11}B NMR, were discussed in a 2008 review.[139] The σ-borane Mn complexes were compared with a σ-borane Re analogue.[139]

In the studies of Re(η^5-$C_5H_4Pr^i$)(CO)(PF_3)Xe by several NMR spectroscopies including ^{19}F-^{129}Xe HMQC and ^{19}F-^{31}P HMQC,[350] the Xe chemical shift was determined to be about δ -6179 with $^2J_{Xe\text{-}P}$ = 41.8 Hz, and $^3J_{Xe\text{-}F}$ = 5.1 at 163 K.[350] ^{15}N NMR was conducted after the addition of Lewis acids and H-bond donor molecules, such as $BAr^F{}_4$ or C_6H_5OH, to ^{15}N-labeled *trans*-Re(N_2)Br(depe)$_2$ [depe = 1,2-bis-(diethylphosphino)ethane].[351] The additions of these acids and donors caused ashift in the ^{15}N NMR resonances to be more shielded. For example, upon addition of $BAr^F{}_4$, one of the peaks shifted from δ -61.3 to -173.3 and the other from δ -91.1 to -93.8.[351]

Organorhenium (VII) oxides complexes with general formulas ReO_3R or $ReO_3R{\bullet}L_n$ (e.g., R = Me, $SiMe_3$, Cp; L = quinuclidine, pyridine; n = 1, 2) were studied by ^{17}O NMR,[352] showing that shifts of the oxo ligands were affected by the donor ability of the R ligands.[352] The ^{17}O shifts of the oxo ligands were also affected by the solvent, especially if the R ligand was not a strong donor or did not cause steric hinderance in the complex.[352] ^{17}O NMR was used to follow the reactions of $EtReO_3$ and (2,6-Me_2-C_6H_3)ReO_3 as epoxidation catalysts in the presence of Bu^tOOH.[353-354] ^{17}O-enriched $MeReO_3$ was used to transfer the labeled ^{17}O to water and subsequently transfer the ^{17}O to the water-sensitive $EtReO_3$ or (2,6-Me_2-C_6H_3)ReO_3.[353-354] ^{17}O NMR showed that the oxygen insertion into the Re-C bond, giving the respective alkoxide trioxorhenium compounds, led to decomposition of the catalyst.[353-354] Other catalytic systems such as aldehyde-olefination using the catalyst $MeReO_2$(PhC≡CPh) and PPh_3 were also investigated using ^{17}O NMR.[355] Water exchange on *fac*-$(CO)_3Re(H_2O)_3^+$ using ^{17}O-enriched water was followed by ^{17}O NMR.[356]

With mono- and bidentate ligands of various nucleophilicities [e.g., CH_3CN, Br^-, Me_2S, CF_3COOH, thiourea, bipy, and phenanthrene (phen)] were followed by ^{17}O NMR as well.[356] The

pK_a values for the successive dissociation of $ReO(H_2O)(CN)_4^+$ were determined to be 1.31 and 3.72 via ^{17}O and ^{13}C NMR.[357] Line broadening of the ^{17}O signals occurred at lower pH values. Other complexes such as $Re_2O_3(CN)_8^{4-}$ and $ReO(NCS)(CN)_4^{2-}$ were also analyzed via ^{17}O NMR.[357]

7. Group 8 (Fe, Ru and Os)

For the three elements, NMR of both the metals and ligands have been reported. Nuclear and NMR properties of the nuclides, including recommended and commonly used references, are given in Table 10. ^{57}Fe, ^{99}Ru and ^{187}Os NMR spectroscopies are, however, challenging mainly from the unfavorable magnetic properties of the nuclides.[1] The spin 1/2 nuclides ^{57}Fe and ^{187}Os have low sensitivity to detection and their receptivities are lower than that of ^{13}C nuclide by about three orders of magnitude.[69] For quadrupolar ^{99}Ru, ^{101}Ru and ^{189}Os, they are much more sensitive than ^{57}Fe and ^{187}Os, but quadrupolar broadening may be substantial, making their detection challenging. The chapter on the NMR of these three metals by Benn in the 1991 book edited by Pregosin gave a detailed review of the literature up to 1990.[1]

Inverse detection methods were developed to increase the sensitivity of the nuclides to indirectly determine chemical shifts by 2-D correlation experiments using coupling (J) to another magnetically active nuclide such as ^1H or ^{31}P. These methods for spin 1/2 nuclides ^{57}Fe[358-360] and ^{187}Os[361-362] using HMQC (Heteronuclear Multiple Quantum Coherence),[4] HSQC (Heteronuclear Single Quantum Coherence)[4] or HMBC (Heteronuclear Multiple Bond Correlation)[4] spectroscopy make the detection and acquisition of their chemical shifts much easier. Both HMQC and HSQC were based on 1-bond coupling such as $^1J_{P\text{-}Fe}$, while HMBC is based on 2-4 bond coupling such as $^{2\text{-}4}J_{P\text{-}Fe}$. The difference between the HMQC and HSQC methods is that during the HMQC evolution, both ^{31}P and ^{57}Fe magnetization evolve. In the HSQC evolution, only ^{57}Fe magnetization is allowed to evolve. Thus, HMQC is affected by the

$^{1}J_{P\text{-}Fe}$ coupling during the evolution, while HSQC is not affected, as there is no ^{31}P magnetization during the evolution.

An alternative to obtain ^{57}Fe NMR for compounds with natural abundance is based on polarization transfer (PT) techniques such as ^{1}H-^{57}Fe INEPT, enhancing the signal/noise ratio with respect to single pulse detection.[363-364]

Table 10.[26] Nuclear and NMR properties of ^{57}Fe, ^{99}Ru and ^{187}Os

Nuclide	Natural abun-dance (%)[a]	Spin	Relative Receptivity		Gyromagnetic ratio (10^7) (rad s^{-1} T^{-1})	Quadrupole moment *Q* (fm^2)	*Ξ* (and frequency, MHz; ^{1}H = 100 MHz, 2.3488 T)	Reference sample
			D^H (^{1}H = 1.00)	D^C (^{13}C = 1.00)				
^{57}Fe	2.119	1/2	7.24 x 10^{-7}	4.25 x 10^{-3}	0.8680624	-	3.237778	$Fe(CO)_5$ (C_6D_6) or Cp_2Fe (δ 1540 in toluene[365])
^{99}Ru	12.76	5/2	1.44 x 10^{-4}	0.848	-1.229	7.9	4.605151	$K_4Ru(CN)_6$ (aq)
^{101}Ru[b]	17.06	5/2	2.71 x 10^{-4}	1.59	-1.377	45.7	5.161369	
^{187}Os	1.96	1/2	2.43 x 10^{-7}	1.43 x 10^{-3}	0.6192895	-	2.282331	OsO_4 (CCl_4)
^{189}Os[c]	16.15	3/2	3.95 x 10^{-4}	2.32	2.10713	85.6	7.765400	

[a] Unless noted, the isotopes are stable. The natural abundances are based on the NIST data.[25]

[b] We did not find a publication in 1990-2019 on ^{101}Ru NMR. It is not used due to the larger quadrupole moment of ^{101}Ru nuclide than ^{99}Ru nuclide. ^{101}Ru properties are listed here for comparison.

[c] We did not find a publication in 1990-2019 on ^{189}Os NMR. It is not used as ^{189}Os is a quadrupolar nuclide and ^{187}Os is not.

7.1. *Iron complexes*

The reported ^{57}Fe NMR shift range is about 12,000 ppm,[358] including complexes with unpaired electrons. The shift is very sensitive to both steric and electronic factors. Thus, it

provides an excellent probe of changes within the coordination sphere of the metal atom.

^{57}Fe shifts of $Fe(CN)_6^{4-}$ (K^+ salt, δ 2455) and $[C(NH_2)_3]_2[Fe(CN)_5(NO)]$ [$C(NH_2)_3^+$ = guanidinium$^+$, δ 2004] in D_2O, two prominent textbook examples in coordination chemistry, were obtained using 25% ^{57}Fe-enriched samples.[366] ^{14}N shifts of δ -5.1 (NO^+), -100 (broad for unresolved *cis* and *trans* CN^- ligands), and -310 for the $C(NH_2)_3^+$ cation in $[C(NH_2)_3]_2[Fe(CN)_5(NO)]$ vs. -105 for $Fe(CN)_6^{4-}$.[366] The fact that the Fe(II) ion in $Fe(CN)_5(NO)^{2-}$ was more shielded than that in $Fe(CN)_6^{4-}$ was the subject of theoretical studies discussed below.

^{57}Fe NMR of iron porphyrin complexes was one major focus of research. ^{57}Fe shifts of several diamagnetic Fe(II) porphyrin carbonyl complexes, including Fe(protoporphyrinate IX)(py-d_5)(CO) (**35**, δ 8205), were reported.[367] Using an inverse detection method based on the ^{31}P-^{57}Fe correlation and 94.5% ^{57}Fe-enriched samples, ^{57}Fe NMR shifts of over 25 diamagnetic Fe(II) porphyrin complexes with PMe_3 ligands were obtained in 5 mm NMR tubes in as little as 20 min.[358] The complexes include $Fe(TPP)(PMe_3)_2$ (**36**, H_2TPP = tetraphenylporphyrin, δ 7652), $Fe(TPP)(PMe_3)(CO)$ (δ 7627), and $Fe(TPP)(PMe_3)(py)$ (δ 8973), and $Fe(OEP)(PMe_3)_2$ (H_2OEP = octaethylporphyrin, δ 7873).[358] A correlation was found between Mössbauer quadrupole splittings (mm/s) and ^{57}Fe NMR shifts of diamagnetic Fe(II) porphyrin complexes such as $Fe(TPP)(PMe_3)_2$ and $Fe(OEP)(PMe_3)_2$.[368] ^{57}Fe shifts of stereo-hindered heme model compounds (with the so-called superstructures) and atropisomers (stereoisomers from hindered rotation about a single bond) showed that the shifts were very sensitive to deformation (ruffling) of the porphyrin geometry.[369-370] ^{57}Fe shifts in metalloporphyrins may be predicted from ^{13}C NMR shifts of the *meso*-C atoms of the TPP^{2-} ligands in the complexes.[370]

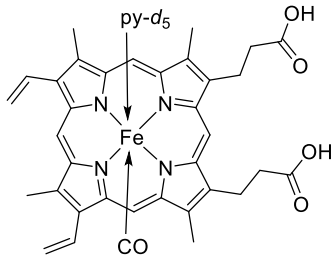

(**35**)

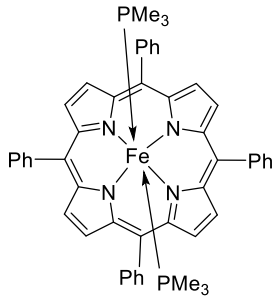

(**36**)

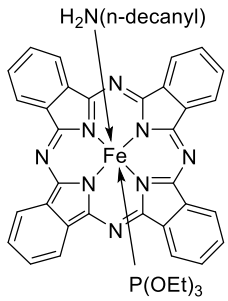

(**37**)

^{57}Fe and ^{15}N shifts in Fe(II) phthalocyanine (Pc) complexes Fe(Pc)[P(OEt)$_3$]L [**37**, L = H_2N(*n*-decanyl)], ^{57}Fe δ 6764; ^{15}N δ -1.34; L = H_2NCH_2Ph, ^{57}Fe δ 6794, ^{15}N δ 3.45] were obtained from ^{31}P-^{57}Fe HMQC and ^{1}H-^{15}N gradient-selected HMQC (*g*HMQC) NMR, respectively.[360] ^{15}N shifts of other diamine complexes Fe(Pc)L$_2$, such as L = H_2N(*n*-decanyl), H_2NCH_2Ph, were also reported.[360]

For organometallic complexes, ^{57}Fe NMR for ferrocene Cp_2Fe with natural abundance was acquired with the ^{1}H-^{57}Fe INEPT polarization transfer (PT) technique.[363] Substituted ferrocenes were a focus of ^{57}Fe NMR studies with a report of ^{57}Fe shifts of CpFe(η^5-C_5H_4R) (R = $SiMe_3$, δ 1626; $SnMe_3$, δ 1611) and Fe(η^5-$C_5H_4R)_2$ (R = CMe_3, δ 1621; R = $SiMe_3$, δ 1728; R = $GeMe_3$, δ 1690; R = $SnMe_3$, δ 1692).[371] For eight ferrocenes with monoamine substituents, ^{15}N and shifts of other nuclides were reported, including CpFe(η^5-$C_5H_4NH_2$) (^{57}Fe δ 1639; ^{15}N δ -345.7) and CpFe(η^5-C_5H_4[N($SiMe_3$)(BEt_2)]) (^{57}Fe δ 1702; ^{15}N δ -285; ^{11}B δ 55.7; ^{29}Si δ 8.4).[372] ^{57}Fe shifts of additional aminoferrocene and 1,1′-diaminoferrocene were reported, such as CpFe(η^5-$C_5H_4NPh_2$) (δ 1664) and Fe(η^5-$C_5H_4NH_2)_2$ (δ 1709).[365] ^{57}Fe shifts of ferrocenes with sulfinylamino[364] or π-acceptor[373] substituents as well as bridged [1]ferrocenophanes Fe[(η^5-$C_5H_4)_2SiMe_2$][374] were also studied. For substituted neutral ferrocenes, there was a linear relationship between Mössbauer quadrupole splittings (mm/s) and ^{57}Fe shifts.[375] The more shielded ^{57}Fe ions (with more upper field ^{57}Fe shifts), the larger the quadrupole splittings.[375]

^{57}Fe, ^{119}Sn, ^{13}C and ^{31}P NMR were used to characterize a series of

$CpFe(SnPh_3)(CO)(PR_3)$ complexes (R = Me, ^{57}Fe δ 447; ^{119}Sn δ 46.71; R = OMe, ^{57}Fe δ 316; ^{119}Sn δ 47.76).[376] ^{57}Fe NMR was used to characterize 35 cyclopentadienyl Fe(II) complexes with the general formulas $CpFe(CO)_2R$, $CpFe(CO)(PPh_3)X$, $CpFe(CO)L(COMe)$ (L = PR_3, and CO) and $(\eta^5\text{-}C_5H_4Y)Fe(CO)(PPh_3)Me$ (Y = Me, $SiMe_3$, NEt_2, Ph, I, COOMe, $COPr^i$),[359] including $CpFe(CO)_2Me$ (δ 684), $CpFe(CO)(PPh_3)H$ (δ 536), $CpFe(CO)(PMe_3)(COMe)$ (δ 1374), and $(\eta^5\text{-}C_5H_4Me)Fe(CO)(PPh_3)Me$ (δ 1367).[359] NMR of dimer $Fe_2(CO)_6(\mu\text{-}SNH)$ was studied, giving ^{57}Fe δ 1315 and ^{15}N δ -374.7.[377] Iron tricarbonyl complexes containing a substituted silole or analogous ligand were also studied by ^{57}Fe NMR.[378]

Inverse-detection techniques were used to indirectly measure ^{57}Fe spin-lattice relaxation times for $CpFe(CO)(PPh_3)(COMe)$ [T_1 = 4.4 s at 9.4 T (or 400 MHz ^1H NMR) and 2.1 s at 14.1 T (600 MHz ^1H NMR)].[379]

As indicated in the ^{57}Fe shifts summarized above, the Fe(II) ion in $Fe(CN)_5(NO)^{2-}$ is more shielded than that in $Fe(CN)_6^{4-}$.[366] Since both complexes were prominent textbook examples in coordination chemistry, the shifts were studied theoretically to provide an understanding. Large geometry dependence of the shifts was found from a combined QM/MM (quantum mechanics/molecular mechanics) approach.[380] Thermal and solvent effects on these shifts were simulated with two molecular-dynamics (MD)-based approaches.[381] The computed trends for the chemical shifts could be rationalized by a large sensitivity of the magnetic shielding on the Fe-ligand distances.[381] ^{57}Fe NMR shifts were calculated by a DFT method for $Fe(CO)_5$, $Fe(CO)_3(H_2C{=}CHCH{=}CH_2)$, $Fe(CO)_3(\text{cyclo-}C_4H_4)$ and $CpFe(CO)_2R$ (R = Me, Bu^n, Pr^i).[382]

In NMR studies of α atoms of ligands, the reaction mixture of excess $^{15}NH_2OH$ and $Fe(CN)_5(NH_3)^{3-}$ at pH 9 was monitored by ^{15}N NMR,[383] leading to the identification of the intermediate species $Fe(CN)_5(N_2H_2)^{3-}$ (δ -76).[383] Several Fe P,N,N pincer complexes, including $(P,N,N)Fe(CO)_2$ [**38**, P,N,N = 2-[(di-tert-butylphosphino)methyl]-6-[1-(2,4,6-mesitylimino)ethyl]pyridine], were characterized by several NMR techniques including $^1H\text{-}^{15}N$ HMQC and $^1H\text{-}^{31}P$ HMQC, giving ^{15}N shifts of δ 258.1 and 259.2 for the pyridine and imido N

atoms in the P,N,N ligand of the complex **38**, respectively.[384]

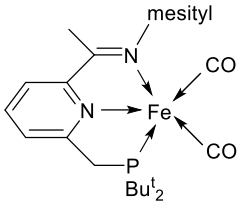

(**38**)

Reaction of electrophile Me_3SiOTf with Fe(0) $Fe(^{15}N_2)(dmpe)_2$ was conducted, followed by addition of triflic acid to the residual product solid in a study of nitrogen fixation. In a test analyzed by ^1H-^{15}N HMQC before the addition of the triflic acid, $Fe(\eta^2\text{-}^{15}N_2H_4)(dmpe)_2^{2+}$ (δ -387.0) and $Fe(^{15}NH_3)_2(dmpe)_2^{2+}$ (δ -422.6) were identified.[385] In another reaction analyzed after the addition of triflic acid, $^{15}NH_4^+$ as well as $FeH(^{15}N_2)(dmpe)_2^+$ were detected.[385] $Fe(NH_3)_2(dmpe)_2^{2+}$ was independently prepared via the treatment of $FeCl_2(dmpe)_2$ with NH_3 in methanol.[385] The nitroxyl ligand in $Fe(CN)_5(HNO)^{3-}$ was analyzed by ^1H (δ 20.2), ^{15}N (δ 640), and ^{17}O (δ 1099) NMR.[386]

The complex $Fe_4(\mu_3\text{-}S)_2(\mu_2\text{-}NO)_2(NO)_6^{2-}$ with bridging and terminal NO ligands was synthesized and characterized via several methods including ^{15}N NMR.[387] An enriched version of $Fe_4(\mu^3\text{-}S)_2(\mu^2\text{-}NO)_2(NO)_6^{2-}$ was prepared as the sample for ^{15}N NMR.[387] At 320 K, there was a single broad singlet at δ 58.3. However, at 220 K, there were signals at δ 200.8 and 200.1 (referenced to $MeNO_2$) for the bridging ^{15}NO ligands and δ 79.7, 73.5, 43.9, 30.3, 27.1, and 21.9 for terminal ^{15}NO ligands.[387] ^{15}N NMR of oxidized ^{15}N-labeled histidine Rieske iron-sulfur protein from the bacterium *Thermus thermophilus* was followed as a function of pH from 11.7 to 5.75 in order to determine the pK_a values of the Fe-bound histidine.[388]

Several reactions of $Cp^*Fe_2(CO)_4(\mu\text{-}CO)(\mu\text{-}PPh_2)$ with various hydrosilanes, such as Ph_2SiH_2 or $(p\text{-tol})_2SiH_2$, were analyzed by ^{29}Si and ^{31}P NMR.[389] Fe(II) dicarbollide 1-(η^6-$Me_nC_6H_{6-}$

$_n$)-*closo*-1,2,3-$FeC_2B_9H_{11}$ (**39**, n = 1-6)[390] and Fe(III) bis(dicarbollide) [3-Fe-(1,2-$C_2B_9H_{11}$)$_2$]$^-$ (**40**),[391] were analyzed via ^{1}H and ^{11}B NMR. For complex [3-Fe-(1,2-$C_2B_9H_{11}$)$_2$]$^-$, DFT calculations were used in order to aid the ^{11}B NMR assignments.[391]

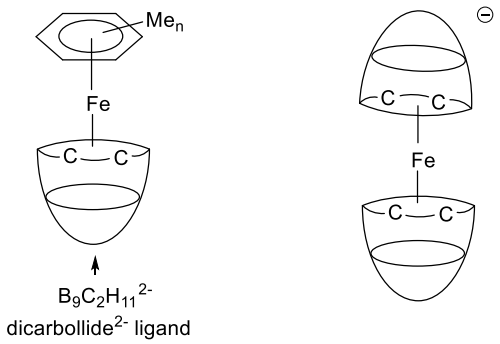

(**39**) (**40**)

Water exchange dynamics of several iron complexes, including porphyrins[392] and polyaminecarboxylates,[393] was studied by ^{17}O NMR.[394-396]

7.2. *Ruthenium complexes*

The range of reported ^{99}Ru NMR shifts we found is ~18000 ppm set by $Ru(OH_2)_6^{2+}$ (δ 16050[397]) and Cp_2Ru (δ -1270 at 346 K[398]). This range was determined in the 1980s.

NMR of ^{99}Ru and ligand donor atoms in metal complexes in aqueous solutions was reviewed in 2016.[399]

^{99}Ru, ^{14}N and ^{17}O NMR were probed to study hydrolysis of $(NH_4)_2[Ru(NO)Cl_5]$ (δ ^{99}Ru 4190; ^{14}N -36; ^{17}O 379), which initially formed *cis*-$Ru(NO)(H_2O)Cl_4^-$ (δ ^{99}Ru 4450; ^{17}O 380 for NO^+ and -79 for H_2O ligand).[400] Subsequently, both isomerization and additional Cl^- replacement in the Ru(II) compound gave *trans*-$Ru(NO)(H_2O)Cl_4^-$ (δ ^{99}Ru 3920; ^{14}N -18; ^{17}O 411 for NO^+ and 0 for H_2O ligand) and *fac*- and *mer*-$Ru(NO)(H_2O)_2Cl_3$, respectively.[400]

^{99}Ru shifts of Ru(II) complexes with N,N chelating ligands, $[Ru(bpy)_3]Cl_2$ (δ 4534, bpy =

2,2′-bipyiridine) and its analogs such as $[Ru(phen)_3]Cl_2$ (δ 4642, phen = phenanthrene), were reported.[401] These were in comparison to δ 7821 of $Ru(NH_3)_6Cl_2$ reported earlier.[398] $[Ru(bpy)_2(2,3\text{-dpp})](PF_6)_2$ [**41**, 2,3-dpp = 2,3-bis(2-pyridyl)pyrazine] containing an N,N pyridyl-substituted pyrazine ligand was characterized by ^{99}Ru NMR (δ 4535).[402]

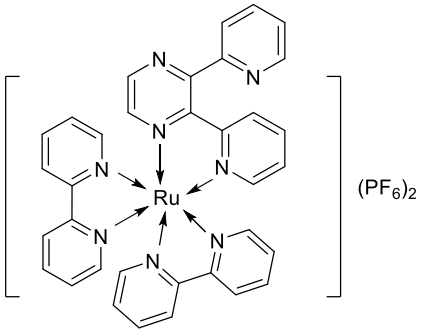

(**41**)

For organometallic Ru(II) complexes, ^{99}Ru shifts of $Ru(CO)_2(dab)XY$ [X, Y = halide, alkyl, SnR_3, $GePh_3$, $PbPh_3$, $Mn(CO)_5$, $CpRu(CO)_2$; dab = Pr^i-N=CH=CH=NPr^i (1,4-diisopropyl-1,4-diaza-1,3-butadiene)] were studied, giving, e.g., δ 1993 (X = Y = Cl^-), 1036 (X = Y = I^-), 794 (X, Y = Me^-, Cl^-), 712 (X, Y = Me^-, Br^-), 551 (X, Y = Me^-, I^-), -316 (X = Y = $SnMe_3$), -116 (X = Y = $SnPh_3$), and 200 (X = Y = $PbPh_3$).[403]

For Ru cluster complexes, the ^{99}Ru shift of $Ru_3(CO)_{12}$ (δ -1208) was reported earlier.[398] Shifts of $HRuCo_3(CO)_{12}$ (δ 202), $(NEt_4)[RuCo_3(CO)_{12}]$ (δ -68), $RuCo_3(CO)_{11}(NO)$ (δ -241 in addition to ^{59}Co NMR shifts discussed below), and $RuCo_2(CO)_{11}$ (δ -597) were obtained,[404] along with their ^{59}Co NMR shifts discussed below. For $RuCo_3(CO)_{12}(NO)$, ^{99}Ru shift at -241 was observed.[404]

Computations of ^{99}Ru shifts were the subject of a few studies using DFT methods.[405-409] ^{99}Ru shifts of several species, including $K_4Ru(CN)_6$, Cp_2Ru, $Ru_3(CO)_{12}$, $Ru(CO)_3Cl_3^-$, $Ru(CO)_2Cl_4^{2-}$, $Ru(bpy)_3^{2+}$, and $Ru(CO)_2(dab)XY$ (X = Y = Cl^-, I^- or $SnMe_3$; X, Y = Me^-, Cl^- or Me^-,

I^-) discussed above, were computed and compared with those from experiments.[408] Relativistic effects, influence of the density functional and solvent effects on *fac*-$Ru(CO)_3I_3^-$ were investigated.[405] Influence of molecular geometry on the nuclear shielding in $RuCl_2(dmso)_4$ and α-$PW_{11}RuO_{39}(dmso)^{5-}$ containing Ru-S bonds was examined, helping the assignment of ^{99}Ru NMR resonances in the compounds.[406]

In the NMR studies of α atoms of ligands, the ^{17}O shift of Ru(VI) dioxo porphyrin complexes such as $Ru(TMP)(=O)_2$ (δ 775 referenced to H_2O; H_2TMP = tetramesitylporphyrin) were studied.[137]

$Ru(H_2O)_6^{2+}$ reacted with H_2 under pressure to give the η^2-H_2 complex $[Ru(H_2)(H_2O)_5]^{2+}$ and was characterized via ^1H (δ -7.65), ^2H (δ -80.4, J_{H-D} = 31.2 Hz) and ^{17}O [δ_{ax} -177.4 (for water ligand *cis* to H_2), δ_{eq} -80.4] NMR.[410]

When a solution of $[RuCl(OEt_2)(PNNP)]^+$ (PNNP = (1S,2S)-N,N-bis[o-(diphenylphosphino)-benzylidene]cyclohexane-1,2-diamine) and N-benzylidene-1,1-diphenylmethanamine is treated with excess ^{15}N-eda (eda = ethyl diazoacetate, N_2=CHCOOEt) -78 °C, the complex *trans*-$RuCl(eda)(PNNP)^+$ was the major species below -20 °C.[411] Reactions of a series of azolylpyridines with $RuCl_2(PMe_3)_4$ yielded $[(N,N)RuCl(PMe_3)_3]$ (**42**) with pyridinylazolate N,N ligands.[412] ^1H-^{15}N HMBC was used to clarify the electronic influence of the substituents on the azolyl ring.[412] ^{15}N-NMR studies were performed at pH 5 of the reaction $Ru(edta)H_2O^-$ with excess ^{15}NO.[413] The ^{15}N NMR of this reaction showed three signals at δ -17.6, 52.4 and 228.5.[413] The first two resonances pertained to coordinated $^{15}NO^+$ and $^{15}NO_2^-$ ligands in $Ru(edta)(NO)(NO_2)^-$, respectively.[413] The shift at δ 228.5 signified the occurrence of free $^{15}NO_2^-$ in solution.[413] Reactions of $[(\eta^6\text{-biphenyl})RuCl(en)]PF_6$ with amino acids *L*-cystine,[414] *L*-methionine,[414] *L*-histidine[415] as well as cytochrome c or the oligonucleotide d(TATGTACCATGTAT) were investigated using ^1H-^{15}N HSQC and ^1H TOCSY.[415]

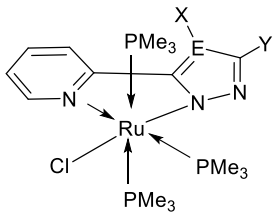

E = C, N
X = H, Br, NO_2
Y = H, Me, Et, Ph, 4-OMe-C_6H_4, NO_2

(**42**)

Several NMR studies, such as ^{1}H-^{31}P HMQC NMR or ^{11}B NMR, and analysis $J_{Si\text{-}H}$ of Ru silane, disilane, and borane complexes were discussed in a 2008 review.[139]

7.3. *Osmium complexes*

^{187}Os is the least sensitive nuclide in the Periodic Table, as shown by its receptivity with respect to ^{13}C in Table 10.[69,416] Inverse detection methods to indirectly determine ^{187}Os chemical shifts by 2-D correlation experiments, which were reported in 1985,[362] significantly expanded the use of ^{187}Os NMR to inorganic compounds.[361] Prior to the development of the techniques, only ^{187}Os NMR shift of OsO_4 was reported.[1]

NMR of ^{187}Os and ligand donor atoms in metal complexes in aqueous solutions was reviewed in 2016.[399]

A ^{19}F-^{187}Os correlation spectrum was used to obtain ^{187}Os shift of *cis*-OsO_2F_4 (δ 1431).[416] The *cis* structure for the Os(VIII) complex is based on DFT calculations.

Several Os(II) complexes were characterized. ^{187}Os NMR of 37 (η^6-arene)Os(PR_3)X_2 complexes (η^6-arene = 1,4-Me,Pr^i-C_6H_4 or *p*-cymene) were probed by either ^{1}H-^{187}Os or ^{31}P-^{187}Os HMBC techniques, yielding, e.g., (η^6-*p*-cymene)Os(PMe_3)X_2 (δ X = Cl^-, -2226; Br^-, -2495; I^-, -3260; H^-, -5265) vs. δ -2431 for (η^6-C_6H_6)Os(PMe_3)Cl_2 and δ -1829 for (η^6-C_6Me_6)Os(PMe_3)Cl_2.[417] The shifts of the 31 (*p*-cymene)Os(PR_3)X_2 complexes span the range of δ -1697 for (*p*-cymene)Os(PCy_3)Cl_2 to -5265 for (η^6-*p*-cymene)Os(PMe_3)H_2.[417] ^{187}Os NMR shifts of several [(η^6-*p*-cymene)Os(CO)(PR_3)I](PF_6) complexes were similarly measured by the HMQC

techniques, giving, e.g., δ -4430 for [(η^6-*p*-cymene)Os(CO)(PMe$_3$)I](PF$_6$).[418] ^{187}Os shifts and $^1J_{Os-C}$ coupling constants of CpOs(CO)$_2$Me (^{187}Os δ -5340, J_{Os-C} = 48.9 Hz) and Cp*Os(CO)$_2$Me (^{187}Os δ -4985, $^1J_{Os-C}$ = 51.5 Hz) were also determined.[418] Inverse-detection techniques, based on the ^{1}H-^{187}Os or ^{31}P-^{187}Os dipole-dipole interactions, were used to indirectly measure ^{187}Os spin-lattice relaxation times (T_1) for (η^6-*p*-cymene)Os(PMe$_3$)(H)Cl at 300 K [T_1 = 4.7 s at 9.4 T and 2.2 s at 14.1 T (600 MHz ^{1}H NMR)].[379]

The ^{187}Os shift of di-arene [Os(η^6-C$_6$H$_5$-Ph)$_2$](OTf)$_2$ (δ -4715) was determined by ^{1}H-^{187}Os HMBC.[419] The δ value in the Os(II) complex was shifted significantly from the average (-3000) ppm of mono-arene complexes [(η^6-arene)Os(PR$_3$)X$_2$](OTf)$_2$ as a result of the increased shielding provided by the second arene ligand in [Os(η^6-C$_6$H$_5$-Ph)$_2$](OTf)$_2$.[419]

^{187}Os shifts of CpOsL$_2$R (L = phosphine, phosphite) were determined from ^{1}H-^{187}Os and ^{31}P-^{187}Os spectra by the inverse detection techniques.[420] For CpOs(PPh$_3$)$_2$X, e.g., the shifts are δ -2595 for X = Cl$^-$, -3008 for X = Br$^-$, and -3530 for X = I$^-$.[420] Coupling constants $^2J_{Os-H}$ and $^1J_{Os-P}$ were determined as well. ^{187}Os spin-lattice relaxation times [T_1, X = Cl$^-$, 0.5 s; Br$^-$, 0.6 s at 9.4 T and 300 K (or 400 MHz ^{1}H NMR)] were determined indirectly by the ^{31}P-^{187}Os dipole-dipole interaction.[420]

^{187}Os NMR of triosmium clusters containing bridging hydrides, including Os$_3$(μ-H)$_2$(CO)$_{10}$ (**43**) and several chelating diphosphine derivatives such as Os$_3$(μ-H)$_2$(CO)$_8$(μ-P,P) [e.g., P,P = Ph$_2$PCH$_2$PPh$_2$ (dppm) (**44**); (*R*)-2,20-bis(di-4-tolylphosphino)-1,10-binaphthyl (tol-BINAP) (**45**)], was studied by HMQC, HSQC and HMBC using $^1J_{H-Os}$ or $^2J_{H-Os}$ couplings.[361] HMQC and HSQC based on one-bond $^1J_{H-Os}$ gave identical δ for the Os atoms (Os^1) directly bound to the bridging H ligands, while HMBC based on two-bond $^2J_{H-Os}$ yielded δ for the Os atom (Os^2) not bound to the H ligands.[361] For Os$_3$(μ-H)$_2$(CO)$_{10}$ (**43**), δ_{Os^1} -11302, δ_{Os^2} -14021. For Os$_3$(μ-H)$_2$(CO)$_8$(μ-dppm) (**44**), δ_{Os^1} -11525, δ_{Os^2} -14001. For Os$_3$(μ-H)$_2$(CO)$_8$(μ-tol-BINAP) (**45**) containing a chelating chiral phosphine ligand, δ (Os^1) -11345, δ (Os^2) -14023.[361] For Os$_3$(μ-H)$_2$(CO)$_{10}$ (**43**)

with two types of Os atoms (two bound to the H ligand and one not bound), the satellite from the long-range $^2J_{H\text{-}Os}$ coupling is buried under the central peak.[421] A method based on varying evolution delays in HMQC spectra led to the extraction of the $^1J_{H\text{-}Os}$ (44 Hz), $^2J_{H\text{-}Os}$ (2 Hz) and $^2J_{H\text{-}C}$ (12 Hz) values for $Os_3(\mu\text{-}H)_2(CO)_{10}$ (**43**).[421]

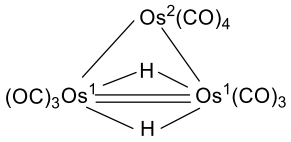

(**43**)

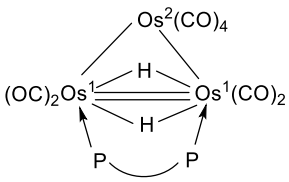

P⌒P = dppm

(**44**)

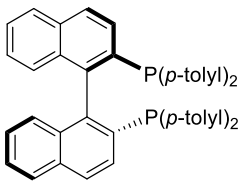

P⌒P = tol-BINAP

(**45**)

A unique NMR method was used to follow σ,π-vinyl interchange in a series of 5,6-dihydro-μ_3-η^3-quinolyl complexes $Os_3(\mu\text{-}H)(CO)_9[\mu_3\text{-}\eta^3\text{-}C_9H_6(5\text{-}R)(6\text{-}R')N]$ such as **46** (R = CMe_2CN, R′ = Me) in **Figure 4**.[422] For a typical σ,π-vinyl interchange involving metal carbonyl complexes in **Figure 4-A**, VT ^{13}C NMR of the CO ligands on the M atoms bound to the σ,π-vinyl moiety was usually used to follow the interchange. At the low temperature limit, environments at the two M atoms were different. The onset of the interchange averaged the environments and the barrier to the interchange could be obtained from the pairwise exchange rates of these CO ligands.[422] However, the chiral centers in, e.g., $Os_3(\mu\text{-}H)(CO)_9[\mu_3\text{-}\eta^3\text{-}C_9H_6(5\text{-}R)(6\text{-}Me)N]$ (R = CMe_2CN, **46**, **Figure 4-B**)[423] made Os^1 and Os^2 (as well as Os^3 and Os^4) atoms to be magnetically non-equivalent, even when the σ-π-vinyl interchange process was rapid on the NMR time scale. The unique NMR method was to examine the $^1H\text{-}^{187}Os$ satellites in ^1H NMR of the hydride ligand of a sample with ^{187}Os at 1.96% natural abundance. The molecules of **46** had essentially one or no ^{187}Os isotope in the cluster because of its low abundance. When the σ,π-vinyl interchange was slow on the NMR time scale at 295 K, there were two isotopomers: One

group of molecules with ^{187}Os isotopes at Os^1 and Os^3 atoms; Another group of molecules with ^{187}Os isotopes at Os^2 and Os^4 atoms. Two sets of ^{1}H-^{187}Os satellites ($^1J_{H\text{-}Os}$ = 30.7 and 35.4 Hz) were present in the hydride resonance at δ -17.00 in the ^{1}H NMR spectrum. At 373 K, the interchange became rapid on the NMR time scale. The two sets of the satellites merged to a single set with $^1J_{H\text{-}Os}$ = average of the two values observed at 295 K.[422] In essence, the interchange was monitored at one Os atom per isotopomer. Thus, two Os atoms did not need to become magnetically equivalent for the process to be averaged on the NMR time scale. Only a single Os atom was required to see an average environment. This method circumvented inherent asymmetry in these quinolyl complexes.[422]

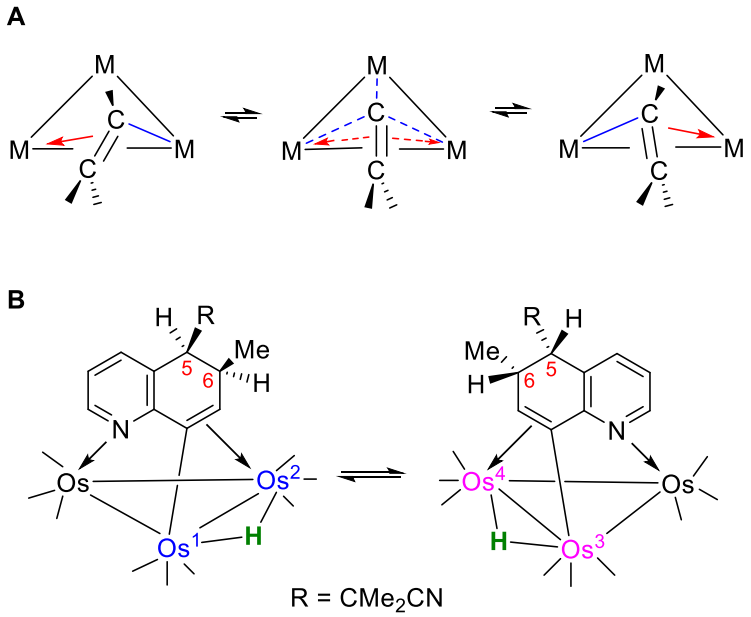

Figure 4. (**A**) σ-π-interchange in μ-η^2-vinyl complexes. (**B**) σ,π-vinyl interchange in *cis*-Os$_3$(μ-H)(CO)$_9$[μ$_3$-η^3-C$_9$H$_4$(5-R)(6-Me)N] (**46**). Os^1 and Os^2 in the left isomer are magnetically inequivalent from Os^3 and Os^4, respectively, in the right isomer.

A hybrid DFT method was implemented to calculate the NMR shielding tensors and ^{187}Os NMR shifts for CpOs(PMe$_3$)$_2$X (H = H, Me, Br).[424]

For NMR of ligands, complexes $TpOs(N)X_2$ (X = CH_3COO^-, Cl^-, CF_3COO^-, CCl_3COO^-, CBr_3COO^-, Br^-, $NO3^-$, 0.5oxalate) were studied via several techniques including ^{15}N NMR using enriched complexes.[425] The ^{15}N singlet for the complexes was between δ 821 and 922.[425] Solvent exchange of H_2O and CH_3CN on *trans*-$Os(en)_2(\eta^2\text{-}H_2)(solvent)^{2+}$ (solvent = H_2O, CH_3CN) was studied as a function of temperature and pressure by ^{17}O NMR line-broadening and isotopic labeling experiments for H_2O and ^1H NMR isotopic labeling experiments for CH_3CN.[426] The rate constants and activation parameters were found to be k_{ex} = 1.59 s^{-1} at 298 K, $\Delta H^{\ddagger}$ = 72.4 kJ/mol ; $\Delta S^{\ddagger}$ = +1.7 J/(mol·K), and $\Delta V^{\ddagger}$ (activation volume)= −1.5 cm^3/mol for water exchange and k_{ex} = 2.74 × 10^{-4} s^{-1} at 298 K, $\Delta H^{\ddagger}$ = 98.0 kJ/mol ; $\Delta S^{\ddagger}$ = +15.6 J/(mol·K), $\Delta V^{\ddagger}$= −0.5 cm^3/mol for acetonitrile exchange.[426]

8. Group 9 (Co, Rh and Ir)

For Co and Rh, NMR of both the metals (^{59}Co, ^{103}Rh) and ligands have been reported. For Ir, we could only find the NMR of the ligands. Nuclear and NMR properties of the nuclides, including recommended and commonly used references, are given in Table 11. ^{59}Co (spin 7/2, natural abundance of 100%) has a relatively large gyromagnetic ratio, thus giving a convenient resonance frequency and a relatively high sensitivity.[1] However, its quadrupole moment is fairly large, and the line width leads to the sensitivity loss. ^{103}Rh, with spin 1/2 and natural abundance of 100%, has a small gyromagnetic ratio, leading to low sensitivity and resonance frequency. In addition, its spin-lattice relaxation, T_1, is relatively long.[1]

Inverse detection methods, similar to those discussed in the section on Group 8 (Fe, Ru and Os), were used for ^{103}Rh NMR to increase the sensitivity of the nuclides.[427-428] 2-D HMQC, based on, e.g, 1-bond coupling $^1J_{P\text{-}Rh}$, makes the acquisition of chemical shifts of spin 1/2 ^{103}Rh much easier.

Table 11.[26] Nuclear and NMR properties of ^{59}Co, ^{103}Rh, ^{191}Ir and ^{193}Ir

Nuclide	Natural abun-dance (%)[a]	Spin	Relative receptivity		Gyromagnetic ratio (10^7) (rad s^{-1} T^{-1})	Quadrupole moment *Q* (fm^2)	*Ξ* (and frequency, MHz; ^1H = 100.0000 MHz, 2.3488 T)	Reference sample
			D^H (^1H = 1.00)	D^C (^{13}C = 1.00)				
^{59}Co	100	7/2	0.278	1.64×10^3	6.332	42.0	23.727074	$K_3Co(CN)_6$ (aq)
^{103}Rh	100	1/2	3.17×10^{-5}	0.186	-0.8468	-	3.186447	$Rh(acac)_3$ ($CDCl_3$)
(^{191}Ir)[b,c]	37.3	3/2	1.09×10^{-5}	6.38×10^{-2}	0.4812	81.6	(1.718)[d]	-
^{193}Ir[b]	62.7	3/2	2.34×10^{-5}	0.137	0.5227	75.1	(1.871)[d]	

[a] Unless noted, the isotopes are stable. The natural abundances are based on the NIST data.[25]

[b] We did not find a publication in 1990-2019 on the ^{191}Ir or ^{193}Ir NMR of a metal complex. None was included in the 1991 book edited by Pregosin.[1]

[c] ^{191}Ir in parenthesis is considered to be the less favorable of the element for NMR.[26]

[d] Value calculated from literature data on nuclear magnetic moments.

8.1. *Cobalt complexes*

^{59}Co NMR is one of the most used metal NMR spectroscopies with many publications. Its application in coordination chemistry was reviewed in detail in 1991,[429] in addition to that in Reference 1. ^{59}Co shifts of about 800 complexes were tabulated, with spin-spin coupling constants *J* for 20 nuclear pairs.[429]

^{59}Co NMR shifts cover the largest known shielding range, including δ 15100 for $Co(H_2O)_6^{3+}$ to -4220 for $KCo(PF_3)_4$, as earlier studies show.[429] Low-spin, octahedral d^6 Co(III) complexes, which are diamagnetic, comprise a large class of compounds probed by ^{59}Co NMR. Their shifts are typically in the range of δ 15100 for $Co(H_2O)_6^{3+}$ to -2600 for $Co[1,2\text{-}C_6H_4(PMe_2)_2]_3^{3+}$.[429] For complexes with Co atoms at lower oxidation states, ^{59}Co shifts include those in $HCo(CO)_4$ (δ -3721), $NaCo(CO)_4$ (δ -3100), $Co_2(CO)_8$ (δ -2101), Cp_2Co^+ (δ -2410), and

$CpCo(C_2H_4)_2$, in addition to Co(-I) $KCo(PF_3)_4$.[429]

In coordination chemistry, $K_3[Co(CN)_6]$, dissolved in organic solvents by cryptand 222, showed the solvent influence on the d-d transition energies and ^{59}Co shift of the complex.[430] Similarly, studies of $[Co(en)_3]Cl_3$,[431] *cis-,trans*-$[Co(en)_2(N_3)_2]NO_3$,[431] K[Co(edta)],[432] and $K_3[Co(ox)_3]$ (ox = oxalate)[432] showed that their ^{59}Co shifts were solvent-dependent. ^{59}Co, ^{13}C and ^{15}N shifts of $Co(CN)_5X^{3-}$ (X = CN^-, Cl^-, Br^-, I^-), $Co(CN)_5(NH_3)^{2-}$ (L = py, NH_3, H_2O), $Co(NH_3)_5(CN)^{2+}$, and $Co(NH_3)_5(NC)^{2+}$ revealed a common tendency that the shifts varied with the identity of the sixth coordinated ligand and correlated with ligand-field parameters including the nephelauxetic ratio.[433] The ligand exchange reactions between $Co(NO_2)_6^{3-}$ and N_3^-, NCS^- or NH_2OH was probed to develop an improved empirical method to estimate the variation of the ligand field strength of the NO_2^- ligand and ^{59}Co shifts.[434]

^{59}Co NMR was shown to be a facile tool to probe configurational isomerism in *fac*-Co(*L*-S,O)$_3$ complexes containing *S,O* ligands [e.g., H(*L*-S,O) = PhC(O)NHC(S)NMeEt].[435] Different configurations of the three ligands led to *EEE, EEZ, EZZ, ZZZ fac*-Co(*L*-S,O)$_3$ configurational isomers, each of which gave a resonance.[435] $Co(dmgBF_2)_2(H_2O)_2$ [$dmgBF_2$ = difluoroboryldimethylglyoximate (**47**)] and its pyridine derivative $Co(dmgBF_2)_2(H_2O)(py)$, both containing a planar N,N,N,N ligand were characterized by ^{59}Co NMR (δ 2996 and 2443, respectively).[436] ^{59}Co NMR of *fac*- and *mer*-$Co(NH_2CH_2CH_2O)_3$ (δ 10175 and 10016, respectively) was reported.[437]

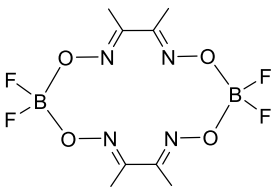

$dmgBF_2$

(**47**)

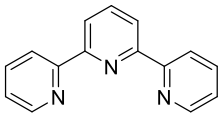

terpy

(**48**)

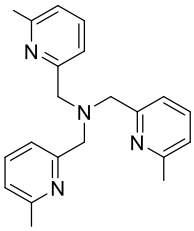

Me_3-tpa

(**49**)

Stereoisomerization of Co(III) complexes with polydentate amine ligands, diethylenetriamine, triethylenetetramine, tetraethylenepentamine, and 1,4,8,11-tetraazacyclotetradecane in aqueous solutions was probed by ^{59}Co NMR.[438] *mer*-[Co(diethylenetriamine)$(NO_2)_2(NH_3)$]Cl was the dominant of four observed isomers.[438] ^{59}Co NMR was used to characterize Co(terpy)F_3 [δ 8179, terpy = 2,2':6',2''-terpyridine (**48**)] and Co(Me_3-tacn)X_3 [δ 9093 for X = F^-; 10190 for X = Cl^-; Me_3-tacn = **2** (R_3 = Me_3)].[439] [Co(tacn)$(H_2O)_3$]$(OTf)_3$ [tacn = **2** (R_3 = H_3)] which was used as a starting material in the preparation of a V complex as described in the section on vanadium complexes,[197] showed a ^{59}Co peak at δ 9535.[440] Reaction of [Co(tacn)$(H_2O)_3$]$(OTf)_3$ with Na_2MoO_4 yielded the polyoxomolybdenate complex, [Co(tacn)]$_2Mo_3O_{12}$, with the ^{59}Co peak moved to δ 9776.[440] ^{59}Co NMR of [Co(tpa)(CO_3)]ClO_4, [Co(Me-tpa)(CO_3)]ClO_4, [Co(Me_2-tpa)(ClO_4)]ClO_4, and [Co(Me_3-tpa)(CO_3)]ClO_4 [tpa = tris(2-pyridylmethyl)amine (δ 7965); Me-tpa (δ 8606), Me_2-tpa (δ 9162), and Me_3-tpa (**49**, δ 10251) as tpa derivatives containing one, two, and three 6-methylpyridyl rings, respectively] are consistent with the decreasing ligand field strength of the *N,N,N,N*-tripodal tetraamine ligands in the order tpa > Me-tpa > Me_2-tpa > Me_3-tpa.[441] Studies of similar tripodal tetraamine complexes also showed the correlation.[442] Co complexes with a *R*-alaninate (**50**) and different tetraamine ligands, including [Co(*R*-alaninate)(N,N,N,N)]$(ClO_4)_2$ [N,N,N,N = 1,9-diamino-3,7-diazanonane (**51**), δ 7935] and its tetramethyl analog [N,N,N,N = (6*R*,8*R*)-6,8-dimethyl-2,5,9,12-tetraazatridecane (**52**), δ 8615] showed that methyl substitutions on the tetraamine ligand significantly affected the ligand field strength, as indicated by characteristic ^{59}Co shifts.[443] ^{59}Co was used to characterize clathrochelate dioximate complexes, such as (H_2NEt_2)[Co(dioximate)$_3(SnCl_3)_2$] (δ 4603) surrounded by a distorted trigonal antiprismatic coordination sphere from a ligand (**53**) with six N atoms cross-linked with $SnCl_3$.[444] Co(III) complex K[Co(oct-dhpta)] [**54**, oct-dhpta = n-heptyl-CO_2-CH[$CH_2N(CH_2CO_2)_2]_2^{4-}$], containing an N,N,O,O,O,O ligand with a long alkyl chain, showed that the ^{59}Co NMR shift (δ 10378) could be

used to probe the aggregation of a surfactant with a Co(III) complex as a polar group.[445]

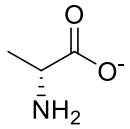

(**50**)

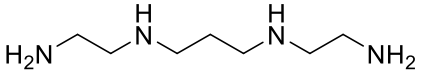

(**51**)

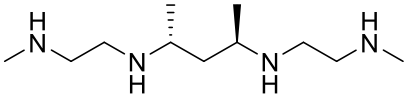

(**52**)

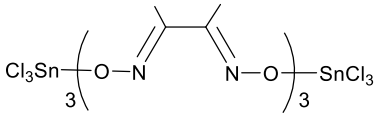

(**53**)

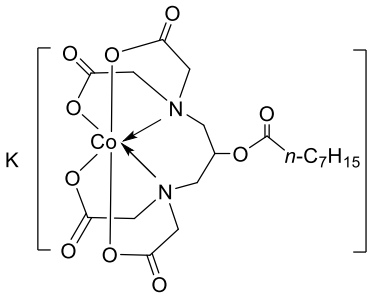

(**54**)

^{59}Co shifts of distibine complexes [Co[1,2-(CH_2SbMe_2)$_2$-C_6H_4]$_2X_2$]Y (X = Br^-, Y = BPh_4^-, δ 4550; X = Y = I^-, δ 6680) were reported,[446] as the shifts of two Co chloride complexes containing the tripodal triphosphine ligand $MeC(CH_2PMe_2)_3$.[447]

Several Co(III) crown thioether complexes were characterized by ^{59}Co NMR, including, e.g., [Co(18S6)]$(ClO_4)_3$ [18S6 = 18-thiacrown-6 or 1,4,7,10,13,16-hexathiacyclooctadecane (**55**), δ 1646].[448] ^{59}Co NMR properties of dithio-, thioseleno- and diseleno-carbamate complexes show, e.g., ^{59}Co NMR of δ 6790, 6850, and 6890 for $Co(S_2CNEt_2)_3$, $Co(SSeCNEt_2)_3$, and $Co(Se_2CNEt_2)_3$, respectively, demonstrating a deshielded shift with increasing substitution of the more electronegative S atoms by Se atoms in the complexes.[449] ^{77}Se shifts of the Se-containing complexes $Co(SSeCNEt_2)_3$ (δ 392, 373) and $Co(Se_2CNEt_2)_3$ (δ 461) were also measured.[449] Both ^{59}Co and ^{77}Se shifts were obtained for diseleno-ether [Co($MeSeCH_2CH_2SeMe$)$_2X_2$]BPh_4 (X = Cl^-, ^{59}Co: *trans*-isomer, δ 8694; *iso*-isomer δ 8310; ^{77}Se: δ 259. X = Br^-, ^{59}Co: *trans*-isomer, δ

8310; *iso*-isomer δ 8228; ^{77}Se: δ 257. X = I^-, ^{59}Co: *trans*- and *iso*-isomer, δ 7689; ^{77}Se: δ 256).[450] ^{59}Co shifts were reported for ditelluro-ether $[Co[1,2\text{-}C_6H_4(TeMe)_2]X_2]BPh_4$ (X = Br^-, *trans*-isomer, δ 8329; *iso*-isomer δ 8248; X = I^-, *trans*- and *iso*-isomer δ 8773).[450] ^{59}Co shifts of *trans*-$[Co(C_{12}H_{24}Se_4)X_2]PF_6$ [$C_{12}H_{24}Se_4$ = 1,5,9,13-tetraselenacyclohexadecane (**56**); X = Cl^-, δ 9590; Br^-, δ 9125; I^-, δ 8436] containing a macrocyclic tetradentate selenoether ligand also showed a similar trend with different halide.[451] For the Cl and Br analogs, ^{77}Se shifts are X = Cl^-, δ 197; Br^-, δ 169.[451] Co(III) complexes with substituted macrobicyclic ligands revealed a correlation of their ^{59}Co shifts with inductive (or polar) substituent constants from a Hammett-type treatment.[452]

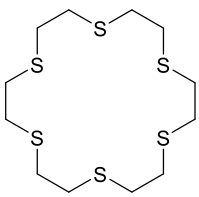

(**55**)

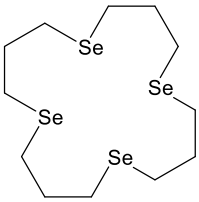

(**56**)

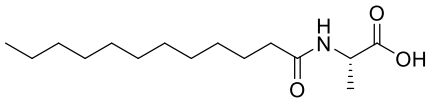

(**57**)

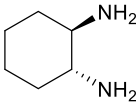

(**58**)

The spin-lattice (or longitudinal) relaxation time T_1 of $Co(acac)_3$ in MeCN was measured at concentrations of 0.020-0.110 M and several temperatures, showing that the relaxation rate was linearly dependent on the concentration of the complex up to approximately 0.080 M.[453] Macroscopic viscosity of the solution was the predominant factor in this dependence.[453]

VT ^{59}Co NMR of 12 octahedral Co(III) complexes were studied to measure spin–lattice relaxation times T_1 and line widths, showing that the quadrupolar mechanism of relaxation was dominant in aqueous solution.[454] The study indicated a need for the use of dilute solutions to measure T_1. Quadrupolar coupling constants in the complexes were determined.[454]

Optical isomers *Δ*- and *Λ*-$[Co(en)_3]$ in aqueous solutions of chiral salts, such as *L*- or *D*-tartrates, show that their ^{59}Co NMR properties (chemical shifts, relaxation rates) were different, which could be used for chiral discrimination.[455] ^{59}Co NMR quadrupole splitting of *Δ*-$[Co(en)_3]$ in

liquid crystals comprising chiral *N*-dodecanoyl-*L*-alanine (**57**) was different than that in liquid crystals comprising its enantiomer *N*-dodecanoyl-*D*-alanine, leading to chiral discrimination.[456] ^{59}Co NMR relaxation studies of *Δ*-[Co(chxn)$_3$]$^{3+}$ ion [chxn = *trans*-(1*R*,2*R*)-1,2-diaminocyclohexane (**58**)] revealed that the decrease in the ^{59}Co NMR relaxation rates, when SO_4^{2-} or PO_4^{3-} anion (<0.1 M) was added, could be attributed to an appreciable decrease in the electric field gradient at the ^{59}Co nucleus by the ion pairing.[457] Similar results were also reported for the interactions between other complexed Co(III) cations[458-459] and anions or between Co(III) complexes[460-462] with surfactants containing different polar groups. For example, in a dilute lyotropic liquid crystal (i.e., dissolving sodium dodecyl sulfate in pentanol and aqueous NaBr), Co(en)$_3^{3+}$ and Co(acac)$_3$ molecules were induced to orientate preferentially, displaying quadrupolar splittings of ^{59}Co NMR signals.[463]

^{59}Co NMR of sterically congested six-coordinate porphyrin complexes Co(TMP)(RIm)$_2^+$ (H_2TMP = tetramesitylporphyrin, an analog of H_2TPP giving the TPP^{2-} anionic ligand in **36**; Rim = imidazole or 1-methylimidazole) and Co(TDCPP)(RIm)$_2^+$ [H_2TDCPP = tetrakis(2,6-dichlorophenyl)porphyrin] showed that the presence of the *ortho* chloro or methyl substituents on the *meso* phenyl groups on the porphyrin ring had a large effect on the ^{59}Co shifts and line widths, when compared to Co(TPP)(RIm)$_2^+$ lacking *ortho* substituents.[464] VT ^{59}Co NMR was used to characterized tetraphenylporphyrinate complexes containing two amine ligands, such as [Co(TPP)(Bu^{n}NH$_2$)$_2$]Cl, and compare them with the NMR of Co(TPP)Cl.[465] For [Co(TPP)(Bu^{n}NH$_2$)$_2$]Cl, ^{59}Co shift range was δ 8019 at -28.5 °C to δ 8293 at 43.1 °C with a linear change with temperature, indicating that the Co(III) ion is less shielded at higher temperatures.[465] Molecular Dynamics (MD) simulations show that the ^{59}Co NMR shift change was due to increased population at thermally excited vibrational levels of the $^1A_1$ ground electronic state.[465]

Similar temperature effects were observed in ^{59}Co NMR of Co(acac)$_3$ and Co(dpm)$_3$ (dpm = dipivaloylmethanate).[466] The exceptional temperature dependence of ^{59}Co NMR shifts

was used for ^{59}Co chemical-shift thermometry, i.e., thermometry via magnetic resonance imaging (MRI) which would provide a powerful noninvasive window into physiological temperature management.[467] Influence of ligand encapsulation on ^{59}Co chemical-shift thermometry was recently studied.[467] Impacts of temperatures on T_1 (spin-lattice) and T_2 (spin-spin) relaxation times in several Co(III) complexes, including $K_3[Co(CN)_6]$, $[Co(NH_3)_6]Cl_3$, and $[Co(en)_3]Cl_3$, were probed with the goal of developing ^{59}Co nuclear spin relaxation thermometry.[468]

Cobaloxime derivatives as vitamin B_{12} models were probed by ^{59}Co NMR,[469-470] showing the electronic and steric influence of axial and equatorial ligands on the NMR shifts.[470] ^{59}Co NMR was also used to characterize Co(II) cobaloxime derivatives.[471] $[(pbt)_2Ru(\mu\text{-L-pyr})Co(dmgBF_2)_2(H_2O)](PF_6)_2$ [**59**, pbt = 2-(2′-pyridyl)benzothiazole, L-pyr = (4-pyridine)oxazolo[4,5-f]phenanthroline, $dmgBF_2$ = difluoroboryldimethylglyoximate (**47**)], containing a tridentate N,N,N ligand bridging Ru(II) and Co(II) ions, was found to be a photocatalyst for H_2 evolution.[471] Similar Co(II) cobaloxime derivatives, such as $Co(dmgBF_2)_2(H_2O)_2$,[472] had been shown to be low spin with one unpaired electron. ^{59}Co shifts of the paramagnetic Co(II) complexes **59** (δ 5401)[471] and $Co(dmgBF_2)_2(H_2O)_2$ (δ 5652),[471] are more deshielded than those of Co(III) cobaloxime derivatives, such as $CoMe(dmgBF_2)_2(H_2O)$ (δ 3888).[470]

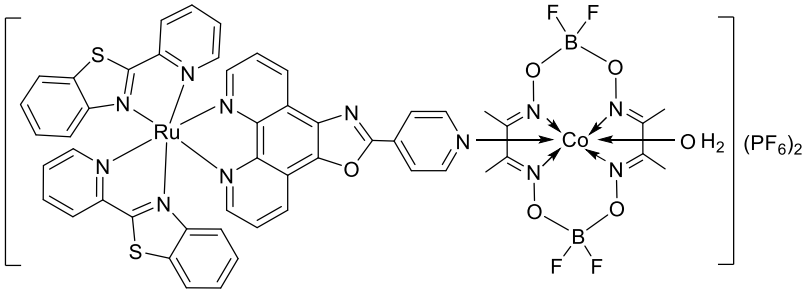

(**59**)

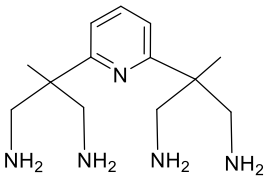

(**60**)

Organometallic Co complexes characterized by ^{59}Co NMR are mainly Co(III) alkyl complexes[470-471,473-474] and carbonyl compounds with Co atoms often at a low oxidation state of I to -I.[249,303,305,404,475-487] Co(III) alkyl complexes include the following: (a) $MeCo(dmgBF_2)_2(H_2O)$, discussed earlier, and other alkyl derivatives;[470-471] (b) $[Co(NH_3)_5Me]S_2O_6$ (δ 7370),[473] $(Et_4N)_3[Co(CN)_5Me]$ (δ -203),[473] *trans*-$[Co(en)_2(NH_3)Me]S_2O_6$ (δ 6400),[473] *trans*-$[Co(en)_2(H_2O)Me]S_2O_6$ (δ 6630),[473] and $[Co(pyN_4)Me](NO_3)_2$ [pyN_4 = 2,6-bis(1′,3′-diamino-2′-methyl-prop-2′-yl)pyridine (**60**), δ 6070] containing the tetrapodal pentadentate amine ligand, pyN_4.[474] In addition to the Co(III) alkyl complexes, ^{59}Co NMR was used to characterize iminiumacetyl complex $(Et_4N)_2[Co(CN)_5(CMe{=}NH_2)]$ (δ 60) and its *N*-methyl and *N,N*-dimethyl derivatives.[488] The iminiumacetyl complex was the product of migratory insertion of a *cis*-CN^- ligand into the Co-Me bond in $Co(CN)_5Me^-$.

Several carbonyl complexes studied by ^{59}Co NMR were derivatives of $MCo_3(CO)_{12}^-$ (M = Fe, Ru),[404,476-479,483,485,487] including $HFeCo_3(CO)_{12}$ (δ -2720),[487] $HRuCo_3(CO)_{12}$ (δ -2760),[487] $HFeCo_3(CO)_{11}(PPh_3)$ (δ -2690 for Co-CO and δ -2467 for Co-P atoms),[487] $HRuCo_3(CO)_{11}(PPh_3)$ (δ -2710 for Co-CO and δ -2564 for Co-P atoms),[487] and $RuCo_3(CO)_{12}(NO)$ (δ -2745 for Co-CO and -486 for Co-NO atoms).[404] References [404], [485] and [487] listed ^{59}Co shifts of additional complexes. 2-D ^{59}Co COSY and DQFCOSY (Double-Quantum-Filtered COSY) were used to probe the scalar coupling constants $^1J_{Co\text{-}Co}$ in such clusters,[481-483] including $HFeCo_3(CO)_{11}L$ [L = PPh_3, $^1J_{Co\text{-}Co}$ = 140 Hz; $P(OMe)_3$, 180 Hz].[481] Other carbonyl complexes studied by ^{59}Co NMR include: (a) Co(I) pseudo-(α-aminoallyl) monomers such as $Co(CO)_3(MeC_3H_3NHPr^i)$ (δ -3118);[475] (b) Isocyanide sulfide complexes $FeCoMo(\mu_3\text{-}S)(CO)_{8\text{-}n}(\eta^5\text{-}C_5H_4COMe)(CNCy)_n$ (n = 1, δ -1640; n = 2, δ -1777; n = 3, δ -1244; Cy = cyclohexyl);[486] (c) Distibine complexes $Co_2(CO)_4(\mu\text{-}CO)_2(\mu\text{-}R_2SbCH_2SbR_2)$ (R = Me, Ph), giving ^{59}Co shifts at δ -1710 and -1820, respectively;[303] (d) Yb(II)-$Co_4(CO)_{11}$ polymeric array, $[(Et_2O)_3YbCo_4(CO)_{11}]_\infty$, probed by VT ^{59}Co NMR, showing δ -170 (apical Co) and -2980 (basal Co) at -105 °C.[489]

Supercritical CO_2 was used as a solvent to study Co carbonyl complexes[249,480,484] and

the hydroformylation reaction.[490] $HCo(CO)_4$ underwent exchanges with $Co_2(CO)_8$ through a H^- ligand transfer, as studied by ^{59}Co NMR line-shape analysis at 80-200 °C and total system pressures up to 370 atm in supercritical CO_2.[484]

Computational studies of ^{59}Co NMR properties of metal complexes,[491-494] including chemical shifts and shielding tensor elements, were performed to, e.g., predict the shifts. DFT studies of the electronic structures in $Co(NH_3)_5X^{(3+n)+}$ (n = 0, X = H_2O; n = -1, X = NO^-, SCN^-, Cl^-, NO_2^-, N_3^-; n = -2, X = CO_3^{2-}, $S_2O_3^{2-}$), offered an insight into the role of the 3d and 4s orbitals in metal-ligand interactions, rationalizing the ^{59}Co NMR trends in the complexes.[495]

Co(II)-mediated interactions between guanine (G) pairs in a self-complementary oligodeoxynucleotides was monitored via ^{15}N NMR.[319] The middle G in a GGG run was shown via both ^{15}N line broadening and HOMO calculations to be the most reactive.[319] To investigate the *trans* influence and chelate ring size,^{15}N NMR shifts in Co(III) complexes with chelated β-alaninato ligands were compared to the shifts of glycinato ligands.[496] Several studies and experiments on cobalamins and corrinoid complexes were conducted via ^{15}N NMR.[497-499]

In order to elucidate Mg(II) binding in an RNA sample (D1κζ), Mg(II)-mimicking Co(III) and Cd(II) were used to probe metal coordination sites in D1κζ.[500] Mg(II) ions initiated the first folding step governed by the κζ element within domain 1 (D1κζ).[500] ^{15}N-labelled samples of D1κζ were titrated with $[Co(NH_3)_6]Cl_3$ at 300 K and monitored via ^1H and ^1H-^{15}N HSQC.[500] The linewidths in the ^{15}N NMR of diamagnetic Co(III) amine and diamine complexes such as $Co(NH_3)_6^{3+}$ and $Co(en)_3^{3+}$ were investigated and compared with those of similar diamagnetic Co(III) complexes.[252] ^{14}N NMR of 20 Co(III) amine compounds, such as $[Co(NH_3)_6]^{3+}$ (δ -422.8) and $Co(NH_3)_5Me^{2+}$ (δ -428.8 for the *cis* and -328.0 for the *trans* isomer), were reported.[501] ^{15}N NMR was used to study the linkage isomerization reaction of the regiospecifically ^{15}N-labelled tetrazole ligand in (5-methyltetrazolato)$Co(NH_3)_5^{2+}$ (**61**).[502] It was shown via ^{15}N NMR that the isomerization was intramolecular and proceeded via η^2 π-bonded intermediates.[502] Rates of the exchange of aqua and hydroxo ligands coordinated to Co(III) amine complexes were examined

via ^{17}O NMR.[503] These complexes contained the tetradentate ligands such as cyclen [cylen = 1,4,7,10-tetraazacyclododecane (**62$_H$**)], *N*-mecyclen [*N*-mecyclen = 1-methyl-1,4,7,10-tetraazacyclododecane (**62$_{Me}$**)], and tren [tren = tris(2-aminoethyl)amine (**63**)].

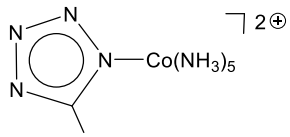

(**61**)

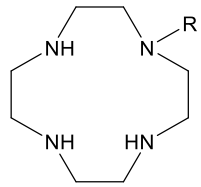

R = H, cylen (**62$_H$**)
Me, *N*-mecyclen (**62$_{Me}$**)

(**62$_H$ and 62$_{Me}$**)

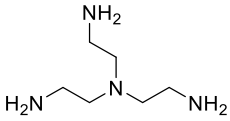

tren

(**63**)

8.2. *Rhodium complexes*

^{103}Rh NMR is one of most widely used transition metal NMR spectroscopies, in part because Rh is used extensively in catalysis. However, ^{103}Rh NMR was challenging mostly due to its low Ξ value and low relative receptivities/sensitivity (Table 11).[69]

^{103}Rh NMR was reviewed in 2004,[427] covering experimental techniques for the insensitive ^{103}Rh detection, use of ^{103}Rh NMR in coordination and organometallic chemistry, and calculations of ^{103}Rh shifts. Another detailed review was published in 2008 about ^{103}Rh NMR.[428] NMR of ^{103}Rh and ligand donor atoms in metal complexes in aqueous solutions was reviewed in 2016.[399] The current brief review will focus on the publications in 2008-2019.

It is noted that the frequency ratio $\Xi(^{103}Rh)$ = 3.186447% [based $Rh(acac)_3$ in saturated $CDCl_3$], recommended by IUPAC in 2001[26] (and updated in 2008[27]), was used in reporting ^{103}Rh shifts of compounds.[28-31] As discussed earlier, this is a unified scale to report NMR chemical shifts of a given nuclide relative to the ^1H resonance of dilute $SiMe_4$ in $CDCl_3$.[26] Advantage of the unified scale is that its use avoids direct handling of any secondary references.[26] The Ξ value was earlier set at 3.160000% for Rh metal,[1,427] which is an alternative value

recommended by IUPAC.[26] Since most ^{103}Rh chemical shifts were measured using the earlier Ξ = 3.160000% scale, we will specifically point out chemical shifts obtained on the new Ξ = 3.186447% scale or using $Rh(acac)_3$ as the external reference. How to convert the ^{103}Rh NMR shifts from the Ξ = 3.160000% scale to the IUPAC Ξ = 3.186447% scale was given in the literature.[28,428] Some publications listed ^{103}Rh shifts in both scales.[28-30]

Rh compounds using ^{103}Rh NMR that we found were typically at Rh(I) and Rh(III) oxidation states. ^{103}Rh shift range of Rh(I) compounds was from δ ~2400 to -2000, while the range for Rh(III) compounds was much larger from δ ~10000 to -1900.[1]

Coordination chemistry focused on Rh(III) complexes. Rh(III) speciation in 3-16 M HNO_3 was probed by ^{103}Rh and ^{15}N NMR, showing that $Rh(H_2O)_{6-n}(NO_3)_n^{3-n}$ (n = 1-4) were the only species in the solutions with the Rh concentration of 0.2-1.3 M.[504] For $Rh(H_2O)_5(NO_3)^{2+}$, ^{103}Rh and ^{15}N shifts were δ 1536 and -9.39, respectively.[504] In concentrated H_2SO_4, Rh(III) speciation studied by ^{103}Rh and ^{17}O NMR[505-506] showed that monomers, such as $Rh(H_2O)_4(SO_4)^+$ (^{103}Rh δ 9883; Ξ = 3.16%) and $Rh(SO_4)_3^{3-}$ (δ 9650), were not the predominant species.[505] Majority of the Rh(III) ions were in symmetric dimers such as $Rh_2(\mu\text{-}SO_4)_2(H_2O)_8^{2+}$ (δ 10069).[506] The ^{17}O NMR peaks at δ -138 and -142 were assigned for coordinated water ligands in $\mu\text{-}SO_4\text{-}Rh\text{-}H_2\mathit{O}$ and $H_2\mathit{O}\text{-}Rh\text{-}H_2\mathit{O}$ containing species, respectively.[506] Additional studies of Rh(III) speciation in H_2SO_4-H_3PO_4 solutions[507] and HF were conducted, showing, e.g., the formation of $Rh(H_2O)_5F^{2+}$ [^{103}Rh δ 2252 relative to $Rh(acac)_3$] and RhF_6^{3-} (δ -529).[508] Rh(III) porphyrin complex $[Rh(TPP)(PEtPh_2)_2]SbF_6$ was characterized by ^{103}Rh NMR using indirect detection, showing δ 2480, 2558 and 2590 (Ξ = 3.16%) at 213, 300 and 333 K, respectively.[509] Ruffled and planar porphyrin conformations were modelled by DFT simulations, leading to moderately accurate ^{103}Rh isotropic shielding tensors.

In organometallic chemistry, ^{103}Rh NMR was used to study both Rh(I) and Rh(III) complexes. In Rh(I) chemistry, cationic Rh(I) diphosphine η^6-arene complexes $[Rh(diphosphine)(\eta^6\text{-}C_6H_6)]BF_4$, such as $[Rh(dppe)(\eta^6\text{-}C_6H_6)]BF_4$ (^{103}Rh δ -1014, Ξ = 3.16%) and

[Rh(*R,R*-Me-DuPhos)(η^6-C_6H_6)]BF_4 [*R,R*-Me-DuPhos = (-)-1,2-bis(2*R*,5*R*-2,5-dimethylphospholano)benzene (**64**)] (^{103}Rh δ -1162), were studied by ^{31}P-^{103}Rh HMQC.[510] For analogous Rh(I) diphosphine cod complexes [Rh(diphosphine)(cod)]PF_6 (cod = 1,5-cyclooctadiene), ^{103}Rh NMR was found to be a powerful tool to assess the electronic and steric contribution of diphosphine ligands on seven complexes.[31] For the complexes with chelating, chiral diphosphine ligands *S,S*-DIOP [**65**, DIOP = 2,3-*O*-isopropylidene-2,3-dihydroxy-1,4-bis(diphenylphosphino)butane], *R*-BINAP [**66**, BINAP = 2,2′-bis(diphenylphosphino)-1,1′-binaphthyl] and *R,R*-Me-DuPhos (**64**), ^{103}Rh NMR was more informative than classical CO-stretching frequency measurements. The following selected ^{103}Rh shifts (Ξ = 3.186447%) were included: [Rh(dppe)(cod)]PF_6, δ -8809; [Rh(*S,S*-DIOP)(cod)]PF_6, δ -8555; [Rh(*R*-BINAP)(cod)]PF_6, δ -8397; [Rh(*S,S*-Me-DuPhos)(cod)]PF_6, δ -8756.[31] Remote C-F-Rh interaction was found in the Rh(I) complex **67**, which was used to obtain the ^{19}F-^{103}Rh HMQC spectrum [^{103}Rh δ -8044 (d, $J_{Rh\text{-}P}$ = 234 Hz, $J_{Rh\text{-}F}$ = 66 Hz) referenced to Rh(acac)$_3$, ^{19}F δ -129.8].[511]

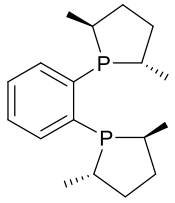

(**64**)

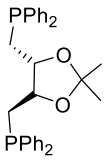

(**65**)

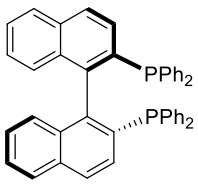

(**66**)

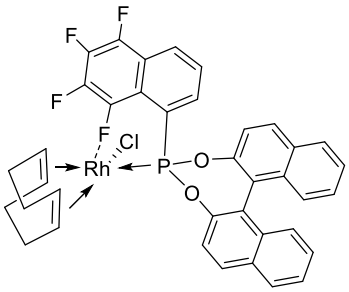

(**67**)

Additional Rh(I) organometallic complexes were studied by ^{103}Rh NMR. Phenyl-bridged dimer *S,S*-[Rh(ArPhPCH$_2$CH$_2$PPhAr)]$_2$(BF_4)$_2$ (Ar = *o*-OMe-C_6H_4) was characterized by ^{31}P-^{103}Rh and ^{1}H-^{103}Rh HMQC, giving ^{103}Rh δ -837.[512-513] This complex and its isomer were a precursor for the asymmetric hydrogenation of prochiral olefins without induction periods. Several Rh(I) β-

diketonates and β-aminoketonates were studied by ^{103}Rh NMR, giving shifts for, e.g., β-diketonates Rh(acac)(CO)(PPh_3) (acac = MeCOCHCOMe$^-$, δ 262), Rh(PhCOCHCOPh)(CO)(PPh_3) (δ 303), and β-aminoketonate Rh[MeCOCHC(NPh)Me](CO)(PPh_3) (δ 190).[514] The shifts of the Rh(I) β-diketonates and β-aminoketonates were compared with earlier reported analogs. Rh(I) complexes [nbd-$(CH_2)_4$-$EPh_2]_2Rh_2(\mu\text{-}Cl)_2$ [**68**, E = P, N; nbd-$(CH_2)_4$-EPh_2 = 2-substituted-2,5-norbornadiene] were catalysts for the polymerization of PhC≡CH and its derivatives.[515] ^{103}Rh NMR together with DFT calculations indicated that the phosphine analog [E = P, δ -7748 referenced to $Rh(acac)_3$, $^1J_{Rh\text{-}P}$ = 166 Hz] existed as mononuclear 16-electron species using the PPh_2 group as a ligand to the Rh(I) ion, while the amide analog (E = N) is a dimer with bridging chloride ligands (δ -7052, -7090). The two resonances for the latter are believed to be from *syn*- and *anti*- isomers and/or isomers with various combinations of (1*S*,4*R*)- and (1*R*,4*S*)-nbd derivatives.[515] Two types of Rh(I) norbornadiene derivatives serve as an initiator in the stereospecific polymerization of PhC≡CH: (a) (nbd)Rh[P(4-F-$C_6H_4)_3$](*o*-napth-C_6H_4) [^{103}Rh δ -7688 on the IUPAC Ξ scale and δ 547 if referenced to Rh metal (using the Ξ = 3.160000% scale); nbd = 2,5-norbornadiene, *o*-napth-C_6H_4 = 2-(naphthalen-2-yl)phenyl];[29] (b) α-Phenylvinylfluorenyl complexes, such as (nbd)Rh[P(4-F-$C_6H_4)_3$](CPh=CFlu) (**69**) [^{103}Rh δ -7862 using the IUPAC Ξ scale and δ 372 if referenced to Rh metal].[30] Rh(I) yldiide complex **70** showed the ^{103}Rh resonance at δ 259.[516] ^{103}Rh NMR was used to characterize the diaminocarbene complex **71** (δ 542) and its derivatives.[517] For the Rh(I) sulfonamido-phosphoramidite (**72**), NMR (^{15}N, ^{31}P and ^{103}Rh) and DFT studies were conducted to probe the AA′MM′XX′ 6 spin system.[518]

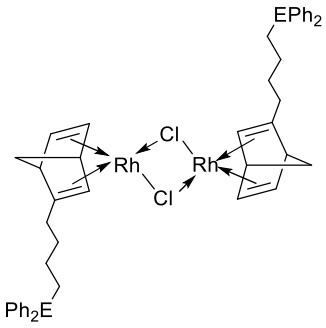

(**68**)

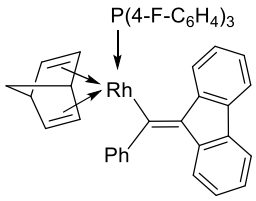

(**69**)

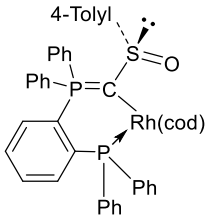

(**70**)

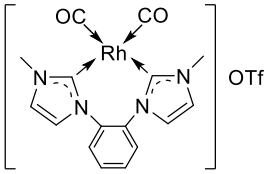

(**71**)

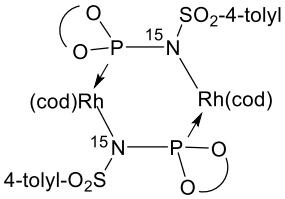

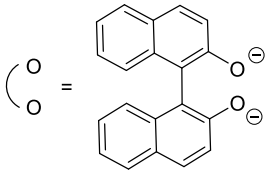

(**72**)

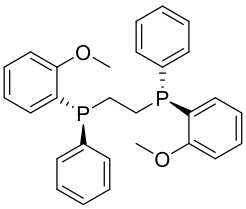

S,S-dipamp

(**73**)

Several Rh(I) trimers $[Rh_3(P,P)_3(\mu_3\text{-}OH)_x(\mu_3\text{-}OMe)_{2\text{-}x}]BF_4$ [e.g., P,P = *S,S*-dipamp = 1,2-ethanediylbis-[(2-methoxyphenyl)phenylphosphine (**73**)] were studied, including by ^{103}Rh NMR using ^{31}P-^{103}Rh HMQC, showing deshielded shifts from δ 97 for the dihydroxide (x = 2), to δ 212 for the mixed hydroxide methoxide (x = 1), and δ 360 for the dimethoxide (x = 0) complex.[513,519] These complexes were possible precatalysts for asymmetric hydrogenation through solvate derivatives. ^{103}Rh NMR was used to characterize Rh(I) heterobinuclear *s*-indacene complexes *anti*-[Cp*M(2,6-diethyl-4,8-dimethyls-indacenediide)Rh(η^4-cod)] (**74**, M = Fe, δ -275; Ru, δ -281).[520]

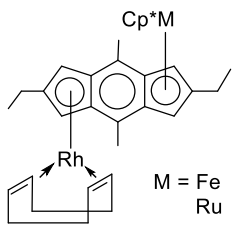

(**74**)

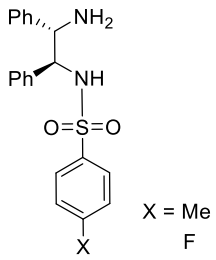

(**75**)

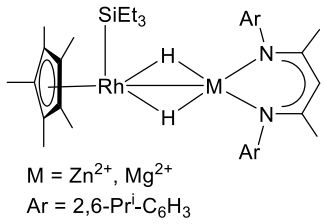

(**76**)

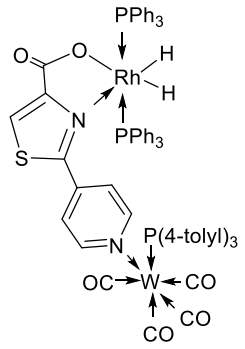

(**77**)

In studies of Rh(III) organometallic chemistry, ^{1}H-^{103}Rh HMBC, using the coupling to the Cp* ligand, led to ^{103}Rh shifts of Rh(III) Cp*RhCl(4-X-dpen) [4-X-dpen = 4-X-1,2-diphenylethylenediamine (**75**); X = Me, δ 2551; X = F, δ 2037 referenced to $Cp^*_2Rh_2Cl_2(\mu\text{-}Cl)_2$ at δ 2303 - This is at the Ξ 3.15% scale rather than Ξ 3.16% scale).[521] ^{1}H-^{15}N HMQC gave ^{15}N shifts of the two complexes: δ -263.6 (d, $^{1}J_{Rh\text{-}N}$ = 14 Hz, NH_2), -210.6 (d, $^{1}J_{Rh\text{-}N}$ = 18 Hz, 4-$MeC_6H_4SO_2N$) for the ^{15}N-labeled former (X = Me) and δ -263.8 (d, $^{1}J_{Rh\text{-}N}$ = 16 Hz, NH_2), -210.2 (d, $^{1}J_{Rh\text{-}N}$ = 21 Hz, 4-F-$C_6H_4SO_2N$) for the latter (X = F).[521] NMR studies of $Cp^*Rh(SiEt_3)(\mu\text{-}H)_2Al(H)$(mesityl-N-CMeCHCMe-N-mesityl) give ^{103}Rh (by ^{1}H-^{103}Rh HMQC using the coupling to the H^- ligand), ^{27}Al and ^{29}Si shifts of δ -1570, 144.7 and 38.6, respectively.[522] Its Mg^{2+} and Zn^{2+} analogs $Cp^*Rh(SiEt_3)(\mu\text{-}H)_2M$(Ar-N-CMeCHCMe-N-Ar) (**76**; M = Zn^{2+}, Mg^{2+}; Ar = 2,6-Pr^i_2-C_6H_3) give the following ^{103}Rh and ^{29}Si shifts: M = Zn^{2+} δ -1743 and 31.6 ($^{1}J_{Rh\text{-}Si}$ = 20.6 Hz); M = Mg^{2+} δ -1540 and 34.7.[522] For the binuclear rhodium and tungsten complex **77** with bridged by 2-(4-pyridyl)thiazole-4-carboxylate, its ^{103}Rh and ^{183}W shifts are δ 510 and δ 1463, respectively.[523]

In computational and theoretical studies, isotope shifts in ^{103}Rh NMR spectra of, e.g., $Rh^{35}Cl_n{}^{37}Cl_{5\text{-}n}(H_2O)^{2-}$ (n = 0-5), were probed by DFT.[524] DFT computations were also performed to provide a computational insight into the ^{103}Rh shift-structure correlations in Rh bis(phosphine) complexes $Rh(cod)(P,P)^+$ [P,P = dmpe, dppe, Me-DuPhos (**64**), DIOP (**65**), BINAP (**66**)].[525] The results showed a linear relationship between computed ^{103}Rh chemical shifts and the mean

Rh−P bond distances.

In the NMR studies of ligands in Rh complexes, ^{15}N NMR was used to follow the irradiation of $[Rh(^{15}NH_3)_5(^{15}NO_2)]^{2+}$ (δ -408, -416) in water in the presence of O_2.[526] The ^{15}N shifts and ^{103}Rh-^{15}N coupling constants for several rhodoximes with the general formula $RhX(Hdmg)_2L$ (**78**) (Hdmg = dimethylglyoximate; L= PPh, pyridine; X = e.g., Cl^-, Br^-, Bu^t, CH_2Cl, CH_2CF_3) were obtained using ^{15}N-^1H HSQC.[527] ^{15}N-^1H HSQC, HMQC, or HMBC NMR was also used to explore the effect of different *N*-containing adducts, such as pyridine or NEt_3, on $Rh_2(O_2CR)_4$ [R = CF_3, Me, $C(OMe)(CF_3)Ph$].[528-531] Complexation of phenylselenenyl-1-phenyl-1-propene (**79**) via the Se atom with $Rh_2(O_2CR)_4$ [R = $C(OMe)(CF_3)Ph$] was monitored via ^{77}Se NMR.[532] VT ^1H studies were also conducted on this system to determine the energy barrier for the selenide exchange when excess selenide was present.[532] $[Rh(C_2H_4)(dtpbb)]_2$ (**80**, dtpbb = di-tert-butylphosphido-boratabenzene) was synthesized and characterized via several NMR, including ^{11}B (δ 23.7) and ^{31}P (δ 23.7).[533]

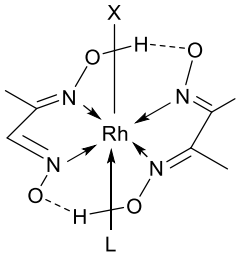

(**78**)

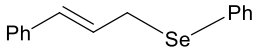

(**79**)

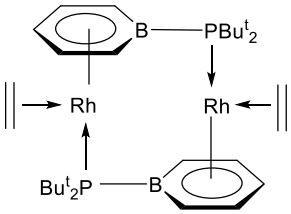

(**80**)

Irradiation of (η^5-$C_5H_4CF_3$)$Rh(PMe_3)(C_2H_4)$ and $CpRh(PR_3)(C_2H_4)$ (R = Me, Ph) in the presence of HBpin and B_2pin_2 (pin =1,2-$O_2C_2Me_4$) was investigated.[534] Photolysis of these Rh complexes with silanes, including $HSiEt_3$, $HSiPr^i_3$, $HSi(OMe)_3$, $HSiMe_2Et$, $HSiMeEt_2$, and H_2SiEt_2, were also conducted.[534] These reactions resulted in the elimination of C_2H_4 and B-H or Si-H oxidative additions to the Rh center.[534] The products were analyzed via NMR including ^{11}B

NMR for those containing B atoms and ^{31}P NMR for all products.[534] Water exchanges of several Rh complexes, such as the Rh trimer $[Rh_3(\mu_3\text{-}O)(\mu\text{-}O_2CCH_3)_6(OH_2)_3]^+$, were explored via ^{17}O NMR as a function of temperature and pressure.[535-537] ^{17}O and NOESY NMR studies were used to study the structures of $[Cp^*Rh(H_2O)_3]^{2+}$ and other Rh aqua complexes at various pH values.[538]

8.3. *Iridium complexes*

As indicated in the footnote of Table 11, we did not find a publication in 1990-2019 on the ^{191}Ir or ^{193}Ir NMR of a metal complex. It was not included in the 1991 book edited by Pregosin[1] or the 2016 review of NMR of platinum group metal complexes in aqueous solutions.[399]

Cp* Ir(III) complex **81** reacted with oxidant $NaIO_4$ [or $(NH_4)_2Ce(NO_3)_6$] forming a blue species (**81**, **Figure 5**) which was characterized by several techniques including ^{17}O NMR for the reaction conducted in $^{17}OH_2$.[539] The results suggested that **82** was an Ir(IV) species with the structure shown in **Figure 5**. The Cp* ligand in **81** was removed during the reactions, and the blue **82** was a catalyst for oxidation of C-H bonds to C-OH bonds and oxidation of water to O_2.[539]

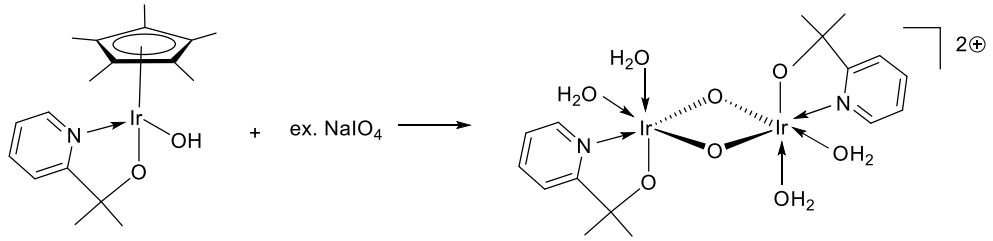

(**81**) (**82**)

Figure 5. Reaction of **81** with $NaIO_4$ to give **82**.

^{15}N NMR was used to analyze $Ir(H)(NH_3)_2(PEt_3)_3^{2+}$ (δ -473.0), $Ir(H)(NH_3)_3(PEt_3)_2^{2+}$ (δ -

425.3), and $Ir(H)(Cl)(NH_3)_2(PEt_3)_2^+$ (δ -461.2).[540] These complexes were found to undergo N-H/O-D scrambling when exposed to D_2O and were also studied via ^2D NMR.[540] Water exchange studies were performed on $Ir(H_2O)_6^{3+}$ and $Ir(H_2O)_5(OH)^{2+}$ via ^{17}O NMR as a function of temperature and pressure at several pH values.[541] The rate constant at 298 K of $[Ir(H_2O)_6]^{3+}$ was 1.1 x 10^{-10} s^{-1}. The exchange rate corresponded to a residence time of about 300 years for this exchange, indicating that the exchange was very slow.[541]

For the use of parahydrogen (*p*-H_2) in the SABRE (Signal Amplification by Reversible Exchange) method to hyperpolarize $[Ir(IMes)(H)_2L_3]Cl$ (IMes = 1,3-dimesitylimidazol-2-ylidene, L = substrate such as indazole or imidazole), see Section 13.6.

9. Group 10 (Ni, Pd and Pt)

Nuclear and NMR properties of the nuclides, including recommended and commonly used references, are given in Table 12. Publications on solution NMR of Group 10 metals are dominated by ^{195}Pt. This is largely because both ^{61}Ni and ^{105}Pd have rather large quadrupole moments, leading to broad resonances of their complexes in non-cubic symmetries. In addition, the low natural abundance of 1.1399% of ^{61}Ni and its small relative receptivities/sensitivity make it challenging to observe the ^{61}Ni NMR of metal complexes.

Table 12.[26] Nuclear and NMR properties of ^{61}Ni, ^{105}Pd and ^{195}Pt

Nuclide	Natural abun-dance (%)[a]	Spin	Relative receptivity		Gyromagnetic ratio (10^7) (rad s^{-1} T^{-1})	Quadrupole moment *Q* (fm^2)	*Ξ* (and frequency, MHz; ^1H = 100.0000 MHz, 2.3488 T)	Reference sample
			D^H (^1H = 1.00)	D^C (^{13}C = 1.00)				
^{61}Ni	1.1399	3/2	4.09 x 10^{-5}	0.240	-2.3948	16.2	8.936051	$Ni(CO)_4$ (neat/C_6D_6)
^{105}Pd	22.33	5/2	2.53 x 10^{-4}	1.49	-1.23	66.0	4.576100	K_2PdCl_6

								(aq)
^{195}Pt	33.78	1/2	3.51 x 10^{-3}	20.7	5.8385	-	21.496784	Na_2PtCl_6 (aq)

[a] Unless noted, the isotopes are stable. The natural abundances are based on the NIST data.[25]

9.1. *Nickel complexes*

^{61}Ni NMR shifts of 22 Ni(0) carbonyl phosphine complexes were recorded with the use of special solenoid glass sample tubes and a solenoid probehead.[542] The complexes included 11 tricarbonyl compounds $Ni(CO)_3(PR_3)$ [including R_3 = Me_3, ^{61}Ni δ 25.8; Ph_3, δ 24.2; Cy_3, δ -11.2; Cy_2H, δ -23.5; Ph_2Cl, δ 48.5; $(OPh)_3$, -129.5] and $[Ni(CO)_3]_2$(μ-dppe) (δ -2.1). Other 11 complexes were dicarbonyl compounds $Ni(CO)_2(PR_3)_2$ with a larger ^{61}Ni shift range. These complexes included $Ni(CO)_2(PMe_3)_2$ (δ 104.0), $Ni(CO)_2$(dppe) (δ -160.5), and $Ni(CO)_2[P(OPh)_3]_2$ (δ -294.0).[542] Description of special solenoid glass sample tubes and a solenoid probehead was provided. ^{61}Ni NMR shifts of $Ni(PMe_3)_4$ (δ 35, 300 K), all-*trans*-cyclododecatriene (**83**, δ 75) and all-*cis*-cyclododecatriene (**84**, δ 22) were reported.[543] DFT computations of the substituent effects on ^{61}Ni NMR chemical shifts of several Ni(0) complexes were performed.[543]

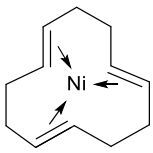

(**83**)

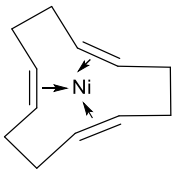

(**84**)

^{31}P and ^{11}B NMR studies of σ-borane nickel complexes, such as diphosphine complexes $(R_2PCH_2CH_2PR_2)Ni(H\text{-}BEt_2)$ (R = Pr^i, Bu^t, Cy), were discussed in a 2008 review.[139]

9.2. *Palladium complexes*

^{105}Pd NMR of Pd(IV) H_2PdCl_6 [in concentrated HCl containing dissolved Cl_2 or aqua

regia (HCl : HNO_3 = 3 : 1)] and H_2PdBr_6 (in a 1:1 mixture of HBr and HNO_3) was first reported in 1984 by Fedotov and Likholobov.[544] In 2016, Fedotov gave more details of ^{105}Pd NMR of K_2PdCl_6 dissolved in concentrated HCl, showing that the resonance shifted to δ 53 at 323 K from δ 0 at 300 K.[399] The temperature coefficient of 2.3 ppm/K for ^{105}Pd NMR of K_2PdCl_6 was close to that of ^{103}Rh NMR of $RhCl_6^{3-}$. ^{105}Pd shift of Pd(II) H_2PdCl_4 in concentrated HCl containing dissolved Cl_2 was found to be δ 28.[399]

Mechanisms of H_2O exchange were studied in the $Pd(OH_2)_4^{2+}$ (^{17}O δ -132), including the measurements of the rates and energy exchange parameters.[399,545]

For the use rapid-injection NMR to study pre-transmetalation intermediates with Pd(II)-O-B linkages, such as (4-F-C_6H_4)(Pr^i_3P)$_2$Pd-O-B(OH)(4-F-C_6H_4),[546-547] in the Suzuki-Miyaura reaction, see Section 13.8.

The cluster complex [K(2,2,2-crypt)]$_4$[Pd_2@Sn_{18}] (2,2,2-crypt = $N(CH_2CH_2OCH_2CH_2OCH_2CH_2)_3N$) was synthesized and characterized by ^{119}Sn NMR (δ -751.3).[548] ^{77}Se NMR was used to characterize palladacycle complexes formed from the reactions of Li_2PdCl_4 with $C_{10}H_7$-1-CH=N-CH_2CH_2SePh or $C_{10}H_7$-1-CH_2NH-CH_2CH_2SePh. The Pd complexes showed ^{77}Se shifts at δ 326.9 and 486.2, respectively.[549]

^{15}N and ^{1}H-^{15}N HMBC NMR were used to characterize Pd complexes, helping to determine their structures, and/or investigate their catalytic activity.[550-554] For example, the coordination mode of 4,5-diazafluoren-9-one (daf) with $Pd(OAc)_2$ was investigated using ^{1}H-^{15}N HMBC, TOCSY, and ROESY.[552] It was found that many complexes could form.[552] These complexes included monomeric and dimeric complexes with chelating, monodentate, and bridging binding modes.[552] DOSY was also used to identify several aggregates including pentameric and hexameric aggregates of systems made via self-assembly reactions of, e.g., N,N′-bis[4-(4-pyridyl)phenyl]acenaphthenequinonediimine (**85**) with Pd(II) diphosphine complexes such as [Pd(dppp)(H_2O)$_2$](OTf)$_2$ [dppp = $Ph_2P(CH_2)_3PPh_2$].[550]

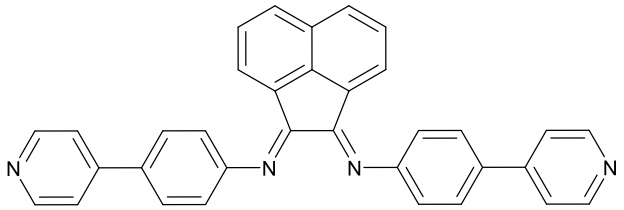

(**85**)

In the reaction of $PdCl_2$ with tppts [tppts = $P(2\text{-}SO_3Na\text{-}C_6H_4)_3$], ^{17}O enriched H_2O was found to give the complex $[PdCl(tppts)_3]^+$ as well as Pd(II) reduction to Pd(0).[555] The reactions were analyzed via ^{17}O, ^{31}P, and ^{35}Cl NMR.[555]

Complexes $MLi_4[Si(3,5\text{-}Me_2pz)_3]_4$ (**86**) (M = Pd, Pt; 3,5-Me_2pz = 3,5-dimethylpyrazolyl) were characterized via several NMR spectroscopies, including ^7Li, ^7Li-^{15}N gHMQC, ^1H-^{29}Si gHMQC, and ^7Li-^{195}Pt HMQC (M = Pd, δ_{Li} 4.23, δ_N 235.4 and 288.0, δ_{Si} 20.3; M = Pt, δ_{Li} 5.22, δ_N 236.2 and 288.9, δ_{Si} 3.7, δ_{Pt} -6639).[556]

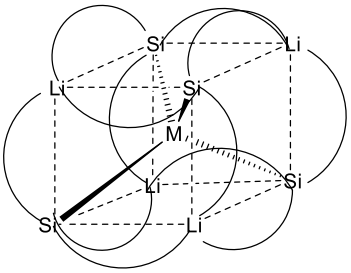

M = Pd or Pt

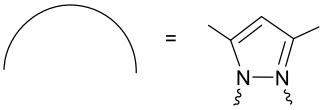

(**86**)

9.3. *Platinum complexes*

^{195}Pt NMR is one of most widely used transition metal NMR spectroscopies[557-558] primarily because platinum chemistry encompasses many areas, including catalysis and

anticancer drugs.[559] ^{195}Pt NMR shits span a wide range of 13000 ppm.[558] ^{195}Pt NMR was reviewed in 2006[557] and 2007.[558] NMR of ^{195}Pt and ligand donor atoms in metal complexes in aqueous solutions was reviewed in 2016.[399] In addition, chemometric uses of ^{195}Pt NMR were reviewed in 2006.[559] Thus, the current article focuses on the publications between 2006 and 2019.

Pt complexes studied by ^{195}Pt NMR include those at 0, I, II, III and IV oxidation states. Among the publication discussed below, a small number of papers were about organometallic complexes containing Pt-C bonds. Thus, we will discuss here the publications on ^{195}Pt NMR by oxidation states of the Pt complexes, including both coordination and organometallic compounds.

Pt(0) complexes $[(Cy_3P)_2Pt{\rightarrow}(\mu\text{-}M){\leftarrow}Pt(PCy_3)_2][B(3,5\text{-}Cl_2\text{-}C_6H_3)_4]$ (M = Ag, Tl) containing bridging, unsupported Ag^+ and Tl^+ cations, were prepared from $Pt(PCy_3)_2$ and $MB(3,5\text{-}C_6H_3Cl_2)_4$.[560] ^{195}Pt NMR spectra of the two products, at δ -4853 and -4697, respectively, revealed a large deshielded shift compared to the starting material $Pt(PCy_3)_2$ (δ -6501), as a result of donating electrons from Pt(0) atoms to M^+ cation.[560]

^{195}Pt NMR was used to characterize the derivatives of Pt(I) phosphinito-bridged dimer $(Cy_2HP)Pt(\mu\text{-}PCy_2)(\kappa^2O,P\text{-}\mu\text{-}O\text{-}PCy_2)Pt(PHCy_2)$ (**87**, **Figure 6**; ^{195}Pt NMR: δ_{Pt^A} -4798; δ_{Pt^B} -5205) with a Pt-Pt bond,[561] such as its sulfur derivative $Cy_2HP)Pt(\mu\text{-}PCy_2)(\kappa^2S,P\text{-}\mu\text{-}S\text{-}PCy_2)Pt(PHCy_2)$ [^{195}Pt NMR: Pt^A, δ -5218; Pt^B, δ -5376]. For the diphosphinito-bridged dimer $(Cy_3P)Pt(\mu\text{-}PCy_2)_2Pt(PCy_3)$ with a Pt-Pt bond, ^{195}Pt resonance was observed at δ -5554.[561]

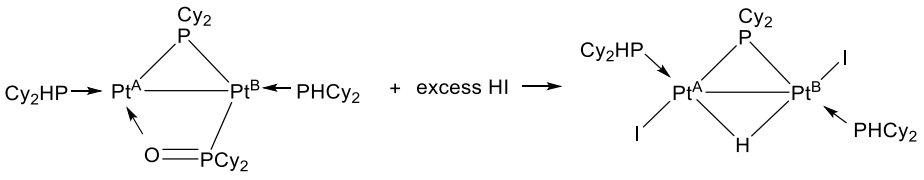

(**87**) (**88**)

Figure 6. Reaction of **87** with HI to give the hydride-bridged complex **88**. The bridging phosphinito ligand uses one σ bond and one dative bond to bind to the Pt atoms, although it is a nearly symmetric bridging ligand in **87**.

In Pt(II) chemistry, protonation of Pt(I) **87** with Brønsted acids led to oxidation of the Pt(I) complex to Pt(II) hydride-bridged Pt-Pt complexes, such as *anti*-I(Cy_2HP)Pt(μ-PCy_2)(μ-H)Pt($PHCy_2$)I (**88**, **Figure 6**; ^{195}Pt NMR: Pt_1, δ -5723, Pt_2, δ -5550).[562] NMR studies, including ^{195}Pt and ^{15}N, were used to characterize Pt(II) chloride complexes (N,N)$PtCl_2$ with pyridine (py), 2,2′-bipyridine (bpy) and 1,10-phenanthroline (phen).[563] The ^{195}Pt and ^{15}N shifts of the complexes are given in Table 13. Various alkyl and aryl derivatives of bpy and phen, such as 5,5′-dimethyl-2,2′-bipyridine (5,5′-dimethyl-bipy), 6,6′-dimethyl-2,2′-bipyridine (6,6′-dimethyl-bipy), and 2,9-dimethyl-1,10-phenanthroline (2,9-dimethyl-phen), were also prepared and probed by NMR.[564] The ^{195}Pt and ^{15}N shifts of the complexes are given in Table 13. ^{195}Pt shifts of square-planar Pt(II) complexes $PtX_mY_{4-m}^{2-}$ ($1 \leq m \leq 4$; X, Y = Cl^-, Br^-, I^-)[565] and Pt(η^2-CH_2=CH_2)(2,9-dimethyl-phen)XY[565-567] showed an inverse linear relationship with the overall sum of ionic radii of halide ligands, suggesting the existence of electric pseudo-ring currents circulating around the Pt–X axes and modulated by the ionic radius of the coordinated halides.[566-567] Pt(II) complex *trans*(N,N)-[Pt(2ppy∗)(2-phenylpyridine)Cl] with an N(1),C(2′)-chelated, deprotonated 2-phenylpyridine ligand (2ppy∗) was also studied.[568] Pt(II) complex [Pt(NH_3)$_3$(1-methylcytosine)](ClO_4)$_2$, containing a mono-dentate 1-methylcytosine (**89**) ligand, shows ^{195}Pt shift at δ -2601.[569] Pt(II)-Ag(I) complexes in **Figure 7** were prepared and the more shielded shifts of the ^{195}Pt resonances in the complexes [than those of the starting Pt(II) complexes] were interpreted as the result of no direct Pt(II) to Ag(I) binding in the products.[570] ^{195}Pt NMR was used to characterize Pt(II) imine and/or oxadiazoline complexes, such as *trans*-$PtCl_2$(mip)(N≡CCH_2CO_2Me) [**90**; δ -2250; mip = NH=C(CH_2CO_2Me)ON=CMe_2 using its imine N atom to bind to the Pt(II) ion] and *cis*-$PtCl_2$(mip)$_2$ (δ -2068).[571] ^{195}Pt shifts of these complexes

were in the δ -2050 to -2330 range.

Table 13. ^{195}Pt and ^{15}N NMR shifts of Pt(II) alkyl and aryl derivatives of bpy and phen[563-564]

Complexes	^{195}Pt shifts (δ)	^{15}N shifts
trans-Pt(py)$_2$Cl$_2$	-1952	-182.3
cis-Pt(py)$_2$Cl$_2$	-2002	-168.0
Pt(bpy)Cl$_2$	-2331	-177.9
Pt(phen)Cl$_2$	-2345	-180.0
Pt(5,5′-dimethyl-bpy)$_2$Cl$_2$	-2315	-178.7
Pt(6,6′-dimethyl-bipy)Cl$_2$	-1888	-167.0
Pt(2,9-dimethyl-phen)Cl$_2$	-1901	-175.2

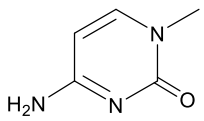

1-methylcytosine

(**89**)

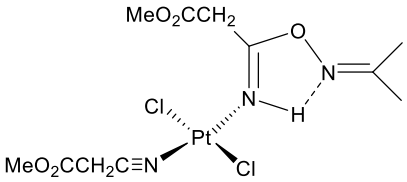

(**90**)

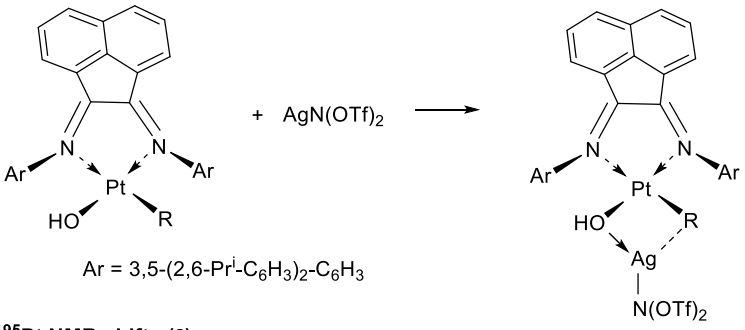

Ar = 3,5-(2,6-Pr^i-C$_6$H$_3$)$_2$-C$_6$H$_3$

^{195}Pt NMR shifts (δ)		
R = OH	-547	-1276
R = Ph	-1485	-2242
R = Me	-1272	-2167

Figure 7. Formation of Pt(II)–Ag(I) complexes and a comparison of ^{195}Pt shifts of the starting

materials and products.

Bioinorganic Pt(II) complexes were also characterized by ^{195}Pt NMR. Mixing *cis*-[Pt(NH_3)$_2$(9-EtGH)Cl](NO_3) containing mononucleobase 9-ethylguanine (9-EtGH = **91**) with 5′-guanosine monophosphate (5′-GMP = **92**) and *N*-acetylmethionine (*N*-ac-L-Met = **93**) in water led to the Cl^- replacement and formation of *cis*-[Pt(NH_3)$_2$(9-EtGH)(5′-GMP)]$^{2+}$ and *cis*-[Pt(NH_3)$_2$(9-EtGH)(*N*-ac-L-Met)]$^{2+}$, showing ^{195}Pt peaks at δ -2432 and -2983, respectively.[572] Reaction of [Pt(dien)Cl]Cl [dien = diethylenetriamine HN($CH_2CH_2NH_2$)$_2$] with selenomethionine [MeSe(CH_2)$_2$CH(NH_2)COOH, a naturally occurring amino acid, abbreviated as SeMet], gave Pt(dien)(SeMet)$^{2+}$ containing a Pt-Se bond as a product, showing ^{195}Pt shift at δ -3420.[573] Analogs of the Pt-Se complex were also characterized by ^{195}Pt NMR.[573] Reaction of Pt(PPh_3)$_4$ with dipyrimidyldiselenide (**94**) led to the oxidation of the Pt(0) complex to the pyrimidyldiselenide Pt(II) complex *trans*-Pt($SeC_4H_3N_2$)$_2$(PPh_3)$_2$ containing two Pt-Se bonds with ^{195}Pt shift at δ -5120 as a triplet due to coupling with two equivalent ^{31}P nuclei.[574]

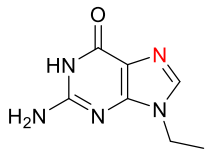

9-EtGH

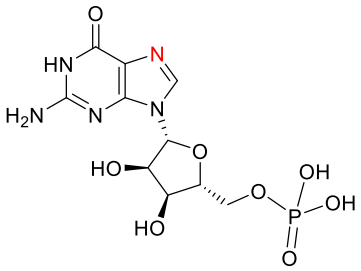

5'-GMP

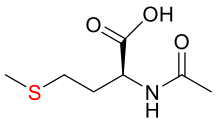

N-acetylmethionine

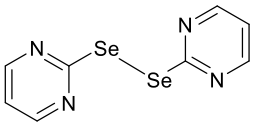

The atoms that form datives bonds with Pt(II) ions are shown in red color.

(**91**) (**92**) (**93**) (**94**)

Pt(II) complex (**95**) with an opening "jaw" ligand dative-bonded to the Pt(II) ion in **Figure 8-A** gave its ^{1}H-decoupled ^{195}Pt NMR resonance at δ -4068 as a triplet of a triplet of a triplet through couplings to three types of P atoms with $^1J_{Pt\text{-}P}$ = 3165 Hz, $^2J_{Pt\text{-}P}$ = 204 Hz and $^3J_{Pt\text{-}P}$ = 57

Hz (**Figure 8-B**).[575] In another Pt(II) complex (**96**) with an opening "jaw" ligand that was σ-bonded to the Pt(II) ion in **Figure 8-C**, ^{195}Pt NMR resonance was observed at δ -4826.[576]

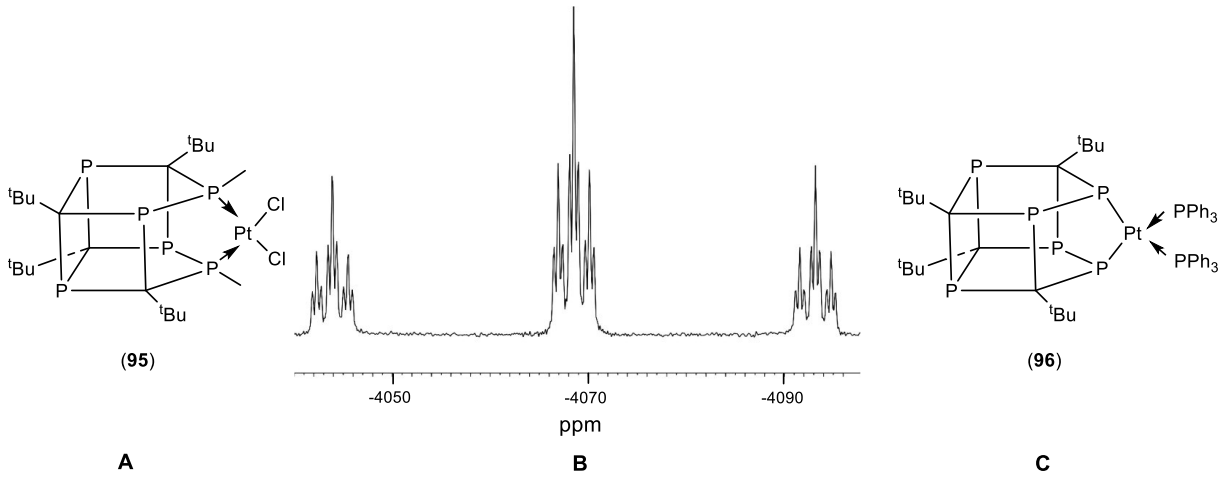

Figure 8. (**A**) Pt(II) complex **95** with an opening ''jaw" ligand dative-bonded to a Pt(II) ion; (**B**) ^{1}H-decoupled ^{195}Pt NMR spectrum of **95**; (**C**) Pt(II) complex **96** with an opening ''jaw" ligand σ-bonded to a Pt(II) ion.

^{195}Pt NMR was used to characterize Pt(II) organometallic complexes, including Pt(COMe)Cl(PPh$_2$[*o*-CH(O$_2$C$_2$H$_4$)-C$_6$H$_4$]) (**97**, δ -3509) and Pt(COMe)Cl(PPh$_2$[*o*-CH(O$_2$C$_2$H$_4$)-C$_6$H$_4$])$_2$ (**98**, δ -3847).[577] Pt(II) complex **99**, containing a diselenastanna-annelated dicarba-*closo*-dodecaborane ligand, was characterized by multinuclear NMR, giving ^{195}Pt (δ -574 referenced to Ξ = 21.4% which is different from 21.496784 MHz in Table 12), ^{119}Sn (δ 58), and ^{31}P shifts (δ 23.8 for P^{A} and 14.6 for P^{B}).[578] An analog of **99** containing the SnPh$_2$ group was also studied by NMR.[578] Stilbene-based Pt(II) complex **100** in **Figure 9** shows long-range through-bond communication, as multi-nuclear NMR studies show.[579] This complex is unstable, converting to the product **101** through oxidative addition of the Br-C bond.

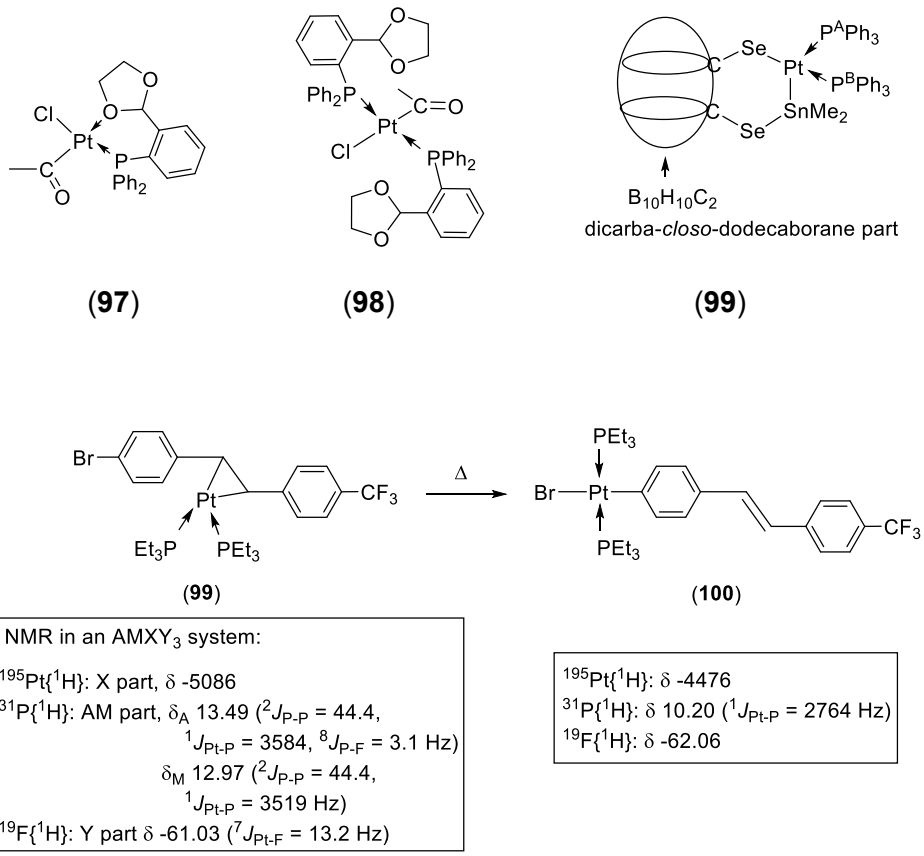

Figure 9. Conversion of **100** to **101** and their NMR properties.

For Pt(III) chemistry, ^{195}Pt and ^{205}Tl NMR were used to characterize $(O_3N)(H_3N)_2Pt(\mu\text{-}NHCOBu^t)_2Tl(NO_3)_2(MeOH)$ (^{195}Pt, δ -980; ^{205}Tl, δ -874; $^1J_{Tl\text{-}Pt}$ = 1.468 x 10^5 Hz) and $[[(O_3N)(H_3N)_2Pt(\mu\text{-}NHCOBu^t)_2]_2Tl]PF_6$ (^{195}Pt, δ -1133; ^{205}Tl, δ -1562; $^1J_{Tl\text{-}Pt}$ = 8.884 x 10^4 Hz), which contain one Pt-Tl bond and two Pt-Tl bonds, respectively.[580] The large $^1J_{Tl\text{-}Pt}$ values for the two complexes are consistent with the presence of Pt-Tl bonds in the complexes. X-ray photoelectron spectra (XPS) studies show that the Pt oxidation states are close to that of Pt(III).[580] A series of head-to-head and head-to-tail amidate-bridged Pt(III) dinuclear complexes, such as **102** and **103**, were probed by ^{195}Pt NMR.[581] The chemical shifts of the two Pt ions (δ 393 and -844) in the head-to-head isomer **102**, in comparison to δ -265 of the head-to-tail isomer **103**, suggested that the Pt^A and Pt^B ions were likely at IV and II oxidations,

respectively.[581] ^{195}Pt NMR was used to study several mixed Pt(II),Pt(III) phosphide derivatives, such as $(C_6F_5)_2Pt^A(\mu\text{-}PPh_2)_2Pt^B(\mu\text{-}PPh_2)_2Pt^C(C_6F_5)_2$ containing the $Pt^A(III)$-$Pt^B(III)$ bond (δ, Pt^A -5336; Pt^B -4393; Pt^C -3783), and to compare the shifts with those of Pt(II) phosphide complexes.[582]

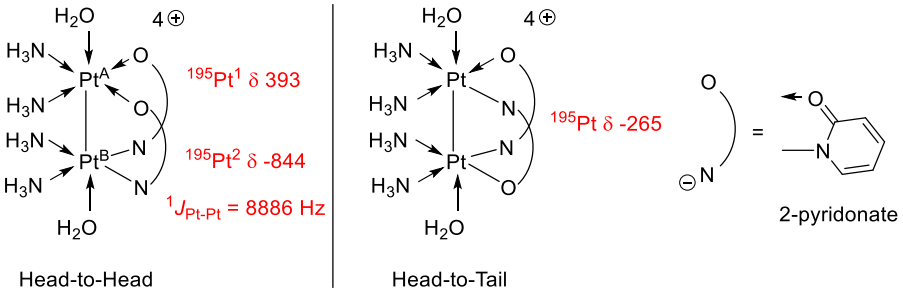

(**102**) (**103**)

For Pt(IV) chemistry, ^{195}Pt NMR was used to investigate the distribution of Pt(IV) products after oxidation of $PtCl_4^{2-}$ by $NaClO_3$, $NaBrO_3$, and H_2O_2 in acidic solutions and, for comparison, by H_2O_2 in water.[583] $^{35/37}$Cl and $^{16/18}$O isotope-resolved ^{195}Pt NMR spectra at 128.8 MHz showed unique spectroscopic 'fingerprints' for unambiguous speciation of $PtCl_m(H_2O)_{6-m}^{4-m}$ (m = 2–5) complexes in an acidic aqueous solution.[584] The detailed fine structure of ^{195}Pt resonance was readily accounted for by an isotopologue and isotopomer model for each complex, showing noticeable differences between stereoisomer pairs such as the *cis/trans*- and *fac/mer*-complexes.[584] For hydroxide derivatives $PtCl_n(OH)_{6-n}^{2-}$ (n = 1-5), analysis of their $^{35/37}$Cl and $^{16/18}$O isotope-resolved ^{195}Pt NMR spectra showed that the greater *trans* influence of the ligands in the order $OH^- > Cl^- > H_2O$ resulted in slightly longer Pt−Cl bonds *trans* to the OH^- ligands in $PtCl_n(OH)_{6-n}^{2-}$ (n = 1-5) (n = 1-5), resulting in the absence of isotopomer effects in contrast to $PtCl_m(H_2O)_{6-m}^{4-m}$ (m = 2–5).[585] ^{195}Pt shifts of $PtX_mY_{6-m}^{2-}$ (1 ≤ m ≤ 6; X, Y = F^-, Cl^-, Br^-, I^-) showed an inverse linear relationship with the overall sum of ionic radii of halide ligands,[565-566] as Pt(II) complexes $PtX_mY_{4-m}^{2-}$ (1 ≤ m ≤ 4; X, Y = Cl^-, Br^-, ^-I)[565] and $Pt(\eta^2\text{-}CH_2{=}CH_2)$(2,9-dimethyl-

phen)XY[565-567] discussed earlier in the paragraph on Pt(II) chemistry. ^{195}Pt NMR study of the speciation of aqueous $PtCl_6^{2-}$, $PtBr_6^{2-}$, and the mixed $PtCl_{6-m}Br_m^{2-}$ (m = 0-6) anions by OH^- substitution was probed.[586] Of the 56 possible $PtCl_{6-m-n}Br_m(OH)_n^{2-}$ (m, n = 0-6) complex anions in solution under dynamic conditions, ^{195}Pt shifts of 52 observable species [spanning over the range of δ 3275 for $Pt(OH)_6^{2-}$ to -1882 for $PtBr_6^{2-}$] were assigned, 33 of which had not been reported previously.[586] ^{195}Pt NMR was used to characterize *cis* bis-stibine complex $PtMe_3I[MeN(CH_2\text{-}2\text{-}C_6H_4SbMe_2)_2]$ (δ -4400) prepared from $PtMe_3I$ and the bis-stibine compound.[265]

Many theoretical and computational studies were conducted in 2007-2019, often involving different DFT methods, to investigate ^{195}Pt NMR shifts/shielings in a variety of complexes.[587-601] The complexes included anticancer agents,[593-594,598-599,601] Pt=O compounds,[587,589] $PtX_mY_{6-m}^{2-}$ (1 ≤ m ≤ 6; X, Y = F^-, Cl^-, Br^-, I^-),[588,590] products from speciation and hydration/solvation of PtX_6^{2-} (X = Cl^-, Br^-),[592,600] and azides (Pt-N_3).[596] Correlation between ^{195}Pt shifts and electronic transitions among *d* orbitals in pincer NCN Pt(II) complexes was studied.[591] ^{195}Pt NMR of $Pt(NHC\text{-}Dip_2)(SiMe_3)_2$ [**104**, NHC-Dip_2 = 2,6-diisopropylphenyl-containing *N*-heterocyclic carbine] with an unusual Y-shaped structure was significantly different from those of Pt(II) complexes but close to those of typical Pt(0) complexes. Theoretical study showed that $Pt(NHC\text{-}Dip_2)(SiMe_3)_2$ was more likely a Pt(0) σ-disilane (**105**) rather than a Pt(II) disilyl complex (**104**).[597]

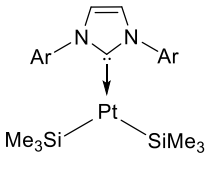

(**104**)

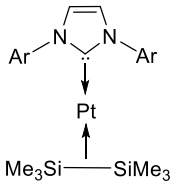

Ar = 2,6-Pr^i_2-C_6H_3

(**105**)

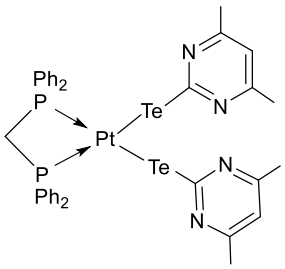

(**106**)

Reactions of Pt(0) $Pt(C_2H_4)(PEt_3)_2$ with diselenides RSeSeR [R = Ph, Fc (ferrocenyl)] gave oxidative addition products *trans*-$Pt(SeR)_2(PEt_3)_2$, giving ^{77}Se NMR shifts of the products [R = Ph, δ 78; R = Fc (Fc = ferrocenyl), δ -47 referenced to $SeMe_2$].[602] $Pt[TeC_4H(4,6\text{-}Me)_2N2]_2(dppm)$ (**106**) with two pyrimidyltelluride ligands gave the ^{125}Te resonance at δ -472 (referenced to $TeMe_2$).[574]

^{1}H-^{195}Pt HMBC of a Pt(IV) mono azido mono triazolato complex (**107**) revealed two ^{195}Pt environments (δ 689 and 785) that showed the complex was in a dynamic exchange (**Figure 10**).[603] This complex was also characterized by other NMR techniques including COSY and ROESY.[603]

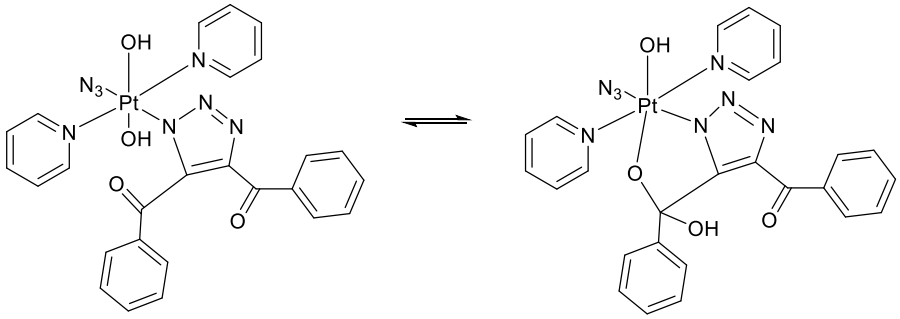

Figure 10. Dynamic exchange between two isomers of complex **107**

Pt(II) complexes with selenium adducts of germa- and stanna-*closo*-dodecaborate $Pt(dppp)(Se\text{-}GeB_{11}H_{11})_2^{2-}$ and $Pt(dppp)(Se\text{-}SnB_{11}H_{11})_2^{2-}$ (**108**) were characterized by NMR including ^{31}P [δ -3.3 (Ge complex) and -1.8 (Sn complex)], ^{77}Se [δ -227.9 (Ge complex), -108.3 (Sn complex)], ^{195}Pt [δ -4777 (Ge complex), -4726 (Sn complex)], and ^{119}Sn [δ -338 (Sn complex)].[604]

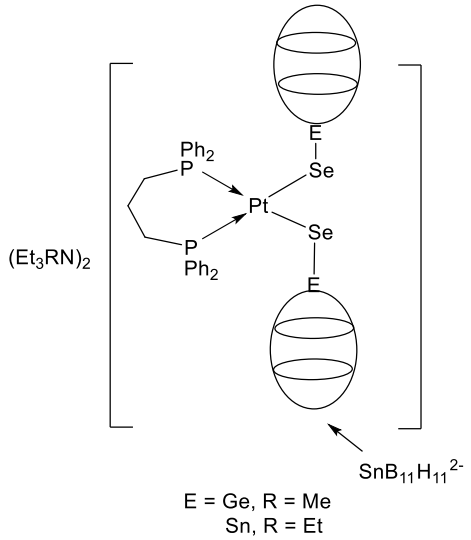

(**108**)

A series of organotin platinum complexes, such as *cis*- and *trans*-$PtPh(Sn_2Ph_5)(PEt_3)_2$ and Pt complexes with bidentate bisstannylene ligands, were synthesized and characterized via ^{31}P and ^{119}Sn NMR.[605-606]

In order to generate a silylene complex, (dippe)PtMeCl [dippe = $Pr^i_2P(CH_2)_2PPr^i_2$] reacted with $(thf)_2LiSiHMes_2$ (Mes = 2,4,6-Me_3-C_6H_2). The product was found to be a silyl complex, (dippe)PtMe($SiHMes_2$), and was analyzed by NMR (^{29}Si, δ -28.70; ^{31}P, δ 66.54).[607] Reaction of the silyl complex (dippe)PtMe($SiHMes_2$) with $B(C_6F_5)_3$ yielded the silylene hydride [(dippe)(H)Pt(=$SiMes_2$)][$MeB(C_6F_5)_3$] (^{31}P, δ 77.2; ^{19}F, δ -132.2, -165.1, -167.2; ^{29}Si, 338.1).[607]

Both 1- and 2-D ^{15}N NMR were used to study Pt complexes, including anticancer compounds, Pt-DNA complexes, *cis*-platin, and other Pt complexes with Pt-N interactions.[608-622] For example, hydrolysis of the ^{15}N-labeled anticancer complexes *cis*-$PtCl_2(NH_3)$(2-picoline) and *cis*-$PtCl_2(NH_3)$(3-picoline) were monitored via ^1H-^{15}N HSQC.[614] After 1 hour, the cross-peaks (δ_H/δ_N) in *cis*-$PtCl_2(NH_3)$(2-picoline) went from δ_H (4.15)/δ_N (-66.52) to δ_H (4.40)/δ_N (-64.41) and δ_H (4.32)/δ_N (-87.25).[614] These peaks pertained to the hydrolysis of the Cl^- *trans* to the 2-picoline and NH_3 ligands, respectively.[614] After 2.5 hours, both Cl^- ligands were replaced as shown by a

new cross-peak at δ_H (4.41)/δ_N (-82.91).[614] A similar experiment was conducted on the *cis*-$PtCl_2(NH_3)$(3-picoline), and the results were compared.[614] Both of the Cl^- ligands in the 2-picoline Pt complex hydrolyzed more slowly than those in the 3-picoline Pt complex.[614] In the 3-picoline Pt complex, the Cl^- ligand *trans* to NH_3 hydrolysed faster than that *trans* to 3-picoline.[614]

A family of platinum bis-boryl complexes, such as $Pt(PPh_3)_2$(Bpin)(Bcat) (**109**, pin = 1,2-$O_2C_2Me_4$, cat = 1,2-$O_2C_6H_4$), were prepared via oxidative addition of unsymmetrical diborane derivatives and analyzed via ^{11}B NMR.[623] Water exchange on $(NCN)Pt(H_2O)^+$ [**110**, N,C,N = 2,6-$(CH_2NMe_2)_2$-C_6H_3] was monitored as a function of pressure and temperature via ^{17}O NMR.[624]

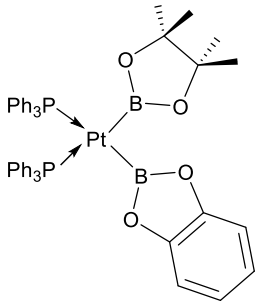

(**109**)

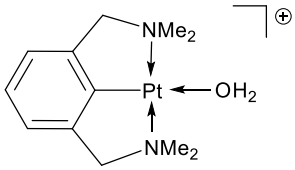

(**110**)

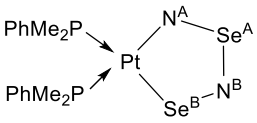

(**111**)

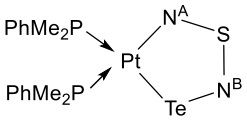

(**112**)

^{15}N-labeled complexes $Pt(Se_2{}^{15}N_2)(PMe_2Ph)_2$ (**111**) and $Pt(TeS^{15}N_2)(PMe_2Ph)_2$ (**112**) have were also analyzed via ^{77}Se, ^{125}Te, and ^{31}P NMR.[625] The following shifts were observed: For **111**, δ_{Pt} -4050, δ_{Se^A} 1819, δ_{Se^B} 1383, $\delta^{15}{}_{N^A}$ 486, $\delta^{15}{}_{N^B}$ 402; For **112**, δ_{Te} 1196, $\delta^{15}{}_{N^A}$ 360, $\delta^{15}{}_{N^B}$ 256.[625]

Characterization of $PtLi_4[Si(3,5\text{-}Me_2pz)_3]_4$[556] (**86**) was discussed in Section 9.2. For ^{77}Se NMR of $(NBu^n{}_4)_2[Pt(C_3Se_5)_2]$ with a diselenolate ligand,[626] see Section 12.2.

10. Group 11 (Cu, Ag and Au)

For Cu and Ag, NMR of both the metals (^{63}Cu, ^{109}Ag) and ligands were reported in 1990-2019. For Au, we found only papers on NMR of ligands. Nuclear and NMR properties of the nuclides, including recommended and commonly used references, are given in Table 14.

Table 14.[26] Nuclear and NMR properties of ^{63}Cu, ^{65}Cu, ^{107}Ag, ^{109}Ag and ^{197}Au

Nuclide	Natural abun-dance (%)[a]	Spin	Relative receptivity		Gyromagnetic ratio (10^7) (rad s^{-1} T^{-1})	Quadrupole moment Q (fm^2)	Ξ (and frequency, MHz; ^{1}H = 100.0000 MHz, 2.3488 T)	Reference sample
			D^H (^{1}H = 1.00)	D^C (^{13}C = 1.00)				
^{63}Cu	69.15	3/2	6.50×10^{-2}	382	7.1117890	-22.0	26.515473	$[Cu(MeCN)_4]ClO_4$ (MeCN)
^{65}Cu	30.85	3/2	3.54×10^{-2}	208	7.60435	-20.4	28.403693	
(^{107}Ag)[b]	51.839	1/2	3.50×10^{-5}	0.205	-1.0889181	-	4.047819	$AgNO_3$ (aq)
^{109}Ag	48.161	1/2	4.94×10^{-5}	0.290	-1.2518634	-	4.653533	
^{197}Au[c]	100	3/2	2.77×10^{-5}	0.162	0.473060	54.7	(1.729)[d]	-

[a] Unless noted, the isotopes are stable. The natural abundances are based on the NIST data.[25]

[b] ^{107}Ag in parenthesis is considered to be the less favorable of the element for NMR.

[c] Although we did not find reports of ^{197}Au NMR, it is listed here for comparison.

[d] Value in parenthesis was calculated from literature data on nuclear magnetic moments.

10.1. *Copper complexes*

Of the two nuclides, both with spin 3/2, ^{63}Cu is more than twice as abundant as ^{65}Cu and has larger relative receptivities. Thus, ^{63}Cu was typically selected for Cu NMR, although both ^{63}Cu and ^{65}Cu were used.[627] Of the two principal oxidation states for copper, Cu(II) complexes with d^9 configuration are often paramagnetic, while Cu(I) complexes are diamagnetic. We found publications in 1999-2019 on ^{63}Cu NMR of Cu(I) complexes.

^{63}Cu NMR of inorganic compounds was reviewed in 1999.[627] Thus, we focus on publications on Cu NMR in 1999-2019 in the current review.

Temperature effect on ^{63}Cu NMR on the nitrile complex $[Cu(PhCN)_4]BF_4$ was studied.[628] ^{63}Cu NMR line widths of CuOTf and $CuClO_4$ in acetonitrile solutions containing salts, water or Cl^- were also investigated.[629] Studies of solvation of Cu(I) salts, such as $CuClO_4$ in mixed solvents of MeCN or PhCN containing other nitriles (EtCN, Pr^iCN), dmso, or D_2O, probed by $^{63}Cu/^{65}Cu$ NMR were reviewed.[630]

Cu phosphine complex $[Cu(dppmb)_2]BF_4$ [dppmb = 1,2-bis(diphenylphosphin omethyl)benzene, *o*-$(CH_2PPh_2)_2$-C_6H_4] gave a ^{63}Cu resonance at δ 193, which is typical for Cu(I)-P_4 complexes.[631] Similarly, phosphine perfluorinated carboxylates, such as $[Cu(dppp)_2](OOCC_2F_5)$, showed broad ^{63}Cu bands at ca. δ 230.[632] ^{63}Cu NMR was used to characterize several Cu(I) phosphite perfluorinated carboxylates, such as $Cu_2[P(OPh)_3]_4(\mu\text{-}OOCC_2F_5)_2$ (δ 105), showing that ^{63}Cu shifts of the phosphites were more shielded than those of phosphine analogs.[633] ^{63}Cu NMR studies of Cu(I) complexes with P-donor ligands, such as phosphines and phosphites, were reviewed in 2006.[634]

In addition to complexes with N- and P-containing ligands, Cu(I) compounds with Sb-containing stibine ligands were characterized by ^{63}Cu NMR. $[Cu(R_2SbCH_2SbR_2)_2]PF_6$ (R = Me, Ph) showed ^{63}Cu resonances at δ -170 (R = Me) and -197 (R = Ph).[635] Their analogs, $[Cu(dmsmb)_2]BF_4$ [dmsmb = 1,2-bis(dimethylstibanylmethyl)benzene, *o*-$(CH_2SbMe_2)_2$-C_6H_4] and $[Cu(bdmsa)_2]BF_4$ [bdmsa = bis(2-dimethylstibanylbenzyl)methylamine, $MeN(CH_2\text{-}o\text{-}SbMe_2\text{-}C_6H_4)_2$] showed ^{63}Cu resonance at δ -171[446] and -203,[265] respectively.

Cu(I) complexes containing chalcogen (S, Se, Te) elements were also studied by ^{63}Cu NMR, including $[Cu[o\text{-}(CH_2EMe)_2\text{-}C_6H_4]_2]BF_4$ (E = S, ^{63}Cu δ 132; E = Se, ^{63}Cu δ -2, ^{77}Se δ 87; E = Te, ^{63}Cu δ 16, ^{125}Te δ 98).[636] Di-tellurium substituted 18-crown-6, 1,4,10,13-tetraoxa-7,16-ditelluracyclooctadecane ([18]aneO_4Te_2, an analog of **1** shown earlier), used its two Te atoms to bind to the Cu(I) ion as a ligand to give $[Cu([18]aneO_4Te_2)_2]BF_4$, showing resonances of ^{63}Cu δ -59 and ^{125}Te δ 166.[637]

A series of organometallic Cu(I) carbonyl complexes with tridentate N,N,N ligands were

investigated by ^{63}Cu NMR, including Tp*Cu-CO (δ 716), [(TpC)Cu-CO]ClO_4 [δ 504, TpC = tris(2-pyridyl)carbinol (**113**)], and [(Me-tacd)Cu-CO]ClO_4 [δ 585, Me-tacd = 1,5,9-trimethyl-1,5,9-triazacyclododecane (**114**)].[638] Intermetalloid cluster Cu@Sn_9^{3-} in [K([2.2.2]-cryptand)]$_3$[Cu@Sn_9] [[2.2.2]-cryptand = **115**] showed ^{63}Cu and ^{119}Sn resonances at δ -330 and -1440 ($^1J_{^{119}Sn-Cu}$ = 280 Hz), respectively.[639] The crystal structure of the cluster revealed that the Cu(I) is in the center of the cluster with an almost spherical environment.

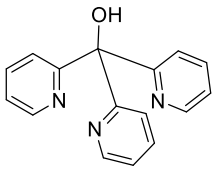

(**113**)

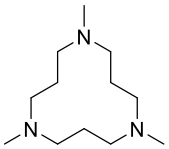

Me-tacd

(**114**)

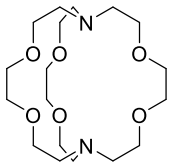

[2.2.2]crypt

(**115**)

^{65}Cu NMR of the Cu^+ site in blue copper protein azurin in frozen solution was investigated at 10 K using an 800 MHz (18.8 T) spectrometer, giving a ^{65}Cu quadrupole coupling constant of ±71.2 MHz which corresponds to an electric field gradient of ±1.49 atomic units at the Cu site and an asymmetry parameter of ~0.2.[640] Azurin is a small, periplasmic, bacterial blue copper protein. The sample used here was 97% ^{65}Cu-enriched. The studies here provided the nuclear quadrupole interaction as an exquisitely sensitive measure of the electron density around Cu(I) ion and the electronic structure and environment. Earlier experiments to obtain nuclear quadrupole interactions in Cu(I) complexes and the reduced form of the enzyme superoxide dismutase were conducted at zero field by nuclear quadrupole resonance (NQR).[640]

For NMR of ligands, reactions of O-phospho-*L*-serine [Ser-P = $(HO)_2P(=O)OCH_2CH(NH_2)CO_2H$] with Cu(II) ions were conducted in order to investigate the coordination of the Cu ion with the amine, carboxyl, or phosphate groups in Ser-P.[641] ^{1}H-^{15}N NMR by the HETCOR method was used to determine if the Cu ion was coordinating to the

amine group.[641] The amine and carboxyl groups were involved in coordination in Cu(Ser-P)$_2$.[641]

^{17}O NMR was used to study the effects of the pressure, temperature, and magnetic field on the water or solvent exchange reactions of $[Cu(tmpa)(H_2O)]^{2+}$ [**116,** tmpa = tris(2-pyridylmethyl)amine],[642] $[Cu(fz)_2(H2O)]^{2-}$ [**117**, fz = ferrozine or 5,6-bis(4-sulfonatophenyl)-3-(2-pyridyl)-1,2,4-triazine],[642] $[Cu(tren)(H_2O)]^{2+}$ (**118**, tren = **63**),[643] and $[Cu(dmf)_6]^{2+}$ (**119**).[644]

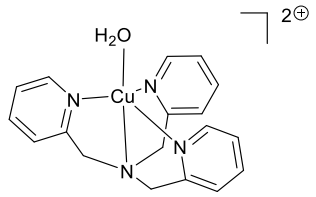

(**116**)

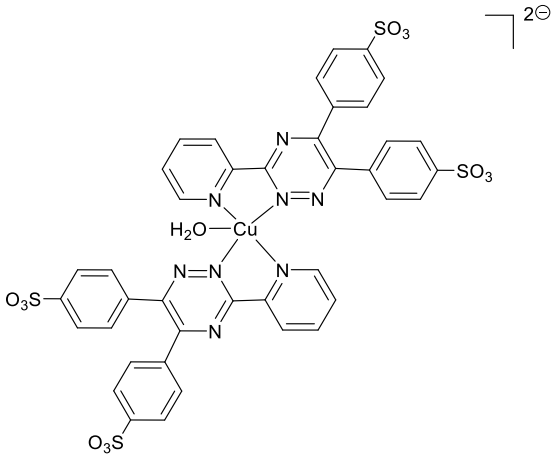

(**117**)

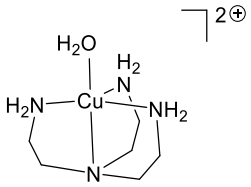

(**118**)

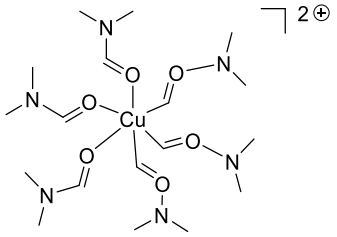

(**119**)

10.2. *Silver complexes*

NMR of ^{109}Ag (spin 1/2) was considered challenging mostly due to its low Ξ value and relative receptivities/sensitivity (Table 14).[69]

Complexes characterized by ^{109}Ag NMR that we found were those at Ag(I) oxidation state.

In Ag complexes coordinated by N-containing ligands, $[Ag(NH_3)_2]NO_3$ in aqueous

NH_3(aq) solution and $[Ag(NH_3)_3]NO_3$ in liquid NH_3(l) showed ^{109}Ag shifts of δ ~450 and ~570, respectively.[645] These shifts were compared with those of Ag^+ salts ($AgNO_3$ or $AgClO_4$) in other liquids such as CD_3CN (δ ~240), PBu^n_3 (δ ~1125) and $P(OMe)_3$ (δ ~1260). The effect of anions was negligible.[645] Dinitramide compounds $AgN(NO_2)_2$, $[Ag(MeCN)][N(NO_2)_2]$, and $[Ag(py)_2][N(NO_2)_2]$ were studied by ^{109}Ag and ^{14}N NMR with the chemical shifts listed in Table 14.[646] ^{109}Ag shift of $[Ag(py)_2][Au(CF_3)_2]$ was found to be at δ 404.[647] When $[Ag(9\text{-EtGH})_2]NO_3$ [9-EtGH = 9-ethylguanine (**91**)] was dissolved, ^{109}Ag NMR showed the equilibria involving the 1:1 complex of Ag:ligand.[648] The ^{109}Ag shift became gradually more deshielded from δ ~200 (at the Ag:ligand ratio = 1:2) to δ ~245 (at 1:4 ratio).[648] For the disilver cryptate complex (**120**) with a thiophene-spaced azacryptand hexa Schiff base, ^1H NMR spectrum revealed three-bond (H-C=N-Ag) coupling of imino CH proton atoms to $^{107,109}Ag$, which was confirmed by the ^{109}Ag INEPT (Insensitive Nuclei Enhanced by Polarization Transfer) spectrum with a peak at δ ~610.[649] Structure of an Ag(I)-mediated cytosine-Ag(I)-cytosine base pair within DNA duplex (**121**) was determined with solution NMR, showing $^1J^{15}_{N\text{-}Ag}$ = 83 and 84 Hz and the N3–Ag–N3 linkage.[650] The ^{109}Ag and ^{15}N (of the N atom bound to the Ag ion) shifts were δ 442 and ~172, respectively.[650] Reaction of $AgPF_6$ with the chiral 5,6-Chiragen ligand (**122**), containing two condensed α-pinene/bipyridine units, gave an enantiomerically pure, helicate $[Ag_6(5,6\text{-Chiragen})_6](PF_6)_6$ in the hexagonal shape.[651] ^{109}Ag NMR spectrum of the hexamer (δ 224) at 221 K showed its equilibrium with the tetramer $[Ag_4(5,6\text{-Chiragen})_4](PF_6)_4$ (δ 249).[652] Ir-Ag mixed metal complexes $Cp^*(pz)Ir(\mu\text{-}pz)_3Ag(PPh_3)$ and $[(Ph_3P)Ag^A(\mu\text{-}pz)Cp^*Ir(\mu\text{-}pz)_2Ag^B(PPh_3)]BF_4$ (**123**, py = pyrazole) were characterized by $^{107,109}Ag$ NMR.[653] For $Cp^*(pz)Ir(\mu\text{-}pz)_3Ag(PPh_3)$, ^{109}Ag shift was observed at δ 902.8; ^{15}N shifts were obtained at N(-Ir) δ -165.5 and N(-Ag) at δ -93.1 with $^1J^{15}_{N\text{-}}{}^{15}_{N}$ = 14.2 Hz, $^1J^{15}_{N\text{-}Ag}$ = 38 Hz and $^2J^{15}_{N\text{-}Ag\text{-}P}$ = 13.6 Hz.[653] For (**123**), ^{109}Ag shifts are at δ 884.3 (for Ag^B) and 562.9 (Ag^A). Its N(-Ir) shifts at δ -168.5 to -170.8 and N(-Ag) shifts at δ -90.7 to -105.2 with $^1J^{15}_{N\text{-}}{}^{15}_{N}$ = 13.5-13.7 Hz, $^1J^{15}_{N\text{-}Ag}$ = 36.5-73.8 Hz and $^2J^{15}_{N\text{-}Ag\text{-}P}$ = 13.2-18.5

Hz.[653] Trisilver complex (**124**) with a chiral ferrocene ligand was studied as a model homogeneous catalyst.[654] The number of coordinated P atoms and the coordination of the chiral side chain were determined using ^{109}Ag-^{31}P, ^{109}Ag-^{1}H, and ^{31}P-^{1}H HSQC and HMQC, showing ^{109}Ag shifts at δ 690 (Ag^{A}) and 540 (Ag^{B}) in **124**.[654]

Table 14. ^{109}Ag and ^{14}N NMR shifts of Ag(I) dinitramide compounds[646]

Complexes	^{109}Ag shifts (δ)	^{14}N shifts
$AgN(NO_2)_2$	137	-17 (*N*O_2), -73 [*N*$(NO_2)_2$]
$[Ag(MeCN)_2][N(NO_2)_2]$	212	-16 (*N*O_2), -68 [*N*$(NO_2)_2$], -157 (MeC*N*)
$[Ag(py)_2][N(NO_2)_2]$	306	-13 (*N*O_2), -91 [*N*$(NO_2)_2$], py in the same region as *N*$(NO_2)_2$, making the two indistinguishable; py may be displaced by solvent THF.

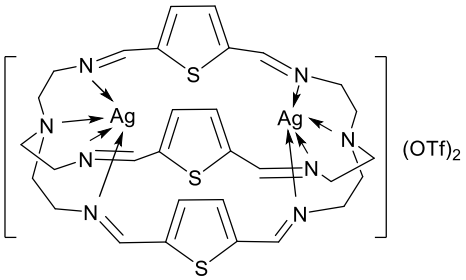

(**120**)

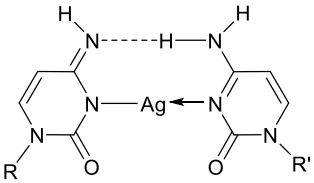

R, R' = sugar of the nucleotide units within DNA

(**121**)

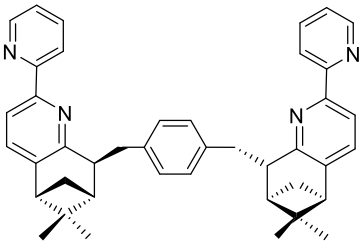

5,6-Chiragen

(**122**)

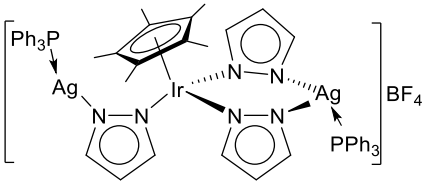

(**123**)

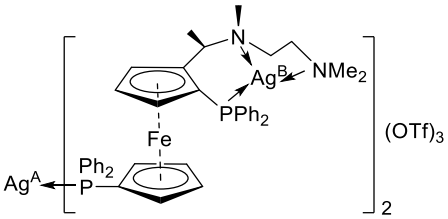

(**124**)

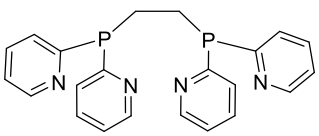

(**125**)

In Ag complexes coordinated only by P-containing ligands, reactions of $AgNO_3$ with 1,2-bis(di-2-pyridylphosphino)ethane (d2pype = **125**) give monomer $[Ag(d2pype)_2]NO_3$ with the $Ag(P,P)_2^+$ structure, dimer $[(d2pype)Ag(\mu\text{-}d2pype)_2Ag(d2pype)](NO_3)_2$ with the $[(P,P)Ag(\mu\text{-}P,P)_2Ag(P,P)]^{2+}$-type cation and a trimer.[655] ^{109}Ag shifts of the monomer and dimer at 243 K were observed at δ 1411 and 1417, respectively. The trimer and analogs with bis(di-*n*-pyridylphosphino)ethane (*n* = 3, 4) were also characterized by ^{109}Ag.[655] For Ag(I) complex **126** with a B-templated catechol phosphine, ^{109}Ag shift was observed at δ 702 with $^1J_{P\text{-}^{107/109}Ag}$ = 571/494 Hz.[656]

Complex with a tetradentate P,S,S,P ligand, $[Ag[Ph_2P(CH_2)_2S(CH_2)_2S(CH_2)_2PPh_2]]BF_4$, was characterized by ^{109}Ag NMR with the resonance at δ 1117.[657]

For Ag(I) complexes with As- (arsine) and Sb (stibine)-containing ligands, several tetra-coordinated compounds were characterized by ^{109}Ag NMR, including $[Ag(AsPh_3)_4]BF_4$ (δ 1056),[658] $[Ag(SbMe_3)_4]BF_4$ (δ 1085),[658] $[Ag(SbPh_3)_4]BF_4$ (δ 1166),[658] and $[Ag(dmap)_2]BF_4$ [δ 1120, dmap = $Me_2Sb(CH_2)_3SbMe_2$].[658] ^{109}Ag shift of $[Ag(dpsm)_2]BF_4$ (dpsm = $Ph_2SbCH_2SbPh_2$) was observed at δ 521, suggesting that the complex is probably di-coordinated (Sb-Ag-Sb).[635]

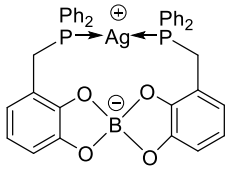

(**126**)

Hmimt

(**127**)

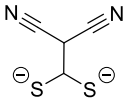

(**128**)

Ag(I) complexes containing chalcogen (S, Se, Te) elements were also studied by ^{109}Ag NMR, including $[Ag[MeE(CH_2)_3EMe]_2]BF_4$ (E = S, ^{109}Ag δ 840; E = Se, ^{109}Ag δ 829, ^{77}Se δ 41; E = Te, ^{109}Ag δ 1053, ^{125}Te δ 24) and their analogs with the $PhE(CH_2)_3EPh$ ligands.[659] [Ag[*o*-

$(EMe)_2$-$C_6H_4]_2]BF_4$ (E = S, ^{109}Ag δ 788; E = Se, ^{109}Ag δ 912, ^{77}Se δ 180; E = Te, ^{109}Ag δ 1128, ^{125}Te δ 433), showing the more deshielded ^{109}Ag shift from the S, Se to the Te analog.[660] For other Ag-S complexes, reaction of Ag(I) ions with 1-methyl-2(3*H*)-imidazolinethione (Hmimt = **127**) led to the formation of $[Ag(Hmimt)_3](NO_3)$, which showed by X-ray crystal diffraction to contain three Ag-S bonds, and showed ^{109}Ag δ 791.5.[661] ^{109}Ag NMR of Ag(I) di-thiourea complex $[Ag[S=C(NH_2)_2]_2]NO_3$ revealed the resonance at δ 671.8,[662] while mono-thiourea complex $Ag[S=C(NH_2)_2]CN$ gave the resonance at δ 651.8.[663] A series of other Ag(I) substituted-thiourea and -thione complexes were characterized by ^{109}Ag NMR,[663-664] showing, e.g., ^{109}Ag δ 654.9 for mono-*N,N*-dimethylthiourea complex $Ag[S=C(NHMe)_2]CN$[663] and δ 656.1 for di-*N,N*-dimethylthiourea complex $[Ag[S=C(NHMe)_2]_2]NO_3$.[664] Hydride complex $(Bu^n{}_4N)_5[Ag_8(H)[S_2CC(CN)_2]_6]$ containing Ag-S bonds with 1,1-dicyanoethylene-2,2-dithiolate (**128**) ligands showed ^{109}Ag δ 1136 and ^{1}H resonance of the hydride ligand at δ 9.65.[665]

For Ag(I) complexes containing S ligands with biological applications, oligomeric Ag(I) thiomalate complex $Na[Ag[O_2CCH(SH)CH_2CO_2]]$ with Ag-S bonds showed ^{109}Ag δ 868.7.[666] Antimicrobial activities of such complexes were studied.[666] Ag(I)-cysteine solution showed a mean Ag-S bond distance of 2.47(2) Å by EXAFS (extended X-ray absorption fine structure) and ^{109}Ag NMR resonance at δ 1103, which were consistent with the product being a partially oligomeric AgS_3 species.[667] For Ag(I)-penicillamine solution, the mean Ag−S bond distance was 2.40(2) Å by EXAFS and ^{109}Ag NMR resonance was observed at δ 922, indicating that mononuclear AgS_2 coordinated complexes dominated in the solution.[667] Here, the studies of the Ag(I)-cysteine and -penicillamine interactions stemmed from the historical use of Ag(I) in antimicrobial agents, as the increasing bacterial resistance against antibiotics renewed the interest in newer and more efficient Ag-based antimicrobial biomaterials.[667]

^{109}Ag shift of $(H_2NPr^i{}_2)Ag[PhCH=C(S)COO]$ containing the di-anionic O,S ligand $PhCH=C(S^-)COO^-$ was at δ 840.8.[668] $Ag(PPh_3)[PhCH=C(SH)COO]$ containing the mono-anionic O,SH ligand showed the ^{109}Ag shift at δ 936.3.[669]

For Ag-Se and Ag-Te complexes, see previous discussion on $[Ag[MeE(CH_2)_3EMe]_2]BF_4$ (E = S, Se, Te),[659] their analogs with the $PhE(CH_2)_3EPh$ ligands,[659] and $[Ag[o\text{-}(EMe)_2\text{-}C_6H_4]_2]BF_4$ (E = S, Se, Te).[660] For other Ag-Se complexes, ^{107}Ag NMR was used to study selenourea complexes $Ag(selenourea)NO_3$ (δ 810.5) and $[Ag(selenourea)_2]NO_3$ (δ 784.3), which are >600 ppm more deshielded than that of $AgNO_3$ (δ 166.0).[670] These resonances are also deshielded from those of Ag-S analogs, $Ag(thiourea)NO_3$ (δ 685.9) and $[Ag(thiourea)_2]NO_3$ (δ 671.8).[670] Various Ag(I)-selenone complexes were probed by ^{109}Ag NMR, including Ag(*N,N*-dimethylselenourea)NO_3 (δ 748.6) and [Ag(*N,N*-dimethylselenourea)$_2$]NO_3 (δ 839.8).[671]

For Ag(I) organometallic complexes (including CN^- compounds), ^{109}Ag NMR was used to study $(Ph_3Te)[Ag(CN)_2]$ (δ 593).[672] Ag(I) trinitromethanide $Ag[C(NO_2)_3]$ in various solvents was studied, showing, e.g., its ^{109}Ag resonance at δ 27.5 in D_2O and at δ 429.7 in CD_3CN.[673] ^{109}Ag NMR was used to characterize hydride-centered heptanuclear silver clusters, $Ag_7(H)[S_2P(OEt)_2]_6$ (δ 1117) with dithiophosphate ligands and its Se analog $Ag_7(H)[Se_2P(OPr^i)_2]_6$ (δ 1126) with diselenophosphate ligands.[674] Ag(I) cluster $Ag_8(\mu_4\text{-}H)[Se_2P(OPr^i)_2]_6^+$ containing H^- bridges (Ag-μ-H-Ag) in tetracapped *T* symmetry inside an Ag_8 core was prepared with PF_6^- anion.[675] Both ^{109}Ag, ^1H-^{109}Ag HMQC and ^{77}Se spectroscopies were used to characterize the complex (^{109}Ag δ 1155 ppm, $^1J_{H\text{-}^{109}Ag}$ = 35.0 Hz; ^{77}Se δ -0.2).[675] Re(I)-Ag(I) hydride-carbonyl clusters $Ag(\mu\text{-}H)_4[Re_2(\mu\text{-}H)(CO)_8]_2^-$, $Ag(\mu\text{-}H)_4[Re_4(\mu\text{-}H)_3(CO)_{16}]_2^-$, and $Ag(\mu\text{-}H)_4[Re_2(\mu\text{-}H)(CO)_8][Re_4(\mu\text{-}H)_3(CO)_{16}]^-$, with OTf^- anions, were studied by ^1H-^{109}Ag HMQC to give ^{109}Ag resonances at δ 1844, 1243, and 1520, respectively.[676] Ag(I) trifluoromethyl complex $[Ag(dmf)_2][Ag(CF_3)_2]$ showed the ^{109}Ag shift of δ 569.8 for the anion $[Ag(CF_3)_2]^-$.[677] Other perfluoroalkyl Ag(I) complexes $[Ag(C_2F_5)_2]^-$ and $[Ag(n\text{-}C_4F_9)_2]^-$ were also characterized by ^{109}Ag NMR.[677] Oligomer Ag(I) $[Ag(C{\equiv}CBu^n)]_m$ showed the ^{109}Ag resonance at δ ~1060.[678]

Ag(III) trifluoromethyl complexes $[Ag(CF_3)_4]^-$ and $[Ag(CF_3)_nX_{4\text{-}n}]^-$ [X = CN^- (n = 1-3), CH_3^-, $^-C{\equiv}CC_6H_{11}$, Cl^-, Br^- (n = 2, 3) and I^- (n = 3); cation = PPh_4^+ or PNP^+ ($Ph_3P{=}N{=}PPh_3^+$)], showing

significantly deshielded ^{109}Ag resonances from Ag(I) complexes, such as δ 2233 for $[Ag(CF_3)_4]^-$, δ 2404 for $Ag(CF_3)_3$(dmf), and δ 2046 for $[Ag(CF_3)_3Me]^-$.[679] ^{109}Ag shifts of the Ag(III) complexes were tabulated in Reference [679].

Several Ag(I) complexes with *N*-heterocyclic carbene (NHC) ligands were studied by ^{109}Ag NMR.[680-684] $[Ag(IMes)_2]$OTf [IMes = 1,3-mesitylimidazol-2-ylidene (**129**)] showed its ^{109}Ag resonance at δ 642.4.[680] *N,N*-diferrocenyl-NHC (**130**) complex [Ag(1,3-diferrocenylimidazol-2-ylidene)$_2$]BPh_4 gave the ^{109}Ag resonance at δ 727.[681] Hydride dimer [(SIDipp)Ag(μ-H)Ag(SIDipp)]OTf (SIDipp = **131**) and its deuteride isotopologue [(SIDipp)Ag(μ-D)Ag(SIDipp)]BF_4, with direct Ag···Ag interactions, showed interesting H/D-^{109}Ag and ^{107}Ag-^{109}Ag couplings in their ^{109}Ag NMR spectra (**Figure 11**).[682] Since naturally occurring silver consists of ca. 52% ^{107}Ag and 48% ^{109}Ag (Table 14), both with spin 1/2, the H^--bridged Ag_2^+ ion therefore comprised a mixture of roughly 1:2:1 (27:50:23) of [^{107}Ag-H-^{107}Ag]$^+$, [^{107}Ag-H-^{109}Ag]$^+$ and [^{109}Ag-H-^{109}Ag]$^+$. Among the three isotopologues, the first with only ^{107}Ag isotopes did not show up in the ^{109}Ag NMR spectrum. The last one, [^{109}Ag-H-^{109}Ag]$^+$, was observed as a doublet split by the H^- ligand with $^1J_{H\text{-}^{109}Ag}$ = 134 Hz. In the middle isotopologue with one ^{107}Ag and one ^{109}Ag ion, [^{107}Ag-H-^{109}Ag]$^+$, the ^{109}Ag signal was split into a doublet of doublets by the ^{1}H and ^{107}Ag nuclides ($^1J_{^{107}Ag\text{-}^{109}Ag}$ = 113 Hz), as shown in **Figure 11-A**.[682] In the spectrum of the D compound in **Figure 11-B**, coupling between ^{109}Ag and ^{2}H (spin 1) gives rise to a 1:1:1 triplet, which ^{107}Ag splits further into a 1:1 doublet of 1:1:1 triplets. This pattern indicates the large ^{109}Ag-^{107}Ag coupling and the smaller ^{109}Ag-^{2}H coupling ($^1J_{D\text{-}^{109}Ag}$ = 18.7 Hz).[682] ^{109}Ag NMR was used to characterize the Ag(I)-NHC complex (dbdpi)Ag(acetate) [δ 476, dbdpi = 1,3-dibenzyl-4,5-diphenylimidazol-2-ylidene (**132**)] and its analogs.[684] The antibiotic activities of the Ag(I)-NHC complex and its analogs was evaluated.[684] ^{1}H(^{13}C)^{109}Ag triple resonance NMR technique was developed to obtain ^{109}Ag NMR resonances in a labile Ag(I)-carbene complex.[683] In Ag complexes, indirect detection of ^{109}Ag resonances via ^{1}H-^{109}Ag HMQC frequently encountered

small or absent $^{1}J_{H\text{-}^{109}Ag}$ couplings or rapid ligand dissociation. H(X)Ag triple resonance spectroscopy used the large one-bond $^{1}J_{X\text{-}^{109}Ag}$ coupling (where X is the relay nuclide). $^{1}H(^{13}C)^{109}Ag$ HMQC NMR experiment was performed for a Ag(I)-NHC complex at natural ^{13}C (1.1%) abundance and variable temperatures, showing that was superior to the $^{1}H\text{-}^{109}Ag$ HMQC detection above -20 °C.[683]

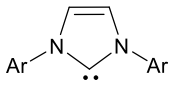

Ar = 2,4,6-Me_3-C_6H_2

N,N-dimesityl-NHC

(**129**)

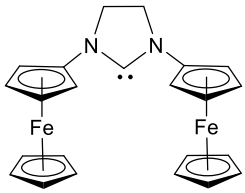

N,N-diferrocenyl-NHC

(**130**)

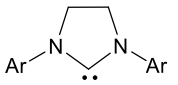

Ar = 2,6-Pr^{i}_2-C_6H_3

SIDipp

(**131**)

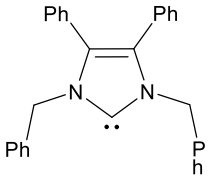

(**132**)

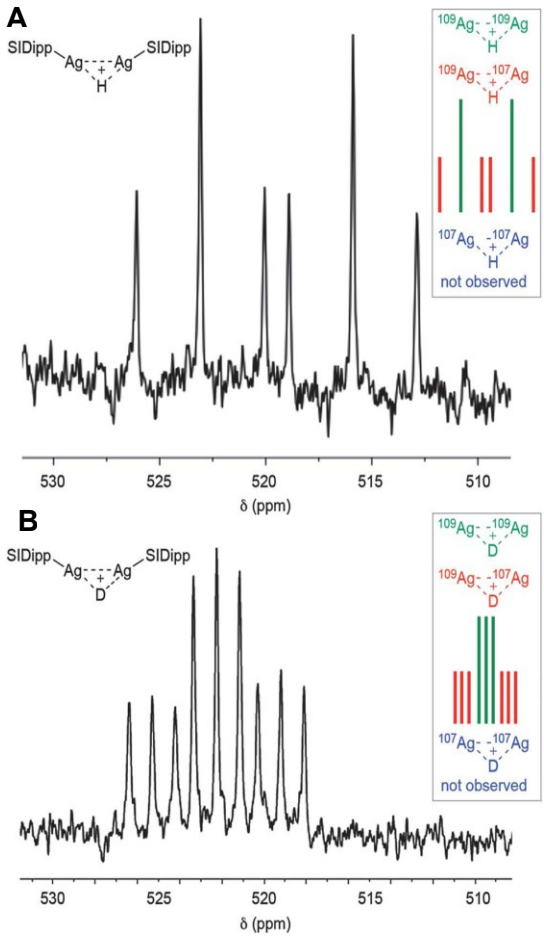

Figure 11. (**A**) ^{109}Ag NMR spectrum of [(SIDipp)Ag(μ-H)Ag(SIDipp)]OTf in CD_2Cl_2. (**B**) ^{109}Ag NMR spectrum of [(SIDipp)Ag(μ-D)Ag(SIDipp)]BF_4 in CD_2Cl_2. Insets: interpretation of signals from each isotopologue. Adapted with permission from Reference [682]. Copyright: Royal Chemical Society.

[HB[3,5-$(CF_3)_2$-Pz]$_3$]AgSn(N_3)[(Pr^n)$_2$ATI] (**133**) [HB(3,5-$(CF_3)_2$-Pz)$_3$ = hydrotris[3,5-bis(trifluoromethyl)pyrazolyl]borate, (Pr^n)$_2$ATI = N-(*n*-propyl)-2-(*n*-propylamino)troponiminate] was characterized by ^{119}Sn NMR, showing a doublet at δ 90 with $^1J^{119}_{Sn-}{}^{107/109}_{Ag}$ = 4866 Hz.[685] ^{119}Sn and ^{29}Si shifts were also reported for products of the reactions between Sn[CH($SiMe_3$)$_2$]$_2$ or Sn[CH($SiMe_3$)$_2$]$_2X_2$ (X = NCO^-, I^-) and AgX (X = NCS^-, CN^-, NCO^-, I^-).[686]

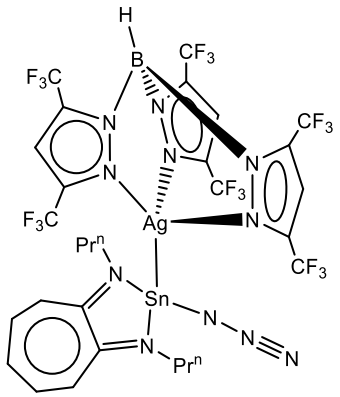

(**133**)

NMR of α atoms of ligands was also used to study Ag complexes. In a DNA oligonucleotide with three consecutive imidazole nucleotides in its center, Ag(I) ions were found to mediate the pairings in three imidazole-Ag-imidazole interactions.[687] The confirmation of the Ag-mediated base pairs was obtained from $^{1}J^{15}_{N-}{}^{107/109}_{Ag}$ (86 Hz) couplings upon using ^{15}N-labelled imidazole.[687] VT ^{31}P NMR was used to study the coordination chemistry of equimolar amounts of Ag(I) with the diphosphine ligands $Ph_2P(CH_2)_nPPh_2$ (n = 6, 8, 10,12).[688] The $^{1}J_{P-}{}^{107}_{Ag}$ for all reaction mixtures was ~500 Hz, indicating that the Ag(I) ion was coordinated to two P atoms in a linear fashion.[688]

10.3. *Gold complexes*

As indicated in the footnote of Table 14, we did not find a publication in 1990-2019 on the ^{197}Au NMR of a metal complex.

Reactions of [Au(*cis*-dach)Cl_2]Cl and [Au(*cis*-dach)$_2$]Cl_3 (*cis*-dach = *cis*-1,2-diaminocyclohexane) with $K^{13}C^{15}N$ were conducted and followed by ^{15}N NMR.[689] For example, after the reaction of [Au(*cis*-dach)Cl_2]Cl with $K^{13}C^{15}N$ in a 1:2 ratio, a signal in the ^{15}N NMR spectrum at δ 281 pertaining to $Au(^{13}C^{15}N)_4^-$ appeared.[689] When the amount of the [Au(*cis*-dach)Cl_2]Cl was increased, the resonance of $Au(^{13}C^{15}N)_4^-$ (δ 262) was observed, showing that it

was produced as a second product.[689]

Synthesis of bis-silyl Au(III) complexes were investigated using DFT calculations and NMR spectroscopy such as ^{31}P and ^{29}Si.[690-691] For example, the reaction of $(Ph_3P)AuCl$ with, e.g., $(PhMe_2Si)_2$ in the presence of $GaCl_3$ at -80 °C produced $[Au(PPh_3)(SiMe_2Ph)_2](GaCl_4)$ (δ_{Si} 40.7, δ_P 60.9).[690]

For ^{77}Se NMR of $(NBu^n_4)[Au(C_3Se_5)_2]$ containing diselenolate ligands,[626] see Section 12.2.

11. Group 12 (Zn, Cd and Hg)

For the three elements, NMR of both the metals (^{67}Zn, ^{113}Cd, and ^{199}Hg) and ligands were reported in 1990-2019. Nuclear and NMR properties of the nuclides, including recommended and commonly used references, are given in Table 15.

Table 15.[26] Nuclear and NMR properties of ^{67}Zn, ^{111}Cd, ^{113}Cd, ^{199}Hg, and ^{201}Hg

Nuclide	Natural abun-dance (%)[a]	Spin	Relative receptivity		Gyromagnetic ratio (10^7) (rad s^{-1} T^{-1})	Quadrupole moment Q (fm^2)	Ξ (and frequency, MHz; ^1H = 100.0000 MHz, 2.3488 T)	Reference sample
			D^H (^1H = 1.00)	D^C (^{13}C = 1.00)				
^{67}Zn	4.04	5/2	1.18×10^{-4}	0.692	1.676688	15.0	6.256803	$Zn(NO_3)_2$ (aq)
(^{111}Cd)[b]	12.80	1/2	1.24×10^{-3}	7.27	-5.6983131	-	21.215480	$Cd(ClO_4)_2$ (aq)[c]
^{113}Cd	12.22	1/2	1.35×10^{-3}	7.94	-5.9609155	-	22.193175	
^{199}Hg	16.87	1/2	1.00×10^{-3}	5.89	4.8457916	-	17.910822	$HgCl_2$ (δ -1550 in D_2O)[e,f]
^{201}Hg[d]	13.18	3/2	1.97×10^{-4}	1.16	-1.788769	38.6	6.611583	

[a] Unless noted, the isotopes are stable. The natural abundances are based on the NIST data.[25]

[b] ^{111}Cd[26] in parenthesis is considered to be the less favorable of the element for NMR.

[c] $CdMe_2$ (neat) is the reference by IUPAC.[26] Most publications have used $Cd(ClO_4)_2$ at δ 0.00 as a reference.[1-2]

[d] ^{199}Hg is a useful spin 1/2 nuclide for NMR.[26]

[e] The highly toxic $HgMe_2$ (neat) is the reference for ^{199}Hg and ^{201}Hg NMR by IUPAC.[26] The high toxicity of $HgMe_2$ means its direct use should be strongly discouraged.[26-27]

[f] In addition to $HgCl_2$ in D_2O, $Hg(ClO_4)_2$ in H_2O at δ -2253 was also used as a secondary reference.[1]

11.1. *Zinc complexes*

The small natural abundance of ^{67}Zn and its low resonance frequency (*Ξ*) lead to slight relative receptivities. In addition, as a spin 5/2 nuclide, it has a quadrupole moment. These properties limited the use of ^{67}Zn NMR in inorganic compounds.[1]

Earlier ^{67}Zn NMR studies by 1990 were reviewed in Reference 1, including following compounds: zincate $Zn(OH)_4^{2-}$ (δ 220 in 16 M KOH), $ZnCl_4^{2-}$ (δ 257), $ZnBr_4^{2-}$ (δ 169), ZnI_4^{2-} (δ -35), $Zn(NH_3)_4^{2+}$ (δ 288), $Zn(SMe)_4^{2-}$ (δ 362), $Zn(SPh)_4^{2-}$ (δ 267), and $Zn(SePh)_4^{2-}$ (δ 224). These complexes are in highly symmetric ligand environment, minimizing the contributions of ^{67}Zn quadrupole moment to the peak width.

In the 1990-2019 period, interactions of silicates with Zn(II) and Al(III) ions in highly alkaline, aqueous solution were studied by ^{67}Zn, ^{29}Si and ^{27}Al NMR.[692] When 0.84 M ZnO and 0.86 M SiO_2 were dissolved in 10.0 M KOH, $(HO)_3ZnOSiO_2(OH)^{4-}$, formed from the reaction of zincate $Zn(OH)_4^{2-}$ with monomeric silicate, was observed at ^{67}Zn δ 286 (line width 2500 Hz) and ^{29}Si δ -71.4. The shift and width of the ^{67}Zn peak in comparison with those of zincate $Zn(OH)_4^{2-}$ (δ 220, width 554 Hz) were consistent with the formation of the Zn(II)-Si(IV) anion with lower symmetry than zincate.[692] ^{29}Si NMR was used to probe reactions of zincate with dimeric silicate and cyclic silicate trimer, forming $(HO)(SiO_2)O(SiO_2)OZn(OH)_3^{6-}$ and $(HO)_3Zn(SiO_3)_3^{7-}$, respectively. Aluminate and zincate, when present together, competed roughly equally for a deficiency of silicate to form $(HO)_3ZnOSiO_2(OH)^{4-}$ and $(HO)_3AlOSiO_2(OH)^{3-}$ which exchanged the ^{29}Si moiety at a fast but measurable rate.[692]

High-energy density aqueous redox flow battery was reported, which was based on the use of Zn/Zn^{2+} and I^-/I_3^- redox couples (Overall reaction: $I_3^- + Zn \rightleftharpoons 3I^- + Zn^{2+}$, E = 1.2986 V).[693] Unlike traditional batteries, such flow-based energy storage systems separated the energy storage and power generation by storing the electro-active species in externally flowing electrolytes (i.e., anolyte and catholyte), while maintaining the redox reactions at the electrode surface.[693] Such a design allowed the redox flow batteries to scale the power and/or energy independently, which was a characteristic advantage. In the aqueous redox flow battery here, $Zn(H_2O)_5(I_3)^+$, a Zn(II)-polyiodide electrolyte was identified and found to initiate precipitation in the catholyte.[693] ^{67}Zn NMR studies were performed on aqueous $ZnNO_3$ and ZnI_2 solutions at different Zn(II) concentrations as well as the pristine and fully charged ZnI_2 catholytes with and without EtOH. The work showed that, when EtOH was present in the aqueous electrolyte solution, Zn(II) ions form $Zn(H_2O)_5(EtOH)^{2+}$ which might partially hinder the formation of $Zn(H_2O)_5(I_3)^+$. In other words, the I_3^- dissociation and subsequent precipitation reaction might be mitigated due to the Zn(II)-EtOH complexation.[693]

DFT quantum chemical investigation was performed on ^{67}Zn NMR shifts and electric field gradients in Zn(II) complexes.[694] The calculated shifts were compared with those from experiments.

NMR studies of α atoms of ligands in Zn(II) complexes were also conducted. The crystal structure of $[MeSi(SiMe_2N(p\text{-tol}))_3Sn]_2Zn$ (**134**) is different from its group 12 analogues $[MeSi(SiMe_2N(p\text{-tol}))_3Sn]_2M$ (M = Cd, Hg) in that the Zn ion formed an asymmetrical complex where there was a Zn-N bond and the Sn-Zn-Sn interaction.[695] The irregularity of the structure was also shown in ^{119}Sn NMR with peaks at δ -153.5 and -91.2.[695] The binding of the Zn(II) ion to the dodecamer $[d(GGTACCGGTACC)]_2$ was investigated via ^{1}H-^{15}N HMBC.[696]

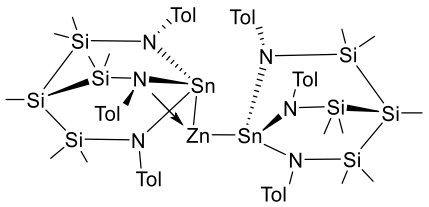

(**134**)

For ^{77}Se NMR of $(PPh_4)_2[Zn(C_3Se_5)_2]$ with a diselenolate ligand,[626] see Section 12.2.

11.2. Cadmium complexes

Cd NMR is relatively easy to obtain, given that both ^{111}Cd and ^{113}Cd are spin 1/2 nuclides with rather high Ξ (and thus frequencies) and receptivities (Table 15). Both ^{111}Cd and ^{113}Cd NMR of inorganic compounds have been reported, although the latter is preferred. Unless noted (in Reference [697]), the discussion below is based on $Cd(ClO_4)_2$ in D_2O as a reference for Cd NMR (Table 15). Effects of solvents such as py, MeCN, MeOH, EtOH on the ^{113}Cd shift of $Cd(ClO_4)_2$ (in comparison to that in D_2O) were probed by ^{113}Cd NMR.[698]

^{113}Cd chemical shifts are very sensitive to the environments that the metal ions are in, including donor atoms, coordination number, geometry and solvent. In Cd-N coordination chemistry, ^{113}Cd NMR spectra were used to study the reactions of ^{15}N-enriched KNCS with $Cd(OTf)_2$ in aqueous solution of acetone and HCF_2Cl (Freon-22) at -110 °C showed $Cd(H_2O)_3(NCS)^+$, $Cd(H_2O)_2(NCS)_2$, $Cd(H_2O)(NCS)_3^-$, and $Cd(NCS)_4^{2-}$ were observed.[699] Each NCS^- substitution led to a deshielded shift of the ^{113}Cd resonance in the δ 19-190 range. ^{15}N shifts of the species were in the δ -39 to -60 range. $^1J_{^{113}Cd-^{15}N}$ decreased continuously from 251 Hz for $Cd(H_2O)_3(NCS)^+$ to 219 Hz for $Cd(NCS)_4^{2-}$.[699] $[Cd(5,5'\text{-diamino-}2,2'\text{-bipyridine})_3]Cl_2$ with a bipy-analog ligand (**135**) was characterized by ^{113}Cd NMR, showing the resonance at δ 254.[700] Exchanges of $CdNO_3$ with benzimidazole (**136**) were studied by ^{113}Cd NMR.[701]

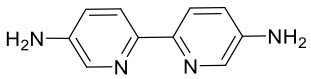

(**135**)

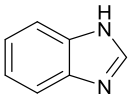

(**136**)

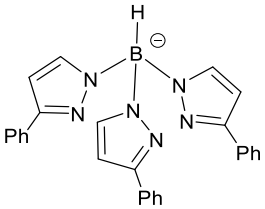

(**137**)

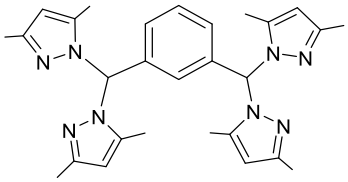

(**138**)

For Cd(II) complexes with mixed N,X ligands, $Tp^{Ph}Cd\text{-}O_2CMe$ with a hydrotris(3-phenylpyrazol-1-yl)borate (Tp^{Ph-} = **137**) ligand, was a catalyst for the formation of polycarbonates from epoxides and CO_2.[702] Binding of the epoxides to the complex was probed by ^{113}Cd NMR, as the activation of an epoxide by interaction with the N_3,O Cd(II) center was a key step in the copolymerization.[702] $[Cd(\mu\text{-}F)(\mu\text{-}dpz)_2Cd](BF_4)_3$ [dpz = *m*-[CH(3,5-dimethyl-1-pz)$_2$]$_2C_6H_4$) (**138**)] with two bridging tetra-dentate N_4 ligands and a bridging F^- ion showed ^{113}Cd shift at δ 25.1 with $^1J^{113}_{Cd-F}$ = 28 Hz.[703]

For chemistry of Cd(II) complexes with *O*-, *S*- or *Se*-containing ligands, complexes with mono- and di-carboxylic acids in aqueous solution were investigated using ^{113}Cd NMR.[704] For mono-carboxylic acids such as HCO_2H, CH_3CO_2H, and $PhCO_2H$, a single averaged chemical shift was observed even at reduced temperature from rapid exchange in solution. In case of di-carboxylic acids $HO_2C(CH_2)_nCO_2H$ (n = 0-3), the ^{113}Cd nuclei showed increasing shielding with larger n.[704] For $(RS)Cd(\mu\text{-}SR)_2Cd(SR)$ [R = $Si(OBu^t)_3$] with mixed S,O-ligands, in which one of O atoms in each $Si(OBu^t)_3$ group formed a dative bond with the Cd(II) ion, ^{113}Cd shift was observed at δ 402.[705]

In Cd(II) organometallic chemistry, several Tp*Cd-R complexes with different alkyl or aryl ligands were studied by ^{113}Cd NMR, including R = Me (δ 437.6), Et (δ 382.9), Pr^n (δ 386.2), Pr^i (δ 338.6), and Ph (δ 359.8).[706] The rather large shift differences between Tp*Cd-Me and Tp*Cd-Et as well as between Tp*Cd-Pr^n and Tp*Cd-Pr^i were attributed to the β effect, i.e., adding a β-C to the alkyl ligands.[706] Perfluoro-alkyl and aryl complexes $Cd(CF_3)_2$, $Cd(C_2F_5)_2$, $Cd(n\text{-}C_3F_7)_2$,

$Cd(i\text{-}C_3F_7)_2$, and $Cd(C_6F_5)_2$ as diglyme adducts, were probed by ^{113}Cd NMR, giving ^{113}Cd shifts (referenced to $CdMe_2$) for $Cd(CF_3)_2$ (δ -489.7), $Cd(C_2F_5)_2$ (δ -432.4), $Cd(n\text{-}C_3F_7)_2$ (δ -439.1), $Cd(i\text{-}C_3F_7)_2$ (δ -288.3), and $Cd(C_6F_5)_2$ (δ -290.0).[697] The shift differences between $Cd(CF_3)_2$ and $Cd(C_2F_5)_2$ as well as between $Cd(n\text{-}C_3F_7)_2$ and $Cd(i\text{-}C_3F_7)_2$ were probably also the result of the β effect,[697] as in Tp*Cd-R.[706]

^{113}Cd NMR was used to study Cd(II) bio-inorganic chemistry,[707-719] including proteins[707-713,719] and enzymes.[714-715] A large range of ^{113}Cd shifts was observed for ^{113}Cd-substituted metalloproteins from δ -100 for Cd(II) with octahedral O ligands to δ 760 ppm for Cd(II) with tetrahedral S ligands.[707] For the tetrahedral S sites in proteins such as rubredoxin and desulforedoxin, ^{113}Cd shifts were ca. δ 720-745. New ^{113}Cd shifts for ^{113}Cd-substituted, overexpressed and mutated homologous desulforedoxin-like $Fe(S\text{-}Cys)_4$ proteins, were obtained to show a correlation between the ^{113}Cd shifts and structures at the metal sites.[707] ^{1}H-^{113}Cd correlation and ^{1}H-^{1}H COSY NMR studies established two distinct protein domains in blue crab *Callinectes sapidus* metallothionein-I.[709] Metallothioneins are small, cysteine-rich found throughout Nature.[710] They are able to bind several different metals with several stoichiometric ratios, making the family of proteins important for essential metal (e.g., Zn^{2+} and Cu^{+}) homeostasis, metal storage, metal donation to nascent metalloenzymes and heavy metal detoxification.[710] In addition, metallothioneins are considered to protect cells against oxidative stress with its 20 cysteines. Investigations of the mechanistic details of metal binding to mammalian metallothioneins, including the use of ^{113}Cd NMR, were reviewed in 2018.[710] For Zn(II)-containing Bud31p, a 157-residue yeast protein containing an unusual Zn_3Cys_9 cluster, ^{113}Cd NMR experiments with ^{113}Cd-substituted samples were performed to reveal the unusual metal cluster in the solution structure of the yeast splicing protein Bud31p.[713] Cd(II) derivatives of ovotransferrin and human serum transferrin were investigated by ^{113}Cd and ^{13}C NMR.[719] ^{113}Cd NMR was also used to observe directly the exchange dynamics of water at a Cd(II) binding site within two *de novo* designed metalloprotein constructs, showing the residence time of the Cd(II)-

bound water molecule was tens of nanoseconds at 20 °C in both proteins.[712] In addition to the proteins and enzymes, Cd(II) bindings to dinucleosides and DNA containing modified nucleosides 4-thio-2′-deoxyuridine (s4dU) and 4-thio-2′-deoxythymidine (s4dT) as metal ion binding sites was probed by ^{113}Cd NMR.[717]

In computational studies of ^{113}Cd NMR, *ab initio* and DFT methods were reproduced to within ~50 ppm of the shifts for Cd(II)-substituted metal ion containing proteins.[720] ^{113}Cd shifts were also calculated using Hartree-Fock and DFT methods for Cd(II) complexes, such as $CdMe_2$, $CdEt_2$, CdMeEt, $Cd(NO_3)_2$•$4H_2O$, and $Cd(O_2CCH_3)_2$•$2H_2O$.[721]

For NMR of ligands, ^{113}Cd NMR of $[MeSi[SiMe_2N(p\text{-tol})]_3Sn]_2Cd$ (**139**) showed two signals (δ 310 and 201), and the ^{119}Sn NMR showed signals at δ -142.7 and -22.2.[695] The crystal structure showed it to be a symmetric molecule. ^{1}H ROESY and VT ^{1}H experiments were conducted to study the dynamic exchange between two isomers of **139** (**Figure 12**).[695] The asymmetric isomer is an analog of the Zn(II) complex **134**.

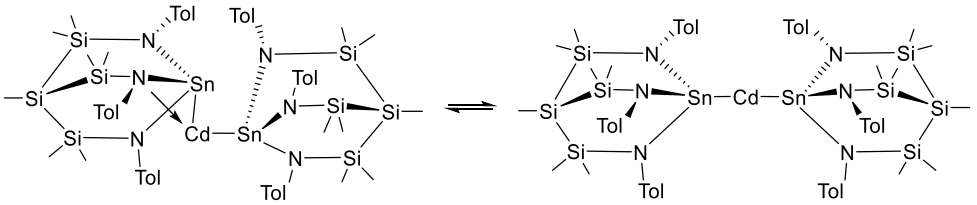

Figure 12. Dynamic exchange between two isomers of **139**.

Tetrahedrally coordinated $(Et_3NH)_6[Cd(SnB_{11}H_{11})_4]$ (**140**) was synthesized via the reaction of stanna-*closo*-dodecaborate with $CdBr_2$ and analyzed via ^{113}Cd (δ -42), ^{119}Sn (δ -377) and ^{11}B (δ -13.8) NMR.[722]

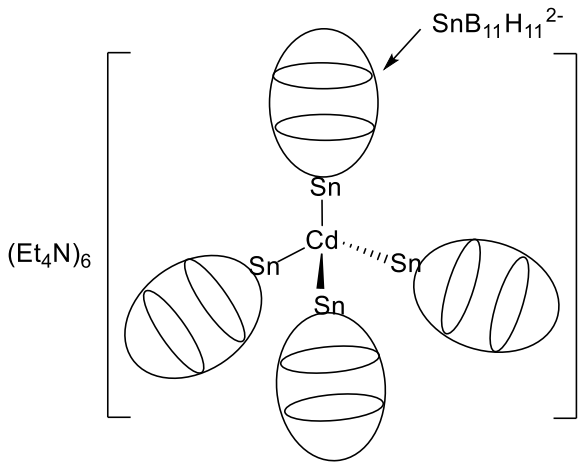

(**140**)

In order to elucidate weaker binding sites for Mg(II) in an RNA sample (D1κζ), Cd(II) was used in order to more easily study these sites in D1κζ by NMR, as discussed earlier in the section on cobalt complexes.[500] ^{15}N-labelled and/or ^{13}C-labelled D1κζ samples were titrated with $Cd(ClO_4)_2$ or $^{113}Cd(NO_3)_2$.[500] ^{1}H, ^{1}H-^{15}N HSQC, ^{31}P, ^{113}Cd, and ^{1}H-^{13}C HSQC NMR spectra were studied after each addition of the metal complex.[500]

11.3. *Mercury complexes*

^{199}Hg [spin 1/2, a natural abundance of 16.87%, relative receptivity D^C = 5.89 with respect to ^{13}C, and Ξ = 17.910822%] is a good nuclide for NMR. There are three major features of ^{199}Hg NMR of inorganic complexes: (a) Chemical exchange often faster than Cd(II) complexes; (b) Large chemical shift anisotropies; (c) Large coupling constants.[1]

^{199}Hg NMR was the subject of a review in 1992.[723] Using multinuclear NMR to probe speciation of Hg complexes was reviewed in 2006.[724]

In Hg(II) coordination chemistry, solvation of $Hg(ClO_4)_2$ in H_2O, dmso, $HC(=S)NMe_2$, and liquid NH_3 was studied by ^{199}Hg NMR.[725] The work showing a pronounced dependence on the coordination number of the Hg(II) ion with ^{199}Hg shifts of >1200 ppm between tetrahedral and

octahedral complexes as well as electron donor properties of the solvents. The ^{199}Hg spin-lattice relaxation times in the solvates were measured in several applied magnetic fields, concentrations, temperatures, and isotope substitutions.[725] Additional studies of solvation of $Hg(ClO_4)_2$ in liquid NH_3 and aqueous ammonia solution (when the molar ratio NH_3:Hg(II) > 4) showed the formation of $[Hg(NH_3)_4](ClO_4)_2$, which was characterized by single-crystal diffraction.[726-727] When $HgCl_2$ or $HgBr_2$ was dissolved in liquid NH_3, $Hg(NH_3)_4^{2+}$ [δ -1065 to -1163 relative to $HgMe_2$ (at δ = 0) or δ 1188 to 1090 relative to $Hg(ClO_4)_2$ (at δ = 0)], although ^{199}Hg NMR indicated weak Hg(II) to Br^- association.[727] In liquid NH_3, HgI_2 formed $Hg(NH_3)_2I_2$ at δ -1902 relative to $HgMe_2$ [δ 351 relative to $Hg(ClO_4)_2$] with the Raman μ(I-Hg-I) symmetric stretching frequency was 132 cm^{-1}.[727] ^{199}Hg NMR shifts of the stable $HgCl_n^{2-n}$ (n = 0-4) were determined in 50 mM aqueous Hg(II) solution as a function of the Cl^- concentration.[728] $HgCl_2[N,N'\text{-}Bu^tNSe(\mu\text{-}NBu^t)_2SeNBu^t]$ was obtained from the [2 + 2] cyclodimerization of t-butylselenium diimide $Se^{IV}(=NBu^t)_2$ with $HgCl_2$, which was characterized by ^{199}Hg (δ -1190) and ^{77}Se (δ 1093) NMR.[729] Linear complex $Hg[N(SiMe_3)_2]_2$ was studied by ^{199}Hg and ^{15}N NMR, including their spin-lattice relaxation times T_1 at 243-403 K, ^{14}N quadrupolar cross-correlation coefficient, and $J^{199}{}_{Hg\text{-}}{}^{15}{}_N$ = 316.2 Hz.[730] Demethylation of $(MeO)_3P{=}O$ by $(NMe_4)_2[Hg(SPh)_4]$ and $(NBu^n{}_4)[Hg(SPh)_3]$ gave MeSPh, $(MeO)_2P(=O)_2^-$, and $Hg(SPh)_3^-$ from $(NMe_4)_2[Hg(SPh)_4]$ and MeSPh and $Hg(SPh)_2[(MeO)_2P(=O)_2]^-$, respectively.[731] ^{199}Hg was used to characterize the reaction mixtures by comparing with ^{199}Hg shifts of $(NMe_4)_2[Hg(SPh)_4]$ (δ -421) and $(NBu^n{}_4)[Hg(SPh)_3]$ (δ -354) in the identification of the products.[731] A series Hg(II) complexes containing thiacrown and related aza and mixed thia/aza macrocycles were characterized by ^{199}Hg NMR.[732] The ^{199}Hg shifts of these complexes are listed in Table 16.

Table 16. ^{199}Hg NMR shifts of Hg(II) thiacrown and related aza and mixed thia/aza complexes[732]

Complexes	^{199}Hg shifts (δ)

$[Hg(9S3)_2](ClO_4)_2$ (9S3 = 1,4,7-trithiacyclonane)	-275
$[Hg(10S3)_2](ClO_4)_2$ (10S3 = 1,4,7-trithiacyclodecane)	-598
$[Hg(12S3)_2](ClO_4)_2$ (12S3 = 1,5,9-trithiacyclododecane)	-795
$[Hg(14S4)](ClO_4)_2$ (14S4 = 1,4,8,11-tetrathiacyclotetradecane)	-827
$[Hg(16S4)](ClO_4)_2$ (16S4 = 1,5,9,13-tetrathiacyclohexadecane)	-1120
$[Hg(15S5)](ClO_4)_2$ (15S5 = 1,4,7,10,13-pentathiacyclopentadecane)	-484
$[Hg(18S6)](ClO_4)_2$ (18S6 = 1,4,7,10,13,16-hexathiacyclooctadecane)	Not observed
$[Hg(18S_4N_2)](PF_6)_2$ ($18S_4N_2$ = 1,4,10,13-tetrathia-7,16-diazacyclooctadecane)	-737 and -816; Two different diastereoisomers from the relative orientations of the two H (in N-H) atoms
$[Hg(9N3)_2](ClO_4)_2$ (9N3 = 1,4,7-triazacyclononane)	-948 and -1313; The solution is believed to be a mixture of $[Hg(9N3)]^{2+}$ and $[Hg(9N3)_2]^{2+}$.

In Hg(II) organometallic chemistry, dependence of ^{199}Hg NMR spectra of a variety of polyfluoroaryl complexes, such as $Hg(C_6F_5)_2$ (δ -851), $Hg(4\text{-}CF_3\text{-}C_6F_4)_2$ (δ -915), $Hg(4\text{-}MeO\text{-}C_6F_4)_2$ (δ -811), $Hg(4\text{-}F\text{-}C_6H_4)_2$ (δ -734), C_6F_5HgEt (δ -604), $(4\text{-}F\text{-}C_6H_4)HgEt$ (δ -536), on solvents (shifts listed above in CH_2Cl_2), concentrations, temperatures, and ligands was studied.[733] ^{199}Hg NMR spectra of substituted vinyl Hg(II) halides, such as ClHC=CHHgCl (*Z*, δ -1141; *E*, δ -1160), PhHC=CHHgBr (*Z*, δ -1018; *E*, δ -1200), and MeHC=CHHgBr (*Z*, δ -1056; *E*, δ -1131), showed that shifts of the *Z* isomers were deshielded from those of the *E* isomers.[734] Experimental (^{199}Hg and ^{13}C NMR) and theoretical studies of $Hg(C{\equiv}CPh)_2$ were conducted to obtain shielding and indirect spin-spin coupling tensors in the presence of a heavy atom.[735]

^{199}Hg and ^{13}C spin-lattice relaxation times were studied to probe solution dynamics of $Hg(C{\equiv}CPh)_2$ and shielding anisotropy of its acetylenic C and Hg nuclides.[736] For thiosulfatemercuriomethanates $Na_n[CH_{4-n}(HgS_2O_3)_n]$ ($1 \leq n \leq 4$), their ^{199}Hg shifts became gradually more deshielded with increasing n: n = 1, δ -677; n = 2, δ -577; n = 3, δ -496; n = 4, δ -453.[737]

A series of Hg-Mo complexes X-Hg-$MoCp(CO)_2(PAr_3)$ (X = F^-, Cl^-, Me^-, OMe^-),[738] $Hg[MoCp(CO)_2(PAr_3)]_2$,[738-739] derivatives with substituted cyclopentadienyl ligands X-Hg-$MoCp^{\#}(CO)_3$[740] and $Hg[MoCp^{\#}(CO)_3]_2$[740] ($Cp^{\#} = C_5HMe_2Ph_2^-$) were studied by ^{199}Hg NMR. ^{199}Hg shits of selected complexes include the following: (a) Hg(I) compounds Cl-Hg-$MoCp(CO)_2[P(4\text{-}Cl\text{-}C_6H_4)_3]$ (δ -523),[738] I-Hg-$MoCp(CO)_2(PPh_3)$ (δ -921),[738] X-Hg-$MoCp^{\#}(CO)_3$ ($Cp^{\#-} = C_5HMe_2Ph_2^-$, X = Cl^-, δ -644; X = Br^-, δ -827; X = I^-, -1169);[740] (b) Hg(0) compounds $Hg[MoCp(CO)_3]_2$ (δ 235.3)[739] and $Hg[MoCp^{\#}(CO)_3]_2$ ($Cp^{\#-} = C_5HMe_2Ph_2^-$, δ 98) with Mo-Hg-Mo bonds.[740]

In Hg bioinorganic chemistry, ^{199}Hg NMR was used probe Hg(II) binding with *L*-cysteine,[741] glutathione,[742] 2-(α-hydroxy-benzyl) thiamin pyrophosphate (Hhbtp) as a model for metal binding in thiamin enzymes,[716] and the metal sites in Hg(II)-mediated thymine (T)–thymine base pair,[743] blue copper proteins,[744] and the metal receptor site in MerR and its protein-DNA complex.[745] In Hg(II) complexes with *L*-cysteine (H_2Cys) in alkaline aqueous solutions structurally were characterized by extended X-ray absorption fine structure (EXAFS) spectroscopy,[741] aided by ^{199}Hg NMR and Raman results. In the reaction of K^+ salt of 2-(α-hydroxy-benzyl) thiamin pyrophosphate, $K^+(hbtp)^-$, with $HgCl_2$, the product was $K_2[Hg(hbtp)_2Cl_2]$ showing ^{199}Hg shift at δ -804.[716] In the reaction of Hg(II) ions with ^{15}N-labeled thymidine (T), one of the four nucleobases in the nucleic acid of DNA, ^{199}Hg and ^{15}N NMR studies indicated that the product was linear T-Hg-T, giving ^{199}Hg δ -1784, ^{15}N δ 184, and $^1J_{^{199}Hg\text{-}^{15}N}$ = 1050 Hz.[743] ^{199}Hg NMR spectra of the ^{199}Hg-substituted blue copper proteins exhibited shifts of δ -749 for

^{199}Hg-plastocyanin and δ -884 for ^{199}Hg-azurin.[744] For the metal receptor site in MerR and its protein-DNA complex,[745] structural insights were provided by ^{199}Hg NMR. The 1- and 2-D NMR data showed a trigonal planar Hg-thiolate coordination environment consisting only of Cys side chains.[745]

In theoretical studies, microsolvation of $(HgMe)^+$ in water, including structures, energies, bonding and ^{199}Hg, ^{13}C and ^{17}O NMR constants (chemical shifts and coupling constants), was investigated by Hartree–Fock (HF) and second-order perturbation theory (MP2) calculations within the scalar and full relativistic frames.[746]

NMR studies of α atoms of ligands in Hg complexes were also conducted. There was only one signal in both the ^{199}Hg (δ -267.8) and ^{119}Sn (δ 266.2) NMR spectra of $[MeSi[SiMe_2N(p\text{-tol})]_3Sn]_2Hg$, an analog of the Cd(II) complex **139** (**Figure 13** in Section 11.2), showing that this complex was a symmetric with respect to the Hg(II) ion and it did not isomerize as its Cd(II) analogue.[695]

The interaction between the oligonucleotide $[d(CGCGAATTCGCG)]_2$ and Hg(II) was studied via several NMR methods including ^{1}H-^{15}N HMQC.[747] The HMQC studies confirmed that the Hg(II) interfered with the AT tract of the oligonucleotide.[747] Hg(II)-mediated T-T (thymine-thymine) pairings were studied via 1-D ^{15}N NMR and 2-D ^{1}H-^{15}N HSQC with *J*-coupling ($^2J_{^{15}N-^{15}N}$) of 2.4 Hz for the N-Hg-N moiety.[748]

The tetrahedrally coordinated $(Me_3NH)_6[Hg(SnB_{11}H_{11})_4]$ was synthesized via the reaction of stanna-*closo*-dodecaborate with Hg_2Cl_2 and analyzed via ^{199}Hg (δ -630), ^{119}Sn (δ -320) and ^{11}B (δ -14.4) NMR.[722] This complex and its Cd analog $(Et_3NH)_6[Cd(SnB_{11}H_{11})_4]$ (**140**), discussed in Section 11.2, were the first examples of coordination complexes with this stanna-*closo*-dodecaborate ligand and group 12 metals.[722]

12. NMR properties shared by complexes of more than two transition metals.

Experimental and theoretical/computational studies

NMR properties shared by complexes of two transition metals are discussed in their respective sections.

12.1. *NMR of metals in the complexes*

We found that NMR chemical shifts of d^0 transition metal compounds showed the following trends:[285] (1) For single-bonded ligands such as M-*H*, M-*C*R_3, M←*N*R_3, M-*Si*R_3 and M←*P*R_3, ^{1}H, ^{13}C, ^{15}N, ^{29}Si and ^{31}P shifts of these α atoms in the complexes of both first- and third-row transition metals are typically more deshielded than those of second-row analogs with a "V-shape" (Trend 1). (2) For multiple-bonded ligands including those with d-p π bonds, such as M=*C*HR, M≡*C*R, M=*N*R, M=*O* and M ⇐ *F*, ^{13}C, ^{15}N, ^{17}O and ^{19}F shifts of the α atoms in the complexes of first-, second- and third-row transition metals become consecutively more shielded (Trend 2).[285] NMR shifts of lanthanum(III) complexes help interpret Trend 1 in Group 3 congeners. Scandide (d-block) and lanthanide (f-block) contractions and relativistic effects were believed to contribute to the NMR shifts, leading to the observed trends. Comparisons were made with NMR chemical shifts of d^n complexes and organic compounds. Since many chemical properties of the second- and third-row congeners such as Zr and Hf are similar, as a result of lanthanide contraction, the NMR chemical shifts were a rare property to distinguish compounds of the otherwise nearly identical congeners. Our narrative interpretations of the trends were provided.[285]

Substituent influence on reported ^{51}V, ^{55}Mn, ^{57}Fe, ^{59}Co, ^{61}Ni, ^{95}Mo, ^{103}Rh, ^{183}W, ^{187}Os and ^{195}Pt NMR shifts (δ) and coupling constants $J_{M\text{-}P}$ (M = Mn, Fe, Mo, Rh, W, Os) in organometallic complexes were analyzed, showing shifts depended on the inductive, resonance, and polarizability effects of substituents.[1,749] The role of polarization effect on the NMR of heavy nuclides (^{51}V, ^{55}Mn, ^{57}Fe, ^{95}Mo, ^{103}Rh, ^{187}Os and ^{195}Pt) was reviewed.[750] Another study was

conducted on the polarizability effect in transition metal CO complexes.[751]

NMR peak line widths of quadrupolar nuclides ^{14}N, ^{53}Cr, ^{59}Co, ^{91}Zr and ^{95}Mo in supercritical solvents and low-viscosity liquefied gases were smaller than in ambient solvents.[249] For example, both ^{53}Cr and ^{14}N (spin 1, natural abundance = 99.636%, Q = 2.044 fm^2, relative sensitivity = 1.00 x 10^{-3}, receptivity = 5.90, gyromagnetic ratio = 1.9337792 x 10^7 rad T^{-1} s^{-1}, Ξ = 7.226317%)[25-26] are quadrupolar nuclides with broad NMR peaks. ^{53}Cr and ^{14}N NMR of $Cr(CO)_5(CNBu^t)$ and $Cr(CO)_4(CNBu^t)_2$ in ambient acetone-d_6, pressurized liquid CO_2 or supercritical CO_2 were compared.[249] For $Cr(CO)_5(CNBu^t)$, ^{53}Cr shifts were δ 17.9, 15.7 and 36.1, respectively, in the three media with peak width reduced from 90 Hz in acetone-d_6 to 35 Hz in the two CO_2 media. Its ^{14}N shifts were δ -171.4, -176.1 and -175.6, respectively, in the three media.[249] For $Cr(CO)_4(CNBu^t)_2$, ^{53}Cr shifts were δ 60.4 and 52.4 in acetone-d_6 and liquid CO_2, respectively, with peak width reduced from 44 Hz in the former to 34 Hz in the latter. Its ^{14}N shifts were δ -174.5 and -178.6 in acetone-d_6 and liquid CO_2, respectively.[249] The studies here tested the reduction of quadrupolar relaxation rates in solvents with low viscosity such as supercritical fluids. In another example, ^{91}Zr peak width of Cp_2ZrCl_2 in thf-containing supercritical CO_2 (CO_2:thf = 93:7; v/v) at 323 K was found to be 210 Hz, a significant decrease from 375 Hz in ambient thf at 296 K.[249] The addition of a small amount of acetone, thf, and CH_2Cl_2 increased the solubilities.

12.2. *NMR of ligand nuclides in the complexes*

Multinuclear NMR was demonstrated to be a good tool to characterize complexes with σ-silane and σ-borane ligands, distinguishing them from the corresponding hydride silyl or hydride boryl oxidative addition products.[139] The studies in the area were reviewed in 2008.[139] Several heterometallic cluster complexes with Mo and Te, including $(Cp^*Mo)_2B_4TeH_5Cl$ and $(Cp^*Mo)_2B_4(\mu_3\text{-}OEt)TeH_3Cl$, were characterized via ^{11}B NMR.[752]

^{119}Sn NMR was used to characterize transition metal complexes $L_nM\text{-}SnR_2$ with terminal

stannylene ligands, including $(OC)_5WSn(OSiPh_3)_2$ (δ -303, $^1J^{119}_{Sn-W}$ = 1660 Hz), $MeSi[SiMe_2N(p\text{-tolyl})]_3Sn\text{-}Rh(PEt_3)(cod)$ (δ -140.5, $^1J^{119}_{Sn-Rh}$ = 846 Hz), and $(Ph_3P)_3Pt\text{-}Sn(acac)_2$ (δ -601, J^{119}_{Sn-Pt} = 1.289 x 10^4 Hz).[753] The research in the area was reviewed in 2009.[753] ^{119}Sn NMR was also used to characterize $CpM(CO)_3[Sn(C_6H_3\text{-}2,6\text{-}Mes_2)]$ (Mes = 2,4,6-Me_3-C_6H_2; M = Cr, Mo, W), $CpM(CO)_3[Sn(C_6H_3\text{-}2,6\text{-}Trip_2)]$ (Trip = 2,4,6-Pr^i_3-C_6H_2; M = Cr, Mo, W), and (η^5-1,3-$Bu^tC_6H_3$)$Mo[Sn(C_6H_2\text{-}2,6\text{-}Trip_2)]$ (δ 2543).[754]

^{15}N coordination shifts in transition metal complexes with *N*-containing heterocycle ligands (azines, azoles and azoloazines like purines or 1,2,4-triazolo-[1,5a]-pyrimidines) were reviewed and discussed with respect to the metal ions and the donor atoms in *trans* position with respect to the ^{15}N atom.[755] Here, the coordination shifts are the differences between ^{15}N shifts of the N atoms in the complex and the free ligand [$\Delta(^{15}N) = \delta_{complex} - \delta_{ligand}$].[755]

^{14}N and ^{15}N NMR studies of imide ligands were conducted for 37 Ta, Mo, W, Re and Os complexes, including $Ru_3(\mu\text{-}H)_2(\mu_3\text{-}^{15}NH)(CO)_9$ (δ -297.7), *trans*-$TaCl(^{15}NPh)(PMe_3)_4$ (δ -76.6), $W(NBu^t)_2(OBu^t)_2$ (δ -11), $[Mo(^{15}NH)(S_2CNEt_2)_3]Cl$ (δ 40.0), *trans*-$[ReCl(^{15}NH)(dppe)_2]Cl_2$ (δ 67.1), and $Os(NBu^t)_4$ (δ 155.6).[756] The studies showed that ^{14}N and ^{15}N NMR spectroscopy was a probe of bonding, bending and fluxionality of the imido ligands.[756] Reviews in 2008[757] and 2013[758] together covered the ^{15}N NMR and the ^{31}P NMR of over 300 complexes. These complexes contain metal ions such as Ni(0), Pd (II), and Au(III) with N- or P-containing heterocyclic ligands such as pyridine, 1,10-phenanthroline, or phosphorin.[758] Line broadening in variable-temperature and -pressure ^{14}N, ^{13}C, and ^{1}H NMR spectra was used to study the exchange of bidentate ethylenediamine (en) ligands in Co(II), Fe(II), and Mn(II) complexes.[759] Further studies of solvent exchange of N-containing ligands 1,3-propanediamine (pa) and n-propylamine (tn) were conducted with variable-temperature ^{14}N NMR, and the results were compared with the data from the en exchange studies.[760] The order of rate constants for these exchanges increases in the order of en < tn < pa for each metal ion. For example, the rate

constants (k^{298}) for Mn(II) are 1.7 x 10^6 s^{-1} for en, 2.5 x 10^6 s^{-1} for tn, and 3.7 x 10^7 s^{-1} for pa.[759-760]

^{1}H-^{15}N HSQC and super-WEFT ^{1}H NMR (WEFT = water elimination Fourier transform), a method to suppress water signals, were used to probe the coordination of Co(II), Ni(II), and Zn(II) ions to a section of DNase domain of colicin E9.[761] The interactions of Ag(I)- and Cd(II)-substituted amicyanin with the periplasmic enzyme MADH (methylamine dehydrogenase) were investigated via several NMR techniques including ^{1}H-^{15}N HSQC and ^{15}N-decoupled TOCSY.[762] ^{15}N and ^{19}F NMR spectroscopies as well as DFT calculations were used to investigate the linearity of the M-NO section of the $[RuF_5NO]^{2-}$ anion by comparing the splitting patters and line widths of the signals of the ^{15}N-enriched and nonenriched samples of $[RuF_5NO]^{2-}$.[763] The data for the Ru compound was compared also to the ^{13}C and ^{15}N NMR of the structurally similar $[Fe(CN)_5NO]^{2-}$ (^{15}N- and ^{13}C-enriched) anion.[763] ^{17}O NMR was also used to probe the kinetic of proton exchange on dioxytetracyanometalate complexes $[MO^2(CN)^4]^{(n+2)-}$ (M = Mo, W, Tc, Re; n = 0,1,2)[764] as well as of oxygen exchange on di- and monoprotonated complexes $[MO(OH_2)(CN)_4]^{n-}$ (M = Mo, W, Tc, Re; n = 1,2) and $[MO(OH)(CN)_4]^{(n+1)-}$ (M = Mo, W, Tc, Re; n = 1,2).[765] ^{17}O NMR has also been used to study water and other oxygen-containing solvent exchanges on metal compounds such as aquapentakis(amine)metal(III) complexes,[766] such as $[Co(CH_2NH_2)(H_2O)]^{3+}$ and paramagnetic aminopolycarbonate complexes, such as $[Fe(TMDTA)]^{2-}$ (TMDTA = trimethylenediaminetetraacetate).[767]

Water and H^+ exchange processes on metal ions, studied by ^{17}O NMR, were the subject of a 2005 review.[768] ^{17}O NMR spectrum of an ^{17}O-enriched sample of $PW_{11}O_{39}^{7-}$ and results from other techniques “indicate that previously assigned terminal Pt-oxo and Au-oxo complexes are in fact cocrystals of the all-tungsten structural analogues with noble metal cations, while the Pd-oxo complex is a disordered Pd(II)-substituted polyoxometalate.”[769] In other words, the oxo wall[770] stands.

^{17}O NMR shifts of oxo metalloporphyrin complexes of Ti, Cr, and Ru, such as

M(TMP)(=O) (H_2TMP = tetramesitylporphyrin) were found to correlate with the strength of the M=O bonds.[137] The fluxional behaviors of $[(Rh(cod))_2(V_4O_{12})]^{2-}$ and $[Rh(cod))(V_4O_{12})]^{3-}$ (cod = η^4-1,5-cyclooctadiene) were studied via ^{51}V and ^{103}Rh NMR along with variable-temperature ^{17}O NMR.[771] Carbonyl complexes $(1,3,5\text{-}Me_3C_6H_3)Cr(CO)_3$, $(1,3,5\text{-}Me_3C_6H_3)W(CO)_3$, $[(1,3,5\text{-}Me_3C_6H_3)Mn(CO)_3]BF_4$, $(1,3,5\text{-}Me_3C_6H_3)Co_4(CO)_9$, $(1,3,5\text{-}Me_3C_6H_3)Ru_6C(CO)_{14}$, and $Ru_6C(CO)_{17}$ show ^{17}O shifts in the range of about δ 340-400.[772] Since the ^{17}O signals could not be observed for all the complexes in a single solvent, various solvents such as CH_3CN, $CDCl_3$, and $(CD_3)_2CO$ were utilized.[772]

^{33}S NMR was used to characterize several bidentate thiometallate complexes $(NEt_4)_2[MS_4]$ (M = Mo, δ 373; M = W, δ 183) and $(NH_4)_2[MS_4]$ (M = Mo, δ 344; M = W, δ 149).[773] ^{33}S NMR was also used to study heterometallic complexes $(NPr^n_4)_2[(CN)CuS_2MS_2]$ (M = Mo, δ 445; M = W, δ 248), $(NPr^n_4)_2[(CN)AgS_2MoS_2]$ (M = Mo, δ 257; M = W, δ 106), $(Pr^n_4N)_2[(CN)CuS_2MoS_2Cu(CN)]$ (M = Mo, δ 139; M = W, δ 16), and $(NPr^n_4)_2[(PhS)CuS_2MoS_2]$ (δ 436).[773]

^{77}Se NMR was used to characterize several complexes with the 1,3-diselenole-2-selone-4,5-diselenolate ligand [$C_3Se_5^{2-}$ (**141**)], including $(PPh_4)_2[Zn(C_3Se_5)_2]$ (δ Se^1, 105; Se^2, 1067; Se^3, 1134), $(NBu^n_4)_2[Pt(C_3Se_5)_2]$ (δ Se^1, 420; Se^2, 1116; Se^3, 1227), and $(NBu^n_4)[Au(C_3Se_5)_2]$ (δ Se^1, 729; Se^2, 1121; Se^3, 1330).[626]

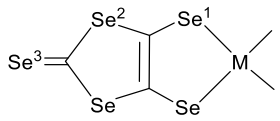

(**141**)

12.3. *Theoretical and computational studies of NMR*

Several reviews on calculations of transition metal NMR parameters,[774-777] including the

DFT methods to calculate NMR shifts,[774-775] methodology and computations of nuclear shielding and spin–spin coupling constants,[776] and developments of theoretical methods between 1999 and 2004.[777]

^{1}H NMR shifts of agostic H atoms in planar d^8 transition metal complexes were in a rather large range of 5 to -10 ppm.[778] When the agostic H atom points to a local Lewis acidic center at the metal, the ^{1}H NMR peak is shifted to be more shielded than that of the complex where the H atom is opposing a local charge concentration at the metal. The origin of the relationship was studied by a topological method.[778]

^{11}B NMR of $(Cp^*M)_2B_5H_9$ (M = Cr, Mo, W) showed shifts of the two types of B atoms directly bound to the metal atoms experienced a large, more shielded shift going from Cr to Mo to W, whereas the shifts for the B atoms connected to the metal atoms via M-H-B bridge bonds were invariant.[779] Molecular orbital analysis of the trend traced the origin to two high-lying filled MOs and two low-lying unfilled MOs, both with M and B character. The energy differences of these sets of MOs correlated well with the observed chemical shifts.[779] DFT computational studies of structures and properties of transition metal dicarbollide complexes were conducted and reproduced the ^{11}B NMR shifts reasonably well.[780]

Thermal effects and vibrational corrections were studied in the calculations of NMR shifts of ^{49}Ti, ^{51}V, ^{55}Mn, and ^{57}Fe shifts.[781]

13. Advanced NMR techniques and methods

This section provides an overview of advanced solution NMR techniques and methods used to characterize transition metal compounds.

13.1. *2-D NMR*

The 2-D NMR methods are discussed in the recent book by Lambert.[4] The use of 2-D NMR to study supramolecular complexes was reviewed in 2007.[782]

2-D NMR methods, in particular, inverse detection such as HMQC, HSQC, or HMBC to increase the sensitivity of the nuclides, indirectly determine chemical shifts of, e.g., ^{57}Fe[358-360] and ^{187}Os[361-362] (Section 7), ^{183}W (Section 5.3), and ^{103}Rh (Section 10). ^{1}H-^{15}N HMBC was also used to obtain ^{15}N (spin 1/2) NMR shifts of complexes at the natural abundance of 0.364%.[240-243,360,521,783] Often, different versions of the techniques such as gradient-selected *g*HMQC, *g*HSQC,[783] and *g*HMBC[240-243,360,521] were used.

In addition to obtaining NMR of the less sensitive nuclides, HMQC,[4] HSQC,[4] and HMBC[4] such as ^{1}H-^{13}C spectra were used to assign 1-D ^{1}H and ^{13}C spectra and structures of the complexes.[6,154,783-786] Homonuclear ^{1}H-^{1}H COSY (Correlated Spectroscopy)[4,6,783,787] and ^{1}H-^{1}H TOCSY (Total Correlated Spectroscopy)[783,787] were also used to assign spectra and structures of the complexes, giving through-bond correlations via spin-spin coupling in the molecules.

When studying H atoms that are close to each other in space but are not bound, ^{1}H-^{1}H NOESY (Nuclear Overhauser Effect Spectroscopy)[4,788] was used to study the signals from the through-space correlations via spin-lattice relaxation,[783,789] including solution structures of ion pairs such as the through-space $^{1}H\cdots{}^{1}H$ interactions between the cation and anion in *trans*-$[Ru(CO)(en)(PMe_3)_2(COMe)]BPh_4$.[790] NOESY could be used to detect chemical and conformational exchanges,[782,791-794] which is also called EXSY when it is used for this purpose.[782,791-792]

^{13}C-^{13}C NOESY was demonstrated to be an attractive alternative for studying large macromolecules.[795] ^{13}C direct detection provides a valuable alternative to ^{1}H detection to overcome fast relaxation because of its smaller magnetic moment.[795] Applications of the ^{13}C-^{13}C NOESY for studying metalloproteins were recently reviewed,[796] including advantages and drawbacks of the method as a function of the molecular size of the metalloproteins. It provided information on the presence/absence of multiple conformations in slow or semi-slow exchange on the NMR chemical shift time scale for amino acid side chains. ^{13}C-^{13}C NOESY was the gold standard for the observation of NMR signals in the 480 kDa ferritin nanocage and for monitoring

its interaction with Fe ions in the protein. When the protein size was decreased, the technique gradually lost its importance as a tool for the detection of the complete spin pattern of the amino acid side chains, as exemplified by Ni-dependent regulatory protein, NikR (molecular mass of the homo-tetramer ~80 kDa). In very small proteins, such as mitochondrial cytochrome *c* (12.3 kDa), only cross peaks between adjacent ^{13}C nuclei were detected, which was used to assign the ^{13}C core resonances of the porphyrin in a uniformly enriched heme.[796]

ROESY[4,797] is a 2-D NMR spectroscopy similar to NOESY. In NOESY, cross relaxation from an initial state of *z*-magnetization is observed. In ROESY, equilibrium magnetization is rotated onto the *x* axis and then locked so it cannot precess. ROESY is particularly suitable for medium size molecules (molecular weight around 700-1200) whose nuclear Overhauser effect is too weak to be detectable.

HOESY (Heteronuclear Overhauser Effect Spectroscopy), such as ^{1}H-^{19}F HOESY,[790,798-800] was used to characterize solution structures of ion pairs such as the through-space $^{1}H\cdots^{19}F$ interactions between peripheral H atoms on the cation and F-containing anion in $[Au(PPh_3)_2]BF_4$.[798]

13.2. *PGSE and DOSY*

Pulsed-Field Gradient Spin-Echo (PGSE) and Diffusion-Ordered Spectroscopy (DOSY) are diffusion NMR techniques to determine the size and shape of many molecular systems in solution.[782,801] When PGSE spectra are presented in a 2-D format, in which the chemical shifts are displayed in one dimension and the diffusion coefficient in the second one, the technique is called DOSY.[4,782] These two techniques were reviewed, especially their applications in inorganic and organometallic chemistry.[782,801] The applications included assessing aggregation state of molecules or supramolecules, character of intermolecular interactions, stability or association constants between different hosts and guests. DOSY has been called “NMR chromatography” for its ability to “separate” the components of a complex mixture according to their diffusion

coefficients.[782]

PGSE measurements using ^{1}H, ^{19}F, ^{31}P or ^{35}Cl NMR were performed on phosphine ligands and transition-metal complexes such as $Pt(PMe_2Ph)_2Cl_2$, $[Pt(PMe_2Ph)Cl(\mu\text{-}Cl)]_2$, [Pd[*o*-$(Ph_3P{=}N)\text{-}C_6H_4$]$(PPh_3)(Me_2NCH_2CH_2NMe_2)$]OTf, demonstrating that the four nuclides were complementary for PGSE.[802] Solvent dependence of the diffusion values of several Pd(II) salts suggested that ion pairing was a major contributor in $HCCl_3$, important in CH_2Cl_2, but small in acetone and MeOH.[802] PGSE NMR studies were performed to determine sizes of dendritic phosphine-gold(I) thiolate complexes.[803]

DOSY studies of *cis*- and *trans*-$[Ta(\mu\text{-}OMe)Me(=NSiMe_3)[N(SiMe_3)_2]]_2$ in equilibrium demonstrated that they existed as dimers in solution.[245] DOSY was used to characterize paramagnetic transition metal complexes, demonstrating that technique was capable of assessing the purity and speciation of paramagnetic complexes, and also provided a convenient method to provide qualitative and sometimes quantitative molecular weight data.[804]

13.3. *EDNMR, HYSCORE and ENDOR*

For paramagnetic compounds with unpaired electrons, electron-electron double resonance (ELDOR)-detected NMR (EDNMR),[805] hyperfine sub-level correlation (HYSCORE),[806-807] and electron-nuclear double resonance (ENDOR)[807-809] were used to detect hyperfine couplings between magnetic nuclides and unpaired electrons, thus helping to elucidate molecular and electronic structures. These techniques were employed to study hyperfine interactions in polyoxometalate $PV_2Mo_{10}O_{40}^{6-}$ with one reduced V(IV) ion.[198] In the ^{17}O-enriched anion, ^{95}Mo, ^{17}O, ^{51}V and ^{31}P nuclides had hyperfine interactions on the EPR resonance. The stronger interactions with ^{95}Mo and ^{17}O were probed by EDNMR and the weaker ones with ^{51}V and ^{31}P were studied by ENDOR.[198] The EDNMR technique[805] led to the observations of EPR, (^{95}Mo and ^{17}O) NMR, and ELDOR transitions and determination of ^{17}O and ^{95}Mo Larmor frequencies.[198] 2-D HYSCORE spectra correlate nuclear frequencies from

different electron-spin manifolds and resolve the hyperfine couplings. The studies here showed that there were two isomers of $PV_2Mo_{10}O_{40}^{6-}$ in solution.[198] ENDOR has also been used to study metalloenzymes and other metalloproteins.[807,809]

13.4. *Measurement of the relaxation time*

Deuterium ^2H NMR spin-lattice relaxation times (T_1) were measured in solution for the D ligands of transition metal hydride complexes and used for the calculation of deuterium quadrupole coupling constants and of the ionic contribution to the M-D bonds.[810]

^{13}C and ^{17}O T_1 times were measured for $M(CO)_6$ (M = Cr, Mo, and W) at two temperatures in $CDCl_3$.[811] ^{13}C T_1 values at two magnetic field strengths were utilized to calculate reorientational correlation times which, together with ^{17}O T_1 values, yielded values for the quadrupole coupling constants for ^{17}O nuclides in the molecules, which were used to investigate π bonding in the compounds.[811] This method was also used to study π bonding in $W(CO)_5L$ (L = pyrazine, pyridine, quinuclidine, NMe_3) and $M(CO)_5$(quinuclidine) (M = Cr, Mo).[812]

Inverse-detection methods were reported to determine spin-lattice relaxation times (T_1) of transition metal nuclides.[379] For insensitive spin 1/2 transition-metal nuclides, direct T_1 measurements were challenging, as very long measurement times were required even for large volumes of highly concentrated or labeled samples. The inverse-detection methods were demonstrated for ^{57}Fe, ^{103}Rh, and ^{187}Os in organometallic complexes.[379]

Indirect measurements of nuclear spin relaxation rates of nuclides with low gyromagnetic ratio (γ) was recently demonstrated using the satellite exchange.[813] The method did not require the observation of the low-γ nuclide, but required that it be scalar-coupled to an NMR observable nuclide, such as ^{31}P or ^1H. Thus, this method was especially attractive for the study of diamagnetic transition metals in complexes. When spin relaxation was dominated by chemical shift anisotropy (CSA), it is possible to determine T_1 of the metal by the method, as illustrated for ^{195}Pt and $^{107/109}Ag$.[813]

13.5. *Dynamic and variable-temperature (VT) NMR from chemical exchanges and reactions*

The use of EXSY to study chemical exchanges was overviewed in Section 13.1.

Other methods to study chemical exchanges were discussed in two monographs published in 1975[814] and 1982.[815] They were also covered in later books on NMR.[6,816]

Exchanges between two isomers or ligands at the NMR time scale may be studied by VT NMR. This method has been widely used to obtain exchange rate constants at different temperatures,[817-820] leading to the calculations of activation energies, enthalpies and entropies.[818-820] For example, alkyl alkylidyne $(Me_3SiCH_2)_3W(\equiv CSiMe_3)(PMe_3)$ and its bis-alkylidene isomer $(Me_3SiCH_2)_2W(=CHSiMe_3)_2(PMe_3)$ were found to undergo tautomerization, reaching an equilibrium.[818,821] The exchange was studied by VT NMR at 273-301 K, giving forward and reverse rate constants k = 1.42 x 10^{-5} s^{-1} and k' = 1.16 x 10^{-6} s^{-1}, respectively, at 278 K. The activation parameters are $\Delta H^{\neq}$ = 67.8 kJ/mol and $\Delta S^{\neq}$ = -92 J/mol·K for the forward reaction and $\Delta H^{\neq}$ = 75.3 kJ/mol and $\Delta S^{\neq}$ = -88 J/mol·K for the reverse reaction.[818,821]

Chemical reaction converting reactants to products were also studied by VT NMR to obtain rate constants.[822-823] Pentaneopentyltantalum $Ta(CH_2Bu^t)_5$ was directly observed as a precursor to the archetypical Schrock-type alkylidene complex $(Bu^tCH_2)_3Ta=CHBu^t$.[822,824] $Ta(CH_2Bu^t)_5$ was, however, short lived, and its ^1H NMR resonances were mixed with those of other species in a fairly narrow region.[824] D-labeled $Ta(CD_2Bu^t)_5$ was prepared and kinetic and mechanistic studies of its conversion to $(Bu^tCD_2)_3Ta=CDBu^t$ were performed by VT NMR at 273-298 K, giving $\Delta H^{\neq}$ = 82.3 kJ/mol and $\Delta S^{\neq}$ = -17 J/mol·K for the α-D abstraction reaction.[822] This work resolved a long-standing issue in inorganic and organometallic chemistry regarding the pathway in the formation of the archetypical alkylidene complex.[822]

The equilibrium mixture of $W(CH_2SiMe_3)_3(\equiv CSiMe_3)(PMe_3)$ and its bis(alkylidene) tautomer $W(CH_2SiMe_3)_2(=CHSiMe_3)_2(PMe_3)$ discussed in a previous paragraph underwent an α-

H abstraction reaction in the presence of PMe_3 to form alkyl alkylidene alkylidyne $W(CH_2SiMe_3)(=CHSiMe_3)(\equiv CSiMe_3)(PMe_3)_2$ at 333.2-363.2 K with the elimination of $SiMe_4$.[823] In the presence of PMe_3, the conversion to $W(CH_2SiMe_3)(=CHSiMe_3)(\equiv CSiMe_3)(PMe_3)_2$ followed first-order kinetics, and the observed rate constant was found to be independent of the concentration of PMe_3, giving activation parameters for the reaction, $\Delta H^{\neq}$ = 118 kJ/mol and $\Delta S^{\neq}$ = 13 J/mol·K.[823]

13.6. *NMR studies using parahydrogen (p-H_2)*

For reactions involving H_2, *p*-H_2 may be used to improve NMR sensitivity and probe the mechanism of reactions such as catalytic hydrogenation of organic substrates. The studies in the areas were reviewed.[825-830]

H_2 with two spin 1/2 nuclides occurred in two isomeric forms, one with its two spins aligned parallel (orthohydrogen, *o*-H_2; spin I = 1, $2I + 1 = 3$) and the other with the spins aligned antiparallel (parahydrogen, *p*-H_2). *p*-H_2 (I = 0, $2I + 1 = 1$) was in a lower energy state than *o*-H_2 in approximately *p*-H_2 : *o*-H_2 = 1 : 3 at room temperature and thermal equilibrium, reflecting the 3-fold degeneracy of *o*-H_2 and nearly equal population of the four energy levels. When H_2 was cooled, *o*-H_2 slowly converted to *p*-H_2, reaching ~1:1 ratio at 77 K. The use of such *p*-H_2-enriched hydrogen in chemical reactions may lead to *p*-H_2-induced polarization (PHIP), as the NMR signal intensity depended on the population difference, giving enhanced signals in the spectra of molecules derived from *p*-H_2.[830] Also, the associated resonances had antiphase character. Before the system re-established the Boltzmann population distribution via relaxation, NMR may be used to probe the newly formed spin state and larger than normal coherences could be generated for detection.[830] Applications of *p*-H_2 NMR included detection of intermediates, rapid product characterization and detection of hereronuclei, deduction of reaction stereochemistry, elucidation of pairwise reaction mechanisms, measurements of

reaction kinetics.[830]

In the reactions of $Pt[(\eta\text{-}CH_2{=}CHSiMe_2)_2O](PCy_3)$ with $HSiEt_3$, *p*-H_2 and PR_3, yielding *cis*-$Pt(PCy_3)(PR_3)(H)_2$ (PR_3 = PCy_2H, PPh_3 or PCy_3), *p*-H_2-enhanced NMR methods enabled the detection of the Pt(II) dihydride complexes which then underwent hydride site interchange and H_2 reductive elimination on the NMR timescale.[831] *p*-H_2-induced polarization was used to investigate alkyne hydrogenation and oligomerization using, e.g., $Pd(dcpe)(OTf)_2$ (dcpe = $Cy_2PCH_2CH_2PCy_2$) as a catalyst precursor.[832] The enhanced NMR resonances led to the identification of an alkyl palladium intermediate $[Pd(dcpe)(CHPhCH_2Ph)]OTf$.[832]

Other NMR techniques were developed based on the use of *p*-H_2, including SABRE (Signal Amplification by Reversible Exchange) as a recently emerged hyperpolarization method.[827,833-835] In this method, hyperpolarization of substrate molecules may be obtained even when they weakly associated to a suitable metal complex together with *p*-H_2. The reversible association provided a transient scalar coupling network through which the spin order of *p*-H_2 could be transferred to the nuclear spins of the substrate.[833] When a suitable co-substrate was used, substrates may be hyperpolarized at concentrations below that of the metal complex.[834]

SABRE approach was used to hyperpolarize the substrates indazole and imidazole in the presence of the co-ligand MeCN in, e.g., $[Ir(IMes)(H)_2L_3]Cl$ [IMes = (**128**), L = indazole or imidazole as substrate] prepared using *p*-H_2.[835] Quantitative trace analysis of mixtures using SABRE hyperpolarization was reported, using $[Ir(IMes)(H)_2L_3]Cl$ (L = substrate).[833] DFT computations and EXAFS studies were performed to study the interaction of $[Ir(IMes)(H)_2L_3]Cl$ (L = py, 1-methyl-1,2,3-triazole) generated by *p*-H_2 with substrate (py) and co-substrate (1-methyl-1,2,3-triazole) as co-substrate that were relevant for SABRE in dilute systems.[834] It was also demonstrated that the hyperpolarized labile ligand/substrate L in $[Ir(IMes)(H)_2L_3]Cl$ (L = nicotinamide, nicotinate, niacin, pyrimidine, and pyrazine), which was obtained from the reaction of IrCl(IMes)(cod) with *p*-H_2 and L, dissociated from the Ir(III) center.[836] The L molecules may then replace an OTf^- ligand in $Pt(OTf)_2(bdppp)$ (bdppp = bis-diphenylphosphinopropane), thus

transferring the hyperpolarization to the second metal complex. ^{31}P NMR resonance of the Pt(II) complex was found to be enhanced.[836] In other words, the hyperpolarization at the initial Ir(III) complex was passed onto the Pt(II) complexes in the SABRE-relay process.[836]

13.7. *High-pressure NMR*

High-pressure NMR were reviewed in 1996, giving details of the technique and its applications in organometallic chemistry.[837]

^{1}H and ^{17}O NMR studies of dmf exchange with $[Ti(dmf)_6]^{3+}$ as a function of pressure were discussed in Section 3.1.[133] The ^{99}Tc NMR spectrum of *fac*-$Tc(^{13}CO)_3(H_2O)_3^+$ under ^{13}CO (49 atm, **Figure 3**) was discussed in Section 6.2.[336-337] In Section 8.1 on Co NMR, the use of ^{59}Co NMR line-shape analysis to study Co carbonyl complexes[249,480,484] and the hydroformylation reaction in supercritical CO_2 was discussed.[484]

High-pressure NMR was often used to study homogeneous catalytic reactions involving, e.g., H_2 or CO.[336-337,838-840] Solution NMR studies under the high pressure of a gas were often conducted in a sapphire NMR tube.[336-337] A new, convenient flow cell for high-pressure NMR for in-situ study of homogeneous catalysis was reported, which could operate over the pressure range 1 to 197 atm and temperature range of -40 to 175 °C.[838] High-pressure NMR was used to study the reaction of Pt(bdpp)Me($SnCl_3$) [bdpp = (2*S*,4*S*)-2,4-bis(diphenylphosphino)pentane (**142**)] with CO and CO/H_2 mixture.[839] Under 49 atm, CO/H_2 = 1/1 pressure at 273 K, Pt(bdpp)MeH was detected, which then converted to [PtMe(CO)(bdpp)]$SnCl_3$ and [Pt(COMe)(CO)(bdpp)]$SnCl_3$.[839] High-pressure NMR studies were conducted on the migratory CO insertion on PtMe(P,P)Cl and [PdMe(P,P)(MeCN)]OTf containing a variety of bidentate, C_s-symmetrical 1,4-diphosphines such as 1,2-$(Ph_2PCH_2)_2$-C_6H_4.[841] The studies yielded rate constants.[841]

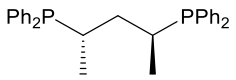

bdpp

(**142**)

High-pressure ^{17}O NMR studies of polyoxoions in water, focusing on the metal ions of interest in environmental chemistry and geochemistry, were reviewed in 2008.[842] These polyoxoions included monomeric $Al(H_2O)_6^{3+}$, $M_3(\mu_3\text{-}E)(\mu\text{-}E)_3(H_2O)_9^{4+}$ (M = Nb, Mo, W; E = S, O), $H_xM_6O_{19}^{(8-x)-}$ (M = Nb, Ta), $H_xM_{10}O_{28}^{(6-x)-}$ (M = V, Nb, Ta), $MO_4Al_{12}(OH)_{24}(H_2O)_{12}^{7/8+}$ (M = Al, Ga, Ge).[842] The 2008 review focused on the clusters for which high-pressure ^{17}O NMR yielded reaction kinetics and activation parameters.[842]

13.8. *Rapid-injection NMR*

A rapid-injection NMR method was reported in 2010 to allow the observation of fast chemical reactions in real time by NMR.[843] Design, validation, and implementation of the system were reported.[843] The method was used to study pre-transmetalation intermediates in the Suzuki-Miyaura reaction, which had been elusive. Species with Pd(II)-O-B linkages, such as $(4\text{-}F\text{-}C_6H_4)(Pr^i_3P)_2Pd\text{-}O\text{-}B(OH)(4\text{-}F\text{-}C_6H_4)$, were identified,[546] with more details of the studies published later.[547]

13.9. *Other advanced NMR techniques and methods*

Several other advanced NMR techniques and methods were used in the studies of transition metal compounds.

LED-illuminated NMR spectroscopy was reported for mechanistic studies of photochemical reactions.[844] This approach involves placing in-situ light illumination [using a light-emitting diode (LED)] inside an NMR spectrometer. This method, e.g., was used to study photodecomposition of a ferrioxalate ion $Fe(C_2O_4)_3^{3-}$ in solution to $Fe(C_2O_4)$ and CO_2 (detected

directly by ^{13}C NMR).[844]

^{1}H NMRD (Nuclear Magnetic Relaxation Dispersion) was used to study phthalate dioxygenase,[845] which was involved in the degradation of phthalate by the soil bacterium, *Pseudomonas cepacia* DB01. T_1^{-1} measurements at magnetic fields between 0.01 and 50 MHz, showing evidence for displacement of water on binding substrate. NMRD is a tool to estimate parameters influencing nuclear relaxation.[845]

Combination of 2-D EXSY and 1-D saturation transfer method was used to study the binding of imidazole, 1-methylimidazole, 1-ethylimidazole to the heme iron in metmyoglobin.[846] Some heme peripheral H resonances were assigned. The rates and equilibrium constants for the binding of the compounds to metmyoglobi were calculated from the EXSY peak amplitudes.[846]

14. Conclusion

Over the 30 year span (1990-2019) covered in the current review, there was much progress in NMR techniques and applications. The vast number of NMR shift data led to the finding of trends of the NMR shifts in transition metal complexes, as we recently found for d^0 complexes.[285] Among the challenges that remain are solution ^{175}Lu, ^{227}Ac, $^{177}Hf/^{179}Hf$, ^{193}Ir and ^{197}Au NMR of their complexes, as we did not find papers on the solution NMR of these nuclides and they were not reported in earlier books.[1,3] We hope to see breakthroughs in the solution NMR of these nuclides. Solution ^{181}Ta and $^{185}Re/^{187}Re$ NMR spectra of their complexes were reported prior to 1990 and we did not find papers on their NMR in our search of the literature since 1990. Similarly, ^{105}Pd NMR of H_2PdX_6 (X = Cl^-, Br^-) was first reported in 1984 with additional details provided in 1996.[399] Given the importance of these transition metals in, e.g., catalysis and materials sciences, we hope to see more use of the NMR of these nuclides in the studies of their complexes. NMR of both metals and ligands will continue to play a critical role in the studies of transition metal complexes.

Acknowledgment

The authors thank the US National Science Foundation (NSF CHE-1900296 and CHE-2055499 to Z.-L.X.), University of Tennessee, and Berry College for support to write this review.

References

1. *Transition Metal Nuclear Magnetic Resonance, P. S. Pregosin Ed.* 1991; Elsevier: Amsterdam.

2. Harris, R. K.; Mann, B. E., *NMR and the Periodic Table*. 1978; Academic Press: London.

3. *Multinuclear NMR*. Mason, J. E., 1987; Plenum Press.

4. Lambert, J. B.; Mazzola, E. P.; Ridge, C. D., *Nuclear Magnetic Resonance Spectroscopy: An Introduction to Principles, Applications, and Experimental Methods*. 2nd ed.; 2019; Wiley: Hoboken, New Jersey. https://www.wiley.com/en-fj/Nuclear+Magnetic+Resonance+Spectroscopy%3A+An+Introduction+to+Principles%2C+Applications%2C+and+Experimental+Methods%2C+2nd+Edition-p-9781119295280

5. Bertini, I.; Luchinat, C.; Parigi, G.; Ravera, E., *NMR of Paramagnetic Molecules: Applications to Metallobiomolecules and Models*. 2nd ed.; 2016; Elsevier. https://www.sciencedirect.com/book/9780444634368/nmr-of-paramagnetic-molecules

6. Pregosin, P. S., *NMR in Organometallic Chemistry*. 2013; Wiley-VCH: Weinheim, Germany. https://www.wiley.com/en-us/NMR+in+Organometallic+Chemistry-p-9783527330133

7. Iggo, J. A.; Liu, J.; Khimyak, Y. Z., Nuclear Magnetic Resonance (NMR) Spectroscopy of Inorganic/Organometallic Molecules. In *Applications of Physical Methods to Inorganic and Bioinorganic Chemistry*, Scott, R. A.; Lukehart, C. M., Eds. Wiley: West Sussex, UK, 2007; pp 315-355 (Also online in *Encyclopedia of Inorganic and Bioinorganic Chemistry*, https://doi.org/10.1002/9781119951438.eibc0295). https://www.wiley.com/en-

us/Applications+of+Physical+Methods+to+Inorganic+and+Bioinorganic+Chemistry-p-9780470032176

8. Berger, S.; Braun, S., *200 and More NMR Experiments: A Practical Course*. 2004; Wiley-VCH: Weinheim. https://www.wiley.com/en-us/200+and+More+NMR+Experiments%3A+A+Practical+Course-p-9783527310678

9. Bertini, I.; Turano, P.; Vila, A. J., Nuclear magnetic resonance of paramagnetic metalloproteins. *Chem. Rev.* **1993,** *93*, 2833-2932. https://doi.org/10.1021/cr00024a009

10. Rehder, D., Metal NMR of organometallic (d-block) systems. *Coord. Chem. Rev.* **1991,** *110*, 161-210. https://doi.org/10.1016/0010-8545(91)80025-9

11. Wrackmeyer, B., Inorganic Chemistry Applications. *eMagRes (earlier Encyclopedia of Magnetic Resonance)* **2011**. https://doi.org/10.1002/9780470034590.emrstm0239.pub2

12. Berger, S.; Braun, S.; Kalinowski, H.-O., *NMR Spectroscopy of the Non-Metallic Elements*. 1997; Wiley. https://www.wiley.com/en-us/NMR+Spectroscopy+of+the+Non+Metallic+Elements-p-9780471967637

13. *Advanced Applications of NMR to Organometallic Chemistry, M. Gielen, R. Willem, B. Wrackmeyer, Eds.* 1996; Wiley: New York. https://www.wiley.com/en-us/Advanced+Applications+of+NMR+to+Organometallic+Chemistry-p-9780471959380

14. Granger, P., NMR of Metallic Nuclei in Clusters. In *Advanced Applications of NMR to Organometallic Chemistry*, Gielen, M.; Willem, R.; Wrackmeyer, B., Eds. Wiely: New York, 1996; pp 313-356.

15. Applications of NMR to Inorganic and Organometallic Chemistry, P. S. Pregosin Ed. *Coord. Chem. Rev.* **2008,** *252*, 2155-2444. https://www.sciencedirect.com/journal/coordination-chemistry-reviews/vol/252/issue/21

16. *Comprehensive Inorganic Chemistry II. From Elements to Applications*. Reedijk, J.; Poeppelmeier, K., 2nd ed.; 2013; Elsevier.

17. *Comprehensive Inorganic Chemistry*. Bailar, J. C. J.; Emeléus, H. J.; Nyholm, R.; Trotman-Dickenson, A. F., 1973. https://www.sciencedirect.com/book/9781483283135/comprehensive-inorganic-chemistry

18. Jensen, W. B., The positions of lanthanum (actinium) and lutetium (lawrencium) in the periodic table. *J. Chem. Edu.* **1982,** *59*, 634. https://doi.org/10.1021/ed059p634

19. Settouti, N.; Aourag, H., A Study of the Physical and Mechanical Properties of Lutetium Compared with Those of Transition Metals: A Data Mining Approach. *JOM* **2015,** *67*, 87-93. https://doi.org/10.1007/s11837-014-1247-x

20. Stein, B. W.; Morgenstern, A.; Batista, E. R.; Birnbaum, E. R.; Bone, S. E.; Cary, S. K.; Ferrier, M. G.; John, K. D.; Pacheco, J. L.; Kozimor, S. A.; Mocko, V.; Scott, B. L.; Yang, P., Advancing Chelation Chemistry for Actinium and Other +3 f-Elements, Am, Cm, and La. *J. Am. Chem. Soc.* **2019,** *141*, 19404-19414. https://doi.org/10.1021/jacs.9b10354

21. Kupče, E.; Wrackmeyer, B., Selective Excitation and Selective Detection in ^{29}Si NMR. In *Advanced Applications of NMR to Organometallic Chemistry*, Gielen, M.; Willem, R.; Wrackmeyer, B., Eds. Wiley: New York, 1996; pp 1-44.

22. Kaseman, D. C.; McKenney, M., Quadrupolar Coupling **2021 (accessed on March 16, 2021)**. tal_Modules_(Physical_and_Theoretical_Chemistry)/Spectroscopy/Magnetic_Resonance_Spectroscopies/Nuclear_Magnetic_Resonance/NMR_-_Theory/NMR_Interactions/Quadrupolar_Coupling

23. Smith, J. A. S., Nuclear quadrupole resonance spectroscopy. General principles. *J. Chem. Edu.* **1971,** *48*, 39. https://doi.org/10.1021/ed048p39

24. Granger, P., Quadrupolar Transition Metal and Lanthanide Nuclei. In *eMagRes*, 2007. https://doi.org/10.1002/9780470034590.emrstm0433

25. NIST: Atomic Weights and Isotopic Compositions for All Elements. **2021**. https://physics.nist.gov/cgi-bin/Compositions/stand_alone.pl?ele=Ti&all=all

26. Harris, R. K.; Becker, E. D.; de Menezes, S. M. C.; Goodfellow, R.; Granger, P., NMR nomenclature. Nuclear spin properties and conventions for chemical shifts(IUPAC Recommendations 2001). *Pure Appl. Chem.* **2001,** *73*, 1795-1818. http://publications.iupac.org/pac/2001/pdf/7311x1795.pdf; https://doi.org/10.1351/pac200173111795

27. Harris, R. K.; Becker, E. D.; de Menezes, S. M. C.; Granger, P.; Hoffman, R. E.; Zilm, K. W., Further conventions for NMR shielding and chemical shifts (IUPAC Recommendations 2008). *Pure Appl. Chem.* **2008,** *80*, 59-84. https://doi.org/10.1351/pac200880010059

28. Zhu, C.; Gras, E.; Duhayon, C.; Lacassin, F.; Cui, X.; Chauvin, R., The Forgotten Nitroaromatic Phosphines as Weakly Donating P-ligands: An N-Aryl-benzimidazolyl Series in RhCl(CO) Complexes. *Chem. Asian J.* **2017,** *12*, 2845-2856. https://doi.org/10.1002/asia.201701078

29. Tan, N. S. L.; Nealon, G. L.; Lynam, J. M.; Sobolev, A. N.; Rowles, M. R.; Ogden, M. I.; Massi, M.; Lowe, A. B., A (2-(naphthalen-2-yl)phenyl)rhodium(i) complex formed by a proposed intramolecular 1,4-ortho-to-ortho′ Rh metal-atom migration and its efficacy as an initiator in the controlled stereospecific polymerisation of phenylacetylene. *Dalton Trans.* **2019,** *48*, 16437-16447. http://dx.doi.org/10.1039/C9DT02953B

30. Tan, N. S. L.; Simpson, P. V.; Nealon, G. L.; Sobolev, A. N.; Raiteri, P.; Massi, M.; Ogden, M. I.; Lowe, A. B., Rhodium(I)-α-Phenylvinylfluorenyl Complexes: Synthesis, Characterization, and Evaluation as Initiators in the Stereospecific Polymerization of Phenylacetylene. *Eur. .J. Inorg. Chem.* **2019,** *2019*, 592-601. https://doi.org/10.1002/ejic.201801411

31. Fabrello, A.; Dinoi, C.; Perrin, L.; Kalck, P.; Maron, L.; Urrutigoity, M.; Dechy-Cabaret, O., Probing the stereo-electronic properties of cationic rhodium complexes bearing chiral

diphosphine ligands by ^{103}Rh NMR. *Magn. Reson. Chem.* **2010,** *48*, 848-856. https://doi.org/10.1002/mrc.2677

32. Emsley, J., *The Elements*. 3rd ed.; 1998; Oxford University Press.

33. Pniok, M.; Kubíček, V.; Havlíčková, J.; Kotek, J.; Sabatie-Gogová, A.; Plutnar, J.; Huclier-Markai, S.; Hermann, P., Thermodynamic and Kinetic Study of Scandium(III) Complexes of DTPA and DOTA: A Step Toward Scandium Radiopharmaceuticals. *Chem. Eur. J.* **2014,** *20*, 7944-7955. https://doi.org/10.1002/chem.201402041

34. Barisic, D.; Diether, D.; Maichle-Mössmer, C.; Anwander, R., Trimethylscandium. *J. Am. Chem. Soc.* **2019,** *141*, 13931-13940. https://doi.org/10.1021/jacs.9b06879

35. Sears, J. M.; Boyle, T. J., Structural properties of scandium inorganic salts. *Coord. Chem. Rev.* **2017,** *340*, 154-171. https://doi.org/10.1016/j.ccr.2016.12.005

36. Hector, A. L.; Levason, W.; Webster, M., Synthesis and properties of scandium, yttrium and lanthanum periodates. Crystal structures of $Y(H_2O)_3\{IO_4(OH)_2\}$ and $Y(H_2O)_2(IO_3)_3$. *Inorg. Chim. Acta* **2000,** *298*, 43-49. https://doi.org/10.1016/S0020-1693(99)00409-0

37. Carravetta, M.; Concistre, M.; Levason, W.; Reid, G.; Zhang, W., Rare Neutral Diphosphine Complexes of Scandium(III) and Yttrium(III) Halides. *Inorg. Chem.* **2016,** *55*, 12890-12896. https://doi.org/10.1021/acs.inorgchem.6b02268

38. Hill, N. J.; Levason, W.; Popham, M. C.; Reid, G.; Webster, M., Scandium halide complexes of phosphine- and arsine-oxides: synthesis, structures and ^{45}Sc NMR studies. *Polyhedron* **2002,** *21*, 1579-1588. https://doi.org/10.1016/S0277-5387(02)01016-1

39. Deakin, L.; Levason, W.; Popham, M. C.; Reid, G.; Webster, M., Syntheses, structures and multinuclear NMR (^{45}Sc, ^{89}Y, ^{31}P) studies of Ph_3PO, Ph_2MePO and Me_3PO complexes of scandium and yttrium nitrates. *J. Chem. Soc., Dalton Trans.* **2000**, 2439-2447. http://dx.doi.org/10.1039/B001669L

40. Levason, W.; Patel, B.; Popham, M. C.; Reid, G.; Webster, M., Scandium, yttrium and lanthanum nitrate complexes of tertiary arsine oxides: synthesis and multinuclear spectroscopic

studies. X-ray structures of $[M(Me_3AsO)_6](NO_3)_3$ (M = Sc or Y), $[Sc(Ph_3AsO)_3(NO_3)_2]NO_3$, $[M''(Ph_3AsO)_4(NO_3)_2]NO_3$ (M″ = Y or La) and $[La(Ph_3AsO)_2(EtOH)(NO_3)_3]$. *Polyhedron* **2001,** *20*, 2711-2720. https://doi.org/10.1016/S0277-5387(01)00889-0

41. Meehan, P. R.; Willey, G. R., Solution state chemistry of scandium(III): a study of scandium-crown ether complexes by 45Sc-NMR spectroscopy. *Inorg. Chim. Acta* **1999,** *284*, 71-75. https://doi.org/10.1016/S0020-1693(98)00279-5

42. Brown, M. D.; Levason, W.; Murray, D. C.; Popham, M. C.; Reid, G.; Webster, M., Primary and secondary coordination of crown ethers to scandium(III). Synthesis, properties and structures of the reaction products of $ScCl_3(thf)_3$, $ScCl_3{\cdot}6H_2O$ and $Sc(NO_3)_3{\cdot}5H_2O$ with crown ethers. *Dalton Trans.* **2003**, 857-865. http://dx.doi.org/10.1039/B210458J

43. Champion, M. J. D.; Farina, P.; Levason, W.; Reid, G., Trivalent scandium, yttrium and lanthanide complexes with thia-oxa and selena-oxa macrocycles and crown ether coordination. *Dalton Trans.* **2013,** *42*, 13179-13189. http://dx.doi.org/10.1039/C3DT51405F

44. Curnock, E.; Levason, W.; Light, M. E.; Luthra, S. K.; McRobbie, G.; Monzittu, F. M.; Reid, G.; Williams, R. N., Group 3 metal trihalide complexes with neutral N-donor ligands – Exploring their affinity towards fluoride. *Dalton Trans.* **2018,** *47*, 6059-6068. http://dx.doi.org/10.1039/C8DT00480C

45. Bartlett, S. A.; Cibin, G.; Dent, A. J.; Evans, J.; Hanton, M. J.; Reid, G.; Tooze, R. P.; Tromp, M., Sc(III) complexes with neutral N_3- and SNS-donor ligands – A spectroscopic study of the activation of ethene polymerisation catalysts. *Dalton Trans.* **2013,** *42*, 2213-2223. http://dx.doi.org/10.1039/C2DT31804K

46. Taydakov, I.; Vaschenko, A.; Strelenko, Y.; Vitukhnovsky, A., An unexpected electro-luminescent properties of scandium(III) heteroaromatic 1,3-diketonate complex. *Inorg. Chim. Acta* **2014,** *414*, 234-239. https://doi.org/10.1016/j.ica.2014.02.013

47. Yang, S.; Wang, C.-r., *Endohedral Fullerenes. From Fundamentals to Applications*. 2014; World Scientific: Singapore. https://doi.org/10.1142/8785

48. *Endohedral Metallofullerenes: Basics and Applications (Ch. 4, NMR Spectroscopic and X-ray crystallographic characterization of endohedral metallofullerenes by Zhang, W.; Chen, M.; Bao, L.; Yamada, M.; Lu, X.; Olmstead, M. M.; Ghiassi, K. B.; Balch, A. L.)*. Lu, X.; Echegoyen, L.; Balch, A. L.; Nagase, S.; Akasaka, T., 2015; CRC Press. https://doi.org/10.1201/b17840

49. Stevenson, S.; Rice, G.; Glass, T.; Harich, K.; Cromer, F.; Jordan, M. R.; Craft, J.; Hadju, E.; Bible, R.; Olmstead, M. M.; Maitra, K.; Fisher, A. J.; Balch, A. L.; Dorn, H. C., Small-bandgap endohedral metallofullerenes in high yield and purity. *Nature* **1999,** *401*, 55-57. https://doi.org/10.1038/43415

50. Dunsch, L.; Yang, S.; Zhang, L.; Svitova, A.; Oswald, S.; Popov, A. A., Metal Sulfide in a C_{82} Fullerene Cage: A New Form of Endohedral Clusterfullerenes. *J. Am. Chem. Soc.* **2010,** *132*, 5413-5421. https://doi.org/10.1021/ja909580j

51. Chen, N.; Beavers, C. M.; Mulet-Gas, M.; Rodríguez-Fortea, A.; Munoz, E. J.; Li, Y.-Y.; Olmstead, M. M.; Balch, A. L.; Poblet, J. M.; Echegoyen, L., $Sc_2S@C_s(10528)$-C_{72}: A Dimetallic Sulfide Endohedral Fullerene with a Non Isolated Pentagon Rule Cage. *J. Am. Chem. Soc.* **2012,** *134*, 7851-7860. https://doi.org/10.1021/ja300765z

52. Wang, T.-S.; Feng, L.; Wu, J.-Y.; Xu, W.; Xiang, J.-F.; Tan, K.; Ma, Y.-H.; Zheng, J.-P.; Jiang, L.; Lu, X.; Shu, C.-Y.; Wang, C.-R., Planar Quinary Cluster inside a Fullerene Cage: Synthesis and Structural Characterizations of $Sc_3NC@C_{80}$-Ih. *J. Am. Chem. Soc.* **2010,** *132*, 16362-16364. https://doi.org/10.1021/ja107843b

53. Zhang, Y.; Popov, A. A., Transition-Metal and Rare-Earth-Metal Redox Couples inside Carbon Cages: Fullerenes Acting as Innocent Ligands. *Organometallics* **2014,** *33*, 4537-4549. https://doi.org/10.1021/om5000387

54. Feng, Y.; Wang, T.; Xiang, J.; Gan, L.; Wu, B.; Jiang, L.; Wang, C., Tuneable dynamics of a scandium nitride cluster inside an Ih-C80 cage. *Dalton Trans.* **2015,** *44*, 2057-2061. http://dx.doi.org/10.1039/C4DT02892A

55. Tang, Q.; Abella, L.; Hao, Y.; Li, X.; Wan, Y.; Rodríguez-Fortea, A.; Poblet, J. M.; Feng, L.; Chen, N., $Sc_2O@C_{2v}(5)$-C_{80}: Dimetallic Oxide Cluster Inside a C_{80} Fullerene Cage. *Inorg. Chem.* **2015,** *54*, 9845-9852. https://doi.org/10.1021/acs.inorgchem.5b01613

56. Yang, T.; Hao, Y.; Abella, L.; Tang, Q.; Li, X.; Wan, Y.; Rodríguez-Fortea, A.; Poblet, J. M.; Feng, L.; Chen, N., $Sc_2O@T_d(19151)$-C_{76}: Hindered Cluster Motion inside a Tetrahedral Carbon Cage Probed by Crystallographic and Computational Studies. *Chem. Eur. J.* **2015,** *21*, 11110 – 11117. https://doi.org/10.1002/chem.201500904

57. Tang, Q.; Abella, L.; Hao, Y.; Li, X.; Wan, Y.; Rodríguez-Fortea, A.; Poblet, J. M.; Feng, L.; Chen, N., $Sc_2O@C_{3v}(8)$-C_{82}: A Missing Isomer of $Sc_2O@C_{82}$. *Inorg. Chem.* **2016,** *55*, 1926-1933. https://doi.org/10.1021/acs.inorgchem.5b02901

58. Wang, Y.; Tang, Q.; Feng, L.; Chen, N., $Sc_2C_2@D_{3h}(14246)$-C_{74}: A Missing Piece of the Clusterfullerene Puzzle. *Inorg. Chem.* **2017,** *56*, 1974-1980. https://doi.org/10.1021/acs.inorgchem.6b02512

59. Yang, W.; Abella, L.; Wang, Y.; Li, X.; Gu, J.; Poblet, J. M.; Rodríguez-Fortea, A.; Chen, N., Mixed Dimetallic Cluster Fullerenes: $ScGdO@C_{3v}(8)$-C_{82} and $ScGdC_2@C_{2v}(9)$-C_{82}. *Inorg. Chem.* **2018,** *57*, 11597-11605. https://doi.org/10.1021/acs.inorgchem.8b01646

60. Zhang, Y.; Krylov, D.; Rosenkranz, M.; Schiemenz, S.; Popov, A. A., Magnetic anisotropy of endohedral lanthanide ions: paramagnetic NMR study of $MSc_2N@C_{80}$-I_h with M running through the whole 4f row. *Chem. Sci.* **2015,** *6*, 2328-2341. http://dx.doi.org/10.1039/C5SC00154D

61. Rinehart, J. D.; Long, J. R., Exploiting single-ion anisotropy in the design of f-element single-molecule magnets. *Chem. Sci.* **2011,** *2*, 2078-2085. http://dx.doi.org/10.1039/C1SC00513H

62. Fu, W.; Wang, X.; Azuremendi, H.; Zhang, J.; Dorn, H. C., 14N and 45Sc NMR study of trimetallic nitride cluster (M3N)6+ dynamics inside a icosahedral C80 cage. *Chem. Commun.* **2011,** *47*, 3858-3860. http://dx.doi.org/10.1039/C0CC03893H

63. Kerdjoudj, R.; Pniok, M.; Alliot, C.; Kubíček, V.; Havlíčková, J.; Rösch, F.; Hermann, P.; Huclier-Markai, S., Scandium(III) complexes of monophosphorus acid DOTA analogues: a thermodynamic and radiolabelling study with ^{44}Sc from cyclotron and from a ^{44}Ti/^{44}Sc generator. *Dalton Trans.* **2016,** *45*, 1398-1409. http://dx.doi.org/10.1039/C5DT04084A

64. Aramini, J. M.; Vogel, H. J., A Scandium-45 NMR Study of Ovotransferrin and Its Half-Molecules. *J. Am. Chem. Soc.* **1994,** *116*, 1988-1993. https://doi.org/10.1021/ja00084a044

65. Germann, M. W.; Aramini, J. M.; Vogel, H. J., Quadrupolar metal ion NMR study of ovotransferrin at 17.6 T. *J. Am. Chem. Soc.* **1994,** *116*, 6971-6972. https://doi.org/10.1021/ja00094a076

66. Wang, B.; Nishiura, M.; Cheng, J.; Hou, Z., Half-sandwich scandium boryl complexes bearing a silylene-linked cyclopentadienyl-amido ligand. *Dalton Trans.* **2014,** *43*, 14215-14218. http://dx.doi.org/10.1039/C4DT01725K

67. Wang, B.; Kang, X.; Nishiura, M.; Luo, Y.; Hou, Z., Isolation, structure and reactivity of a scandium boryl oxycarbene complex. *Chem. Sci.* **2016,** *7*, 803-809. http://dx.doi.org/10.1039/C5SC03138A

68. Levy, G. C.; Rinaldi, P. L.; Bailey, J. T., Yttrium-89 NMR. A possible spin relaxation probe for studying metal ion interactions with organic ligands. *J. Magn. Reson.* **1980,** *40*, 167-173. https://doi.org/10.1016/0022-2364(80)90237-1

69. Mann, B. E., The Cinderella Nuclei. *Annu. Rep. NMR Spectrosc.* **1991,** *23*, 141-207. https://doi.org/10.1016/S0066-4103(08)60277-X

70. Schaverien, C. J., Alkoxides as ancillary ligands in organolanthanide chemistry: Synthesis of, reactivity of, and olefin polymerization by the μ-hydride-μ-alkyl compounds

[Y(C_5Me_5)($OC_6H_3{}^tBu_2$)]$_2$(μ-H)(μ-alkyl). *Organometallics* **1994,** *13*, 69-82. https://doi.org/10.1021/om00013a017

71. Hultzsch, K. C.; Voth, P.; Beckerle, K.; Spaniol, T. P.; Okuda, J., Single-Component Polymerization Catalysts for Ethylene and Styrene: Synthesis, Characterization, and Reactivity of Alkyl and Hydrido Yttrium Complexes Containing a Linked Amido−Cyclopentadienyl Ligand. *Organometallics* **2000,** *19*, 228-243. https://doi.org/10.1021/om990583p

72. Eppinger, J.; Spiegler, M.; Hieringer, W.; Herrmann, W. A.; Anwander, R., C2-Symmetric ansa-Lanthanidocene Complexes. Synthesis via Silylamine Elimination and β-SiH Agostic Rigidity. *J. Am. Chem. Soc.* **2000,** *122*, 3080-3096. https://doi.org/10.1021/ja992786a

73. Arndt, S.; Beckerle, K.; Zeimentz, P. M.; Spaniol, T. P.; Okuda, J., Cationic Yttrium Methyl Complexes as Functional Models for Polymerization Catalysts of 1,3-Dienes. *Angew. Chem. Int. Ed.* **2005,** *44*, 7473-7477. https://doi.org/10.1002/anie.200502915

74. Barisic, D.; Schneider, D.; Maichle-Mössmer, C.; Anwander, R., Formation and Reactivity of an Aluminabenzene Ligand at Pentadienyl-Supported Rare-Earth Metals. *Angew. Chem. Int. Ed.* **2019,** *58*, 1515-1518. https://doi.org/10.1002/anie.201812515

75. Zimmermann, M.; Frøystein, N. Å.; Fischbach, A.; Sirsch, P.; Dietrich, H. M.; Törnroos, K. W.; Herdtweck, E.; Anwander, R., Homoleptic Rare-Earth Metal(III) Tetramethylaluminates: Structural Chemistry, Reactivity, and Performance in Isoprene Polymerization. *Chem. Eur. J.* **2007,** *13*, 8784-8800. https://doi.org/10.1002/chem.200700534

76. Yuan, Y.; Chen, Y.; Li, G.; Xia, W., Synthesis and Structural Features of Boratabenzene Rare-Earth Metal Alkyl Complexes. *Organometallics* **2010,** *29*, 3722-3728. https://doi.org/10.1021/om1005116

77. Wrackmeyer, B.; Klimkina, E. V.; Milius, W., Five- and Four-Coordinate 1,3-Diaza-2-yttria- and 1,3-Diaza-2-scandia-[3]ferrocenophanes. *Eur. J. Inorg. Chem.* **2008,** *2008*, 3340-3347. https://doi.org/10.1002/ejic.200800399

78. Schädle, C.; Fischbach, A.; Herdtweck, E.; Törnroos, K. W.; Anwander, R., Reactivity of Yttrium Carboxylates Toward Alkylaluminum Hydrides. *Chem. Eur. J.* **2013,** *19*, 16334-16341. https://doi.org/10.1002/chem.201302944

79. Pernin, C. G.; Ibers, J. A., Bis(cyclopentadienyl)yttrium Complexes of the Ligand $[N(QPPh_2)_2]^-$ (Q = S, Se): Synthesis, Structure, and NMR Properties of $Cp_2Y[\eta^3\text{-}N(QPPh_2)_2]$. *Inorg. Chem.* **1999,** *38*, 5478-5483. https://doi.org/10.1021/ic990602n

80. Kilimann, U.; Edelmann, F. T., Cyclooctatetraenyl-komplexe der frühen übergangsmetalle und lanthanoide: II. Neue cyclooctatetraenyl-halsandwich-komplexe des yttriums. *J. Organomet. Chem.* **1994,** *469*, C5-C9. https://doi.org/10.1016/0022-328X(94)80089-8

81. Palumbo, C. T.; Halter, D. P.; Voora, V. K.; Chen, G. P.; Ziller, J. W.; Gembicky, M.; Rheingold, A. L.; Furche, F.; Meyer, K.; Evans, W. J., Using Diamagnetic Yttrium and Lanthanum Complexes to Explore Ligand Reduction and C–H Bond Activation in a Tris(aryloxide)mesitylene Ligand System. *Inorg. Chem.* **2018,** *57*, 12876-12884. https://doi.org/10.1021/acs.inorgchem.8b02053

82. Bovens, E.; Hoefnagel, M. A.; Boers, E.; Lammers, H.; van Bekkum, H.; Peters, J. A., Multinuclear Magnetic Resonance Study on the Structure and Dynamics of Lanthanide(III) Complexes of Cyclic DTPA Derivatives in Aqueous Solution. *Inorg. Chem.* **1996,** *35*, 7679-7683. https://doi.org/10.1021/ic960540q

83. Hall, C. D.; Tucker, J. H. R.; Sheridan, A.; Chu, S. Y. F.; Williams, D. J., Complex formation between 1,1′-(1,4,10,13-tetraoxa-7,16-diazacyclooctadecane-7,16-dicarbonyl)ferrocene and yttrium perchlorate. *J. Chem. Soc., Dalton Trans.* **1992**, 3133-3136. http://dx.doi.org/10.1039/DT9920003133

84. Platas-Iglesias, C.; Corsi, D. M.; Elst, L. V.; Muller, R. N.; Imbert, D.; Bünzli, J.-C. G.; Tóth, É.; Maschmeyer, T.; Peters, J. A., Stability, structure and dynamics of cationic

lanthanide(iii) complexes of N,N′-bis(propylamide)ethylenediamine-N,N′-diacetic acid. *Dalton Trans.* **2003**, 727-737. http://dx.doi.org/10.1039/B211060A

85. Fratiello, A.; Kuboanderson, V.; Bolanos, E. L.; Haigh, D.; Laghaei, F.; Perrigan, R. D., A Hydrogen-1, Nitrogen-15, and Yttrium-89 NMR-Study of Yttrium(III)-Isothiocyanate Complexes in Aqueous Solvent Mixtures. *J. Magn. Reson. A* **1994,** *107*, 56-66. https://doi.org/10.1006/jmra.1994.1047

86. Ishiguro, S.-i.; Umebayashi, Y.; Kato, K.; Nakasone, S.; Takahashi, R., Solvation structure and bromo complexation of neodymium(III) and yttrium(III) ions in solvent mixtures of N,N-dimethylformamide and N,N-dimethylacetamide. *Phys. Chem. Chem. Phys.* **1999,** *1*, 2725-2732. http://dx.doi.org/10.1039/A901225G

87. Gleizes, A.; Sans-Lenain, S.; Medus, D.; Hovnanian, N.; Miele, P.; Foulon, J. D., Yttrium tetramethylheptanedionates: syntheses, crystal and molecular structures and thermal behaviours of $Y(thd)_3 \cdot H_2O$ and $Y(thd)_3$ (thd = tBuC(O)CHC(O)tBu). *Inorg. Chim. Acta* **1993,** *209*, 47-53. https://doi.org/10.1016/S0020-1693(00)84979-8

88. Popovici, C.; Fernández, I.; Oña-Burgos, P.; Roces, L.; García-Granda, S.; Ortiz, F. L., Synthesis and structure of tridentate bis(phosphinic amide)-phosphine oxide complexes of yttrium nitrate. Applications of ^{31}P,^{89}Y NMR methods in structural elucidation in solution. *Dalton Trans.* **2011,** *40*, 6691-6703. http://dx.doi.org/10.1039/C1DT10194C

89. Fernández, I.; Yañez-Rodríguez, V.; Ortiz, F. L., ^{31}P,^{89}Y Shift correlation. Application to the speciation of yttrium complexes with triphenylphosphine oxide. *Dalton Trans.* **2011,** *40*, 2425-2428. http://dx.doi.org/10.1039/C0DT01733G

90. Bradley, D. C.; Chudzynska, H.; Hursthouse, M. B.; Motevalli, M., The synthesis and characterization of volatile complexes of fluorinated alkoxides of yttrium. X-ray structures of $[Y\{OCMe(CF_3)_2\}_3(thf)_3]$ and $[Y\{OCMe(CF_3)_2\}_3(diglyme)]$. *Polyhedron* **1993,** *12*, 1907-1918. https://doi.org/10.1016/S0277-5387(00)81430-8

91. Tripathi, U. M.; Singh, A.; Mehrotra, R. C., Preparation and characterization of heteroleptic tetraisopropoxoaluminato-yttrium(III) complexes. *Polyhedron* **1993,** *12*, 1947-1952. https://doi.org/10.1016/S0277-5387(00)81435-7

92. Coan, P. S.; Huffman, J. C.; Caulton, K. G., Strategy for synthesis of an yttrium/copper(I) complex with an oxo ligand environment. *Inorg. Chem.* **1992,** *31*, 4207-4209. https://doi.org/10.1021/ic00046a041

93. White, R. E.; Hanusa, T. P., Prediction of 89Y NMR Chemical Shifts in Organometallic Complexes with Density Functional Theory. *Organometallics* **2006,** *25*, 5621-5630. https://doi.org/10.1021/om060695y

94. Nockemann, P.; Thijs, B.; Lunstroot, K.; Parac-Vogt, T. N.; Görller-Walrand, C.; Binnemans, K.; Van Hecke, K.; Van Meervelt, L.; Nikitenko, S.; Daniels, J.; Hennig, C.; Van Deun, R., Speciation of Rare-Earth Metal Complexes in Ionic Liquids: A Multiple-Technique Approach. *Chem. Eur. J.* **2009,** *15*, 1449-1461. https://doi.org/10.1002/chem.200801418

95. Le Natur, F.; Calvez, G.; Guégan, J.-P.; Le Pollès, L.; Trivelli, X.; Bernot, K.; Daiguebonne, C.; Neaime, C.; Costuas, K.; Grasset, F.; Guillou, O., Characterization and Luminescence Properties of Lanthanide-Based Polynuclear Complexes Nanoaggregates. *Inorg. Chem.* **2015,** *54*, 6043-6054. https://doi.org/10.1021/acs.inorgchem.5b00947

96. Holz, R. C.; Horrocks, W. D. W., Yttrium-89 NMR spectroscopy, a new probe for calcium-binding proteins. *J. Magn. Reson.* **1990,** *89*, 627-631. https://doi.org/10.1016/0022-2364(90)90349-E

97. Bruno, J.; Herr, B. R.; Horrocks, W. D., Laser-induced luminescence studies of europium hexaazamacrocycle $Eu(HAM)^{3+}$. An evaluation of complex stability and the use of the gadolinium analog as a relaxation agent in yttrium-89 NMR. *Inorg. Chem.* **1993,** *32*, 756-762. https://doi.org/10.1021/ic00057a041

98. Rudovský, J.; Botta, M.; Hermann, P.; Koridze, A.; Aime, S., Relaxometric and solution NMR structural studies on ditopic lanthanide(iii) complexes of a phosphinate analogue of DOTA

with a fast rate of water exchange. *Dalton Trans.* **2006**, 2323-2333. http://dx.doi.org/10.1039/B518147J

99. Jindal, A. K.; Merritt, M. E.; Suh, E. H.; Malloy, C. R.; Sherry, A. D.; Kovács, Z., Hyperpolarized ^{89}Y Complexes as pH Sensitive NMR Probes. *J. Am. Chem. Soc.* **2010,** *132*, 1784-1785. https://doi.org/10.1021/ja910278e

100. Lumata, L.; Jindal, A. K.; Merritt, M. E.; Malloy, C. R.; Sherry, A. D.; Kovacs, Z., DNP by Thermal Mixing under Optimized Conditions Yields >60 000-fold Enhancement of 89Y NMR Signal. *J. Am. Chem. Soc.* **2011,** *133*, 8673-8680. https://doi.org/10.1021/ja201880y

101. Miéville, P.; Jannin, S.; Helm, L.; Bodenhausen, G., Kinetics of Yttrium−Ligand Complexation Monitored Using Hyperpolarized 89Y as a Model for Gadolinium in Contrast Agents. *J. Am. Chem. Soc.* **2010,** *132*, 5006-5007. https://doi.org/10.1021/ja1013954

102. Casey, C. P.; Tunge, J. A.; Lee, T.-Y.; Carpenetti, D. W., Kinetics and Mechanism of Formation of Yttrium Alkyl Complexes from $(Cp^*_2YH)_2$ and Alkenes. *Organometallics* **2002,** *21*, 389-396. https://doi.org/10.1021/om010817g

103. Chen, Z.; Morel-Desrosiers, N.; Morel, J.-P.; Detellier, C., A ^{139}La NMR study of the interactions between the La(III) cation and D-ribose in aqueous solution. *Can. J. Chem.* **1994,** *72*, 1753-1757. https://doi.org/10.1139/v94-221

104. Biruš, M.; van Eldik, R.; Gabričević, M.; Zahl, A., ^{139}La NMR Kinetic Study of Lanthanum(III) Complexation with Acetohydroxamic Acid. *Eur. J. Inorg. Chem.* **2002,** *2002*, 819-825. https://doi.org/10.1002/1099-0682(200203)2002:4<819::AID-EJIC819>3.0.CO;2-E

105. Israëli, Y.; Bonal, C.; Detellier, C.; Morel, J.-P.; Morel-Desrosiers, N., Complexation of the La(III) cation by p-sulfonatocalix[4]arene. A 139La NMR study. *Can. J. Chem.* **2002,** *80*, 163-168. https://doi.org/10.1139/v02-005

106. Boyle, T. J.; Ottley, L. A. M.; Alam, T. M.; Rodriguez, M. A.; Yang, P.; McIntyre, S. K., Structural characterization of methanol substituted lanthanum halides. *Polyhedron* **2010,** *29*, 1784-1795. https://doi.org/10.1016/j.poly.2010.02.027

107. Lammers, H.; van der Heijden, A. M.; van Bekkum, H.; Geraldes, C. F. G. C.; Peters, J. A., Multinuclear NMR study of the interactions between the La(III) complex of DTPA-bis(glucamide) and Zn(II) or borate. *Inorg. Chim. Acta* **1998,** *268*, 249-255. https://doi.org/10.1016/S0020-1693(97)05752-6

108. Chen, Z.; Van Westrenen, J.; Van Bekkum, H.; Peters, J. A., Synthesis of polyhydroxy carboxylates. 5. Metal ion catalyzed O-alkylation of ethylene glycol with maleate. A multinuclear NMR study of the lanthanide(III) complexes present in the reaction mixture of the lanthanide(III)-catalyzed reaction. *Inorg. Chem.* **1990,** *29*, 5025-5031. https://doi.org/10.1021/ic00350a005

109. Taube, R.; Windisch, H.; Hemling, H.; Schumann, H., Komplexkatalyse: LIII1LII. Mitteilung siehe [7].1. Darstellung und Charakterisierung der Bis(η3-allyl)lanthanhalogenid-Komplexe La(η3-C3H5)2X·2THF (X=Cl, Br, I) als Präkatalysatoren für die stereospezifische Butadienpolymerisation, ein Beitrag zur weiteren Klärung der katalytischen Struktur-Wirkungsbeziehung. *J. Organomet. Chem.* **1998,** *555*, 201-210. https://doi.org/10.1016/S0022-328X(97)00753-5

110. Taube, R.; Windisch, H.; Weiβenborn, H.; Hemling, H.; Schumann, H., Komplexkatalyse LI. Komplexe des Tris(allyl)lanthans mit verschiedenen Donorliganden La(η3-C3H5)3 · L (L:DME, TMED, 2HMPT) und ihre katalytischen Eigenschaften in der stereospezifischen Butadienpolymerisation. *J. Organomet. Chem.* **1997,** *548*, 229-236. https://doi.org/10.1016/S0022-328X(97)00406-3

111. Windisch, H.; Scholz, J.; Taube, R.; Wrackmeyer, B., 139La-NMR-spektroskopie an allyllanthan(III)-komplexen. *J. Organomet. Chem.* **1996,** *520*, 23-30. https://doi.org/10.1016/0022-328X(96)06259-6

112. Guan, J.; Shen, Q.; Fischer, R. D., Crystal structure, conformational diversity and solution NMR spectroscopy of four tris(indenyl)lanthanoid(III) tetrahydrofuran adducts: [Ln(C9H7)3 · THF] (Ln = La, Pr, Nd, Sm). *J. Organomet. Chem.* **1997,** *549*, 203-212. https://doi.org/10.1016/S0022-328X(97)00565-2

113. Beletskaya, I. P.; Voskoboynikov, A. Z.; Chuklanova, E. B.; Kirillova, N. I.; Shestakova, A. K.; Parshina, I. N.; Gusev, A. I.; Magomedov, G. K. I., Bimetallic lanthanide complexes with lanthanide-transition metal bonds. Molecular structure of $(C_4H_8O)(C_5H_5)_2LuRu(CO)_2(C_5H_5)$. The use of ^{139}La NMR spectroscopy. *J. Am. Chem. Soc.* **1993,** *115*, 3156-3166. https://doi.org/10.1021/ja00061a015

114. Kato, H.; Taninaka, A.; Sugai, T.; Shinohara, H., Structure of a Missing-Caged Metallofullerene: La2@C72. *J. Am. Chem. Soc.* **2003,** *125*, 7782-7783. https://doi.org/10.1021/ja0353255

115. Suzuki, M.; Mizorogi, N.; Yang, T.; Uhlik, F.; Slanina, Z.; Zhao, X.; Yamada, M.; Maeda, Y.; Hasegawa, T.; Nagase, S.; Lu, X.; Akasaka, T., La2@Cs(17 490)-C76: A New Non-IPR Dimetallic Metallofullerene Featuring Unexpectedly Weak Metal–Pentalene Interactions. *Chem. Eur. J.* **2013,** *19*, 17125-17130. https://doi.org/10.1002/chem.201302821

116. Wakahara, T.; Yamada, M.; Takahashi, S.; Nakahodo, T.; Tsuchiya, T.; Maeda, Y.; Akasaka, T.; Kako, M.; Yoza, K.; Horn, E.; Mizorogi, N.; Nagase, S., Two-dimensional hopping motion of encapsulated La atoms in silylated La2@C80. *Chem. Commun.* **2007**, 2680-2682. http://dx.doi.org/10.1039/B703473C

117. Yamada, M.; Wakahara, T.; Nakahodo, T.; Tsuchiya, T.; Maeda, Y.; Akasaka, T.; Yoza, K.; Horn, E.; Mizorogi, N.; Nagase, S., Synthesis and Structural Characterization of Endohedral Pyrrolidinodimetallofullerene: La2@C80(CH2)2NTrt. *J. Am. Chem. Soc.* **2006,** *128*, 1402-1403. https://doi.org/10.1021/ja056560l

118. Akasaka, T.; Lu, X.; Kuga, H.; Nikawa, H.; Mizorogi, N.; Slanina, Z.; Tsuchiya, T.; Yoza, K.; Nagase, S., Dichlorophenyl Derivatives of La@C_{3v}(7)-C_{82}: Endohedral Metal Induced Localization of Pyramidalization and Spin on a Triple-Hexagon Junction. *Angew. Chem. Int. Ed.* **2010,** *49*, 9715-9719. https://doi.org/10.1002/anie.201004318

119. Lin, S.-J.; Wakagi, T.; Matsuzawa, H.; Yoshimura, E., Lanthanum binding to aqualysin I, a thermostable serine protease, as probed by lanthanum-139 nuclear magnetic resonance

spectrometry. *J. Inorg. Biochem.* **1999,** *77*, 205-208. https://doi.org/10.1016/S0162-0134(99)00195-6

120. Johnson, L.; Verraest, D. L.; Besemer, A. C.; van Bekkum, H.; Peters, J. A., Complexation of LnIII and CaII Cations with 3,4-Dicarboxyinulin and Model Compounds: Methyl 3,4-Dicarboxy-α-d-fructofuranoside and 3,4-Dicarboxynystose, As Studied by Multinuclear Magnetic Resonance Spectroscopy and Potentiometry. *Inorg. Chem.* **1996,** *35*, 5703-5710. https://doi.org/10.1021/ic960103b

121. Fratiello, A.; Kubo-Anderson, V.; Bolanos, E.; Perrigan, R. D.; Saenz, L.; Stoll, S. M., A direct hydrogen-1, carbon-13, and nitrogen-15 NMR study of lutetium(III)-isothiocyanate complexation in aqueous solvent mixtures. *J. Solution Chem.* **1996,** *25*, 1071-1082. https://doi.org/10.1007/BF00972922

122. Skarnemark, G.; Skålberg, M., The half-life of 228Ac. *Int. J. Appl. Radiat. Isot.* **1985,** *36*, 439-441. https://doi.org/10.1016/0020-708X(85)90206-6

123. Foris, A., 47,49Ti and 13C NMR spectra of titanium-containing catalysts. *Magn. Reson. Chem.* **2000,** *38*, 1044-1046. https://doi.org/10.1002/1097-458X(200012)38:12<1044::AID-MRC773>3.0.CO;2-M

124. Hafner, A.; Duthaler, R. O.; Marti, R.; Rihs, G.; Rothe-Streit, P.; Schwarzenbach, F., Enantioselective syntheses with titanium carbohydrate complexes. Part 7. Enantioselective allyltitanation of aldehydes with cyclopentadienyldialkoxyallyltitanium complexes. *J. Am. Chem. Soc.* **1992,** *114*, 2321-2336. https://doi.org/10.1021/ja00033a005

125. Hafner, A.; Okuda, J., Titanium NMR data for some titanium half-sandwich complexes bearing substituted cyclopentadienyl ligands. *Organometallics* **1993,** *12*, 949-950. https://doi.org/10.1021/om00027a052

126. Sarsfield, M. J.; Ewart, S. W.; Tremblay, T. L.; Roszak, A. W.; Baird, M. C., Synthesis of a series of new, highly electrophilic, monocyclopentadienyltitanium olefin polymerization initiators*J. Chem. Soc., Dalton Trans.* **1997**, 3097-3104. http://dx.doi.org/10.1039/A703112B

127. Erben, M.; Růžička, A.; Picka, M.; Pavlík, I., 47, 49Ti NMR spectra of half-sandwich titanium(IV) complexes. *Magn. Reson. Chem.* **2004,** *42*, 414-417. https://doi.org/10.1002/mrc.1354

128. Erben, M.; Merna, J.; Hermanová, S.; Císařová, I.; Padělková, Z.; Dušek, M., Fluorosilyl-Substituted Cyclopentadienyltitanium(IV) Complexes: Synthesis, Structure, and Styrene Polymerization Behavior. *Organometallics* **2007,** *26*, 2735-2741. https://doi.org/10.1021/om070098r

129. Traill, P. R.; Young, C. G., Application of a transverse NMR probe in the detection of broad titanium-49 resonances from Ti(IV) and Ti(II) compounds. *J. Magn. Reson.* **1990,** *90*, 551-556. https://doi.org/10.1016/0022-2364(90)90059-I

130. Carlin, R. T.; Osteryoung, R. A.; Wilkes, J. S.; Rovang, J., Studies of Titanium(IV) Chloride in a Strongly Lewis Acidic Molten Salt: Electrochemistry and Titanium NMR and Electronic Spectroscopy. *Inorg. Chem.* **1990,** *29*, 3003-3009. http://doi.org/10.1021/ic00341a030

131. Brueggermann, K.; Czernuszewicz, R. S.; Kochi, J. K., Charge-transfer structures of aromatic electron donor-acceptor complexes with titanium tetrachloride. Ground-state and excited-state spectroscopy for redox processes. *J. Phys. Chem.* **1992,** *96*, 4405-4414. https://doi.org/10.1021/j100190a052

132. Bühl, M.; Mauschick, F. T., Density functional computation of ^{49}Ti NMR chemical shifts. *Magn. Reson. Chem.* **2004,** *42*, 737-744. https://doi.org/10.1002/mrc.1405

133. Dellavia, I.; Helm, L.; Merbach, A. E., High-pressure NMR kinetics. 54. N,N-dimethylformamide exchange on hexakis(N,N-dimethylformamide)titanium(III): a variable-temperature and pressure proton and oxygen-17 NMR study. *Inorg. Chem.* **1992,** *31*, 2230-2233. https://doi.org/10.1021/ic00037a043

134. Finn, M. G.; Sharpless, K. B., Mechanism of asymmetric epoxidation. 2. Catalyst structure. *J. Am. Chem. Soc.* **1991,** *113*, 113-126. https://doi.org/10.1021/ja00001a019

135. Reynolds, M. S.; Butler, A., Oxygen-17 NMR, Electronic, and Vibrational Spectroscopy of Transition Metal Peroxo Complexes: Correlation with Reactivity. *Inorg. Chem.* **1996,** *35*, 2378-2383. https://doi.org/10.1021/ic951212d

136. Camporeale, M.; Cassidei, L.; Mello, R.; Troisi, L.; Curci, R.; Sciacovelli, O., The oxygen-17 NMR of some side-bonded dioxygen species. *Studies in Organic Chemistry* **1988,** *33*, 201-210.

137. Fujii, H.; Kurahashi, T.; Tosha, T.; Yoshimura, T.; Kitagawa, T., 17O NMR study of oxo metalloporphyrin complexes: Correlation with electronic structure of MO moiety. *J. Inorg. Biochem.* **2006,** *100*, 533-541. https://doi.org/10.1016/j.jinorgbio.2006.01.009

138. Kilpatrick, A. F. R.; Green, J. C.; Cloke, F. G. N., Reactivity of a Dititanium Bis(pentalene) Complex toward Heteroallenes and Main-Group Element–Element Bonds. *Organometallics* **2017,** *36*, 352-362. https://doi.org/10.1021/acs.organomet.6b00791

139. Alcaraz, G.; Sabo-Etienne, S., NMR: A good tool to ascertain σ-silane or σ-borane formulations? *Coord. Chem. Rev.* **2008,** *252*, 2395-2409. https://doi.org/10.1016/j.ccr.2008.02.006

140. Bühl, M.; Hopp, G.; von Philipsborn, W.; Beck, S.; Prosenc, M.-H.; Rief, U.; Brintzinger, H.-H., Zirconium-91 Chemical Shifts and Line Widths as Indicators of Coordination Geometry Distortions in Zirconocene Complexes. *Organometallics* **1996,** *15*, 778-785. https://doi.org/10.1021/om950757c

141. Fedotov, M. A.; Belyaev, A. V., A study of the hydrolysis of ZrF_6^{2-} and the structure of intermediate hydrolysis products by ^{19}F and ^{91}Zr NMR in the 9.4 T field. *J. Struct. Chem.* **2011,** *52*, 69-74. https://doi.org/10.1134/S0022476611010094

142. Janiak, C.; Versteeg, U.; Lange, K. C. H.; Weimann, R.; Hahn, E., The influence of electronic and steric effects and the importance of polymerization conditions in the ethylene polymerization with zirconocene/MAO catalysts. *J. Organomet. Chem.* **1995,** *501*, 219-234. https://doi.org/10.1016/0022-328X(95)05647-8

143. Janiak, C.; Lange, K. C. H.; Versteeg, U.; Lentz, D.; Budzelaar, P. H. M., Ethene Polymerization Activity and Coordination Gap Aperture in non-ansa Alkyl-substituted Cyclopentadienyl- and Phospholyl-zirconium/MAO Catalysts. *Chem. Ber.* **1996,** *129*, 1517-1529. https://doi.org/10.1002/cber.19961291219

144. Siedle, A. R.; Newmark, R. A.; Gleason, W. B.; Lamanna, W. M., Reactions of bis(cyclopentadienyl)dimethylzirconium with fluorocarbon acids. Structure, dynamic properties, and zirconium-91 NMR spectra of (C5H5)2Zr[HC(SO2CF3)2-O,O'][HC(SO2CF3)2-O]. *Organometallics* **1990,** *9*, 1290-1295. https://doi.org/10.1021/om00118a061

145. Janiak, C.; Lange, K. C. H.; Scharmann, T. G., Zirconium-chelate and mono-η-cyclopentadienyl zirconium-chelate/ methylalumoxane systems as soluble Ziegler–Natta olefin polymerization catalysts. *Appl. Organomet. Chem.* **2000,** *14*, 316-324. https://doi.org/10.1002/(SICI)1099-0739(200006)14:6<316::AID-AOC990>3.0.CO;2-U

146. Bühl, M., NMR Chemical Shifts of Zr@C_{28}. How Shielded Can ^{91}Zr Get? *J. Phys. Chem. A* **1997,** *101*, 2514-2517. https://doi.org/10.1021/jp963882q

147. Aberg, M.; Glaser, J., Oxygen-17 and proton NMR study of the tetranuclear hydroxo zirconium complex in aqueous solution. *Inorg. Chim. Acta* **1993,** *206*, 53-61. https://doi.org/10.1016/S0020-1693(00)89259-2

148. Gozum, J. E.; Wilson, S. R.; Girolami, G. S., Zirconium and hafnium polyhydrides. 2. Preparation and characterization of M3H6(BH4)6(PMe3)4 and M2H4(BH4)4(dmpe)2. *J. Am. Chem. Soc.* **1992,** *114*, 9483-92. https://doi.org/10.1021/ja00050a029

149. Manke, D. R.; Nocera, D. G., Bis(alkylamido)phenylborane Complexes of Zirconium, Hafnium, and Vanadium. *Inorg. Chem.* **2003,** *42*, 4431-4436. https://doi.org/10.1021/ic0340478

150. Woo, H. G.; Heyn, R. H.; Tilley, T. D., σ-Bond metathesis reactions for d0 metal-silicon bonds that produce zirconocene and hafnocene hydrosilyl complexes. *J. Am. Chem. Soc.* **1992,** *114*, 5698-707. https://doi.org/10.1021/ja00040a032

151. Chen, C.-H.; Shih, W.-C.; Hilty, C., In Situ Determination of Tacticity, Deactivation, and Kinetics in [*rac*-(C_2H_4(1-Indenyl)$_2$)ZrMe][B(C_6F_5)$_4$] and [Cp_2ZrMe][B(C_6F_5)$_4$]-Catalyzed Polymerization of 1-Hexene Using ^{13}C Hyperpolarized NMR. *J. Am. Chem. Soc.* **2015,** *137*, 6965-6971. https://doi.org/10.1021/jacs.5b04479

152. Rocchigiani, L.; Busico, V.; Pastore, A.; Macchioni, A., Probing the interactions between all components of the catalytic pool for homogeneous olefin polymerisation by diffusion NMR spectroscopy. *Dalton Trans.* **2013,** *42*, 9104-9111. http://doi.org/10.1039/c3dt00041a

153. Frey, U.; Helm, L.; Merbach, A. E., A variable-pressure 2D proton NMR study of the mechanism of trimethyl phosphate intermolecular exchange and cis/trans-isomerization of tetrachlorobis(trimethyl phosphate)zirconium(IV). *Helv. Chim. Acta* **1990,** *73*, 199-202. http://doi.org/10.1002/hlca.19900730123

154. Cook, T. M.; Steren, C. A.; Xue, Z.-L., Syntheses and characterization of hepta-coordinated Group 4 amidinate complexes. *Dalton Trans.* **2018,** *47*, 11030-11040. http://dx.doi.org/10.1039/C8DT02523A

155. Xie, X.; Jones, J. N.; Hughbanks, T., Excision of Zirconium Iodide Clusters from Highly Cross-Linked Solids. *Inorg. Chem.* **2001,** *40*, 522-527. https://doi.org/10.1021/ic000651w

156. Nakata, N.; Fujita, T.; Sekiguchi, A., A Stable Schrock-Type Hafnium-Silylene Complex. *J. Am. Chem. Soc.* **2006,** *128*, 16024-16025. https://doi.org/10.1021/ja067251d

157. Erich, L. C.; Gossard, A. C.; Hartless, R. L., Magnetic moment of 181Ta. *J. Chem. Phys.* **1973,** *59*, 3911-3912. https://aip.scitation.org/doi/abs/10.1063/1.1680576

158. Rehder, D.; Basler, W., Tantalum-181 solution NMR spectroscopy. *J. Magn. Reson.* **1986,** *68*, 157-160. https://doi.org/10.1016/0022-2364(86)90325-2

159. de Oliveira, V.; da Silva San Gil, R. A.; Lachter, E. R., Synthesis and characterization of two new niobium(V) diperoxo complexes containing 8-quinolinolate as the ligand. *Polyhedron* **2001,** *20*, 2647-2649. https://doi.org/10.1016/S0277-5387(01)00870-1

160. Levason, W.; Light, M. E.; Reid, G.; Zhang, W., Soft diphosphine and diarsine complexes of niobium(V) and tantalum(V) fluorides: synthesis, properties, structures and comparisons with the corresponding chlorides. *Dalton Trans.* **2014,** *43*, 9557-9566. http://dx.doi.org/10.1039/C4DT01029A

161. Talay, R.; Rehder, D., Vanadium-metal bonds in carbonylvanadium complexes: A 51V NMR spectroscopic investigation. *J. Organomet. Chem.* **1984,** *262*, 25-32. https://doi.org/10.1016/S0022-328X(00)99119-8

162. Howarth, O. W., Vanadium-51 NMR. *Prog. NMR Spec.* **1990,** *22*, 453-485. https://doi.org/10.1016/0079-6565(90)80007-5

163. Rehder, D., Biological Applications of ^{51}V NMR Spectroscopy. In *Vanadium in Biological Systems: Physiology and Biochemistry*, Chasteen, N. D., Ed. Kluwer Academic Publishers: 1990; pp 173-197.

164. Rehder, D., Vanadium NMR of organovanadium complexes. *Coord. Chem. Rev.* **2008,** *252*, 2209-2223. https://doi.org/10.1016/j.ccr.2008.01.008

165. Rehder, D.; Polenova, T.; Bühl, M., Vanadium-51 NMR. *Annu. Rep. NMR Spectrosc.* **2007,** *62*, 49-114. https://doi.org/10.1016/S0066-4103(07)62002-X

166. Angus-Dunne, S. J.; Paul, P. C.; Tracey, A. S., A ^{51}V NMR investigation of the interactions of aqueous vanadate with hydroxylamine. *Can. J. Chem.* **1997,** *75*, 1002-1010. https://cdnsciencepub.com/doi/abs/10.1139/v97-120

167. Ramos, M. L.; Justino, L. L. G.; Fonseca, S. M.; Burrows, H. D., NMR, DFT and luminescence studies of the complexation of V(V) oxoions in solution with 8-hydroxyquinoline-5-sulfonate. *New J. Chem.* **2015,** *39*, 1488-1497. http://dx.doi.org/10.1039/C4NJ01873G

168. Yamaki, R. T.; Paniago, E. B.; Carvalho, S.; Lula, I. S., Interaction of 2-amino-N-hydroxypropanamide with vanadium(V) in aqueous solution. *J. Chem. Soc., Dalton Trans.* **1999**, 4407-4412. http://dx.doi.org/10.1039/A907249G

169. Dörnyei, Á.; Garribba, E.; Jakusch, T.; Forgó, P.; Micera, G.; Kiss, T., Vanadium(iv,v) complexes of d-saccharic and mucic acids in aqueous solution. *Dalton Trans.* **2004**, 1882-1891. http://dx.doi.org/10.1039/B401443J

170. Miranda, C. T.; Carvalho, S.; Yamaki, R. T.; Paniago, E. B.; Borges, R. H. U.; De Bellis, V. M., pH-metric, UV–Vis and 51V NMR study of vanadium(V) coordination to α-aminohydroxamic acids in aqueous solutions. *Polyhedron* **2010,** *29*, 897-903. https://doi.org/10.1016/j.poly.2009.10.020

171. Miyazaki, Y.; Matsuoka, S.; Fujimori, T.; Kai, Y.; Yoshimura, K., Coordination properties of aqueous vanadate complexes with nitrogen- and oxygen-containing multidentate ligands. *Polyhedron* **2017,** *134*, 79-87. https://doi.org/10.1016/j.poly.2017.05.056

172. Yang, L.; la Cour, A.; Anderson, O. P.; Crans, D. C., 4-Hydroxypyridine-2,6-dicarboxylatodioxovanadate(V) Complexes: Solid State and Aqueous Chemistry. *Inorg. Chem.* **2002,** *41*, 6322-6331. https://doi.org/10.1021/ic0201598

173. Crans, D. C.; Yang, L.; Jakusch, T.; Kiss, T., Aqueous Chemistry of Ammonium (Dipicolinato)oxovanadate(V): The First Organic Vanadium(V) Insulin-Mimetic Compound. *Inorg. Chem.* **2000,** *39*, 4409-4416. https://doi.org/10.1021/ic9908367

174. Durupthy, O.; Coupé, A.; Tache, L.; Rager, M.-N.; Maquet, J.; Coradin, T.; Steunou, N.; Livage, J., Spectroscopic Investigation of Interactions between Dipeptides and Vanadate(V) in Solution. *Inorg. Chem.* **2004,** *43*, 2021-2030. https://doi.org/10.1021/ic0301019

175. Castro, M. M. C. A.; Geraldes, C. F. G. C.; Gameiro, P.; Pereira, E.; Castro, B.; Rangel, M., Structural study of the interaction of vanadate with the ligand 1,2-dimethyl-3-hydroxy-4-pyridinone (Hdmpp) in aqueous solution. *J. Inorg. Biochem.* **2000,** *80*, 177-179. https://doi.org/10.1016/S0162-0134(00)00028-3

176. Elvingson, K.; Crans, D. C.; Pettersson, L., Speciation in Vanadium Bioinorganic Systems. 4. Interactions between Vanadate, Adenosine, and ImidazoleAn Aqueous

Potentiometric and 51V NMR Study. *J. Am. Chem. Soc.* **1997,** *119*, 7005-7012. https://doi.org/10.1021/ja9630497

177. Maurya, M. R.; Jangra, N.; Avecilla, F.; Correia, I., 4,6-Diacetyl Resorcinol Based Vanadium(V) Complexes: Reactivity and Catalytic Applications. *Eur. J. Inorg. Chem.* **2019,** *2019*, 314-329. https://doi.org/10.1002/ejic.201801243

178. Levinger, N. E.; Rubenstrunk, L. C.; Baruah, B.; Crans, D. C., Acidification of Reverse Micellar Nanodroplets by Atmospheric Pressure CO2. *J. Am. Chem. Soc.* **2011,** *133*, 7205-7214. https://doi.org/10.1021/ja2011737

179. Bányai, I.; Conte, V.; Pettersson, L.; Silvagni, A., On the Nature of VV Species in Hydrophilic Ionic Liquids: A Spectroscopic Approach. *Eur. J. Inorg. Chem.* **2008,** *2008*, 5373-5381. https://doi.org/10.1002/ejic.200800673

180. Bell, R. C.; Castleman, A. W.; Thorn, D. L., Vanadium Oxide Complexes in Room-Temperature Chloroaluminate Molten Salts. *Inorg. Chem.* **1999,** *38*, 5709-5715. https://doi.org/10.1021/ic990693o

181. Cotton, F. A.; Wilkinson, G.; Murillo, C. A.; Bochmann, M., *Advanced Inorganic Chemistry*. 6 ed.; 1999; Wiley-Interscience.

182. Fedotov, M. A.; Maksimovskaya, R. I., NMR structural aspects of the chemistry of V, Mo, W polyoxometalates. *J. Struct. Chem.* **2006,** *47*, 952-978. https://doi.org/10.1007/s10947-006-0413-6

183. Crans, D. C.; Rithner, C. D.; Theisen, L. A., Application of time-resolved vanadium-51 2D NMR for quantitation of kinetic exchange pathways between vanadate monomer, dimer, tetramer, and pentamer. *J. Am. Chem. Soc.* **1990,** *112*, 2901-2908. https://doi.org/10.1021/ja00164a009

184. Andersson, I.; Pettersson, L.; Hastings, J. J.; Howarth, O. W., Oxygen and vanadium exchange processes in linear vanadate oligomers. *J. Chem. Soc., Dalton Trans.* **1996**, 3357-3361. http://dx.doi.org/10.1039/DT9960003357

185. Pettersson, L.; Andersson, I.; Howarth, O. W., Tridecavanadate, [H12V13O40]3. *Inorg. Chem.* **1992,** *31*, 4032-4033. https://doi.org/10.1021/ic00046a003

186. Kuwajima, S.; Kikukawa, Y.; Hayashi, Y., Small-Molecule Anion Recognition by a Shape-Responsive Bowl-Type Dodecavanadate. *Chem. Asian J.* **2017,** *12*, 1909-1914. https://doi.org/10.1002/asia.201700489

187. Hastings, J. J.; Howarth, O. W., 183W nuclear magnetic resonance of α-[H2W11VO40]7− and α-[H2W11MoO40]6−. *Polyhedron* **1993,** *12*, 847-849. https://doi.org/10.1016/S0277-5387(00)81767-2

188. Grigoriev, V. A.; Cheng, D.; Hill, C. L.; Weinstock, I. A., Role of Alkali Metal Cation Size in the Energy and Rate of Electron Transfer to Solvent-Separated 1:1 [(M+)(Acceptor)] (M+ = Li+, Na+, K+) Ion Pairs. *J. Am. Chem. Soc.* **2001,** *123*, 5292-5307. https://doi.org/10.1021/ja010074q

189. Howarth, O. W.; Hastings, J. J., Monotungstononavanadate and mer-tritungstotrivanadate. *Polyhedron* **1990,** *9*, 143-146. https://doi.org/10.1016/S0277-5387(00)84259-X

190. Howarth, O. W.; Hastings, J. J., Aqueous vanadosilicates. *J. Chem. Soc., Dalton Trans.* **1996**, 4189-4192. http://dx.doi.org/10.1039/DT9960004189

191. Howarth, O. W.; Pettersson, L.; Andersson, I., Aqueous molybdovanadates at high Mo:V ratio. *J. Chem. Soc., Dalton Trans.* **1991**, 1799-1812. http://dx.doi.org/10.1039/DT9910001799

192. Andersson, I.; Hastings, J. J.; Howarth, O. W.; Pettersson, L., Aqueous tungstovanadate equilibria. *J. Chem. Soc., Dalton Trans.* **1996**, 2705-2711. http://dx.doi.org/10.1039/DT9960002705

193. Hastings, J. J.; Howarth, O. W., Molybdotungstovanadates [V2MoW(4–)O19]4–. *J. Chem. Soc., Dalton Trans.* **1995**, 2891-2893. http://dx.doi.org/10.1039/DT9950002891

194. Son, J.-H.; Ohlin, C. A.; Johnson, R. L.; Yu, P.; Casey, W. H., A Soluble Phosphorus-Centered Keggin Polyoxoniobate with Bicapping Vanadyl Groups. *Chem. Eur. J.* **2013,** *19*, 5191-5197. https://doi.org/10.1002/chem.201204563

195. Ueda, T.; Ohnishi, M.; Kawamoto, D.; Guo, S.-X.; Boas, J. F.; Bond, A. M., Voltammetric behavior of 1- and 4-[S2VVW17O62]5− in acidified acetonitrile. *Dalton Trans.* **2015,** *44*, 11660-11668. http://dx.doi.org/10.1039/C5DT01530H

196. Abramov, P. A.; Davletgildeeva, A. T.; Moroz, N. K.; Kompankov, N. B.; Santiago-Schübel, B.; Sokolov, M. N., Cation-Dependent Self-assembly of Vanadium Polyoxoniobates. *Inorg. Chem.* **2016,** *55*, 12807-12814. https://doi.org/10.1021/acs.inorgchem.6b02108

197. Sugiarto; Kawamoto, K.; Hayashi, Y., Strategic Isolation of a Polyoxocation Mimicking Vanadium(V) Oxide Layered-Structure by Stacking of [H2V2O8]4− Anions Bridged by (1,4,7-Triazacyclononane)Co(III) Complexes. *Front. Chem.* **2018,** *6*, 375. https://www.frontiersin.org/article/10.3389/fchem.2018.00375

198. Kaminker, I.; Goldberg, H.; Neumann, R.; Goldfarb, D., High-Field Pulsed EPR Spectroscopy for the Speciation of the Reduced [PV2Mo10O40]6− Polyoxometalate Catalyst Used in Electron-Transfer Oxidations. *Chem. Eur. J.* **2010,** *16*, 10014-10020. https://doi.org/10.1002/chem.201000944

199. Justino, Licínia L. G.; Ramos, M. L.; Caldeira, M. M.; Gil, Victor M. S., Peroxovanadium(V) Complexes of L-Lactic Acid as Studied by NMR Spectroscopy. *Eur. J. Inorg. Chem.* **2000,** *2000*, 1617-1621. https://doi.org/10.1002/1099-0682(200007)2000:7<1617::AID-EJIC1617>3.0.CO;2-B

200. Ballistreri, F. P.; Barbuzzi, E. G. M.; Tomaselli, G. A.; Toscano, R. M., Insulin mimesis of vanadium derivatives. Oxidation of cysteine by V(V) oxo diperoxo complexes. *J. Inorg. Biochem.* **2000,** *80*, 173-176. https://doi.org/10.1016/S0162-0134(00)00027-1

201. Tracey, A. S.; Jaswal, J. S., Reactions of peroxovanadates with amino acids and related compounds in aqueous solution. *Inorg. Chem.* **1993,** *32*, 4235-4243. https://doi.org/10.1021/ic00072a015

202. Conte, V.; Di Furia, F.; Moro, S., 51V-NMR investigation on the formation of peroxo vanadium complexes in aqueous solution: Some novel observations. *J. Mole. Catal.* **1994,** *94*, 323-333. https://doi.org/10.1016/0304-5102(94)00149-9

203. Conte, V.; Furia, F. D.; Moro, S., Solvation, preferential solvation and complexation by the solvent of peroxovanadium complexes studied by 51V NMR spectroscopy. Correlations with the oxidative reactivity. *Inorg. Chim. Acta* **1998,** *272*, 62-67. https://doi.org/10.1016/S0020-1693(97)05976-8

204. Talsi, E. P.; Shalyaev, K. V., 51V NMR and EPR study of the mechanistic details of oxidation with VO(O2) (Pic) (H2O)2. *J. Mole. Catal.* **1994,** *92*, 245-255. https://doi.org/10.1016/0304-5102(94)00069-7

205. Andersson, I.; Angus-Dunne, S.; Howarth, O.; Pettersson, L., Speciation in vanadium bioinorganic systems: 6. Speciation study of aqueous peroxovanadates, including complexes with imidazole. *J. Inorg. Biochem.* **2000,** *80*, 51-58. https://doi.org/10.1016/S0162-0134(00)00039-8

206. Justino, L. n. L. G.; Ramos, M. L. s.; Caldeira, M. M.; Gil, V. M. S., Peroxovanadium(V) complexes of glycolic acid as studied by NMR spectroscopy. *Inorg. Chim. Acta* **2000,** *311*, 119-125. https://doi.org/10.1016/S0020-1693(00)00317-0

207. Justino, L., L. G.; Ramos, M. L.; Caldeira, M. M.; Gil, V. M. S., NMR spectroscopy study of the peroxovanadium(V) complexes of l-malic acid. *Inorg. Chim. Acta* **2003,** *356*, 179-186. https://doi.org/10.1016/S0020-1693(03)00466-3

208. Schmidt, H.; Andersson, I.; Rehder, D.; Pettersson, L., A Potentiometric and 51V NMR Study of the Aqueous H+/H2VO4−/H2O2/L-α-Alanyl-L-histidine System. *Chem. Eur. J.* **2001,** *7*, 251-257. https://doi.org/10.1002/1521-3765(20010105)7:1<251::AID-CHEM251>3.0.CO;2-9

209. Zhang, J.; Yu, X.; Zeng, B.; Cai, S.; Chen, Z., Spectroscopic and theoretical study on the interaction between diperoxovanadate complexes and glycyl-histidine. *Spectrochim. Acta A* **2010,** *77*, 825-831. https://doi.org/10.1016/j.saa.2010.08.013

210. Zeng, B.; Zhu, X.; Cai, S.; Chen, Z., Interactions between diperoxovanadate complex and amide ligands in aqueous solution. *Spectrochim. Acta A* **2007,** *67*, 202-207. https://doi.org/10.1016/j.saa.2006.07.003

211. Vennat, M.; Brégeault, J.-M.; Herson, P., Mixed crystals containing the dioxo complex [{Ph3SiO}2VO2]− and novel pentacoordinated oxoperoxo complex [{Ph3SiO}2VO(O2)]−: X-ray crystal structure and assessment as oxidation catalysts. *Dalton Trans.* **2004**, 908-913. http://dx.doi.org/10.1039/B400657G

212. Bonchio, M.; Bortolini, O.; Conte, V.; Moro, S., Characterization and Reactivity of Triperoxo Vanadium Complexes In Protic Solvents. *Eur. J. Inorg. Chem.* **2001,** *2001*, 2913-2919. https://doi.org/10.1002/1099-0682(200111)2001:11<2913::AID-EJIC2913>3.0.CO;2-T

213. Kwong, D. W. J.; Chan, O. Y.; Wong, R. N. S.; Musser, S. M.; Vaca, L.; Chan, S. I., DNA-Photocleavage Activities of Vanadium(V)−Peroxo Complexes. *Inorg. Chem.* **1997,** *36*, 1276-1277. https://doi.org/10.1021/ic960909b

214. Butenko, N.; Pinheiro, J. P.; Da Silva, J. P.; Tomaz, A. I.; Correia, I.; Ribeiro, V.; Costa Pessoa, J.; Cavaco, I., The effect of phosphate on the nuclease activity of vanadium compounds. *J. Inorg. Biochem.* **2015,** *147*, 165-176. https://doi.org/10.1016/j.jinorgbio.2015.04.010

215. Wittenkeller, L.; Abraha, A.; Ramasamy, R.; De Freitas, D. M.; Theisen, L. A.; Crans, D. C., Vanadate interactions with bovine copper,zinc-superoxide dismutase as probed by vanadium-51 NMR spectroscopy. *J. Am. Chem. Soc.* **1991,** *113*, 7872-7881. https://doi.org/10.1021/ja00021a008

216. Wolff, F.; Choukroun, R.; Lorber, C.; Donnadieu, B., Reactivity of B(C6F5)3 with Oxovanadium(V) Complexes VOL3 (L = OCH2CF3, NEt2): Formation of the Organometallic

Vanadium(V) Complex [VO(μ-OCH2CF3)(OCH2CF3)(C6F5)]2 and the Lewis Acid Adduct [(Et2N)3VO·B(C6F5)3]. *Eur. .J. Inorg. Chem.* **2003,** *2003*, 628-632. https://doi.org/10.1002/ejic.200390086

217. Zamaraev, K., New possibilities of NMR in mechanistic studies of homogeneous and heterogeneous catalysis. *J. Mole. Catal.* **1993,** *82*, 275-324. https://doi.org/10.1016/0304-5102(93)80037-U

218. Bonchio, M.; Bortolini, O.; Carraro, M.; Conte, V.; Primon, S., Vanadium catalyzed reduction of dioxygen to hydrogen peroxide: an oscillating process. *J. Inorg. Biochem.* **2000,** *80*, 191-194. https://doi.org/10.1016/S0162-0134(00)00031-3

219. Ishikawa, E.; Kihara, D.; Togawa, Y.; Ookawa, C., Cyclooctene Epoxidation by Hydrogen Peroxide in the Presence of Vanadium-Substituted Lindqvist-Type Polyoxotungstate [VW5O19]3–. *Eur. J. Inorg. Chem.* **2019,** *2019*, 402-409. https://doi.org/10.1002/ejic.201800869

220. Zakzeski, J.; Burton, S.; Behn, A.; Head-Gordon, M.; Bell, A. T., Spectroscopic investigation of the species involved in the rhodium-catalyzed oxidative carbonylation of toluene to toluic acid. *Phys. Chem. Chem. Phys.* **2009,** *11*, 9903-9911. http://dx.doi.org/10.1039/B906883J

221. Chahkandi, M., ^{51}V NMR, ^{17}O NMR, and UV–Vis computational studies of new VBPO functional models: Bromide oxidation reaction. *Polyhedron* **2016,** *109*, 92-98. https://doi.org/10.1016/j.poly.2016.02.006

222. Vijayakumar, M.; Li, L.; Nie, Z.; Yang, Z.; Hu, J. Z., Structure and stability of hexa-aqua V(III) cations in vanadium redox flow battery electrolytes. *Phys. Chem. Chem. Phys.* **2012,** *14*, 10233-10242. https://doi.org/10.1039/c2cp40707h

223. Jura, M.; Levason, W.; Ratnani, R.; Reid, G.; Webster, M., Six- and eight-coordinate thio- and seleno-ether complexes of NbF5 and some comparisons with NbCl5 and NbBr5 adducts. *Dalton Trans.* **2010,** *39*, 883-891. http://dx.doi.org/10.1039/B916336K

224. Benjamin, S. L.; Chang, Y.-P.; Gurnani, C.; Hector, A. L.; Huggon, M.; Levason, W.; Reid, G., Niobium(v) and tantalum(v) halide chalcogenoether complexes – towards single source CVD precursors for ME_2 thin films. *Dalton Trans.* **2014,** *43*, 16640-16648. http://dx.doi.org/10.1039/C4DT02694B

225. Henderson, R. A.; Hughes, D. L.; Stephens, A. N., The chemistry of niobium and tantalum dithiocarbamato-complexes. Part 4. The co-ordination isomers of NbCl3(S2CNEt2)2 and the X-ray crystal structure of [NbCl3(S2CNEt2)2]. *J. Chem. Soc., Dalton Trans.* **1990**, 1097-1099. http://dx.doi.org/10.1039/DT9900001097

226. Dilworth, J. R.; Henderson, R. A.; Hills, A.; Hughes, D. L.; Macdonald, C.; Stephens, A. N.; Walton, D. R. M., The chemistry of niobium and tantalum dithiocarbamato-complexes. Part 1. Synthesis, structure, and protonation of dinitrogen-bridged complexes. *J. Chem. Soc., Dalton Trans.* **1990**, 1077-1085. http://dx.doi.org/10.1039/DT9900001077

227. Lee, G. R.; Crayston, J. A., Niobium-93 nuclear magnetic resonance studies of the solvolysis of NbCl5 by alcohols. *J. Chem. Soc., Dalton Trans.* **1991**, 3073-3076. http://dx.doi.org/10.1039/DT9910003073

228. Karaliota, A.; Kamariotaki, M.; Hatzipanayioti, D., Spectroscopic studies of NbCl5 and TaCl5 in methanol solutions. An investigation of the alcoholysis and the formation of organic compounds. *Transit. Met. Chem.* **1997,** *22*, 411-417. https://doi.org/10.1023/A:1018582406721

229. Lee, G. R.; Crayston, J. A., Hydrolysis of acetonitrile in the presence of NbCl5. *Polyhedron* **1996,** *15*, 1817-1821. https://doi.org/10.1016/0277-5387(95)00432-7

230. Amini, M. M.; Fazaeli, Y.; Mohammadnezhad, G.; Khavasi, H. R., Structural and spectroscopic characterizations of tetra-nuclear niobium(V) complexes of quinolinol derivatives. *Spectrochim. Acta A* **2015,** *144*, 192-199. https://doi.org/10.1016/j.saa.2015.02.077

231. Lu, Y.-J.; Lalancette, R.; Beer, R. H., Deoxygenation of Polynuclear Metal−Oxo Anions: Synthesis, Structure, and Reactivity of the Condensed Polyoxoanion

[(C4H9)4N]4(NbW5O18)2O. *Inorg. Chem.* **1996,** *35*, 2524-2529. https://doi.org/10.1021/ic951197c

232. Rehder, D.; Rodewald, D., Metal NMR of Organovanadium, -Niobium and -Tantalum Compounds. In *Advanced Applications of NMR to Organometallic Chemistry*, Gielen, M.; Willem, R.; Wrackmeyer, B., Eds. Wiley: New York, 1996; pp 291-311.

233. Calderazzo, F.; Felten, C.; Pampaloni, G.; Rehder, D., New alkyne complexes of niobium(I). *J. Chem. Soc., Dalton Trans.* **1992**, 2003-2007. http://dx.doi.org/10.1039/DT9920002003

234. Cheatham, L. K.; Graham, J. J.; Apblett, A. W.; Barron, A. R., The molecular structure of (allyl)bis(methylcyclopentadienyl)niobium(III). *Polyhedron* **1991,** *10*, 1075-1078. https://doi.org/10.1016/S0277-5387(00)81371-6

235. Hulley, E. B.; Williams, V. A.; Hirsekorn, K. F.; Wolczanski, P. T.; Lancaster, K. M.; Lobkovsky, E. B., Application of 93Nb NMR spectroscopy to (silox)3Nb(Xn/Lm) complexes (silox=tBu3SiO): Where does (silox)3Nb(NN)Nb(silox)3 appear? *Polyhedron* **2016,** *103*, 105-114. https://doi.org/10.1016/j.poly.2015.10.005

236. Sugimoto, M.; Kanayama, M.; Nakatsuji, H., Theoretical study on metal NMR chemical shifts: niobium complexes. *J. Phys. Chem.* **1992,** *96*, 4375-4381. https://doi.org/10.1021/j100190a048

237. Bühl, M.; Wrackmeyer, B., Density-functional computation of ^{93}Nb NMR chemical shifts. *Magn. Reson. Chem.* **2010,** *48*, S61-S68. https://doi.org/10.1002/mrc.2624

238. Zhou, Q.; Ye, M.; Ma, W.; Li, D.; Ding, B.; Chen, M.; Yao, Y.; Gong, X.; Hou, Z., Ionic Liquid Stabilized Niobium Oxoclusters Catalyzing Oxidation of Sulfides with Exceptional Activity. *Chem. Eur. J.* **2019,** *25*, 4206-4217. https://doi.org/10.1002/chem.201806178

239. Klemperer, W. G.; Marek, K. A., An 17O NMR Study of Hydrolyzed NbV in Weakly Acidic and Basic Aqueous Solutions. *Eur. J. Inorg. Chem.* **2013,** *2013*, 1762-1771. http://doi.porg/10.1002/ejic.201201231

240. Galajov, M.; García, C.; Gómez, M.; Gómez-Sal, P., Trialkyl imido niobium and tantalum compounds: synthesis, structural study and migratory insertion reactions. *Dalton Trans.* **2011,** *40*, 2797-2804. http://dx.doi.org/10.1039/C0DT01449D

241. Galajov, M.; García, C.; Gómez, M., Tri-chlorido, 2-methylallyl and 2-butenyl tert-butylimido niobium and tantalum complexes: Synthesis, multinuclear NMR spectroscopy and reactivity. *Dalton Trans.* **2011,** *40*, 413-420. http://dx.doi.org/10.1039/C0DT00878H

242. Elorriaga, D.; Galajov, M.; García, C.; Gómez, M.; Gómez-Sal, P., Hydridotris(3,5-dimethylpyrazolyl)borate Dimethylamido Imido Niobium and Tantalum Complexes: Synthesis, Reactivity, Fluxional Behavior, and C–H Activation of the NMe2 Function. *Organometallics* **2012,** *31*, 5089-5100. https://doi.org/10.1021/om300437e

243. Galájov, M.; García, C.; Gómez, M.; Gómez-Sal, P.; Temprado, M., Synthesis and DFT, Multinuclear Magnetic Resonance, and X-ray Structural Studies of Iminoacyl Imido Hydridotris(3,5-dimethylpyrazolyl)borate Niobium and Tantalum(V) Complexes. *Organometallics* **2014,** *33*, 2277-2286. https://doi.org/10.1021/om5002028

244. Bregel, D. C.; Oldham, S. M.; Lachicotte, R. J.; Eisenberg, R., A New Tantalum Dinitrogen Complex and a Parahydrogen-Induced Polarization Study of Its Reaction with Hydrogen. *Inorg. Chem.* **2002,** *41*, 4371-4377. http://doi.org/10.1021/ic025578j

245. Hunter, S. C.; Chen, S.-J.; Steren, C. A.; Richmond, M. G.; Xue, Z.-L., Syntheses and Characterization of Tantalum Alkyl Imides and Amide Imides. DFT Studies of Unusual α-SiMe3 Abstraction by an Amide Ligand. *Organometallics* **2015,** *34*, 5687-5696. https://doi.org/10.1021/acs.organomet.5b00558

246. Malito, J., Molybdenum-95 NMR Spectroscopy. In *Annu. Rep. NMR Spectrosc.*, Webb, G. A., Ed. 1996; pp 151-206. https://doi.org/10.1016/S0066-4103(08)60050-2

247. Bouten, R.; Baerends, E. J.; van Lenthe, E.; Visscher, L.; Schreckenbach, G.; Ziegler, T., Relativistic Effects for NMR Shielding Constants in Transition Metal Oxides Using the

Zeroth-Order Regular Approximation. *J. Phys. Chem. A* **2000,** *104*, 5600-5611. https://doi.org/10.1021/jp994480w

248. Dutta, R.; Chakraborty, S.; Bose, P.; Ghosh, P., Aerial CO2 Trapped as CO32– Ions in a Dimeric Capsule That Efficiently Extracts Chromate, Sulfate, and Thiosulfate from Water by Anion-Exchange Metathesis. *Eur. J. Inorg. Chem.* **2014,** *2014*, 4134-4143. https://doi.org/10.1002/ejic.201402139

249. Gaemers, S.; Groenevelt, J.; Elsevier, Cornelis J., Transition Metal (53Cr, 59Co, 91Zr, and 95Mo) and 14N NMR Spectroscopy of Coordination Compounds Containing Nitrogen Donor Ligands in Low-Viscosity Fluids. *Eur. J. Inorg. Chem.* **2001,** *2001*, 829-835. https://doi.org/10.1002/1099-0682(200103)2001:3<829::AID-EJIC829>3.0.CO;2-F

250. Bühl, M., Density-functional computation of ^{53}Cr NMR chemical shifts. *Magn. Reson. Chem.* **2006,** *44*, 661-668. https://doi.org/10.1002/mrc.1807

251. Aldrich, K. E.; Billow, B. S.; Holmes, D.; Bemowski, R. D.; Odom, A. L., Weakly Coordinating yet Ion Paired: Anion Effects on an Internal Rearrangement. *Organometallics* **2017,** *36*, 1227-1237. http://doi.org/10.1021/acs.organomet.6b00839

252. Fujihara, T.; Kaizaki, S., Diamagnetic behaviour of high-resolution nitrogen-14 nuclear magnetic resonance spectra for co-ordinated nitrogens in paramagnetic chromium(III) diamine complexes. *J. Chem. Soc., Dalton Trans.* **1993**, 2521-2524. http://dx.doi.org/10.1039/DT9930002521

253. Braunschweig, H.; Colling, M.; Kollann, C.; Merz, K.; Radacki, K., [$(OC)_5Cr{=}BSi(SiMe_3)_3$]: A Terminal Borylene Complex with an Electronically Unsaturated Boron Atom. *Angew. Chem. Int. Ed,* **2001,** *40*, 4198-4200. https://doi.org/10.1002/1521-3773(20011119)40:22<4198::AID-ANIE4198>3.0.CO;2-E

254. Grieves, R. A.; Mason, J., Patterns of 95Mo shielding in organometallic and inorganic chemistry. *Polyhedron* **1986,** *5*, 415-421. https://doi.org/10.1016/S0277-5387(00)84943-8

255. Brito, J. A.; Teruel, H.; Massou, S.; Gómez, M., ^{95}Mo NMR: a useful tool for structural studies in solution. *Magn. Reson. Chem.* **2009,** *47*, 573-577. https://doi.org/10.1002/mrc.2431

256. Ramos, M. L.; Justino, L. L. G.; Abreu, P. E.; Fonseca, S. M.; Burrows, H. D., Oxocomplexes of Mo(VI) and W(VI) with 8-hydroxyquinoline-5-sulfonate in solution: structural studies and the effect of the metal ion on the photophysical behaviour. *Dalton Trans.* **2015,** *44*, 19076-19089. http://dx.doi.org/10.1039/C5DT03473F

257. Ramos, M. L.; Justino, L. L. G.; Gil, V. M. S.; Burrows, H. D., NMR and DFT studies of the complexation of W(VI) and Mo(VI) with 3-phospho-D-glyceric and 2-phospho-D-glyceric acids. *Dalton Trans.* **2009**, 9616-9624. http://dx.doi.org/10.1039/B905933D

258. Szalontai, G.; Kiss, G.; Bartha, L., Equilibria of mononuclear oxomolybdenum(VI) complexes of triethanolamine.: A multinuclear dynamic magnetic resonance study of structure and exchange mechanisms. *Spectrochim. Acta A* **2003,** *59*, 1995-2007. https://doi.org/10.1016/S1386-1425(02)00445-6

259. Unoura, K.; Suzuki, T.; Nagasawa, A.; Yamazaki, A.; Fukuda, Y., Electrochemical and 95Mo NMR studies of triply-bridged dinuclear oxomolybdenum(V) complexes with various dithiocarbamates. *Inorg. Chim. Acta* **1999,** *292*, 7-15. https://doi.org/10.1016/S0020-1693(99)00163-2

260. Wong, T. C.; Huang, Q.; Nianyong, Z.; Wu, X., 95Mo NMR studies of five heterometallic trinuclear incomplete cubane-like clusters. *Polyhedron* **1997,** *16*, 2987-2990. https://doi.org/10.1016/S0277-5387(97)00050-8

261. Nguyen, T. T.; Jung, J.; Trivelli, X.; Trébosc, J.; Cordier, S.; Molard, Y.; Le Pollès, L.; Pickard, C. J.; Cuny, J.; Gautier, R., Evaluation of 95Mo Nuclear Shielding and Chemical Shift of [Mo6X14]2– Clusters in the Liquid Phase. *Inorg. Chem.* **2015,** *54*, 7673-7683. https://doi.org/10.1021/acs.inorgchem.5b00396

262. Akagi, S.; Fujii, S.; Kitamura, N., Zero-Magnetic-Field Splitting in the Excited Triplet States of Octahedral Hexanuclear Molybdenum(II) Clusters: $[\{Mo_6X_8\}Y_6]^{2-}$ (X, Y = Cl, Br, I). *J. Phys. Chem. A* **2018,** *122*, 9014-9024. https://doi.org/10.1021/acs.jpca.8b09339

263. Maksimovskaya, R. I.; Maksimov, G. M., 95Mo and 17O NMR Studies of Aqueous Molybdate Solutions. *Inorg. Chem.* **2007,** *46*, 3688-3695. https://doi.org/10.1021/ic061549n

264. Brunner, H.; Mijolovic, D.; Wrackmeyer, B.; Nuber, B., NMR analysis of trinuclear silver(I) complexes with μ_2-H bridged group VI metallocene hydrides as ligands and X-ray structure analysis of $\{[(\eta^5\text{-MeC}_5H_4)_2Mo(\mu_2\text{-H})_2]_2Ag\}PF_6$. *J. Organomet. Chem.* **1999,** *579*, 298-303. https://doi.org/10.1016/S0022-328X(99)00012-1

265. Jura, M.; Levason, W.; Reid, G.; Webster, M., Preparation and properties of cyclic and open-chain Sb/N-donor ligands. *Dalton Trans.* **2009**, 7811-7819. http://dx.doi.org/10.1039/B909226A

266. Levason, W.; Ollivere, L. P.; Reid, G.; Tsoureas, N.; Webster, M., Synthesis, spectroscopic and structural characterisation of molybdenum, tungsten and manganese carbonyl complexes of tetrathio- and tetraseleno-ether ligands. *J. Organomet. Chem.* **2009,** *694*, 2299-2308. https://doi.org/10.1016/j.jorganchem.2009.03.041

267. Levason, W.; Reid, G.; Tolhurst, V.-A., Transition metal complexes of 1,3-dihydrobenzo[c]tellurophene: synthesis, spectroscopy and crystal structures. *J. Chem. Soc., Dalton Trans.* **1998**, 3411-3416. http://dx.doi.org/10.1039/A805183F

268. Cybulski, P. A.; Gillis, D. J.; Baird, M. C., Molybdenum-95 T1 measurements of molybdenum hexacarbonyl encapsulated in NaY zeolite. *Inorg. Chem.* **1993,** *32*, 460-462. https://doi.org/10.1021/ic00056a019

269. Li, L.-F.; You, X.-Z., Topological Index and Its Applications. I. *Chi. Sci. Bull.* **1993,** *38*, 1358-1363.

270. Randic, M., Characterization of molecular branching. *J. Am. Chem. Soc.* **1975,** *97*, 6609-6615. https://doi.org/10.1021/ja00856a001

271. Zhang, H.; Xin, H., Bonding Parameter Topological Index and Its Applications in Correlation with XY, XY_2, XY_3, and XY_4 Molecular Properties. *Chin. J. Chem. Phys. (in Chinese with English abstract)* **1989,** *2*, 413-419.

272. Teruel, H.; Sierralta, A., Molecular orbital studies in95Mo NMR shielding for[MoOnS(4 − n)]2− anions: Relations between chemical shift and molybdenum orbital electron populations. *Polyhedron* **1996,** *15*, 2215-2221. https://doi.org/10.1016/0277-5387(95)00476-9

273. Farkas, E.; Csoka, H.; Toth, I., New insights into the solution equilibrium of molybdenum(VI)-hydroxamate systems: 1H and 17O NMR spectroscopic study of Mo(VI)-desferrioxamine B and Mo(VI)-monohydroxamic acid systems. *Dalton Trans.* **2003**, 1645-1652. https://doi.org/10.1039/B300431G

274. Santos, M. A.; Gama, S.; Pessoa, J. C.; Oliveira, M. C.; Toth, I.; Farkas, E., Complexation of molybdenum(VI) with bis(3-hydroxy-4-pyridinone)amino acid derivatives. *Eur. J. Inorg. Chem.* **2007**, 1728-1737. http://doi.org/10.1002/ejic.200601088

275. Burroughs, B. A.; Bursten, B. E.; Chen, S.; Chisholm, M. H.; Kidwell, A. R., Metathesis of Nitrogen Atoms within Triple Bonds Involving Carbon, Tungsten, and Molybdenum. *Inorg. Chem.* **2008,** *47*, 5377-5385. https://doi.org/10.1021/ic8003917

276. Chisholm, M. H.; Delbridge, E. E.; Kidwell, A. R.; Quinlan, K. B., Nitrogen atom exchange between molybdenum, tungsten and carbon. A convenient method for N-15 labeling. *Chem. Commun.* **2003**, 126-127. https://doi.org/10.1039/B210286B

277. Zhang, S.; Appel, A. M.; Bullock, R. M., Reversible Heterolytic Cleavage of the H-H Bond by Molybdenum Complexes: Controlling the Dynamics of Exchange Between Proton and Hydride. *J. Am. Chem. Soc.* **2017,** *139*, 7376-7387. https://doi.org/10.1021/jacs.7b03053

278. Chiang, M.-H.; Antonio, M. R.; Soderholm, L., Energetics of the Preyssler anion's molecular orbitals: quantifying the effect of the encapsulated-cation's charge. *Dalton Trans.* **2004**, 3562-3567. http://dx.doi.org/10.1039/B412337A

279. Bajpe, S. R.; Breynaert, E.; Robeyns, K.; Houthoofd, K.; Absillis, G.; Mustafa, D.; Parac-Vogt, T. N.; Maes, A.; Martens, J. A.; Kirschhock, C. E. A., Chromate-Mediated One-Step Quantitative Transformation of PW_{12} into P_2W_{20} Polyoxometalates. *Eur. J. Inorg. Chem.* **2012,** *2012*, 3852-3858. https://doi.org/10.1002/ejic.201200440

280. Duval, S.; Béghin, S.; Falaise, C.; Trivelli, X.; Rabu, P.; Loiseau, T., Stabilization of Tetravalent 4f (Ce), 5d (Hf), or 5f (Th, U) Clusters by the [α-SiW9O34]10– Polyoxometalate. *Inorg. Chem.* **2015,** *54*, 8271-8280. https://doi.org/10.1021/acs.inorgchem.5b00786

281. Nomiya, K.; Saku, Y.; Yamada, S.; Takahashi, W.; Sekiya, H.; Shinohara, A.; Ishimaru, M.; Sakai, Y., Synthesis and structure of dinuclear hafnium(IV) and zirconium(IV) complexes sandwiched between 2 mono-lacunary α-Keggin polyoxometalates. *Dalton Trans.* **2009**, 5504-5511. http://dx.doi.org/10.1039/B902296A

282. Sprangers, C. R.; Marmon, J. K.; Duncan, D. C., Where Are the Protons in α-[HxW12O40](8-x)- (x = 2−4)? *Inorg. Chem.* **2006,** *45*, 9628-9630. https://doi.org/10.1021/ic061370c

283. Smith, B. J.; Patrick, V. A., Quantitative Determination of Aqueous Dodecatungstophosphoric Acid Speciation by NMR Spectroscopy. *Aust. J. Chem.* **2004,** *57*, 261-268. https://doi.org/10.1071/CH02037

284. Lenoble, G.; Hasenknopf, B.; Thouvenot, R., A Strategy for the Analysis of Chiral Polyoxotungstates by Multinuclear (31P, 183W) NMR Spectroscopy Applied to the Assignment of the 183W NMR Spectra of α1-[P2W17O61]10- and α1-[YbP2W17O61]7. *J. Am. Chem. Soc.* **2006,** *128*, 5735-5744. https://doi.org/10.1021/ja0575934

285. Xue, Z.-L.; Cook, T. M.; Lamb, A. C., Trends in NMR chemical shifts of d0 transition metal compounds. *J. Organomet. Chem.* **2017,** *852*, 74-93. https://doi.org/10.1016/j.jorganchem.2017.03.044

286. Kamata, K.; Hirano, T.; Kuzuya, S.; Mizuno, N., Hydrogen-Bond-Assisted Epoxidation of Homoallylic and Allylic Alcohols with Hydrogen Peroxide Catalyzed by Selenium-Containing

Dinuclear Peroxotungstate. *J. Am. Chem. Soc.* **2009,** *131*, 6997-7004. https://doi.org/10.1021/ja901289r

287. Kamata, K.; Kimura, T.; Sunaba, H.; Mizuno, N., Scope of chemical fixation of carbon dioxide catalyzed by a bifunctional monomeric tungstate. *Catal. Today* **2014,** *226*, 160-166. https://doi.org/10.1016/j.cattod.2013.09.054

288. Carlton, L.; Emdin, A.; Lemmerer, A.; Fernandes, M. A., A tungsten-183 NMR study of cis and trans isomers of $[W(CO)_4(PPh_3)(PR_3)]$(PR_3 = phosphine, phosphite). *Magn. Reson. Chem.* **2008,** *46*, S56-S62. https://doi.org/10.1002/mrc.2300

289. Fuchs, A.; Gudat, D.; Nieger, M.; Schmidt, O.; Sebastian, M.; Nyulaszi, L.; Niecke, E., 1,3-Diphospholene-4-ylidene Chromium (Tungsten) Pentacarbonyl Complexes Formed by CO Insertion into the Ring of a 1,3-Diphosphacyclobutane-2,4-diyl-2-ide—Complexes of a Phosphanyl Carbene or a Phosphonium Ylide? *Chem. Eur. J.* **2002,** *8*, 2188-2196. https://doi.org/10.1002/1521-3765(20020503)8:9<2188::AID-CHEM2188>3.0.CO;2-F

290. Vilà-Nadal, L.; Sarasa, J. P.; Rodríguez-Fortea, A.; Igual, J.; Kazansky, L. P.; Poblet, J. M., Towards the Accurate Calculation of 183W NMR Chemical Shifts in Polyoxometalates: The Relevance of the Structure. *Chem. Asian J.* **2010,** *5*, 97-104. https://doi.org/10.1002/asia.200900263

291. Chermette, H.; Lefebvre, F., Theoretical study of the four isomers of $[SiW_{11}O_{39}]^{8-}$: Structure, stability and physical properties. *C. R. Chimie* **2012,** *15*, 143-151. https://doi.org/10.1016/j.crci.2011.09.002

292. Vankova, N.; Heine, T.; Kortz, U., NMR Chemical Shifts of Metal Centres in Polyoxometalates: Relativistic DFT Predictions. *Eur. J. Inorg. Chem.* **2009,** *2009*, 5102-5108. https://doi.org/10.1002/ejic.200900865

293. Bagno, A.; Bonchio, M.; Autschbach, J., Computational Modeling of Polyoxotungstates by Relativistic DFT Calculations of ^{183}W NMR Chemical Shifts. *Chem. Eur. J.* **2006,** *12*, 8460-8471. https://doi.org/10.1002/chem.200600488

294. Bagno, A., Counterion effects on the ^{183}W NMR spectra of the lacunary Keggin polyoxotungstate $[PW_{11}O_{39}]^{7-}$. Relativistic DFT calculations. *C. R. Chim.* **2012,** *15*, 118-123. https://doi.org/10.1016/j.crci.2011.07.008

295. Gracia, J.; Poblet, J. M.; Autschbach, J.; Kazansky, L. P., Density-Functional Calculation of the 183W and 17O NMR Chemical Shifts for Large Polyoxotungstates. *Eur. J. Inorg. Chem.* **2006,** *2006*, 1139-1148. https://doi.org/10.1002/ejic.200500832

296. Kazansky, L. P.; Chaquin, P.; Fournier, M.; Hervé, G., Analysis of 183W and 17O NMR chemical shifts in polyoxometalates by extended Hückel mo calculations. *Polyhedron* **1998,** *17*, 4353-4364. https://doi.org/10.1016/S0277-5387(98)00218-6

297. Howarth, O. W., Oxygen-17 NMR study of aqueous peroxotungstates. *Dalton Trans.* **2004**, 476-481. http://dx.doi.org/10.1039/B313243A

298. Sakharov, S. G.; Buslaev, Y. A.; Tkáč, I., Multinuclear NMR Study of the Structure and Intramolecular Dynamics of (η2-Acetone phenylhydrazonato)tetrafluorooxotungsten(VI). *Inorg. Chem.* **1996,** *35*, 5514-5519. https://doi.org/10.1021/ic950330y

299. Malinowska, A.; Kochel, A.; Szymańska-Buzar, T., An anionic binuclear complex of tungsten(II), [(μ-Cl)3{W(SnCl3)(CO)3}2]−, and its reactivity towards norbornene. *J. Organomet. Chem.* **2007,** *692*, 3994-3999. https://www.sciencedirect.com/science/article/pii/S0022328X07004226

300. Connolly, J.; R. J. Genge, A.; Levason, W.; D. Orchard, S.; J. A. Pope, S.; Reid, G., Cationic manganese(I) tricarbonyl complexes with group 15 and 16 donor ligands: synthesis, multinuclear NMR spectroscopy and crystal structures. *J. Chem. Soc., Dalton Trans.* **1999**, 2343-2352. http://dx.doi.org/10.1039/A902820J

301. K. Davies, M.; C. Durrant, M.; Levason, W.; Reid, G.; L. Richards, R., Synthesis, spectroscopic and structural studies on transition metal carbonyl complexes of cyclic di- and tetra-selenoether ligands. *J. Chem. Soc., Dalton Trans.* **1999**, 1077-1084. http://dx.doi.org/10.1039/A809853K

302. Grossbruchhaus, V.; Rehder, D., Synthesis and properties of the open clusters (LnM)3 μ 3-E (LnM · η 5-CpMo/W(CO)3, Mn(CO)5; E = P, As, Sb, Bi and V). *Inorg. Chim. Acta* **1990,** *172*, 141-145. https://doi.org/10.1016/S0020-1693(00)80848-8

303. Hill, A. M.; Levason, W.; Webster, M.; Albers, I., Complexes of Distibinomethane Ligands. 1. Iron, Cobalt, Nickel, and Manganese Carbonyl Complexes. *Organometallics* **1997,** *16*, 5641-5647. https://doi.org/10.1021/om9706121

304. Holmes, N. J.; Levason, W.; Webster, M., Triphenylstibine substituted manganese and rhenium carbonyls: synthesis and multinuclear NMR spectroscopic studies. X-ray crystal structures of ax-[Mn2(CO)9(SbPh3)], [Mn(CO)5(SbPh3)][CF3SO3] and fac-[Re(CO)3Cl(SbPh3)2]. *J. Organomet. Chem.* **1998,** *568*, 213-223. https://doi.org/10.1016/S0022-328X(98)00763-3

305. Klingler, R. J.; Rathke, J. W., Thermodynamics for the hydrogenation of dimanganese decacarbonyl. *Inorg. Chem.* **1992,** *31*, 804-808. https://doi.org/10.1021/ic00031a021

306. Torocheshnikov, V.; Rentsch, D.; von Philipsborn, W., ^{55}Mn, ^{13}C coupling constants of some σ- and π-organomanganese complexes. *Magn. Reson. Chem.* **1994,** *32*, 348-352. https://doi.org/10.1002/mrc.1260320607

307. Levason, W.; Orchard, S. D.; Reid, G., Ditelluroether Complexes of Manganese and Rhenium Carbonyl Halides: Synthesis and IR and Multinuclear NMR Spectroscopic and Structural Studies. Comparison of the Bonding Properties of Dithio-, Diseleno-, and Ditelluroethers in Low-Valent Carbonyl Systems. *Organometallics* **1999,** *18*, 1275-1280. https://doi.org/10.1021/om980867u

308. Petz, W.; Rehder, D., Evidence for the formation of Mn2(CO)9(CS). *Organometallics* **1990,** *9*, 856-859. https://doi.org/10.1021/om00117a050

309. Pope, S. J. A.; Reid, G., Phosphine, arsine and stibine complexes of manganese(I) carbonyl halides: synthesis, multinuclear NMR spectroscopic studies, redox properties and

crystal structures. *J. Chem. Soc., Dalton Trans.* **1999**, 1615-1622. http://dx.doi.org/10.1039/A900875F

310. Rentsch, D.; Nill, L.; von Philipsborn, W.; Sidler, D. R.; Rybczynski, P. J.; DeShong, P., ^{13}C, ^{17}O and ^{55}Mn NMR studies on substituted manganese carbonyl complexes. A contribution to the mechanism of demetalation reactions. *Magn. Reson. Chem.* **1998,** *36*, S54-S60. https://doi.org/10.1002/(SICI)1097-458X(199806)36:13<S54::AID-OMR292>3.0.CO;2-L

311. DeShong, P.; Soli, E. D.; Slough, G. A.; Sidler, D. R.; Elango, V.; Rybczynski, P. J.; Vosejpka, L. J. S.; Lessen, T. A.; Le, T. X.; Anderson, G. B.; von Philipsborn, W.; Vöhler, M.; Rentsch, D.; Zerbe, O., Glycosylmanganese pentacarbonyl complexes: an organomanganese-based approach to the synthesis of C-glycosyl derivatives. *J. Organomet. Chem.* **2000,** *593-594*, 49-62. https://doi.org/10.1016/S0022-328X(99)00431-3

312. Heuer, B.; Matthews, M. L.; Reid, G.; Ripley, M., A comparison of the ligating properties of the mixed P/O- and P/S-donor ligands Ph2P(CH2)2O(CH2)2O(CH2)2PPh2 and Ph2P(CH2)2S(CH2)2S(CH2)2PPh2 with Group 6 and 7 carbonyls. *J. Organomet. Chem.* **2002,** *655*, 55-62. https://doi.org/10.1016/S0022-328X(02)01413-4

313. Christendat, D.; Wharf, I.; Lebuis, A.-M.; Butler, I. S.; Gilson, D. F. R., Synthesis and spectroscopic and X-ray structural characterisation of some para-substituted triaryltin(pentacarbonyl)manganese(I) complexes. *Inorg. Chim. Acta* **2002,** *329*, 36-44. https://doi.org/10.1016/S0020-1693(01)00792-7

314. Wrackmeyer, B.; Hofmann, T.; Herberhold, M., Characterization of manganese sandwich complexes by 55Mn NMR spectroscopy. *J. Organomet. Chem.* **1995,** *486*, 255-258. https://doi.org/10.1016/0022-328X(94)05052-D

315. Tanimura, H.; Kitahori, A.; Kuzuoka, C.; Honda, Y.; Hada, M., Calculations and Electronic Analyses of 55Mn and 13C Nuclear Magnetic Shielding Constants for Mn(CO)5X (X = H, F, Cl, Br, I, and CH3) and M(CO)(NH3)3 (M = Cr2+, Fe2+, Cu+, and Zn2+). *Bull. Chem. Soc. Jpn.* **2010,** *83*, 514-519. https://doi.org/10.1246/bcsj.20090344

316. Sharma, R.; Zhang, J.; André Ohlin, C., pH-Dependent solution dynamics of a manganese(ii) polyoxometalate, [Mn4(H2O)2(P2W15O56)2]16−, and [Mn(H2O)6]2+. *Dalton Trans.* **2015,** *44*, 19068-19071. http://dx.doi.org/10.1039/C5DT03138A

317. Lieb, D.; Zahl, A.; Shubina, T. E.; Ivanović-Burmazović, I., Water Exchange on Manganese(III) Porphyrins. Mechanistic Insights Relevant for Oxygen Evolving Complex and Superoxide Dismutation Catalysis. *J. Am. Chem. Soc.* **2010,** *132*, 7282-7284. https://doi.org/10.1021/ja1014585

318. Mundlapati, V. R.; Jena, P.; Acharya, A. N.; Kar, A. K.; Dash, A. C.; Biswal, H. S., Water exchange reaction of a manganese catalase mimic: oxygen-17 NMR relaxometry study on (aqua)manganese(iii) in a salen scaffold and its reactions in a mildly basic medium. *RSC Adv.* **2016,** *6*, 111739-111746. http://dx.doi.org/10.1039/C6RA23154C

319. Okamoto, A.; Kanatani, K.; Taiji, T.; Saito, I., 15N NMR Study on Site-Selective Binding of Metal Ions to Guanine Runs in DNA: A Good Correlation with HOMO Distribution. *J. Am. Chem. Soc.* **2003,** *125*, 1172-1173. https://doi.org/10.1021/ja0279388

320. Alberto, R.; Braband, H.; Nadeem, Q., Bioorganometallic Technetium and Rhenium Chemistry: Fundamentals for Applications. *Chimia* **2020,** *74*, 953-959. https://doi.org/10.2533/chimia.2020.953

321. Sutton, A. D.; John, G. H.; Sarsfield, M. J.; Renshaw, J. C.; May, I.; Martin, L. R.; Selvage, A. J.; Collison, D.; Helliwell, M., Spectroscopic Evidence for the Direct Coordination of the Pertechnetate Anion to the Uranyl Cation in [UO2(TcO4)(DPPMO2)2]+. *Inorg. Chem.* **2004,** *43*, 5480-5482. https://doi.org/10.1021/ic049588r

322. Sarsfield, M. J.; Sutton, A. D.; May, I.; John, G. H.; Sharrad, C.; Helliwell, M., Coordination of pertechnetate [TcO4]− to actinides. *Chem. Commun.* **2004**, 2320-2321. http://dx.doi.org/10.1039/B404424J

323. Mikhalev, V. A., 99Tc NMR Spectroscopy. *Radiochem.* **2005,** *47*, 319-333. https://doi.org/10.1007/s11137-005-0097-3

324. Balasekaran, S. M.; Hagenbach, A.; Drees, M.; Abram, U., $[Tc^{II}(NO)(trifluoroacetate)_4F]^{2-}$ – synthesis and reactions. *Dalton Trans.* **2017,** *46*, 13544-13552. http://dx.doi.org/10.1039/C7DT03084C

325. Poineau, F.; Burton-Pye, B. P.; Maruk, A.; Kirakosyan, G.; Denden, I.; Rego, D. B.; Johnstone, E. V.; Sattelberger, A. P.; Fattahi, M.; Francesconi, L. C.; German, K. E.; Czerwinski, K. R., On the nature of heptavalent technetium in concentrated nitric and perchloric acid. *Inorg. Chim. Acta* **2013,** *398*, 147-150. https://doi.org/10.1016/j.ica.2012.12.028

326. Poineau, F.; Weck, P. F.; German, K.; Maruk, A.; Kirakosyan, G.; Lukens, W.; Rego, D. B.; Sattelberger, A. P.; Czerwinski, K. R., Speciation of heptavalent technetium in sulfuric acid: structural and spectroscopic studies. *Dalton Trans.* **2010,** *39*, 8616-8619. http://dx.doi.org/10.1039/C0DT00695E

327. Soderquist, C.; Weaver, J.; Cho, H.; McNamara, B.; Sinkov, S.; McCloy, J., Properties of Pertechnic Acid. *Inorg. Chem.* **2019,** *58*, 14015-14023. https://doi.org/10.1021/acs.inorgchem.9b01999

328. Poineau, F.; Weck, P. F.; Burton-Pye, B. P.; Denden, I.; Kim, E.; Kerlin, W.; German, K. E.; Fattahi, M.; Francesconi, L. C.; Sattelberger, A. P.; Czerwinski, K. R., Reactivity of HTcO4 with methanol in sulfuric acid: Tc-sulfate complexes revealed by XAFS spectroscopy and first principles calculations. *Dalton Trans.* **2013,** *42*, 4348-4352. http://dx.doi.org/10.1039/C3DT32951H

329. Cho, H.; de Jong, W. A.; McNamara, B. K.; Rapko, B. M.; Burgeson, I. E., Temperature and Isotope Substitution Effects on the Structure and NMR Properties of the Pertechnetate Ion in Water. *J. Am. Chem. Soc.* **2004,** *126*, 11583-11588. https://doi.org/10.1021/ja047447i

330. Hansen, P. E., Isotope effects in nuclear shielding. *Prog. Nucl. Magn. Reson. Spectrosc.* **1988,** *20*, 207-255. https://doi.org/10.1016/0079-6565(88)80002-5

331. Tarasov, V. P.; Kirakosyan, G. A.; German, K. E., 99Tc NMR determination of the oxygen isotope content in 18O-enriched water. *Magn. Reson. Chem.* **2018,** *56*, 183-189. https://doi.org/10.1002/mrc.4680

332. Oehlke, E.; Alberto, R.; Abram, U., Synthesis, Characterization, and Structures of R3EOTcO3 Complexes (E = C, Si, Ge, Sn, Pb) and Related Compounds. *Inorg. Chem.* **2010,** *49*, 3525-3530. https://doi.org/10.1021/ic1001094

333. Tooyama, Y.; Braband, H.; Spingler, B.; Abram, U.; Alberto, R., High-Valent Technetium Complexes with the [99TcO3]+ Core from in Situ Prepared Mixed Anhydrides of [99TcO4]- and Their Reactivities. *Inorg. Chem.* **2008,** *47*, 257-264. https://doi.org/10.1021/ic701908q

334. Grundler, P. V.; Helm, L.; Alberto, R.; Merbach, A. E., Relevance of the Ligand Exchange Rate and Mechanism of fac-[(CO)3M(H2O)3]+ (M = Mn, Tc, Re) Complexes for New Radiopharmaceuticals. *Inorg. Chem.* **2006,** *45*, 10378-10390. https://doi.org/10.1021/ic061578y

335. Hall, G. B.; Andersen, A.; Washton, N. M.; Chatterjee, S.; Levitskaia, T. G., Theoretical Modeling of 99Tc NMR Chemical Shifts. *Inorg. Chem.* **2016,** *55*, 8341-8347. https://doi.org/10.1021/acs.inorgchem.6b00458

336. Aebischer, N.; Schibli, R.; Alberto, R.; Merbach, A. E., Complete Carbonylation of *fac*-$[Tc(H_2O)_3(CO)_3]^+$ under CO Pressure in Aqueous Media: A Single Sample Story! *Angew. Chem. Int. Ed.* **2000,** *39*, 254-256. https://doi.org/10.1002/(SICI)1521-3773(20000103)39:1<254::AID-ANIE254>3.0.CO;2-F

337. Helm, L., Ligand exchange and complex formation kinetics studied by NMR exemplified on fac-[(CO)3M(H2O)]+ (M=Mn, Tc, Re). *Coord. Chem. Rev.* **2008,** *252*, 2346-2361. https://doi.org/10.1016/j.ccr.2008.01.009

338. Chatterjee, S.; Hall, G. B.; Engelhard, M. H.; Du, Y.; Washton, N. M.; Lukens, W. W.; Lee, S.; Pearce, C. I.; Levitskaia, T. G., Spectroscopic Characterization of Aqua [*fac*-$Tc(CO)_3]^+$ Complexes at High Ionic Strength. *Inorg. Chem.* **2018,** *57*, 6903-6912. https://doi.org/10.1021/acs.inorgchem.8b00490

339. Miroslavov, A. E.; Braband, H.; Sidorenko, G. V.; Stepanova, E. S.; Lumpov, A. A.; Alberto, R., Synthesis of [99TcX(CO)5] (X = Cl, Br, I) at ambient pressure. *J. Organomet. Chem.* **2018,** *871*, 56-59. https://doi.org/10.1016/j.jorganchem.2018.06.028

340. Miroslavov, A. E.; Gurziy, V. V.; Tyupina, M. Y.; Lumpov, A. A.; Sidorenko, G. V.; Polotskii, Y. S.; Suglobov, D. N., Technetium and rhenium pentacarbonyl perchlorates: Structure and reactivity. *J. Organomet. Chem.* **2013,** *745-746*, 219-225. https://doi.org/10.1016/j.jorganchem.2013.07.019

341. Schibli, R.; Marti, N.; Maurer, P.; Spingler, B.; Lehaire, M.-L.; Gramlich, V.; Barnes, C. L., Syntheses and Characterization of Dicarbonyl−Nitrosyl Complexes of Technetium(I) and Rhenium(I) in Aqueous Media: Spectroscopic, Structural, and DFT Analyses. *Inorg. Chem.* **2005,** *44*, 683-690. https://doi.org/10.1021/ic049599k

342. Ackermann, J.; Abdulkader, A.; Scholtysik, C.; Jungfer, M. R.; Hagenbach, A.; Abram, U., [TcI(NO)X(Cp)(PPh_3)] Complexes (X^- = I^-, I3–, SCN^-, CF3SO3$^-$, or CF3COO$^-$) and Their Reactions. *Organometallics* **2019,** *38*, 4471-4478. https://doi.org/10.1021/acs.organomet.9b00620

343. Bühl, M.; Golubnychiy, V., Density-functional computation of ^{99}Tc NMR chemical shifts. *Magn. Reson. Chem.* **2008,** *46*, S36-S44. https://doi.org/10.1002/mrc.2276

344. Mancini, D. T.; Souza, E. F.; Caetano, M. S.; Ramalho, T. C., 99Tc NMR as a promising technique for structural investigation of biomolecules: theoretical studies on the solvent and thermal effects of phenylbenzothiazole complex. *Magn. Reson. Chem.* **2014,** *52*, 129-137. https://doi.org/10.1002/mrc.4043

345. Dwek, R. A.; Luz, Z.; Shporer, M., Nuclear magnetic resonance of aqueous solutions of sodium perrhenate. *J. Phys. Chem.* **1970,** *74*, 2232-2233. https://doi.org/10.1021/j100909a038

346. Müller, A.; Krickemeyer, E.; Bögge, H.; Penk, M.; Rehder, D., Thiorhenates [ReS4]-, [ReS9]-, and [ReOS8]-: simple synthesis with Sx2- solutions, structural data, and 185/187 Re-NMR studies. *Chimia* **1986,** *40*, 50-52.

347. Klobasa, D. G.; Burkert, P. K., 185Re and 187Re solid-state NMR of metaperrhenates. *Magn. Reson. Chem.* **1987,** *25*, 154-157. https://doi.org/10.1002/mrc.1260250213

348. Keçeci, A.; Rehder, D., IR, 31P, 55Mn and i85,i87Re NMR Spectroscopic Investigations of Some Carbonylmanganese and -rhenium Complexes. *Z. Naturforsch. B* **1981,** *36*, 20-26. https://zfn.mpdl.mpg.de/data/Reihe_B/36/ZNB-1981-36b-0020.pdf

349. Herrmann, W. A.; Fischer, R. W.; Scherer, W.; Rauch, M. U., Methyltrioxorhenium(VII) as Catalyst for Epoxidations: Structure of the Active Species and Mechanism of Catalysis. *Angew. Chem. Int. Ed.* **1993,** *32*, 1157-1160. https://doi.org/10.1002/anie.199311571

350. Ball, G. E.; Darwish, T. A.; Geftakis, S.; George, M. W.; Lawes, D. J.; Portius, P.; Rourke, J. P., Characterization of an organometallic xenon complex using NMR and IR spectroscopy. *Proc. Natl. Acad. Sci. USA* **2005,** *102*, 1853-1858. http://doi.org/10.1073/pnas.0406527102

351. Shanahan, J. P.; Szymczak, N. K., Hydrogen Bonding to a Dinitrogen Complex at Room Temperature: Impacts on N2 Activation. *J. Am. Chem. Soc.* **2019,** *141*, 8550-8556. https://doi.org/10.1021/jacs.9b02288

352. Herrmann, W. A.; Kneuper, H.-J., Mehrfachbindungen zwischen Hauptgruppenelementen und Übergangsmetallen: LIII.125Te- und 77Se-Kernresonanzspektren von Übergangsmetall-komplexen mit “nackten” Tellur- bzw. Selen-Brückenliganden. *J. Organomet. Chem.* **1988,** *348*, 193-197. https://doi.org/10.1016/0022-328X(88)80395-4

353. Hofmann, B. J.; Huber, S.; Reich, R. M.; Drees, M.; Kühn, F. E., Ethyltrioxorhenium – Catalytic application and decomposition pathways. *J. Organomet. Chem.* **2019,** *885*, 32-38. https://doi.org/10.1016/j.jorganchem.2019.02.004

354. Huber, S.; Cokoja, M.; Drees, M.; Mínk, J.; Kühn, F. E., Xylyltrioxorhenium – the first arylrhenium(vii) oxide applicable as an olefin epoxidation catalyst. *Catal. Sci. Technol.* **2013,** *3*, 388-393. http://dx.doi.org/10.1039/C2CY20371E

355. Santos, A. M.; Romão, C. C.; Kühn, F. E., (η2-Alkyne)methyl(dioxo)rhenium Complexes as Aldehyde-Olefination Catalysts. *J. Am. Chem. Soc.* **2003,** *125*, 2414-2415. https://doi.org/10.1021/ja021315c

356. Salignac, B.; Grundler, P. V.; Cayemittes, S.; Frey, U.; Scopelliti, R.; Merbach, A. E.; Hedinger, R.; Hegetschweiler, K.; Alberto, R.; Prinz, U.; Raabe, G.; Kölle, U.; Hall, S., Reactivity of the Organometallic fac-[(CO)3ReI(H2O)3]+ Aquaion. Kinetic and Thermodynamic Properties of H2O Substitution. *Inorg. Chem.* **2003,** *42*, 3516-3526. https://doi.org/10.1021/ic0341744

357. Roodt, A.; Leipoldt, J. G.; Helm, L.; Merbach, A. E., Carbon-13 and oxygen-17, NMR studies of the solution and equilibrium behavior of selected oxocyanorhenate(V) complexes. *Inorg. Chem.* **1992,** *31*, 2864-2868. https://doi.org/10.1021/ic00039a036

358. Mink, L. M.; Polam, J. R.; Christensen, K. A.; Bruck, M. A.; Walker, F. A., Electronic Effects in Transition Metal Porphyrins. 8. The Effect of Porphyrin Substituents, Axial Ligands, "Steric Crowding", Solvent, and Temperature on the 57Fe Chemical Shifts of a Series of Model Heme Complexes. *J. Am. Chem. Soc.* **1995,** *117*, 9329-9339. https://doi.org/10.1021/ja00141a027

359. Meier, E. J. M.; Koźmiński, W.; Linden, A.; Lustenberger, P.; von Philipsborn, W., 57Fe NMR Study of Ligand Effects in Cyclopentadienyliron Complexes. *Organometallics* **1996,** *15*, 2469-2477. https://doi.org/10.1021/om950989b

360. Oña-Burgos, P.; Casimiro, M.; Fernández, I.; Navarro, A. V.; Fernández Sánchez, J. F.; Carretero, A. S.; Gutiérrez, A. F., Octahedral iron(ii) phthalocyanine complexes: multinuclear NMR and relevance as NO2 chemical sensors. *Dalton Trans.* **2010,** *39*, 6231-6238. http://dx.doi.org/10.1039/B924429H

361. Stchedroff, M. J.; Moberg, V.; Rodriguez, E.; Aliev, A. E.; Böttcher, J.; Steed, J. W.; Nordlander, E.; Monari, M.; Deeming, A. J., Synthesis, characterisation and natural abundance 187Os NMR spectroscopy of hydride bridged triosmium clusters with chiral diphosphine ligands. *Inorg. Chim. Acta* **2006,** *359*, 926-937. https://doi.org/10.1016/j.ica.2005.06.048

362. Cabeza, J. A.; Mann, B. E.; Brevard, C.; Maitlis, P. M., Dinuclear p-cymeneosmium hydride complexes; the measurement of ^{187}Os chemical shifts using ^{1}H-{^{187}Os} two-dimensional NMR spectroscopy. *J. Chem. Soc., Chem. Commun.* **1985**, 65-67. http://dx.doi.org/10.1039/C39850000065

363. Wrackmeyer, B.; Tok, O. L.; Herberhold, M., 57Fe NMR of Ferrocenes by 1H−57Fe INEPT Techniques. *Organometallics* **2001,** *20*, 5774-5776. https://doi.org/10.1021/om010756m

364. Wrackmeyer, B.; Klimkina, E. V.; Milius, W.; Siebenbürger, M.; Tok, O. L.; Herberhold, M., Ferrocenes Bearing Sulfinylamino Groups. *Eur. .J. Inorg. Chem.* **2007,** *2007*, 103-109. https://doi.org/10.1002/ejic.200600326

365. Wrackmeyer, B.; Klimkina, E. V.; Maisel, H. E.; Tok, O. L.; Herberhold, M., 57Fe NMR spectroscopy of ferrocenes derived from aminoferrocene and 1,1′ -diaminoferrocene. *Magn. Reson. Chem.* **2008,** *46*, S30-S35. https://doi.org/10.1002/mrc.2284

366. Janiak, C.; Dorn, T.; Paulsen, H.; Wrackmeyer, B., Synthesis of Isotope Enriched (CN3H6)2[57Fe(CN)5NO] starting from 57Fe. *Z. Anorg. Allg. Chem.* **2001,** *627*, 1663-1668. https://doi.org/10.1002/1521-3749(200107)627:7<1663::AID-ZAAC1663>3.0.CO;2-#

367. Baltzer, L.; Landergren, M., Iron-57 nuclear magnetic resonance chemical shifts of hindered iron porphyrins. Ruffling as a possible mechanism for d-orbital energy level inversion. *J. Am. Chem. Soc.* **1990,** *112*, 2804-2805. https://doi.org/10.1021/ja00163a054

368. Polam, J. R.; Wright, J. L.; Christensen, K. A.; Walker, F. A.; Flint, H.; Winkler, H.; Grodzicki, M.; Trautwein, A. X., Valence Electron Cloud Asymmetry from Two Points of View: A Correlation between Mössbauer Quadrupole Splittings and 57Fe NMR Chemical Shifts of Diamagnetic Iron(II) Porphyrinates. *J. Am. Chem. Soc.* **1996,** *118*, 5272-5276. https://doi.org/10.1021/ja954096m

369. Gerothanassis, I. P.; Kalodimos, C. G.; Hawkes, G. E.; Haycock, P., The Effects of Atropisomerism and Porphyrin Deformation on ^{57}Fe Shieldings in Superstructured Hemoprotein Models. *J. Magn. Reson.* **1998,** *131*, 163-165. https://doi.org/10.1006/jmre.1997.1350

370. Kalodimos, C. G.; Gerothanassis, I. P.; Rose, E.; Hawkes, G. E.; Pierattelli, R., Iron-57 Nuclear Shieldings as a Quantitative Tool for Estimating Porphyrin Ruffling in Hexacoordinated Carbonmonoxy Heme Model Compounds in Solution. *J. Am. Chem. Soc.* **1999,** *121*, 2903-2908. https://doi.org/10.1021/ja983889q

371. Wrackmeyer, B.; Ayazi, A.; Maisel, H. E.; Herberhold, M., 57Fe-NMR spectroscopy revisited: ferrocene derivatives containing heterosubstituents. *J. Organomet. Chem.* **2001,** *630*, 263-265. https://doi.org/10.1016/S0022-328X(01)01008-7

372. Wrackmeyer, B.; Maisel, H. E.; Herberhold, M., N-Ferrocenyl Amines Bearing Boryl and Silyl Substituents at the Nitrogen Atom, Studied by 57Fe NMR Spectroscopy. *Z. Naturforsch. B* **2001,** *56*, 1373-1375. https://doi.org/10.1515/znb-2001-1221

373. Wrackmeyer, B.; Tok, O. L.; Ayazi, A.; Maisel, H. E.; Herberhold, M., 57Fe NMR spectroscopy of ferrocenes bearing π-acceptor substituents. *Magn. Reson. Chem.* **2004,** *42*, 827-830. https://doi.org/10.1002/mrc.1401

374. Wrackmeyer, B.; Tok, O. L.; Ayazi, A.; Hertel, F.; Max, H., 57Fc NMR spectroscopy of some sila- [I J fcrroccnophancs and a phospha- [I J fcrrocenophane. *Z. Naturforsch. B* **2002,** *57*, 305-308.

375. Houlton, A.; Miller, J. R.; Roberts, R. M. G.; Silver, J., Studies of the bonding in iron(II) cyclopentadienyl and arene sandwich compounds. Part 2. Correlations and interpretations of carbon-13 and iron-57 nuclear magnetic resonance and iron-57 mössbauer data. *J. Chem. Soc., Dalton Trans.* **1991**, 467-470. http://dx.doi.org/10.1039/DT9910000467

376. Mampa, R. M.; Fernandes, M. A.; Carlton, L., Iron-57 NMR and Structural Study of [Fe(η5-Cp)(SnPh3)(CO)(PR3)] (PR3 = Phosphine, Phosphite). Separation of Steric and

Electronic σ and π Effects. *Organometallics* **2014,** *33*, 3283-3299. https://doi.org/10.1021/om4011593

377. Wrackmeyer, B.; Herberhold, M., NMR parameters of the tetrahedrane [Fe2(CO)6(μ-SNH)], studied by experiment and DFT. *Struct. Chem.* **2006,** *17*, 79-83. https://doi.org/10.1007/s11224-006-9030-4

378. Wrackmeyer, B.; Seidel, G.; Köster, R., Isotope-induced chemical shifts 1Δ12/13C(29Si) and 57Fe NMR of organosubstituted 2,5-dihydro-1,2,5-azasilaboroles, a silole and their tricarbonyliron complexes†. *Magn. Reson. Chem.* **2000,** *38*, 520-524. https://doi.org/10.1002/1097-458X(200007)38:7<520::AID-MRC681>3.0.CO;2-A

379. Koźmiński, W.; von Philipsborn, W., Spin–Lattice Relaxation Times of Transition-Metal Nuclei from Inverse-Detection Experiments*. *J. Magn. Reson. A* **1995,** *116*, 262-265. https://doi.org/10.1006/jmra.1995.0018

380. Bühl, M.; Mauschick, F. T.; Terstegen, F.; Wrackmeyer, B., Remarkably Large Geometry Dependence of ^{57}Fe NMR Chemical Shifts. *Angew. Chem. Int. Ed.* **2002,** *41*, 2312-2315. https://doi.org/10.1002/1521-3773(20020703)41:13<2312::AID-ANIE2312>3.0.CO;2-P

381. Bühl, M.; Mauschick, F. T., Thermal and solvent effects on ^{57}Fe NMR chemical shifts. *Phys. Chem. Chem. Phys.* **2002,** *4*, 5508-5514. http://dx.doi.org/10.1039/B202894H

382. Bühl, M.; Malkina, O. L.; Malkin, V. G., Computations of ^{57}Fe-NMR Chemical Shifts with the SOS-DFPT Method. *Helv. Chim. Acta* **1996,** *79*, 742-754. https://doi.org/10.1002/hlca.19960790317

383. Alluisetti, G. E.; Almaraz, A. E.; Amorebieta, V. T.; Doctorovich, F.; Olabe, J. A., Metal-Catalyzed Anaerobic Disproportionation of Hydroxylamine. Role of Diazene and Nitroxyl Intermediates in the Formation of N_2, N_2O, NO^+, and NH_3. *J. Am. Chem. Soc.* **2004,** *126*, 13432-13442. https://doi.org/10.1021/ja046724i

384. Butschke, B.; Fillman, K. L.; Bendikov, T.; Shimon, L. J. W.; Diskin-Posner, Y.; Leitus, G.; Gorelsky, S. I.; Neidig, M. L.; Milstein, D., How Innocent are Potentially Redox Non-Innocent

Ligands? Electronic Structure and Metal Oxidation States in Iron-PNN Complexes as a Representative Case Study. *Inorg. Chem.* **2015,** *54*, 4909-4926. https://doi.org/10.1021/acs.inorgchem.5b00509

385. Field, L. D.; Hazari, N.; Li, H. L., Nitrogen Fixation Revisited on Iron(0) Dinitrogen Phosphine Complexes. *Inorg. Chem.* **2015,** *54*, 4768-4776. https://doi.org/10.1021/acs.inorgchem.5b00211

386. Gao, Y.; Toubaei, A.; Kong, X.; Wu, G., Acidity and Hydrogen Exchange Dynamics of Iron(II)-Bound Nitroxyl in Aqueous Solution. *Angew. Chem. Int. Ed.* **2014,** *53*, 11547-51. https://doi.org/10.1002/anie.201407018

387. Yeh, S.-W.; Tsou, C.-C.; Liaw, W.-F., The dinitrosyliron complex [Fe4(μ3-S)2(μ2-NO)2(NO)6]2− containing bridging nitroxyls: 15N (NO) NMR analysis of the bridging and terminal NO-coordinate ligands. *Dalton Trans.* **2014,** *43*, 9022-9025. http://dx.doi.org/10.1039/C4DT00450G

388. Lin, I.-J.; Chen, Y.; Fee, J. A.; Song, J.; Westler, W. M.; Markley, J. L., Rieske protein from Thermus thermophilus: 15N NMR titration study demonstrates the role of iron-ligated histidines in the pH dependence of the reduction potential. *J. Am. Chem. Soc.* **2006,** *128*, 10672-10673. https://doi.org/10.1021/ja0627388

389. Hashimoto, H.; Tobita, H.; Ogino, H., Redistribution reactions of hydrosilanes mediated by the unsymmetrical and homometallic phosphido-bridged complex (η5-C5Me5)Fe2(CO)4(μ-CO)(μ-PPh2). *J. Organomet. Chem.* **1995,** *499*, 205-211. https://doi.org/10.1016/0022-328X(95)00301-6

390. Štíbr, B.; Bakardjiev, M.; Holub, J.; Růžička, A.; Padělková, Z.; Štěpnička, P., Additive Character of Electron Donation by Methyl Substituents within a Complete Series of Polymethylated [1-(η6-MenC6H6−n)-closo-1,2,3-FeC2B9H11] Complexes. Linear Correlations of the NMR Parameters and FeII/III Redox Potentials with the Number of Arene Methyls. *Inorg. Chem.* **2011,** *50*, 3097-3102. https://doi.org/10.1021/ic2000798

391. Pennanen, T. O.; Macháček, J.; Taubert, S.; Vaara, J.; Hnyk, D., Ferrocene-like iron bis(dicarbollide), [3-FeIII-(1,2-C2B9H11)2]−. The first experimental and theoretical refinement of a paramagnetic 11B NMR spectrum. *Phys. Chem. Chem. Phys.* **2010,** *12*, 7018-7025. http://dx.doi.org/10.1039/B923891C

392. Jee, J.-E.; Wolak, M.; Balbinot, D.; Jux, N.; Zahl, A.; van Eldik, R., A Comparative Mechanistic Study of the Reversible Binding of NO to a Water-Soluble Octa-Cationic FeIII Porphyrin Complex. *Inorg. Chem.* **2006,** *45*, 1326-1337. https://doi.org/10.1021/ic051339v

393. Schneppensieper, T.; Seibig, S.; Zahl, A.; Tregloan, P.; van Eldik, R., Influence of Chelate Effects on the Water-Exchange Mechanism of Polyaminecarboxylate Complexes of Iron(III). *Inorg. Chem.* **2001,** *40*, 3670-3676. https://doi.org/10.1021/ic001304p

394. Mizuno, M.; Funahashi, S.; Nakasuka, N.; Tanaka, M., Water exchange of the (o-phenylenediamine-N,N,N',N'-tetraacetato)ferrate(III) complex in aqueous solution as studied by variable-temperature, -pressure, and -frequency oxygen-17 NMR techniques. *Inorg. Chem.* **1991,** *30*, 1550-1553. https://doi.org/10.1021/ic00007a023

395. Livramento, J. B.; Sour, A.; Borel, A.; Merbach, A. E.; Tóth, É., A starburst-shaped heterometallic compound incorporating six densely packed gd(3+) ions. *Chem. Eur. J.* **2006,** *12*, 989-1003. https://doi.org/10.1002/chem.200500969

396. Maigut, J.; Meier, R.; Zahl, A.; van Eldik, R., Effect of Chelate Dynamics on Water Exchange Reactions of Paramagnetic Aminopolycarboxylate Complexes. *Inorg. Chem.* **2008,** *47*, 5702-5719. https://doi.org/10.1021/ic702421z

397. Bernhard, P.; Helm, L.; Ludi, A.; Merbach, A. E., Direct measurement of a prominent outer-sphere electron self-exchange: kinetic parameters for the hexaaquaruthenium(II)/(III) couple determined by oxygen-17 and ruthenium-99 NMR. *J. Am. Chem. Soc.* **1985,** *107*, 312-317. https://doi.org/10.1021/ja00288a005

398. Brevard, C.; Granger, P., Ruthenium NMR spectroscopy: a promising structural and analytical tool. General trends and applicability to organometallic and inorganic chemistry. *Inorg. Chem.* **1983,** *22*, 532-535. https://doi.org/10.1021/ic00145a033

399. Fedotov, M. A., Applications of nuclear magnetic resonance to study the structure of platinum-group metal complexes in aqueous solutions. *J. Struct. Chem.* **2016,** *57*, 563-613. https://doi.org/10.1134/S0022476616030203

400. Emel'yanov, V. A.; Fedotov, M. A.; Belyaev, A. V.; Tkachev, S. V., A multinuclear magnetic resonance study of transformations of ruthenium(II) nitrosyl chloride complexes in aqueous solutions. *Russ. J. Inorg. Chem.* **2013,** *58*, 956-963. https://doi.org/10.1134/S003602361308007X

401. Orellana, G.; Kirsch-De Mesmaeker, A.; Turro, N. J., Ruthenium-99 NMR spectroscopy of ruthenium(II) polypyridyl complexes. *Inorg. Chem.* **1990,** *29*, 882-885. https://doi.org/10.1021/ic00329a063

402. Ferrari, M. B.; Fava, G. G.; Pelosi, G.; Predieri, G.; Vignali, C.; Denti, G.; Serroni, S., Crystal and molecular structure of [Ru(bpy)2(2,3-dpp)]Cl2 • 3H2O • CH3CN and 1H and 99Ru NMR spectra of [Ru(bpy)2(2,n-dpp)][PF6]2 (bpy=2,2′ -bipyridine, dpp=bis (2-pyridyl)pyrazine, n=3 or 5). *Inorg. Chim. Acta* **1998,** *275-276*, 320-326. https://doi.org/10.1016/S0020-1693(97)06068-4

403. Gaemers, S.; van Slageren, J.; O'Connor, C. M.; Vos, J. G.; Hage, R.; Elsevier, C. J., 99Ru NMR Spectroscopy of Organometallic and Coordination Complexes of Ruthenium(II). *Organometallics* **1999,** *18*, 5238-5244. https://doi.org/10.1021/om990477n

404. Braunstein, P.; Rosé, J.; Granger, P.; Richert, T., ^{59}Co and ^{99}Ru NMR investigation of heterometallic carbonyl clusters. Reactivity of $[MCo_3(CO)_{12}]^-$ (M = Fe, Ru) towards NO^+; formation of $RuCo_3(CO)_{11}(NO)$ and $FeCo_2(\mu_3\text{-}NH)(CO)_9$. *Magn. Reson. Chem.* **1991,** *29*, S31-S37. https://doi.org/10.1002/mrc.1260291309

405. Autschbach, J.; Zheng, S., Density functional computations of ^{99}Ru chemical shifts: relativistic effects, influence of the density functional, and study of solvent effects on *fac*-$[Ru(CO)_3I_3]^-$. *Magn. Reson. Chem.* **2006,** *44*, 989-1007. https://doi.org/10.1002/mrc.1885

406. Bagno, A.; Bonchio, M., DFT Calculations of ^{99}Ru Chemical Shifts with All-Electron and Effective Core Potential Basis Sets. *Eur. .J. Inorg. Chem.* **2002,** *2002*, 1475-1483. https://doi.org/10.1002/1099-0682(200206)2002:6<1475::AID-EJIC1475>3.0.CO;2-J

407. Bagno, A.; Bonchio, M., Relativistic DFT calculation of ^{99}Ru NMR parameters: chemical shifts and spin–spin coupling constants. *Magn. Reson. Chem.* **2004,** *42*, S79-S87. https://doi.org/10.1002/mrc.1412

408. Bühl, M.; Gaemers, S.; Elsevier, C. J., Density-Functional Computation of ^{99}Ru NMR Parameters. *Chem. Eur. J.* **2000,** *6*, 3272-3280. https://doi.org/10.1002/1521-3765(20000901)6:17<3272::AID-CHEM3272>3.0.CO;2-E

409. Ramalho, T. C.; Bühl, M.; Figueroa-Villar, J. D.; de Alencastro, R. B., Computational NMR Spectroscopy of Transition-Metal/Nitroimidazole Complexes: Theoretical Investigation of Potential Radiosensitizers. *Helv. Chim. Acta* **2005,** *88*, 2705-2721. https://doi.org/10.1002/hlca.200590210

410. Grundler, P. V.; Yazyev, O. V.; Aebischer, N.; Helm, L.; Laurenczy, G.; Merbach, A. E., Kinetic studies on the first dihydrogen aquacomplex, [Ru(H2)(H2O)5]2+: Formation under H2 pressure and catalytic H/D isotope exchange in water. *Inorg. Chim. Acta* **2006,** *359*, 1795-1806. https://doi.org/10.1016/j.ica.2005.06.056

411. Egloff, J.; Ranocchiari, M.; Schira, A.; Schotes, C.; Mezzetti, A., Highly Enantioselective Ruthenium/PNNP-Catalyzed Imine Aziridination: Evidence of Carbene Transfer from a Diazoester Complex. *Organometallics* **2013,** *32*, 4690-4701. https://doi.org/10.1021/om400735p

412. Muller, K.; Sun, Y.; Heimermann, A.; Menges, F.; Niedner-Schatteburg, G.; van Wüllen, C.; Thiel, W. R., Structure–Reactivity Relationships in the Hydrogenation of Carbon Dioxide with

Ruthenium Complexes Bearing Pyridinylazolato Ligands. *Chem. Eur. J.* **2013,** *19*, 7825-7834. https://doi.org/10.1002/chem.201204199

413. Wanat, A.; Schneppensieper, T.; Karocki, A.; Stochel, G.; Eldik, R. v., Thermodynamics and kinetics of RuIII(edta) as an efficient scavenger for nitric oxide in aqueous solution. *J. Chem. Soc., Dalton Trans.* **2002**, 941-950. http://dx.doi.org/10.1039/B108236C

414. Wang, F.; Chen, H.; Parkinson, J. A.; Murdoch, P. d. S.; Sadler, P. J., Reactions of a Ruthenium(II) Arene Antitumor Complex with Cysteine and Methionine. *Inorg. Chem.* **2002,** *41*, 4509-4523. https://doi.org/10.1021/ic025538f

415. Wang, F.; Bella, J.; Parkinson, J. A.; Sadler, P. J., Competitive reactions of a ruthenium arene anticancer complex with histidine, cytochrome c and an oligonucleotide. *J. Biol. Inorg. Chem.* **2005,** *10*, 147-155. https://doi.org/10.1007/s00775-004-0621-5

416. Christe, K. O.; Dixon, D. A.; Mack, H. G.; Oberhammer, H.; Pagelot, A.; Sanders, J. C. P.; Schrobilgen, G. J., Osmium tetrafluoride dioxide, *cis*-OsO_2F_4. *J. Am. Chem. Soc.* **1993,** *115*, 11279-11284. https://doi.org/10.1021/ja00077a029

417. Bell, A. G.; Koźmiński, W.; Linden, A.; von Philipsborn, W., ^{187}Os NMR Study of (η6-Arene)osmium(II) Complexes: Separation of Electronic and Steric Ligand Effects. *Organometallics* **1996,** *15*, 3124-3135. https://doi.org/10.1021/om960053i

418. Gisler, A.; Schaade, M.; Meier, E. J. M.; Linden, A.; von Philipsborn, W., 187Os, 31P and 17O NMR study of carbonylated and alkylated (p-cymene)OsI (L)PR3 complexes. *J. Organomet. Chem.* **1997,** *545-546*, 315-326. https://doi.org/10.1016/S0022-328X(97)00376-8

419. Gray, J. C.; Pagelot, A.; Collins, A.; Fabbiani, F. P. A.; Parsons, S.; Sadler, P. J., Organometallic Osmium(II) and Ruthenium(II) Biphenyl Sandwich Complexes: X-ray Crystal Structures and 187Os NMR Spectroscopic Studies in Solution. *Eur. .J. Inorg. Chem.* **2009,** *2009*, 2673-2677. https://doi.org/10.1002/ejic.200900244

420. Benn, R.; Brenneke, H.; Joussen, E.; Lehmkuhl, H.; Lopez Ortiz, F., Probing osmium-187 NMR of complexes containing ^{187}Os in natural abundance via indirect heteronuclear 2-

dimensional NMR spectroscopy. *Organometallics* **1990,** *9*, 756-761. https://doi.org/10.1021/om00117a034

421. Stchedroff, M. J.; Aime, S.; Gobetto, R.; Salassa, L.; Nordlander, E., 187Os subspectra in 1H and 31P{1H} spectra of triosmium carbonyl clusters. *Magn. Reson. Chem.* **2002,** *40*, 107-113. https://doi.org/10.1002/mrc.962

422. Beatty, S. T.; Bergman, B.; Rosenberg, E.; Dastru', W.; Gobetto, R.; Milone, L.; Viale, A., Conformational constraints and σ–π-vinyl interchange in μ_3-η^3-5,6-dihydroquinoline triosmium complexes. *J. Organomet. Chem.* **2000,** *593-594*, 226-231. https://doi.org/10.1016/S0022-328X(99)00661-0

423. Bergman, B.; Holmquist, R.; Smith, R.; Rosenberg, E.; Ciurash, J.; Hardcastle, K.; Visi, M., Functionalizing Heterocycles by Electron-Deficient Bonding to a Triosmium Cluster. *J. Am. Chem. Soc.* **1998,** *120*, 12818-12828. https://doi.org/10.1021/ja981445e

424. Krykunov, M.; Ziegler, T.; van Lenthe, E., Implementation of a Hybrid DFT Method for Calculating NMR Shieldings Using Slater-Type Orbitals with Spin−Orbital Coupling Included. Applications to 187Os, 195Pt, and 13C in Heavy-Metal Complexes. *J. Phys. Chem. A* **2009,** *113*, 11495-11500. https://doi.org/10.1021/jp901991s

425. Dehestani, A.; Kaminsky, W.; Mayer, J. M., Tuning the Properties of the Osmium Nitrido Group in TpOs(N)X2 by Changing the Ancillary Ligand. *Inorg. Chem.* **2003,** *42*, 605-611. https://doi.org/10.1021/ic0260264

426. Frey, U.; Li, Z.-W.; Matras, A., Mechanism for Solvent Exchange on trans-[Os(en)2(η2-H2)S]2+. *Inorg. Chem.* **1996,** *35*, 981-984. https://doi.org/10.1021/ic9510775

427. Ernsting, J. M.; Gaemers, S.; Elsevier, C. J., ^{103}Rh NMR spectroscopy and its application to rhodium chemistry. *Magn. Reson. Chem.* **2004,** *42*, 721-736. https://doi.org/10.1002/mrc.1439

428. Carlton, L., Rhodium-103 NMR. *Annu. Rep. NMR Spectrosc.* **2008,** *63*, 49-178. https://doi.org/10.1016/S0066-4103(07)63003-8

429. Yamasaki, A., Cobalt-59 Nuclear Magnetic Resonance Spectroscopy in Coordination Chemistry. *J. Coord. Chem.* **1991,** *24*, 211-260. https://doi.org/10.1080/00958979109407886

430. Taura, T., Solvent Influence on UV, 59Co, and 13C NMR of [Co(CN)6]3− and Its Solvation Site. *Bull. Chem. Soc. Jpn.* **1990,** *63*, 1105-1110. https://doi.org/10.1246/bcsj.63.1105

431. Ho, K. K. W.; Choy, W. Y.; Yuxin, C.; Auyeung, S. C. F., Solvent-Dependent 59Co NMR-Study of [Co(en)3]Cl3 and cis,trans-[Co-(en)2(N3)2]NO3. *J. Magn. Reson. A* **1994,** *108*, 196-200. https://doi.org/10.1006/jmra.1994.1110

432. Taura, T., Spectrochemical Series for the Outersphere Coordination of Carboxylatocobaltate(III) Complexes with Solvent Molecules. *Bull. Chem. Soc. Jpn.* **1991,** *64*, 2362-2371. https://doi.org/10.1246/bcsj.64.2362

433. Fujihara, T.; Kaizaki, S., Correlation of 13C, 15N and 59Co nuclear magnetic resonance chemical shifts with ligand-field parameters for pentacyanocobaltate(III) complexes. *J. Chem. Soc., Dalton Trans.* **1993**, 1275-1279. http://dx.doi.org/10.1039/DT9930001275

434. Au-Yeung, S. C. F.; Kwong, K. W.; Buist, R. J., Multinuclear NMR study of the crystal field strength of the nitro ligand and the empirical estimation of the cobalt-59 NMR chemical shifts of cobalt-nitro complexes. *J. Am. Chem. Soc.* **1990,** *112*, 7482-7488. https://doi.org/10.1021/ja00177a005

435. Barnard, I.; Koch, K. R., ^{59}Co NMR, a facile tool to demonstrate EEE, EEZ, EZZ and ZZZ configurational isomerism in *fac*-[Co(L-κ S,O)$_3$] complexes derived from asymmetrically substituted N,N-dialkyl-N′-aroylthioureas. *Inorg. Chim. Acta* **2019,** *495*, 119019. https://doi.org/10.1016/j.ica.2019.119019

436. Lawrence, M. A. W.; Celestine, M. J.; Artis, E. T.; Joseph, L. S.; Esquivel, D. L.; Ledbetter, A. J.; Cropek, D. M.; Jarrett, W. L.; Bayse, C. A.; Brewer, M. I.; Holder, A. A., Computational, electrochemical, and spectroscopic studies of two mononuclear cobaloximes: the influence of an axial pyridine and solvent on the redox behaviour and evidence for pyridine

coordination to cobalt(i) and cobalt(ii) metal centres. *Dalton Trans.* **2016,** *45*, 10326-10342. http://dx.doi.org/10.1039/C6DT01583B

437. Kotovaya, A. S.; Shova, S. G.; Simonov, Y. A.; Roshu, T.; Sandu, I.; Gulya, A. P., New crystal forms of tris(2-aminoethanolato-O,N)cobalt(III): Structures and properties. *Rus. J. Coord. Chem.* **2006,** *32*, 841-847. https://doi.org/10.1134/S1070328406110121

438. Kapanadze, T. S. H.; Kokunov, Y. V.; Buslaev, Y. A., A 59Co NMR study of stereoisomerism of cobalt(III) complexes with polydentate aminochelate ligands. *Polyhedron* **1990,** *9*, 2803-2808. https://doi.org/10.1016/S0277-5387(00)84183-2

439. Blower, P. J.; Levason, W.; Luthra, S. K.; McRobbie, G.; Monzittu, F. M.; Mules, T. O.; Reid, G.; Subhan, M. N., Exploring transition metal fluoride chelates – synthesis, properties and prospects towards potential PET probes. *Dalton Trans.* **2019,** *48*, 6767-6776. http://dx.doi.org/10.1039/C8DT03696A

440. Sugiarto; Tagami, T.; Kawamoto, K.; Hayashi, Y., Synthesis of cationic molybdenum–cobalt heterometallic clusters protected against hydrolysis by macrocyclic triazacyclononane complexes. *Dalton Trans.* **2018,** *47*, 9657-9664. http://dx.doi.org/10.1039/C8DT01226A

441. Cheyne, S. E.; McClintock, L. F.; Blackman, A. G., Stabilization of Coordinated Carbonate in Aqueous Acidic Solution: Steric Inhibition of Protonation in Co(III) Complexes Containing Chelated Carbonate. *Inorg. Chem.* **2006,** *45*, 2610-2618. https://doi.org/10.1021/ic0521325

442. McClintock, L. F.; Bagaria, P.; Kjaergaard, H. G.; Blackman, A. G., Co(III) complexes of the type [(L)Co(O2CO)]+ (L=tripodal tetraamine ligand): Synthesis, structure, DFT calculations and 59Co NMR. *Polyhedron* **2009,** *28*, 1459-1468. https://doi.org/10.1016/j.poly.2009.03.010

443. Yashiro, M.; Yoshikawa, S.; Yano, S., Regulation of the ligand field strength of a cobalt(III) complex by methyl substitutions on a tetraamine ligand: an important factor for the dissociation of a generally inert chelated amino acidato ligand from a cobalt(III) complex. *Inorg. Chem.* **1993,** *32*, 4166-4167. https://doi.org/10.1021/ic00071a036

444. Voloshin, Y. Z.; Belsky, V. K.; Trachevskii, V. V., Macrobicyclic d-metal tris-dioximates obtained by cross-linking with p-block elements—VII. Clathrochelate tris-dioximates of cobalt(III) formed by tin tetrachloride. *Polyhedron* **1992,** *11*, 1939-1948. https://doi.org/10.1016/S0277-5387(00)83743-2

445. Yano, S.; Kato, M.; Tsukahara, K.; Sato, M.; Shibahara, T.; Lee, K.; Sugihara, Y.; Iida, M.; Goto, K., Chemical Modification of Metal Complexes. An Efficient Procedure for O-Acylation of an Anionic Metal Complex Having a Noncoordinated Hydroxyl Group. *Inorg. Chem.* **1994,** *33*, 5030-5035. ^{59}Co shift of δ 2203 vs $Co(NH_3)_6^{3+}$ reported in this paper was converted to δ 10 409 vs $Co(CN)_6^{3-}$ by authors of the current article based on the data in A. Yamasaki, *J. Coord. Chem.* **1991**, *24*, 211. https://doi.org/10.1021/ic00100a030

446. Levason, W.; Matthews, M. L.; Reid, G.; Webster, M., Synthesis and characterisation of transition metal halide complexes of the xylyl-distibine, 1,2-bis(dimethylstibanylmethyl)benzene. *Dalton Trans.* **2004**, 554-561. http://dx.doi.org/10.1039/B400214H

447. Suzuki, T.; Tsukuda, T.; Kiki, M.; Kaizaki, S.; Isobe, K.; Takagi, H. D.; Kashiwabara, K., Preparation, crystal structures and spectroscopic properties of novel [MIIICl3−n(P)3+n]n+ (M=Co, Rh; n=0, 1, 2 or 3) series of complexes containing tripodal tridentate phosphine, 1,1,1-tris(dimethylphosphinomethyl)ethane. *Inorg. Chim. Acta* **2005,** *358*, 2501-2512. https://doi.org/10.1016/j.ica.2005.02.008

448. Grant, G. J.; Shoup, S. S.; Hadden, C. E.; VanDerveer, D. G., Cobalt(III) complexes of crown thioethers: the crystal structure of (1,4,7,11,14,17-hexathiacycloeicosane) cobalt (III) tetrafluoroborate dihydrate. *Inorg. Chim. Acta* **1998,** *274*, 192-200. https://doi.org/10.1016/S0020-1693(97)06054-4

449. Dietzsch, W.; Duffy, N. V.; Katsoulos, G. A.; Olk, B., Multinuclear (1H, 13C, 59Co, 77Se) NMR studies of thioseleno- and diselenocarbamato complexes of cobalt(III) and indium(III) in CDCl3 solution. *Inorg. Chim. Acta* **1991,** *184*, 89-97. https://doi.org/10.1016/S0020-1693(00)83049-2

450. Brown, J. L.; Kemmitt, T.; Levason, W., Cobalt(III) complexes of neutral selenium and tellurium donor ligands: synthesis and nuclear magnetic resonance studies. *J. Chem. Soc., Dalton Trans.* **1990**, 1513-1515. http://dx.doi.org/10.1039/DT9900001513

451. Levason, W.; Quirk, J. J.; Reid, G., Synthesis and characterisation of selenoether macrocyclic complexes of CoIII, RhIII and IrIII: crystal structures of trans-[CoBr2([16]aneSe4)]BPh4 and trans-[IrBr2([16]aneSe4)]BPh4([16]aneSe4= 1,5,9,13-tetraselenacyclohexadecane). *J. Chem. Soc., Dalton Trans.* **1996**, 3713-3719. http://dx.doi.org/10.1039/DT9960003713

452. Lawrance, G. A.; Lay, P. A.; Sargeson, A. M., Organic substituent effects in macrobicyclic (hexaamine)cobalt(III/II) complexes: a new method of obtaining polar substituent constants. *Inorg. Chem.* **1990,** *29*, 4808-4816. https://doi.org/10.1021/ic00348a042

453. Kanakubo, M.; Ikeuchi, H.; Sato, G. P., Concentration Dependence of Cobalt-59 Longitudinal Relaxation Times of Tris(acetylacetonato)cobalt(III) in Acetonitrile. *J. Magn. Reson. A* **1995,** *112*, 13-16. https://doi.org/10.1006/jmra.1995.1003

454. Kirby, C. W.; Puranda, C. M.; Power, W. P., Cobalt-59 Nuclear Magnetic Relaxation Studies of Aqueous Octahedral Cobalt(III) Complexes. *J. Phys. Chem.* **1996,** *100*, 14618-14624. https://doi.org/10.1021/jp9614254

455. Iida, M.; Mizuno, Y.; Koine, N., 59Co NMR Spectroscopic Chiral Discrimination of [Co(en)3]3+ Enantiomers in Ionic Interacting Systems. *Bull. Chem. Soc. Jpn.* **1995,** *68*, 1337-1344. https://doi.org/10.1246/bcsj.68.1337

456. Iida, M.; Mizuno, Y.; Koine, N., Chiral Discrimination in the Interactions between [Co(en)3]3+ and Cholesteric Liquid Crystals by 59Co NMR Spectroscopy. *Chem. Lett.* **1994,** *23*, 481-484. https://doi.org/10.1246/cl.1994.481

457. Iida, M.; Nakamori, T.; Mizuno, Y.; Masuda, Y., Appreciable Effects of Ion Pairings on the 59Co Electric Field Gradient in the NMR Relaxation of [Co(chxn)3]3+. *J. Phys. Chem.* **1995,** *99*, 4347-4352. https://doi.org/10.1021/j100012a068

458. Iida, M.; Miyagawa, Y.; Kohri, S., Interactions of Some Cationic Cobalt(III) Complexes with Anions Studied by the 59Co NMR Chemical Shifts. *Bull. Chem. Soc. Jpn.* **1993,** *66*, 2398-2401. https://doi.org/10.1246/bcsj.66.2398

459. Sotomayor, J.; Santos, H.; Pina, F., Application of 59Co NMR to the investigation of interactions between cobalt sepulchrate and various counterions. *Can. J. Chem.* **1991,** *69*, 567-569. https://doi.org/10.1139/v91-085

460. Iida, M.; Miyagawa, Y.; Kohri, S.; Ikemoto, Y., A 59Co NMR Study of the Interactions of Some Cobalt(III) Complexes in Nematic Lyomesophases. *Bull. Chem. Soc. Jpn.* **1993,** *66*, 2840-2846. https://doi.org/10.1246/bcsj.66.2840

461. Iida, M.; Mizuno, Y.; Miyagawa, Y., Estimation of the Ratio of Hidden Multivalent Ions in Nematic Lyomesophases by Using Heteronuclear NMR. *Bull. Chem. Soc. Jpn.* **1994,** *67*, 1531-1537. https://doi.org/10.1246/bcsj.67.1531

462. Iida, M.; Tracey, A. S., Cobalt-59 NMR investigation of hexacyanocobaltate(3-) and hexaamminecobalt(3+) interactions in nematic liquid crystalline surfactant solutions. *J. Phys. Chem.* **1991,** *95*, 7891-7896. https://doi.org/10.1021/j100173a062

463. Pellizer, G.; Asaro, F.; Pergolese, B., NMR investigations of Co(III) coordination compounds oriented in a dilute lyotropic liquid crystal. *Magn. Reson. Chem.* **2004,** *42*, 756-759. https://doi.org/10.1002/mrc.1420

464. Bang, H.; Edwards, J. O.; Kim, J.; Lawler, R. G.; Reynolds, K.; Ryan, W. J.; Sweigart, D. A., Cobalt-59 NMR of six-coordinate cobalt(III) tetraphenylporphyrin complexes. 4. The effect of phenyl ortho substituents on chemical shift, line width, and structure. *J. Am. Chem. Soc.* **1992,** *114*, 2843-2852. https://doi.org/10.1021/ja00034a014

465. Munro, O. Q.; Shabalala, S. C.; Brown, N. J., Structural, Computational, and ^{59}Co NMR Studies of Primary and Secondary Amine Complexes of Co(III) Porphyrins. *Inorg. Chem.* **2001,** *40*, 3303-3317. https://doi.org/10.1021/ic000976c

466. Kanakubo, M.; Uda, T.; Ikeuchi, H.; Satô, G. P., Solvent and Temperature Dependence of 59Co NMR Chemical Shifts of Tris(acetylacetonato)cobalt(III) and Tris(dipivaloylmethanato)cobalt(III). *J. Solution Chem.* **1998,** *27*, 645-653. https://doi.org/10.1023/A:1022645924321

467. Ozvat, Tyler M.; Peña, M. E.; Zadrozny, J. M., Influence of ligand encapsulation on cobalt-59 chemical-shift thermometry. *Chem. Sci.* **2019,** *10*, 6727-6734. http://dx.doi.org/10.1039/C9SC01689A

468. Ozvat, T. M.; Johnson, S. H.; Rappé, A. K.; Zadrozny, J. M., Ligand Control of 59Co Nuclear Spin Relaxation Thermometry. *Magnetochemistry* **2020,** *6*, 58. https://www.mdpi.com/2312-7481/6/4/58

469. Celestine, M. J.; Joseph, L. S.; Holder, A. A., Kinetics and mechanism of the oxidation of a cobaloxime by sodium hypochlorite in aqueous solution: Is it an outer-sphere mechanism? *Inorg. Chim. Acta* **2017,** *454*, 254-265. https://doi.org/10.1016/j.ica.2016.07.013

470. Tavagnacco, C.; Balducci, G.; Costa, G.; Täschler, K.; von Philipsborn, W., Electronic and Steric Influence of Axial and Equatorial Ligands in Vitamin B12 Model Complexes Derived from Cobaloxime: Electrochemical and 59Co-NMR Studies. *Helv. Chim. Acta* **1990,** *73*, 1469-1480. https://doi.org/10.1002/hlca.19900730527

471. Cropek, D. M.; Metz, A.; Müller, A. M.; Gray, H. B.; Horne, T.; Horton, D. C.; Poluektov, O.; Tiede, D. M.; Weber, R. T.; Jarrett, W. L.; Phillips, J. D.; Holder, A. A., A novel ruthenium(ii)–cobaloxime supramolecular complex for photocatalytic H2 evolution: synthesis, characterisation and mechanistic studies. *Dalton Trans.* **2012,** *41*, 13060-13073. http://dx.doi.org/10.1039/C2DT30309D

472. Bakac, A.; Brynildson, M. E.; Espenson, J. H., Characterization of the structure, properties, and reactivity of a cobalt(II) macrocyclic complex. *Inorg. Chem.* **1986,** *25*, 4108-4114. https://doi.org/10.1021/ic00243a012

473. Kofod, P.; Harris, P.; Larsen, S., NMR Spectroscopic Characterization of Methylcobalt(III) Compounds with Classical Ligands. Crystal Structures of [Co(NH3)5(CH3)]S2O6, trans-[Co(en)2(NH3)(CH3)]S2O6 (en = 1,2-Ethanediamine), and [Co(NH3)6]-mer,trans-[Co(NO2)3(NH3)2(CH3)]2-trans- [Co(NO2)4(NH3)2]. *Inorg. Chem.* **1997,** *36*, 2258-2266. https://doi.org/10.1021/ic961264i

474. Grohmann, A.; Heinemann, F. W.; Kofod, P., The methylcobalt(III) complex of a tetrapodal pentadentate amine ligand, 2,6-bis(1′,3′-diamino-2′-methyl-prop-2′-yl)pyridine. *Inorg. Chim. Acta* **1999,** *286*, 98-102. https://doi.org/10.1016/S0020-1693(98)00367-3

475. Beers, O. C. P.; Elsevier, C. J.; Ernsting, J. M.; De Ridder, D. J. A.; Stam, C. H., Reactions of monoazadienes with metal carbonyl complexes. 14. Pseudo-allyl complexes from monoazadienes and cobalt carbonyl [$Co_2(CO)_8$] by activation of dihydrogen under mild conditions. *Organometallics* **1992,** *11*, 3886-3893. https://doi.org/10.1021/om00059a063

476. Bouherour, S.; Braunstein, P.; Rosé, J.; Toupet, L., Metallosite Selectivity Studies in Reactions of Tetrahedral MCo_3 Carbonyl Clusters (M = Fe, Ru) with Cyclohexylphosphine. Skeletal Rearrangements Leading to Tri- and Pentanuclear Phosphinidene Clusters and Crystal Structures of $RuCo_4(\mu_4\text{-PCy})(\mu\text{-CO})_2(CO)_{11}$ and $RuCo_2(\mu_3\text{-PCy})(CO)_9$. *Organometallics* **1999,** *18*, 4908-4915. https://doi.org/10.1021/om9902840

477. Braunstein, P.; Jiao, F. Y.; Rosé, J.; Granger, P.; Balegroune, F.; Bars, O.; Grandjean, D., Structural and cobalt-59 nuclear magnetic resonance study of heterosite reactivities of alkynes in Ru–Co carbonyl–nitrosyl clusters. *J. Chem. Soc., Dalton Trans.* **1992**, 2543-2550. http://dx.doi.org/10.1039/DT9920002543

478. Braunstein, P.; Mourey, L.; Rose, J.; Granger, P.; Richert, T.; Balegroune, F.; Grandjean, D., Selectivity in substitution chemistry of mixed-metal, tetrahedral MCo_3 (M = iron, ruthenium) carbonyl clusters: cobalt-59 NMR study and crystal structure of $RuCo_3(\mu_3\text{-H})(\mu\text{-CO})_3(CO)_8(NMe_3)$. *Organometallics* **1992,** *11*, 2628-2634. https://doi.org/10.1021/om00043a054

479. Braunstein, P.; Rose, J.; Toussaint, D.; Jaaskelainen, S.; Ahlgren, M.; Pakkanen, T. A.; Pursiainen, J.; Toupet, L.; Grandjean, D., Site-Selective Substitution Reactions and Isomerizations in Tetrahedral MCo_3 Carbonyl Clusters (M = Fe, Ru) with N, P, S, and Te Donor Ligands. Crystal Structures of $HRuCo_3(CO)_{10}(PMe_2Ph)_2$ and $HRuCo_3(CO)_9(PMe_2Ph)_3$. *Organometallics* **1994,** *13*, 2472-2479. https://doi.org/10.1021/om00018a046

480. Chen, M. J.; Klingler, R. J.; Rathke, J. W.; Kramarz, K. W., In Situ High-Pressure NMR Studies of $Co_2(CO)_6[P(p\text{-}CF_3C_6H_4)_3]_2$ in Supercritical Carbon Dioxide: Ligand Substitution, Hydrogenation, and Hydroformylation Reactions. *Organometallics* **2004,** *23*, 2701-2707. https://doi.org/10.1021/om030600h

481. Kempgens, P.; Elbayed, K.; Raya, J.; Granger, P.; Rosé, J.; Braunstein, P., Investigation of Tetrahedral Mixed-Metal Carbonyl Clusters by Two-Dimensional 59Co COSY and DQFCOSY NMR Experiments. *Inorg. Chem.* **2006,** *45*, 3378-3383. https://doi.org/10.1021/ic051544a

482. Kempgens, P.; Rosé, J., Determination of 1J(59Co–59Co) scalar coupling constants in the tetrahedral mixed-metal cluster HFeCo3(CO)10(PCyH2)(PPh2[CH2C(O)Ph]) using COSY-type NMR experiments. *J. Magn. Reson.* **2011,** *209*, 88-93. https://doi.org/10.1016/j.jmr.2010.12.007

483. Kempgens, P.; Raya, J.; Elbayed, K.; Granger, P.; Rosé, J.; Braunstein, P., Theoretical Study of Two-Dimensional COSY Experiments for S = 7/2 Spins: Application to 59Co in the Tetrahedral Cluster HFeCo3(CO)11PPh2H. *J. Magn. Reson.* **2000,** *142*, 64-73. https://doi.org/10.1006/jmre.1999.1903

484. Klingler, R. J.; Rathke, J. W., High-Pressure NMR Investigation of Hydrogen Atom Transfer and Related Dynamic Processes in Oxo Catalysis. *J. Am. Chem. Soc.* **1994,** *116*, 4772-4785. https://doi.org/10.1021/ja00090a025

485. Richert, T.; Elbayed, K.; Raya, J.; Granger, P.; Braunstein, P.; Rosé, J., 59Co NMR in Tetrahedral Clusters. *Magn. Reson. Chem.* **1996,** *34*, 689-696. https://doi.org/10.1002/(SICI)1097-458X(199609)34:9<689::AID-OMR955>3.0.CO;2-U

486. Song, L.-C.; Luo, C.-C.; Hu, Q.-M.; Chen, J.; Wang, H.-G., Unexpected Metallosite-Selective CO Substitution of Heteronuclear Tetrahedral (μ3-S)FeCoM (M = Mo, W) Carbonyl Clusters with Cyclohexyl Isocyanide: 59Co NMR and 57Fe Mössbauer Spectra of (μ3-S)FeCoMo(CO)8-n(η5-C5H4COMe)(C6H11NC)n (n = 1−3) and Crystal Structures of (μ3-S)FeCoM(CO)8-n(η5-C5H4R)(C6H11NC)n (M = Mo, W; R = MeCO, MeO2C; n = 1, 2). *Organometallics* **2001,** *20*, 4510-4516. https://doi.org/10.1021/om0104262

487. Braunstein, P.; Rose, J.; Granger, P.; Raya, J.; Bouaoud, S. E.; Grandjean, D., Cobalt-59 NMR study of cluster reactions: solvent and ligand effects in mixed-metal, tetrahedral MCo_3 (M = iron, ruthenium) carbonyl clusters. Crystal structure of $FeCo_3(\mu_3\text{-}H)(\mu\text{-}CO)_3(CO)_8(PPh_2H)$. *Organometallics* **1991,** *10*, 3686-3693. https://doi.org/10.1021/om00056a046

488. Kofod, P.; Harris, P.; Larsen, S., Migratory Insertion of Hydrogen Isocyanide in the Pentacyano(methyl)cobaltate(III) Anion. *Inorg. Chem.* **2003,** *42*, 244-249. https://doi.org/10.1021/ic020353u

489. Plečnik, C. E.; Liu, S.; Chen, X.; Meyers, E. A.; Shore, S. G., Lanthanide−Transition-Metal Carbonyl Complexes: New [Co4(CO)11]2- Clusters and Lanthanide(II) Isocarbonyl Polymeric Arrays. *J. Am. Chem. Soc.* **2004,** *126*, 204-213. https://doi.org/10.1021/ja0304852

490. Rathke, J. W.; Klingler, R. J.; Krause, T. R., Propylene hydroformylation in supercritical carbon dioxide. *Organometallics* **1991,** *10*, 1350-1355. https://doi.org/10.1021/om00051a027

491. Bühl, M.; Grigoleit, S.; Kabrede, H.; Mauschick, F. T., Simulation of 59Co NMR Chemical Shifts in Aqueous Solution. *Chem. Eur. J.* **2006,** *12*, 477-488. https://doi.org/10.1002/chem.200500285

492. Godbout, N.; Oldfield, E., Density Functional Study of Cobalt-59 Nuclear Magnetic Resonance Chemical Shifts and Shielding Tensor Elements in Co(III) Complexes. *J. Am. Chem. Soc.* **1997,** *119*, 8065-8069. https://doi.org/10.1021/ja970981o

493. Grigoleit, S.; Bühl, M., Computational 59Co NMR Spectroscopy: Beyond Static Molecules. *J. Chem. Theory Comput.* **2005,** *1*, 181-193. https://doi.org/10.1021/ct049920o

494. Chan, J. C. C.; Au-Yeung, S. C. F., Density Functional Study of ^{59}Co Chemical Shielding Tensors Using Gauge-Including Atomic Orbitals. *J. Phys. Chem. A* **1997,** *101*, 3637-3640. https://doi.org/10.1021/jp962200w

495. Chan, J. C. C.; Wilson, P. J.; Au-Yeung, S. C. F.; Webb, G. A., Density Functional Study of the Electronic Structures of $[Co(NH_3)_5X]^{(3+n)+}$ Complexes. Insight into the Role of the 3d and 4s Orbitals in Metal−Ligand Interactions. *J. Phys. Chem. A* **1997,** *101*, 4196-4201. https://doi.org/10.1021/jp962201o

496. Juranić, N.; Macura, S., Nitrogen-15 NMR coordination shifts of β-alanine and glycine in cobalt(III) complexes. *Inorg. Chim. Acta* **1994,** *217*, 213-215. https://doi.org/10.1016/0020-1693(93)03768-6

497. Brown, K. L.; Gupta, B. D., Heteronuclear NMR studies of Cobalamins. 10. Nitrogen-15 NMR studies of [15N]cyanocobalt corrins. *Inorg. Chem.* **1990,** *29*, 3854-3860. https://doi.org/10.1021/ic00344a040

498. Brown, K. L.; Evans, D. R., Heteronuclear NMR studies of cobalt corrinoids. 14. Amide proton and nitrogen-15 NMR studies of base-on cobalamins. *Inorg. Chem.* **1993,** *32*, 2544-2548. https://doi.org/10.1021/ic00063a055

499. Brown, K. L.; Evans, D. R.; Zou, X.; Wu, G. Z., Heteronuclear NMR studies of cobalt corrinoids. 16. Indirect detection of the nitrogen-15 NMR resonances of the axial 5,6-dimethylbenzimidazole nucleotide and of corrin ring N22 and N23 via the heteronuclear multiple-quantum coherence (HMQC) experiment. *Inorg. Chem.* **1993,** *32*, 4487-4488. https://doi.org/10.1021/ic00073a003

500. Bartova, S.; Pechlaner, M.; Donghi, D.; Sigel, R. K., Studying metal ion binding properties of a three-way junction RNA by heteronuclear NMR. *J. Biol. Inorg. Chem.* **2016,** *21*, 319-328. http://doi.org/10.1007/s00775-016-1341-3

501. Kofod, P., 14N NMR of amminecobalt(III) compounds. *Magn. Reson. Chem.* **2003,** *41*, 531-534. https://doi.org/10.1002/mrc.1210

502. Jackson, W. G.; Cortez, S., π-Bonded Intermediates in Linkage Isomerization Reactions of a Tetrazole Coordinated to Pentaamminecobalt(III): An 15N NMR Study. *Inorg. Chem.* **1994,** *33*, 1921-1927. https://doi.org/10.1021/ic00087a031

503. Brasch, N. E.; Buckingham, D. A.; Clark, C. R.; Rogers, A. J., ^{17}O NMR Study of Solvent Exchange in Some Aqueous $[Co(tren)(X)(OH_2/OH)]^{n+}$, $[Co(cyclen)(X)(OH_2/OH)]^{n+}$, and $[Co(N\text{-}Mecyclen)(X)(OH_2/OH)]^{n+}$ Systems (X = NH_3, OH_2/OH; n = 3, 2, 1). *Inorg. Chem.* **1998,** *37*, 4865-4871. https://doi.org/10.1021/ic980221u

504. Vasilchenko, D.; Vorob'eva, S.; Tkachev, S.; Baidina, I.; Belyaev, A.; Korenev, S.; Solovyov, L.; Vasiliev, A., Rhodium(III) Speciation in Concentrated Nitric Acid Solutions. *Eur. .J. Inorg. Chem.* **2016,** *2016*, 3822-3828. https://doi.org/10.1002/ejic.201600523

505. Belyaev, A. V.; Fedotov, M. A.; Vorob'eva, S. N., Formation of mononuclear rhodium(III) sulfates: ^{103}Rh and ^{17}O NMR study. *Rus. J. Coord. Chem.* **2009,** *35*, 577-581. https://doi.org/10.1134/S1070328409080041

506. Belyaev, A. V.; Fedotov, M. A.; Vorob'eva, S. N., ^{103}Rh and ^{17}O NMR study of oligomer rhodium(III) sulfates in aqueous solutions. *Rus. J. Coord. Chem.* **2009,** *35*, 824. https://doi.org/10.1134/S1070328409110062

507. Belyaev, A. V.; Vorob'eva, S. N.; Fedotov, M. A., ^{103}Rh, ^{17}O, and ^{31}P NMR study of Rh(III) complex formation in acidic sulfate-phosphate media. *Rus. J. Coord. Chem.* **2012,** *57*, 231-236. https://doi.org/10.1134/S0036023612020040

508. Belyaev, A. V., State of Rh(III) in Hydrofluoric Acid Solutions. *Rus. J. Coord. Chem.* **2018,** *63*, 162-168. https://doi.org/10.1134/S003602361802002X

509. Munro, O. Q.; Camp, G. L.; Carlton, L., Structural, ^{103}Rh NMR and DFT Studies of a Bis(phosphane)RhIII–Porphyrin Derivative. *Eur. .J. Inorg. Chem.* **2009,** *2009*, 2512-2523. https://doi.org/10.1002/ejic.200800837

510. Fischer, C.; Thede, R.; Drexler, H.-J.; König, A.; Baumann, W.; Heller, D., Investigations into the Formation and Stability of Cationic Rhodium Diphosphane η6-Arene Complexes. *Chem. Eur. J.* **2012,** *18*, 11920-11928. https://doi.org/10.1002/chem.201201587

511. Stanek, K.; Czarniecki, B.; Aardoom, R.; Rüegger, H.; Togni, A., Remote C−F−Metal Interactions in Late-Transition-Metal Complexes. *Organometallics* **2010,** *29*, 2540-2546. https://doi.org/10.1021/om100261e

512. Preetz, A.; Baumann, W.; Fischer, C.; Drexler, H.-J.; Schmidt, T.; Thede, R.; Heller, D., Asymmetric Hydrogenation. Dimerization of Solvate Complexes: Synthesis and Characterization of Dimeric [Rh(DIPAMP)]22+, a Valuable Catalyst Precursor. *Organometallics* **2009,** *28*, 3673-3677. https://doi.org/10.1021/om801199q

513. References for the NMR shifts are not provided in the paper.

514. Twigge, L.; Swarts, J. C.; Conradie, J., $_{103}$Rh NMR shifts of Rh^{I}-β-diketonato and Rh^{I}-β-aminoketonato complexes influenced by different substituents. *Polyhedron* **2019,** *169*, 14-23. https://doi.org/10.1016/j.poly.2019.04.052

515. Onishi, N.; Shiotsuki, M.; Masuda, T.; Sano, N.; Sanda, F., Polymerization of Phenylacetylenes Using Rhodium Catalysts Coordinated by Norbornadiene Linked to a Phosphino or Amino Group. *Organometallics* **2013,** *32*, 846-853. https://doi.org/10.1021/om301147n

516. Zurawinski, R.; Lepetit, C.; Canac, Y.; Mikolajczyk, M.; Chauvin, R., From Neutral to Anionic η1-Carbon Ligands: Experimental Synthesis and Theoretical Analysis of a Rhodium−Yldiide Complex. *Inorg. Chem.* **2009,** *48*, 2147-2155. https://doi.org/10.1021/ic802104f

517. Canac, Y.; Lepetit, C.; Abdalilah, M.; Duhayon, C.; Chauvin, R., Diaminocarbene and Phosphonium Ylide Ligands: A Systematic Comparison of their Donor Character. *J. Am. Chem. Soc.* **2008,** *130*, 8406-8413. https://doi.org/10.1021/ja801159v

518. Patureau, F. W.; Groß, J.; Ernsting, J. M.; van Wüllen, C.; Reek, J. N. H., P-N Bridged Dinuclear Rh-METAMORPhos Complexes: NMR and Computational Studies. *Eur. .J. Inorg. Chem.* **2018,** *2018*, 3761-3769. https://doi.org/10.1002/ejic.201800397

519. Preetz, A.; Baumann, W.; Drexler, H.-J.; Fischer, C.; Sun, J.; Spannenberg, A.; Zimmer, O.; Hell, W.; Heller, D., Trinuclear Rhodium Complexes and Their Relevance for Asymmetric Hydrogenation. *Chem. Asian J.* **2008,** *3*, 1979-1982. https://doi.org/10.1002/asia.200800184

520. Adams, C.; Morales-Verdejo, C.; Morales, V.; MacLeod-Carey, D.; Manríquez, J. M.; Chávez, I.; Muñoz-Castro, A.; Delpech, F.; Castel, A.; Gornitzka, H.; Rivière-Baudet, M.; Rivière, P.; Molins, E., Heterobinuclear s-Indacene Rhodium Complexes: Synthesis and Characterization. *Eur. .J. Inorg. Chem.* **2009,** *2009*, 784-791. https://doi.org/10.1002/ejic.200800920

521. Blacker, A. J.; Duckett, S. B.; Grace, J.; Perutz, R. N.; Whitwood, A. C., Reactivity, Structures, and NMR Spectroscopy of Half-Sandwich Pentamethylcyclopentadienyl Rhodium Amido Complexes Relevant to Transfer Hydrogenation. *Organometallics* **2009,** *28*, 1435-1446. https://doi.org/10.1021/om8009969

522. Ekkert, O.; White, A. J. P.; Toms, H.; Crimmin, M. R., Addition of aluminium, zinc and magnesium hydrides to rhodium(iii). *Chem. Sci.* **2015,** *6*, 5617-5622. http://dx.doi.org/10.1039/C5SC01309G

523. Mampa, R. M.; Fernandes, M. A.; Carlton, L., Preparation and NMR study of trimetallic complexes of platinum and tungsten bridged by 4-pyridylacetylide and a binuclear complex of rhodium and tungsten bridged by 2-(4-pyridyl)thiazole-4-carboxylate (PTC): structure of [(Ph3P)2Rh(H)2(μ-PTC)W(CO)4(P(4-MeC6H4)3)]. *Transit. Met. Chem.* **2013,** *38*, 219-224. https://doi.org/10.1007/s11243-012-9681-5

524. Davis, J. C.; Bühl, M.; Koch, K. R., Probing Isotope Shifts in ^{103}Rh and ^{195}Pt NMR Spectra with Density Functional Theory. *J. Phys. Chem. A* **2013,** *117*, 8054-8064. https://doi.org/10.1021/jp405453c

525. Ortuño, M. A.; Castro, L.; Bühl, M., Computational Insight into ^{103}Rh Chemical Shift–Structure Correlations in Rhodium Bis(phosphine) Complexes. *Organometallics* **2013,** *32*, 6437-6444. https://doi.org/10.1021/om400774y

526. Nadolinny, V.; Belyaev, A.; Komarovskikh, A.; Tkachev, S.; Yushina, I., The photochemical generation of superoxide Rh(III) complexes. *New J. Chem.* **2018,** *42*, 15231-15236. http://dx.doi.org/10.1039/C8NJ02570C

527. Hopp Rentsch, G.; Kozminski, W.; von Philipsborn Fioretta Asaro, W.; Pellizer, G., Transition Metal NMR Spectroscopy. One-bond ^{103}Rh,^{15}N coupling constants of axial and equatorial ligands in rhodoximes. *Magn. Reson. Chem.* **1997,** *35*, 904-907. https://doi.org/10.1002/(SICI)1097-458X(199712)35:12<904::AID-OMR231>3.0.CO;2-%23

528. Rozwadowski, Z.; Nowak-Wydra, B., Chiral recognition of Schiff bases by 15N NMR spectroscopy in the presence of a dirhodium complex. Deuterium isotope effect on 15N chemical shift of the optically active Schiff bases and their dirhodium tetracarboxylate adducts. *Magn. Reson. Chem.* **2008,** *46*, 974-978. https://doi.org/10.1002/mrc.2280

529. Jaźwiński, J.; Duddeck, H., Pyridine and aminide derivatives as ligands in 1 : 1 Rh2[tfa]4 adducts: 1H, 13C and 15N NMR study. *Magn. Reson. Chem.* **2003,** *41*, 921-926. https://doi.org/10.1002/mrc.1263

530. Jaźwiński, J., Studies on adducts of rhodium(II) tetraacetate and rhodium(II) tetratrifluoroacetate with some amines in CDCl3 solution using 1H, 13C and 15N NMR. *J. Mol. Struct.* **2005,** *750*, 7-17. https://doi.org/10.1016/j.molstruc.2005.03.035

531. Bocian, W.; Jaźwiński, J.; Sadlej, A., ^{1}H, ^{13}C and ^{15}N NMR studies on adducts formation of rhodium(II) tetraacylates with some azoles in $CDCl_3$ solution. *Magn. Reson. Chem.* **2008,** *46*, 156-165. https://doi.org/10.1002/mrc.2149

532. Duddeck, H.; Malik, S.; Gáti, T.; Tóth, G.; Choudhary, M. I., Complexation of selenium to (R)-Rh2(MTPA)4: thermodynamics and stoichiometry. *Magn. Reson. Chem.* **2002,** *40*, 153-156. https://doi.org/10.1002/mrc.990

533. Perez, V.; Audet, P.; Bi, W.; Fontaine, F.-G., Phosphidoboratabenzene–rhodium(i) complexes as precatalysts for the hydrogenation of alkenes at room temperature and atmospheric pressure. *Dalton Trans.* **2016,** *45*, 2130-2137. http://dx.doi.org/10.1039/C5DT03109E

534. Câmpian, M. V.; Harris, J. L.; Jasim, N.; Perutz, R. N.; Marder, T. B.; Whitwood, A. C., Comparisons of Photoinduced Oxidative Addition of B−H, B−B, and Si−H Bonds at Rhodium(η^5-cyclopentadienyl)phosphine Centers. *Organometallics* **2006,** *25*, 5093-5104. https://doi.org/10.1021/om060500m

535. Houston, J. R.; Yu, P.; Casey, W. H., Water Exchange from the Oxo-Centered Rhodium(III) Trimer [Rh3(μ3-O)(μ-O2CCH3)6(OH2)3]+: A High-Pressure 17O NMR Study. *Inorg. Chem.* **2005,** *44*, 5176-5182. https://doi.org/10.1021/ic050537j

536. Laurenczy, G.; Rapaport, I.; Zbinden, D.; Merbach, A. E., Variable-pressure oxygen-17 NMR study of water exchange on hexaaquarhodium(III). *Magn. Reson. Chem.* **1991,** *29*, S45-S51. https://doi.org/10.1002/mrc.1260291311

537. Drljaca, A.; Zahl, A.; van Eldik, R., High-Pressure Oxygen-17 NMR Study of the Dihydroxo-Bridged Rhodium(III) Hydrolytic Dimer. Mechanistic Evidence for Limiting Dissociative Water Exchange Pathways. *Inorg. Chem.* **1998,** *37*, 3948-3953. https://doi.org/10.1021/ic971074n

538. Eisen, M. S.; Haskel, A.; Chen, H.; Olmstead, M. M.; Smith, D. P.; Maestre, M. F.; Fish, R. H., Aqueous Organometallic Chemistry: Structure and Dynamics in the Formation of (.eta.5-Pentamethylcyclopentadienyl)rhodium Aqua Complexes as a Function of pH. *Organometallics* **1995,** *14*, 2806-2812. https://doi.org/10.1021/om00006a029

539. Hintermair, U.; Sheehan, S. W.; Parent, A. R.; Ess, D. H.; Richens, D. T.; Vaccaro, P. H.; Brudvig, G. W.; Crabtree, R. H., Precursor Transformation during Molecular Oxidation Catalysis with Organometallic Iridium Complexes. *J. Am. Chem. Soc.* **2013,** *135*, 10837-10851. https://doi.org/10.1021/ja4048762

540. Koelliker, R.; Milstein, D., Evidence for an unprecedented Ir(H)(NH3) .dblarw. Ir(H2)(NH2) equilibrium and hydrogen exchange between NH and CH bonds. *J. Am. Chem. Soc.* **1991,** *113*, 8524-8525. https://doi.org/10.1021/ja00022a051

541. Cusanelli, A.; Frey, U.; Richens, D. T.; Merbach, A. E., The Slowest Water Exchange at a Homoleptic Mononuclear Metal Center: Variable-Temperature and Variable-Pressure 17O NMR Study on [Ir(H2O)6]3+. *J. Am. Chem. Soc.* **1996,** *118*, 5265-5271. https://doi.org/10.1021/ja954071n

542. Behringer, K. D.; Blümel, J., ^{61}Ni NMR spectroscopy of di- and tricarbonylnickel complexes. *Magn. Reson. Chem.* **1995,** *33*, 729-733. https://doi.org/10.1002/mrc.1260330907

543. Bühl, M.; Peters, D.; Herges, R., Substituent effects on ^{61}Ni NMR chemical shifts. *Dalton Trans.* **2009**, 6037-6044. http://dx.doi.org/10.1039/B902308A

544. Fedotov, M. A.; Likholobov, V. A., First direct observation of 105Pd NMR in solution. *Bull. Acad. Sci. USSR, Div. Chem. Sci. (Engl. Transl.)* **1984,** *33*, 1751-1751. https://doi.org/10.1007/BF00959235

545. Helm, L.; Elding, L. I.; Merbach, A. E., Water-Exchange Mechanism of Tetraaquapalladium(II). A Variable-Pressure and Variable-Temperature Oxygen-17 NMR Study. *Helv. Chim. Acta* **1984,** *67*, 1453-1460. https://doi.org/10.1002/hlca.19840670605

546. Thomas, A. A.; Denmark, S. E., Pre-transmetalation intermediates in the Suzuki-Miyaura reaction revealed: The missing link. *Science* **2016,** *352*, 329-332. http://doi.org/10.1126/science.aad6981

547. Thomas, A. A.; Wang, H.; Zahrt, A. F.; Denmark, S. E., Structural, Kinetic, and Computational Characterization of the Elusive Arylpalladium(II)boronate Complexes in the Suzuki–Miyaura Reaction. *J. Am. Chem. Soc.* **2017,** *139*, 3805-3821. https://doi.org/10.1021/jacs.6b13384

548. Kocak, F. S.; Zavalij, P.; Lam, Y.-F.; Eichhorn, B. W., Solution Dynamics and Gas-Phase Chemistry of Pd2@Sn184−. *Inorg. Chem.* **2008,** *47*, 3515-3520. https://doi.org/10.1021/ic701699d

549. Bhaskar, R.; Sharma, A. K.; Yadav, M. K.; Singh, A. K., Sonogashira (Cu and amine free) and Suzuki coupling in air catalyzed via nanoparticles formed in situ from Pd(ii) complexes of chalcogenated Schiff bases of 1-naphthaldehyde and their reduced forms. *Dalton Trans.* **2017,** *46*, 15235-15248. http://dx.doi.org/10.1039/C7DT02701J

550. Holló-Sitkei, E.; Szalontai, G.; Lois, I.; Gömöry, Á.; Pollreisz, F.; Párkányi, L.; Jude, H.; Besenyei, G., Sterically-Directed Consecutive and Size-Selective Self-Assembly of Palladium Diphosphane Complexes with an Ar-BIAN Ligand: Unexpected Formation of Pentameric and Hexameric Aggregates. *Chem. Eur. J.* **2009,** *15*, 10620-10633. https://doi.org/10.1002/chem.200901126

551. Requet, A.; Colin, O.; Bourdreux, F.; Salim, S. M.; Marque, S.; Thomassigny, C.; Greck, C.; Farjon, J.; Prim, D., Pyridylalkylamine ligands and their palladium complexes: structure and reactivity revisited by NMR. *Magn. Reson. Chem.* **2014,** *52*, 273-278. https://doi.org/10.1002/mrc.4058

552. White, P. B.; Jaworski, J. N.; Fry, C. G.; Dolinar, B. S.; Guzei, I. A.; Stahl, S. S., Structurally Diverse Diazafluorene-Ligated Palladium(II) Complexes and Their Implications for Aerobic Oxidation Reactions. *J. Am. Chem. Soc.* **2016,** *138*, 4869-4880. https://doi.org/10.1021/jacs.6b01188

553. Corbi, P. P.; Massabni, A. C., 1H–15N NMR studies of the complex bis(S-allyl-l-cysteinate)palladium(II). *Spectrochim. Acta A* **2006,** *64*, 418-419. https://doi.org/10.1016/j.saa.2005.07.039

554. Strong, E. T. J.; Cardile, S. A.; Brazeau, A. L.; Jennings, M. C.; McDonald, R.; Jones, N. D., Chiral, Hemilabile Palladium(II) Complexes of Tridentate Oxazolidines, Including C2-Symmetric “Pincers”. *Inorg. Chem.* **2008,** *47*, 10575-10586. https://doi.org/10.1021/ic8011926

555. Papadogianakis, G.; Peters, J. A.; Maat, L.; Sheldon, R. A., Catalytic conversions in water: 17O, {1H}31P and 35Cl NMR study of a novel stoichiometric redox reaction between PdCl2, tppts and H2O [tppts = P(C6H4-m-SO3Na)3]. *J. Chem. Soc., Chem. Commun.* **1995**, 1105-1106. http://dx.doi.org/10.1039/C39950001105

556. Armbruster, F.; Augenstein, T.; Oña-Burgos, P.; Breher, F., Homoleptic Tetrakis(silyl) Complexes of Pd0 and Pt0 Featuring Metal-Centred Heterocubane Structures: Evidence for the Existence of the Corresponding Mononuclear PdI and PtI Complexes. *Chem. Eur. J.* **2013,** *19*, 17899-17906. https://doi.org/10.1002/chem.201303299

557. Priqueler, J. R. L.; Butler, I. S.; Rochon, F. D., An Overview of 195Pt Nuclear Magnetic Resonance Spectroscopy. *Appl. Spectrosc. Rev.* **2006,** *41*, 185-226. https://doi.org/10.1080/05704920600620311

558. Still, B. M.; Kumar, P. G. A.; Aldrich-Wright, J. R.; Price, W. S., 195Pt NMR—theory and application. *Chem. Soc. Rev.* **2007,** *36*, 665-686. http://dx.doi.org/10.1039/B606190G

559. Gabano, E.; Marengo, E.; Bobba, M.; Robotti, E.; Cassino, C.; Botta, M.; Osella, D., 195Pt NMR spectroscopy: A chemometric approach. *Coord. Chem. Rev.* **2006,** *250*, 2158-2174. https://doi.org/10.1016/j.ccr.2006.02.011

560. Braunschweig, H.; Dewhurst, R. D.; Hupp, F.; Schneider, C., Silver(I) and thallium(I) cations as unsupported bridges between two metal bases. *Chem. Commun.* **2014,** *50*, 15685-15688. http://dx.doi.org/10.1039/C4CC08508F

561. Gallo, V.; Latronico, M.; Mastrorilli, P.; Nobile, C. F.; Polini, F.; Re, N.; Englert, U., Reactivity of a Phosphinito-Bridged PtI−PtI Complex with Nucleophiles: Substitution versus Addition. *Inorg. Chem.* **2008,** *47*, 4785-4795. https://doi.org/10.1021/ic800045u

562. Latronico, M.; Polini, F.; Gallo, V.; Mastrorilli, P.; Calmuschi-Cula, B.; Englert, U.; Re, N.; Repo, T.; Räisänen, M., Site Selectivity in the Protonation of a Phosphinito Bridged PtI−PtI Complex: a Combined NMR and Density-Functional Theory Mechanistic Study. *Inorg. Chem.* **2008,** *47*, 9779-9796. https://doi.org/10.1021/ic800508t

563. Pazderski, L.; Szłyk, E.; Sitkowski, J.; Kamieński, B.; Kozerski, L.; Toušek, J.; Marek, R., Experimental and quantum-chemical studies of 15N NMR coordination shifts in palladium and platinum chloride complexes with pyridine, 2,2′-bipyridine and 1,10-phenanthroline. *Magn. Reson. Chem.* **2006,** *44*, 163-170. https://doi.org/10.1002/mrc.1740

564. Pawlak, T.; Pazderski, L.; Sitkowski, J.; Kozerski, L.; Szłyk, E., 1H, 13C, 195Pt and 15N NMR structural correlations in Pd(II) and Pt(II) chloride complexes with various alkyl and aryl derivatives of 2,2′-bipyridine and 1,10-phenanthroline. *Magn. Reson. Chem.* **2011,** *49*, 59-64. https://doi.org/10.1002/mrc.2704

565. Benedetti, M.; De Castro, F.; Fanizzi, F. P., Square-Planar Pt^{II} versus Octahedral Pt^{IV} Halido Complexes: ^{195}Pt NMR Explained by a Simple Empirical Approach. *Eur. .J. Inorg. Chem.* **2016,** *2016*, 3957-3962. https://doi.org/10.1002/ejic.201600573

566. Benedetti, M.; de Castro, F.; Antonucci, D.; Papadia, P.; Fanizzi, F. P., General cooperative effects of single atom ligands on a metal: a ^{195}Pt NMR chemical shift as a function of coordinated halido ligands' ionic radii overall sum. *Dalton Trans.* **2015,** *44*, 15377-15381. http://dx.doi.org/10.1039/C5DT02285A

567. Benedetti, M.; Papadia, P.; Girelli, C. R.; De Castro, F.; Capitelli, F.; Fanizzi, F. P., X-ray structures versus NMR signals in pentacoordinate $[PtX_2(\eta^2\text{-}CH_2CH_2)(Me_2phen)]$ (X = Cl, Br, I) complexes. *Inorg. Chim. Acta* **2015,** *428*, 8-13. https://doi.org/10.1016/j.ica.2015.01.003

568. Pazderski, L.; Pawlak, T.; Sitkowski, J.; Kozerski, L.; Szłyk, E., 1H, 13C, 15N and 195Pt NMR studies of Au(III) and Pt(II) chloride organometallics with 2-phenylpyridine. *Magn. Reson. Chem.* **2009,** *47*, 932-941. https://doi.org/10.1002/mrc.2491

569. Sanz Miguel, P. J.; Lax, P.; Lippert, B., (Dien)MII (M=Pd, Pt) and (NH3)3PtII complexes of 1-methylcytosine: Linkage and rotational isomerism, metal-promoted deamination, and pathways to dinuclear species. *J. Inorg. Biochem.* **2006,** *100*, 980-991. https://doi.org/10.1016/j.jinorgbio.2006.02.017

570. Lohr, T. L.; Piers, W. E.; Sgro, M. J.; Parvez, M., Silver ion enhanced C–H activation in Pt(ii) hydroxo complexes. *Dalton Trans.* **2014,** *43*, 13858-13864. http://dx.doi.org/10.1039/C4DT01934B

571. Lasri, J.; Adília Januário Charmier, M.; da Silva, M. F. C. G.; Pombeiro, A. J. L., Mixed unsymmetric oxadiazoline and/or imine platinum(ii) complexes. *Dalton Trans.* **2007**, 3259-3266. http://dx.doi.org/10.1039/B704329E

572. Strukl, J. V.; de Paula, Q. A.; Yang, X.; Qu, Y.; Farrell, N. P., Comparison of cis and trans-Platinum Mononucleobase Compounds with DNA and Protein Models. *Aust. J. Chem.* **2008,** *61*, 694-699. https://doi.org/10.1071/CH08227

573. Williams, K. M.; Dudgeon, R. P.; Chmely, S. C.; Robey, S. R., Reaction of platinum(II) diamine and triamine complexes with selenomethionine. *Inorg. Chim. Acta* **2011,** *368*, 187-193. https://doi.org/10.1016/j.ica.2011.01.002

574. Chauhan, R. S.; Sharma, R. K.; Kedarnath, G.; Cordes, D. B.; Slawin, A. M. Z.; Jain, V. K., Reactivity of dipyrimidyldiselenides with $[M(PPh_3)_4]$ and 2-pyrimidylchalcogenolates with $[MCl_2(diphosphine)]$ (M = Pd or Pt). *J. Organomet. Chem.* **2012,** *717*, 180-186. https://doi.org/10.1016/j.jorganchem.2012.06.036

575. Al-Ktaifani, M. M.; Coles, M. P.; Crossley, I. R.; Evans, L. T. J.; Hitchcock, P. B.; Lawless, G. A.; Nixon, J. F., Opening "Jaws": Functionalisation of the hexaphosphapentaprismane cage, $P_6C_4{}^tBu_4$, affording $X_2P_6C_4{}^tBu_4$ (X = Me, I), crystal and molecular structures of $X_2P_6C_4{}^tBu_4$ (X = Me, I) and [*cis*-$PtCl_2Me_2P_6C_4{}^tBu_4$]. *J. Organomet. Chem.* **2009,** *694*, 4223-4229. https://doi.org/10.1016/j.jorganchem.2009.09.002

576. Al-Ktaifani, M. M.; Hitchcock, P. B.; Nixon, J. F., Facile insertion and halogen migration reactions of the hexaphosphapentaprismane cage $P_6C_4{}^tBu_4$ with zerovalent and divalent platinum complexes. *Dalton Trans.* **2008**, 1132-1135. http://dx.doi.org/10.1039/B719064F

577. Kluge, T.; Mendicute-Fierro, C.; Bette, M.; Rodríguez-Diéguez, A.; Garralda, M. A.; Steinborn, D., On the Reactivity of Platina-β-diketone and Acetylplatinum(II) Complexes toward

2-(Diphenylphosphanyl)benzaldehyde and Its Dioxolane Derivative. *Eur. .J. Inorg. Chem.* **2013,** *2013*, 5418-5427. https://doi.org/10.1002/ejic.201300779

578. Wrackmeyer, B.; Hernández, Z. G.; Kempe, R.; Herberhold, M., Diselenastanna-, -sila- and -carbacycles with an annelated dicarba-closo-dodecaborane(12) unit. *Appl. Organometal. Chem.* **2007,** *21*, 108-116. https://doi.org/10.1002/aoc.1181

579. Zenkina, O. V.; Konstantinovski, L. E.; Shimon, L. J. W.; Diskin-Posner, Y.; Iron, M. A.; van der Boom, M. E., Long-Range Through-Bond Heteronuclear Communication in Platinum Complexes. *Inorg. Chem.* **2009,** *48*, 4021-4030. https://doi.org/10.1021/ic801940h

580. Chen, W.; Liu, F.; Matsumoto, K.; Autschbach, J.; Le Guennic, B.; Ziegler, T.; Maliarik, M.; Glaser, J., Spectral and Structural Characterization of Amidate-Bridged Platinum−Thallium Complexes with Strong Metal−Metal Bonds. *Inorg. Chem.* **2006,** *45*, 4526-4536. https://doi.org/10.1021/ic051678o

581. Iwatsuki, S.; Isomura, E.; Wada, A.; Ishihara, K.; Matsumoto, K., 195Pt NMR Spectra of Head-to-Head and Head-to-Tail Amidato-Bridged Platinum(III) Dinuclear Complexes. *Eur. .J. Inorg. Chem.* **2006,** *2006*, 2484-2490. https://doi.org/10.1002/ejic.200500954

582. Ara, I.; Forniés, J.; Fortuño, C.; Ibáñez, S.; Martín, A.; Mastrorilli, P.; Gallo, V., Unsymmetrical Platinum(II) Phosphido Derivatives: Oxidation and Reductive Coupling Processes Involving Platinum(III) Complexes as Intermediates. *Inorg. Chem.* **2008,** *47*, 9069-9080. https://doi.org/10.1021/ic8011124

583. Murray, P.; Koch, K. R., A 195Pt NMR study of the oxidation of [PtCl4]2− with chlorate, bromate, and hydrogen peroxide in acidic aqueous solution. *J. Coord. Chem.* **2010,** *63*, 2561-2577. https://doi.org/10.1080/00958972.2010.493212

584. Murray, P.; Gerber, W. J.; Koch, K. R., 35/37Cl and 16/18O isotope resolved 195Pt NMR: unique spectroscopic 'fingerprints' for unambiguous speciation of [PtCln(H2O)6−n]4−n (n = 2–5) complexes in an acidic aqueous solution. *Dalton Trans.* **2012,** *41*, 10533-10542. http://dx.doi.org/10.1039/C2DT31201H

585. Engelbrecht, L.; Murray, P.; Koch, K. R., Isotope Effects in 195Pt NMR Spectroscopy: Unique 35/37Cl- and 16/18O-Resolved “Fingerprints” for All [PtCl6–n(OH)n]2– (n = 1–5) Anions in an Alkaline Solution and the Implications of the Trans Influence. *Inorg. Chem.* **2015,** *54*, 2752-2764. https://doi.org/10.1021/ic502901d

586. Kramer, J.; Koch, K. R., 195Pt NMR Chemical Shift Trend Analysis as a Method to Assign New Pt(IV)−Halohydroxo Complexes. *Inorg. Chem.* **2007,** *46*, 7466-7476. https://doi.org/10.1021/ic700804t

587. Bagno, A.; Bini, R., NMR Spectra of Terminal Oxo Gold and Platinum Complexes: Relativistic DFT Predictions. *Angew. Chem. Int. Ed.* **2010,** *49*, 1083-1086. https://doi.org/10.1002/anie.200905507

588. Burger, M. R.; Kramer, J.; Chermette, H.; Koch, K. R., A comparison of experimental and DFT calculations of ^{195}Pt NMR shielding trends for $[PtX_nY_{6-n}]^{2-}$ (X, Y = Cl, Br, F and I) anions. *Magn. Reson. Chem.* **2010,** *48*, S38-S47. https://doi.org/10.1002/mrc.2607

589. Efremenko, I.; Poverenov, E.; Martin, J. M. L.; Milstein, D., DFT Study of the Structure and Reactivity of the Terminal Pt(IV)-Oxo Complex Bearing No Electron-Withdrawing Ligands. *J. Am. Chem. Soc.* **2010,** *132*, 14886-14900. https://doi.org/10.1021/ja105197x

590. Fowe, E. P.; Belser, P.; Daul, C.; Chermette, H., Assessment of theoretical prediction of the NMR shielding tensor of 195PtClxBr6−x2− complexes by DFT calculations: experimental and computational results. *Phys. Chem. Chem. Phys.* **2005,** *7*, 1732-1738. http://dx.doi.org/10.1039/B500574D

591. Hashemi, M., Correlation between 195Pt chemical shifts and the electronic transitions among d orbitals in pincer NCN Pt(II) complexes: A theoretical study and application of Ramsey’s equation. *Spectrochim. Acta A* **2015,** *151*, 438-442. https://doi.org/10.1016/j.saa.2015.06.122

592. Koch, K. R.; Burger, M. R.; Kramer, J.; Westra, A. N., 195Pt NMR and DFT computational methods as tools towards the understanding of speciation and

hydration/solvation of [PtX6]2− (X = Cl−, Br−) anions in solution. *Dalton Trans.* **2006**, 3277-3284. http://dx.doi.org/10.1039/B605182K

593. Oziminski, W. P.; Garnuszek, P.; Bednarek, E.; Dobrowolski, J. C., The platinum complexes with histamine: Pt(II)(Hist)Cl2, Pt(II)(Iodo-Hist)Cl2 and Pt(IV)(Hist)2Cl2. *Inorg. Chim. Acta* **2007,** *360*, 1902-1914. https://doi.org/10.1016/j.ica.2006.10.004

594. Semenov, V. A.; Samultsev, D. O.; Rusakova, I. L.; Krivdin, L. B., Computational Multinuclear NMR of Platinum Complexes: A Relativistic Four-Component Study. *J. Phys. Chem. A* **2019,** *123*, 4908-4920. https://doi.org/10.1021/acs.jpca.9b02867

595. Sterzel, M.; Autschbach, J., Toward an Accurate Determination of 195Pt Chemical Shifts by Density Functional Computations: The Importance of Unspecific Solvent Effects and the Dependence of Pt Magnetic Shielding Constants on Structural Parameters. *Inorg. Chem.* **2006,** *45*, 3316-3324. https://doi.org/10.1021/ic052143y

596. Sutter, K.; Autschbach, J., Computational Study and Molecular Orbital Analysis of NMR Shielding, Spin–Spin Coupling, and Electric Field Gradients of Azido Platinum Complexes. *J. Am. Chem. Soc.* **2012,** *134*, 13374-13385. https://doi.org/10.1021/ja3040762

597. Takagi, N.; Sakaki, S., A Theoretical Study of an Unusual Y-Shaped Three-Coordinate Pt Complex: Pt(0) σ-Disilane Complex or Pt(II) Disilyl Complex? *J. Am. Chem. Soc.* **2012,** *134*, 11749-11759. https://doi.org/10.1021/ja304110h

598. Truflandier, L. A.; Sutter, K.; Autschbach, J., Solvent Effects and Dynamic Averaging of 195Pt NMR Shielding in Cisplatin Derivatives. *Inorg. Chem.* **2011,** *50*, 1723-1732. https://doi.org/10.1021/ic102174b

599. Tsipis, A. C.; Karapetsas, I. N., Accurate prediction of 195Pt NMR chemical shifts for a series of Pt(ii) and Pt(iv) antitumor agents by a non-relativistic DFT computational protocol. *Dalton Trans.* **2014,** *43*, 5409-5426. http://dx.doi.org/10.1039/C3DT53594K

600. Tsipis, A. C.; Karapetsas, I. N., Accurate prediction of 195Pt-NMR chemical shifts for hydrolysis products of [PtCl6]2− in acidic and alkaline aqueous solutions by non-relativistic DFT

computational protocols. *J. Coord. Chem.* **2015,** *68*, 3788-3804. https://doi.org/10.1080/00958972.2015.1083095

601. Tsipis, A. C.; Karapetsas, I. N., Prediction of 195Pt NMR of photoactivable diazido- and azine-Pt(IV) anticancer agents by DFT computational protocols. *Magn. Reson. Chem.* **2017,** *55*, 145-153. https://doi.org/10.1002/mrc.4523

602. Morley, C. P.; Webster, C. A.; Vaira, M. D., Oxidative addition of (PhSe)2 and (FcSe)2 to zerovalent palladium and platinum trialkylphosphine complexes (Fc=ferrocenyl, [Fe(η5-C5H5)(η5-C5H4)]). *J. Organomet. Chem.* **2006,** *691*, 4244-4249. https://doi.org/10.1016/j.jorganchem.2006.06.035

603. Yao, K.; Bertran, A.; Morgan, J.; Hare, S. M.; Rees, N. H.; Kenwright, A. M.; Edkins, K.; Bowen, A. M.; Farrer, N. J., A novel Pt(iv) mono azido mono triazolato complex evolves azidyl radicals following irradiation with visible light. *Dalton Trans.* **2019,** *48*, 6416-6420. http://dx.doi.org/10.1039/C9DT01156K

604. Dimmer, J.-A.; Hornung, M.; Eichele, K.; Wesemann, L., Selenium adducts of germa- and stanna-closo-dodecaborate: coordination at platinum, structural studies and NMR spectroscopy. *Dalton Trans.* **2012,** *41*, 8989-8996. http://dx.doi.org/10.1039/C2DT30478C

605. Al-Allaf, T. A. K., Reactions of organotin(IV) compounds with platinum complexes: Part II. Oxidative addition of SnR_xCl_{4-x} to $[Pt(COD)_2]$ and subsequent reactions with tertiary phosphines. *J. Organomet. Chem.* **1999,** *590*, 25-35. https://doi.org/10.1016/S0022-328X(99)00408-8

606. Zabula, A. V.; Pape, T.; Hepp, A.; Hahn, F. E., Coordination chemistry of bisstannylenes with platinum(0). *Dalton Trans.* **2008**, 5886-5890. http://dx.doi.org/10.1039/B809878F

607. Mitchell, G. P.; Tilley, T. D., Generation of a Silylene Complex by the 1,2-Migration of Hydrogen from Silicon to Platinum. *Angew. Chem. Int. Ed,* **1998,** *37*, 2524-2526. https://doi.org/10.1002/(SICI)1521-3773(19981002)37:18<2524::AID-ANIE2524>3.0.CO;2-H

608. Liu, Y.; Intini, F. P.; Natile, G.; Sletten, E., Kinetic study of the reaction between an antitumor 15N labeled trans-platinum iminoether complex and GMP by [1H, 15N] HMQC NMR. *J. Chem. Soc., Dalton Trans.* **2002**, 3489-3495. http://dx.doi.org/10.1039/B203572N

609. Liu, Y.; Pacifico, C.; Natile, G.; Sletten, E., Antitumor trans Platinum Complexes can Form Cross-Links with Adjacent Purine Groups. *Angew. Chem. Int. Ed,* **2001,** *40*, 1226-1228. https://doi.org/10.1002/1521-3773(20010401)40:7<1226::AID-ANIE1226>3.0.CO;2-U

610. Liu, Y.; Vinje, J.; Pacifico, C.; Natile, G.; Sletten, E., Formation of Adenine−N3/Guanine−N7 Cross-Link in the Reaction of trans-Oriented Platinum Substrates with Dinucleotides. *J. Am. Chem. Soc.* **2002,** *124*, 12854-12862. https://doi.org/10.1021/ja027251n

611. Berners-Price, S. J.; Frenkiel, T. A.; Ranford, J. D.; Sadler, P. J., Nuclear magnetic resonance studies of N – H bonds in platinum anticancer complexes: detection of reaction intermediates and hydrogen bonding in guanosine 5′ -monophosphate adducts of $[PtCl_2(NH_3)_2]$. *J. Chem. Soc., Dalton Trans.* **1992**, 2137-2139. http://dx.doi.org/10.1039/DT9920002137

612. Berners-Price, S. J.; Davies, M. S.; Cox, J. W.; Thomas, D. S.; Farrell, N., Competitive Reactions of Interstrand and Intrastrand DNA-Pt Adducts: A Dinuclear-Platinum Complex Preferentially Forms a 1,4-Interstrand Cross-Link Rather than a 1,2 Intrastrand Cross-link on Binding to a GG 14-Mer Duplex. *Chem. Eur. J.* **2003,** *9*, 713-725. https://doi.org/10.1002/chem.200390080

613. Chen, Y.; Guo, Z.; del Socorro Murdoch, P.; Zang, E.; J. Sadler, P., Interconversion between S- and N-bound L-methionine adducts of $Pt(dien)^{2+}$ (dien = diethylenetriamine) via dien ring-opened intermediates. *J. Chem. Soc., Dalton Trans.* **1998**, 1503-1508. http://dx.doi.org/10.1039/A709282B

614. Chen, Y.; Guo, Z.; Parsons, S.; Sadler, P. J., Stereospecific and Kinetic Control over the Hydrolysis of a Sterically Hindered Platinum Picoline Anticancer Complex. *Chem. Eur. J.* **1998,**

4, 672-676. https://doi.org/10.1002/(SICI)1521-3765(19980416)4:4<672::AID-CHEM672>3.0.CO;2-8

615. Gorle, A. K.; Zhang, J.; Berners-Price, S. J.; Farrell, N. P., Influence of geometric isomerism on the binding of platinum anticancer agents with phospholipids. *Dalton Trans.* **2019,** *48*, 9791-9800. http://dx.doi.org/10.1039/C9DT00753A

616. Qu, Y.; Farrell, N., Association of mononuclear and dinuclear platinum tetraamine cations with nucleotides studied by 15N NMR relaxation. *Inorg. Chim. Acta* **1996,** *245*, 265-267. https://doi.org/10.1016/0020-1693(95)04815-4

617. Ruhayel, R. A.; Berners-Price, S. J.; Farrell, N. P., Competitive formation of both long-range 5′ – 5′ and short-range antiparallel 3′ – 3′ DNA interstrand cross-links by a trinuclear platinum complex on binding to a 10-mer duplex. *Dalton Trans.* **2013,** *42*, 3181-3187. http://dx.doi.org/10.1039/C2DT32079G

618. Watson, A. A.; Fairlie, D. P., Ammonia and Carbon Dioxide from Urea. Multinuclear NMR Study of the Activation of Urea by Platinum(II). *Inorg. Chem.* **1995,** *34*, 3087-3092. https://doi.org/10.1021/ic00115a041

619. Kelly, P. F.; Sheppard, R. N.; Woollins, J. D., Reinvestigation into the isomerization of mer-PtCl2(S4N4)(PMe2Ph). *Polyhedron* **1992,** *11*, 2605-2609. https://doi.org/10.1016/S0277-5387(00)80229-6

620. Cubo, L.; Thomas, D. S.; Zhang, J.; Quiroga, A. G.; Navarro-Ranninger, C.; Berners-Price, S. J., [1H,15N] NMR studies of the aquation of cis-diamine platinum(II) complexes. *Inorg. Chim. Acta* **2009,** *362*, 1022-1026. https://doi.org/10.1016/j.ica.2008.03.117

621. Davies, M. S.; Hall, M. D.; Berners-Price, S. J.; Hambley, T. W., [1H, 15N] Heteronuclear Single Quantum Coherence NMR Study of the Mechanism of Aquation of Platinum(IV) Ammine Complexes. *Inorg. Chem.* **2008,** *47*, 7673-7680. https://doi.org/10.1021/ic8006734

622. Pregosin, P. S.; Rüegger, H.; Wombacher, F.; Van Koten, G.; Grove, D. M.; Wehman-Ooyevaar, I. C. M., New Pt … H□N bonds characterized by 15N-filtered and 2D NOESY 1H NMR spectroscopy. *Magn. Reson. Chem.* **1992,** *30*, 548-551. https://doi.org/10.1002/mrc.1260300616

623. Drescher, W.; Borner, C.; Tindall, D. J.; Kleeberg, C., Exploring unsymmetrical diboranes(4) as boryl ligand precursors: platinum(ii) bis-boryl complexes. *RSC Adv.* **2019,** *9*, 3900-3911. http://dx.doi.org/10.1039/C9RA00170K

624. Frey, U.; Grove, D. M.; van Koten, G., Fast water exchange on a Pt(II) center: variable temperature and pressure17O NMR study at 14.1 tesla of the ionic arylplatinum species [PtC6H3(CH2NMe2)2-2,6 (OH2)]+ (OSO2CF3)−. *Inorg. Chim. Acta* **1998,** *269*, 322-325. https://doi.org/10.1016/S0020-1693(97)05791-5

625. Ginn, V. C.; Kelly, P. F.; Woollins, J. D., Multinuclear NMR studies upon 15N labelled metalla-chalcogen-nitrogen complexes. *Polyhedron* **1994,** *13*, 1501-1506. https://doi.org/10.1016/S0277-5387(00)83444-0

626. Matsubayashi, G.-e.; Yokozawa, A., Selenium-77 NMR of C3Se5-metal complexes (C3Se52−=1,3-diselenole-2-selone-4,5-diselenolate). *Inorg. Chim. Acta* **1993,** *208*, 95-97. https://doi.org/10.1016/S0020-1693(00)82889-3

627. Malito, J., Copper-63 NMR Spectroscopy. *Annu. Rep. NMR Spectrosc.* **1999,** *38*, 265-287. https://doi.org/10.1016/S0066-4103(08)60039-3

628. Falcomer, V. A. S.; Lemos, S. S.; Martins, G. B. C.; Casagrande, G. A.; Burrow, R. A.; Lang, E. S., Synthesis, structural characterization and reactivity of copper(I)-nitrile complexes: Crystal and molecular structure of [Cu(BzCN)4][BF4]. *Polyhedron* **2007,** *26*, 3871-3875. https://doi.org/10.1016/j.poly.2007.04.007

629. Irangu, J. K.; Jordan, R. B., Copper-63 NMR Line width Study of the Copper(I)−Acetonitrile System. *Inorg. Chem.* **2003,** *42*, 3934-3942. https://doi.org/10.1021/ic030020c

630. Gill, D.; Pathania, V., Chapter Ten - The Chemistry of Monovalent Copper in Solutions of Pure and Mixed Nonaqueous Solvents. *Adv. Inorg. Chem.* **2016,** *68*, 441-481. https://doi.org/10.1016/bs.adioch.2015.11.001

631. Brown, M. D.; Levason, W.; Reid, G.; Watts, R., Synthesis spectroscopic and structural properties of transition metal complexes of the o-xylyl diphosphine o-$C_6H_4(CH_2PPh_2)_2$. *Polyhedron* **2005,** *24*, 75-87. https://doi.org/10.1016/j.poly.2004.10.008

632. Szłyk, E.; Kucharek, R.; Szymańska, I.; Pazderski, L., Synthesis and characterization of Cu(I) chelate complexes with 1,3-bis(diphenylphosphino)propane, 1,2-bis(diphenylphosphino)benzene and perfluorinated carboxylates. *Polyhedron* **2003,** *22*, 3389-3393. https://doi.org/10.1016/j.poly.2003.09.006

633. Szłyk, E.; Szymańska, I., Studies of new volatile copper(I) complexes with triphenylphosphite and perfluorinated carboxylates. *Polyhedron* **1999,** *18*, 2941-2948. https://doi.org/10.1016/S0277-5387(99)00199-0

634. Szymańska, I., 63Cu and 31P Nuclear Magnetic Resonance for Characterization of Cu(I) Complexes with P-Donor Ligands. *Pol. J. Chem.* **2006,** *80*, 1095-1117. http://yadda.icm.edu.pl/baztech/element/bwmeta1.element.baztech-article-BUJ6-0007-0010?q=bwmeta1.element.baztech-volume-0137-5083-polish_journal_of_chemistry-2006-vol__80_nr_7;9&qt=CHILDREN-STATELESS

635. Even, T.; Genge, A. R. J.; Hill, A. M.; Holmes, N. J.; Levason, W.; Webster, M., Synthesis, properties and structures of complexes of platinum metal halides and Group 11 metals with two distibinomethane ligands, R2SbCH2SbR2 (R = Me or Ph). *J. Chem. Soc., Dalton Trans.* **2000**, 655-662. http://dx.doi.org/10.1039/A908296D

636. Levason, W.; Nirwan, M.; Ratnani, R.; Reid, G.; Tsoureas, N.; Webster, M., Transition metal complexes with wide-angle dithio-, diseleno- and ditelluroethers: properties and structural systematics. *Dalton Trans.* **2007**, 439-448. http://dx.doi.org/10.1039/B613501C

637. Hesford, M. J.; Levason, W.; Matthews, M. L.; Reid, G., Synthesis and complexation of the mixed tellurium–oxygen macrocycles 1-tellura-4,7-dioxacyclononane, [9]aneO2Te, and 1,10-ditellura-4,7,13,16-tetraoxacyclooctadecane, [18]aneO4Te2 and their selenium analogues. *Dalton Trans.* **2003**, 2852-2858. http://dx.doi.org/10.1039/B303365C

638. Kujime, M.; Kurahashi, T.; Tomura, M.; Fujii, H., 63Cu NMR Spectroscopy of Copper(I) Complexes with Various Tridentate Ligands: CO as a Useful 63Cu NMR Probe for Sharpening 63Cu NMR Signals and Analyzing the Electronic Donor Effect of a Ligand. *Inorg. Chem.* **2007,** *46*, 541-551. https://doi.org/10.1021/ic060745r

639. Scharfe, S.; Fässler, T. F.; Stegmaier, S.; Hoffmann, S. D.; Ruhland, K., [Cu@Sn9]3− and [Cu@Pb9]3−: Intermetalloid Clusters with Endohedral Cu Atoms in Spherical Environments. *Chem. Eur. J.* **2008,** *14*, 4479-4483. https://doi.org/10.1002/chem.200800429

640. Lipton, A. S.; Heck, R. W.; de Jong, W. A.; Gao, A. R.; Wu, X.; Roehrich, A.; Harbison, G. S.; Ellis, P. D., Low Temperature 65Cu NMR Spectroscopy of the Cu+ Site in Azurin. *J. Am. Chem. Soc.* **2009,** *131*, 13992-13999. https://doi.org/10.1021/ja901308v

641. Jastrzab, R.; Lomozik, L., Coordination mode in the binary systems of copper(II)/O-phospho-L-serine. *J. Coord. Chem.* **2009,** *62*, 710-720. https://doi.org/10.1080/00958970802317855

642. Neubrand, A.; Thaler, F.; Koerner, M.; Zahl, A.; Hubbard, C. D.; van Eldik, R., Mechanism of water exchange on five-coordinate copper(II) complexes. *J. Chem. Soc., Dalton Trans.* **2002**, 957-961. https://doi.org/10.1039/b107458j

643. Powell, D. H.; Merbach, A. E.; Fabian, I.; Schindler, S.; van Eldik, R., Evidence for a Chelate-Induced Changeover in the Substitution Mechanism of Aquated Copper(II). Volume Profile Analyses of Water Exchange and Complex-Formation Reactions. *Inorg. Chem.* **1994,** *33*, 4468-73. https://doi.org/10.1021/ic00098a011

644. Powell, D. H.; Furrer, P.; Pittet, P.-A.; Merbach, A. E., Solvent Exchange and Jahn-Teller Inversion on Cu2+ in Water and N,N'-Dimethylformamide: A High-Pressure 17O NMR Study. *J. Phys. Chem.* **1995,** *99*, 16622-16629. https://doi.org/10.1021/j100045a022

645. Nilsson, K. B.; Persson, I.; Kessler, V. G., Coordination Chemistry of the Solvated AgI and AuI Ions in Liquid and Aqueous Ammonia, Trialkyl and Triphenyl Phosphite, and Tri-n-butylphosphine Solutions. *Inorg. Chem.* **2006,** *45*, 6912-6921. https://doi.org/10.1021/ic060175v

646. Ang, H.-G.; Fraenk, W.; Karaghiosoff, K.; Klapötke, T. M.; Mayer, P.; Nöth, H.; Sprott, J.; Warchhold, M., Synthesis, Characterization, and Crystal Structures of Cu, Ag, and Pd Dinitramide Salts. *Z. Anorg. Allg. Chem.* **2002,** *628*, 2894-2900. https://doi.org/10.1002/1521-3749(200213)628:13<2894::AID-ZAAC2894>3.0.CO;2-R

647. Zopes, D.; Hegemann, C.; Tyrra, W.; Mathur, S., [(CF3)4Au2(C5H5N)2] – a new alkyl gold(ii) derivative with a very short Au–Au bond. *Chem. Commun.* **2012,** *48*, 8805-8807. http://dx.doi.org/10.1039/C2CC33735E

648. Menzer, S.; Hillgeris, E. C.; Lippert, B., Preparation, X-ray structure and solution behavior of [Ag(9-EtGH-N7)2]NO3·H2O (9-EtGH=9-ethylguanine). *Inorg. Chim. Acta* **1993,** *210*, 167-171. https://doi.org/10.1016/S0020-1693(00)83323-X

649. Drew, M. G. B.; Harding, C. J.; Howarth, O. W.; Lu, Q.; Marrs, D. J.; Morgan, G. G.; McKee, V.; Nelson, J., Thiophene-linked azacryptand sites for dicopper and disilver; thiophene sulfur as an inert spacer? *J. Chem. Soc., Dalton Trans.* **1996**, 3021-3030. http://dx.doi.org/10.1039/DT9960003021

650. Dairaku, T.; Furuita, K.; Sato, H.; Šebera, J.; Nakashima, K.; Kondo, J.; Yamanaka, D.; Kondo, Y.; Okamoto, I.; Ono, A.; Sychrovský, V.; Kojima, C.; Tanaka, Y., Structure Determination of an AgI-Mediated Cytosine–Cytosine Base Pair within DNA Duplex in Solution with 1H/15N/109Ag NMR Spectroscopy. *Chem. Eur. J.* **2016,** *22*, 13028-13031. https://doi.org/10.1002/chem.201603048

651. Mamula, O.; von Zelewsky, A.; Bernardinelli, G., Completely Stereospecific Self-Assembly of a Circular Helicate. *Angew. Chem. Int. Ed.* **1998,** *37*, 289-293. https://doi.org/10.1002/(SICI)1521-3773(19980216)37:3<289::AID-ANIE289>3.0.CO;2-M

652. Mamula, O.; Monlien, F. J.; Porquet, A.; Hopfgartner, G.; Merbach, A. E.; von Zelewsky, A., Self-Assembly of Multinuclear Coordination Species with Chiral Bipyridine Ligands: Silver Complexes of 5,6-CHIRAGEN(o,m,p-xylidene) Ligands and Equilibrium Behaviour in Solution. *Chem. Eur. J.* **2001,** *7*, 533-539. https://doi.org/10.1002/1521-3765(20010119)7:2<533::AID-CHEM533>3.0.CO;2-Q

653. Carmona, D.; Oro, L. A.; Lamata, M. P.; Jimeno, M. L.; Elguero, J.; Belguise, A.; Lux, P., Argentotropism in (Pentamethylcyclopentadienyl)iridium Complexes with Pyrazole Ligands: Multinuclear DNMR Experiments. *Inorg. Chem.* **1994,** *33*, 2196-2203. https://doi.org/10.1021/ic00088a022

654. Lianza, F.; Macchioni, A.; Pregosin, P.; Ruegger, H., Multidimensional 109Ag, 31P, and 1H HMQC and HSQC NMR studies on a model homogeneous catalyst. Reactions of a chiral ferrocenylphosphine with Ag(CF3SO3). *Inorg. Chem.* **1994,** *33*, 4999-5002. https://doi.org/10.1021/ic00100a025

655. Berners-Price, S. J.; Bowen, R. J.; Harvey, P. J.; Healy, P. C.; Koutsantonis, G. A., Silver(I) nitrate adducts with bidentate 2-, 3- and 4-pyridyl phosphines. Solution ^{31}P and [^{31}P – ^{109}Ag] NMR studies of 1：2 complexes and crystal structure of dimeric [{Ag(d2pype)(μ-d2pype)}$_2$][NO_3]$_2$·2CH_2Cl_2 [d2pype = 1,2-bis(di-2-pyridylphosphino)ethane]. *J. Chem. Soc., Dalton Trans.* **1998**, 1743-1750. http://dx.doi.org/10.1039/A709098F

656. Chikkali, S. H.; Gudat, D.; Lissner, F.; Nieger, M.; Schleid, T., Boron templated catechol phosphines as bidentate ligands in silver complexes. *Dalton Trans.* **2007**, 3906-3913. http://dx.doi.org/10.1039/B708252E

657. Doel, C. L.; Gibson, A. M.; Reid, G.; Frampton, C. S., Synthesis and multinuclear NMR studies on copper and silver complexes of multidentate phosphine and mixed phospha/thia ligands. Single crystal structure of [Cu(P2S2)]PF6 (P2S2 = Ph2PCH2CH2SCH2CH2SCH2CH2PPh2). *Polyhedron* **1995,** *14*, 3139-3146. https://doi.org/10.1016/0277-5387(95)00042-Q

658. Hill, A. M.; Levason, W.; Webster, M., Synthesis and 109Ag NMR Studies of Homoleptic Silver(I) Stibines. *Inorg. Chem.* **1996,** *35*, 3428-3430. https://doi.org/10.1021/ic9515618

659. Black, J. R.; Champness, N. R.; Levason, W.; Reid, G., Homoleptic silver(I) complexes with dithio-, diseleno- and ditelluro-ethers: synthesis, structures and multinuclear nuclear magnetic resonance studies. *J. Chem. Soc., Dalton Trans.* **1995**, 3439-3445. http://dx.doi.org/10.1039/DT9950003439

660. Black, J. R.; Champness, N. R.; Levason, W.; Reid, G., Homoleptic Copper(I) and Silver(I) Complexes with o-Phenylene-Backboned Bis(thioethers), Bis(selenoethers), and Bis(telluroethers): Synthesis, Multinuclear NMR Studies, and Crystal Structures of [Cu{o-$C_6H_4(SeMe)_2$}2]PF_6, [Cu{o-$C_6H_4(TeMe)_2$}2]PF_6, and [Agn{μ-o-C_6H4(SeMe)2}$_n${o-$C_6H_4(SeMe)_2$}$_n$]$[BF_4]_n$·nCH_2Cl_2. *Inorg. Chem.* **1996,** *35*, 1820-1824. https://doi.org/10.1021/ic951139r

661. Casa, J.; García Martínez, E.; Sánchez, A.; Sánchez González, A.; Sordo, J.; Casellato, U.; Graziani, R., Complexes of Ag(I) with 1-methyl-2(3H)-imidazolinethione. The crystal structure of tris[1-methyl-2(3H)-imidazolinethione]-silver(I) nitrate. *Inorg. Chim. Acta* **1996,** *241*, 117-123. https://doi.org/10.1016/0020-1693(95)04729-8

662. Ahmad, S.; Isab, A. A.; Perzanowski, H. P., Silver(I) complexes of thiourea. *Transit. Met. Chem.* **2002,** *27*, 782-785. https://doi.org/10.1023/A:1020350023536

663. Ahmad, S.; Isab, A. A.; Ashraf, W., Multinuclear NMR (^{1}H, ^{13}C, ^{15}N and ^{107}Ag) studies of the silver cyanide complexes of thiourea and substituted thioureas. *Inorg. Chem. Commun.* **2002,** *5*, 816-819. https://doi.org/10.1016/S1387-7003(02)00567-1

664. Isab, A. A.; Ahmad, S.; Arab, M., Synthesis of silver(I) complexes of thiones and their characterization by 13C, 15N and 107Ag NMR spectroscopy. *Polyhedron* **2002,** *21*, 1267-1271. https://doi.org/10.1016/S0277-5387(02)00981-6

665. Liao, P.-K.; Liu, K.-G.; Fang, C.-S.; Liu, C. W.; Fackler, J. P.; Wu, Y.-Y., A Copper(I) Homocubane Collapses to a Tetracapped Tetrahedron Upon Hydride Insertion. *Inorg. Chem.* **2011,** *50*, 8410-8417. https://doi.org/10.1021/ic2009896

666. Nomiya, K.; Onoue, K.-I.; Kondoh, Y.; Kasuga, N. C.; Nagano, H.; Oda, M.; Sakuma, S., Synthesis and characterization of oligomeric, anionic thiomalato-silver(I) complexes with biological activities. *Polyhedron* **1995,** *14*, 1359-1367. https://doi.org/10.1016/0277-5387(94)00393-S

667. Leung, B. O.; Jalilehvand, F.; Mah, V.; Parvez, M.; Wu, Q., Silver(I) Complex Formation with Cysteine, Penicillamine, and Glutathione. *Inorg. Chem.* **2013,** *52*, 4593-4602. https://doi.org/10.1021/ic400192c

668. Barreiro, E.; Casas, J. S.; Couce, M. D.; Sánchez, A.; Seoane, R.; Sordo, J.; Varela, J. M.; Vázquez-López, E. M., Synthesis and antimicrobial activities of silver(I) sulfanylcarboxylates. Structural isomers with identically or unequally coordinated Ag centers in an Ag_4S_4 ring. *Dalton Trans.* **2007**, 3074-3085. http://dx.doi.org/10.1039/B702936E

669. Barreiro, E.; Casas, J. S.; Couce, M. D.; Sánchez, A.; Sordo, J.; Varela, J. M.; Vázquez-López, E. M., New structural features in triphenylphosphinesilver(I) sulfanylcarboxylates. *Dalton Trans.* **2005**, 1707-1715. http://dx.doi.org/10.1039/B501309G

670. Ahmad, S.; Isab, A. A., Silver(I) complexes of selenourea (^{13}C and ^{15}N labeled); characterization by ^{13}C, ^{15}N and ^{107}Ag NMR. *Inorg. Chem. Commun.* **2002,** *5*, 355-357. https://doi.org/10.1016/S1387-7003(02)00405-7

671. Ahmad, S.; Isab, A. A.; Arnold, A. P., Synthesis and Spectroscopic Characterization of Silver(I) Complexes of Selenones. *J. Coord. Chem.* **2003,** *56*, 539-544. https://doi.org/10.1080/0095897031000101457

672. Klapötke, T. M.; Krumm, B.; Mayer, P.; Piotrowski, H.; Schwab, I.; Vogt, M., Synthesis and Structures of Triorganotelluronium Pseudohalides. *Eur. .J. Inorg. Chem.* **2002,** *2002*, 2701-2709. https://doi.org/10.1002/1099-0682(200210)2002:10<2701::AID-EJIC2701>3.0.CO;2-G

673. Klapötke, T. M.; Krumm, B.; Moll, R.; Penger, A.; Sproll, S. M.; Berger, R. J. F.; Hayes, S. A.; Mitzel, N. W., Structures of Energetic Acetylene Derivatives HC≡CCH2ONO2, (NO2)3CCH2C≡CCH2C(NO2)3 and Trinitroethane, (NO2)3CCH3. *Z. Naturforsch. B* **2013,** *68*, 719-731. https://doi.org/10.5560/znb.2013-2311

674. Liu, C. W.; Lin, Y.-R.; Fang, C.-S.; Latouche, C.; Kahlal, S.; Saillard, J.-Y., [Ag7(H){E2P(OR)2}6] (E = Se, S): Precursors for the Fabrication of Silver Nanoparticles. *Inorg. Chem.* **2013,** *52*, 2070-2077. https://doi.org/10.1021/ic302482p

675. Liu, C. W.; Chang, H.-W.; Sarkar, B.; Saillard, J.-Y.; Kahlal, S.; Wu, Y.-Y., Stable Silver(I) Hydride Complexes Supported by Diselenophosphate Ligands. *Inorg. Chem.* **2010,** *49*, 468-475. https://doi.org/10.1021/ic901408n

676. Donghi, D.; Maggioni, D.; D'Alfonso, G.; Beringhelli, T., Rhenium–silver bicyclic “spiro” hydrido-carbonyl clusters: NMR investigation of their formation and reversible fragmentation. *J. Organomet. Chem.* **2014,** *751*, 462-470. https://doi.org/10.1016/j.jorganchem.2013.07.002

677. Naumann, D.; Wessel, W.; Hahn, J.; Tyrra, W., Darstellung, NMR-spektroskopische Charakterisierung und reaktionen von perfluoralkylsilber(I)-verbindungen. *J. Organomet. Chem.* **1997,** *547*, 79-88. https://doi.org/10.1016/S0022-328X(97)00105-8

678. Létinois-Halbes, U.; Pale, P.; Berger, S., Triphenylphosphane complex formation with hexyn-1-yl silver. *Magn. Reson. Chem.* **2004,** *42*, 831-834. https://doi.org/10.1002/mrc.1403

679. Eujen, R.; Hoge, B.; Brauer, D. J., Preparation and NMR Spectra of the (Trifluoromethyl)argentates(III) [Ag(CF3)nX4-n]-, with X = CN (n = 1−3), CH3, C:CC6H11, Cl, Br (n = 2, 3), and I (n = 3), and of Related Silver(III) Compounds. Structures of [PPh4][trans-

Ag(CF3)2(CN)2] and [PPh4][Ag(CF3)3(CH3)]. *Inorg. Chem.* **1997,** *36*, 1464-1475. https://doi.org/10.1021/ic9610445

680. Arduengo, A. J.; Dias, H. V. R.; Calabrese, J. C.; Davidson, F., Homoleptic carbene-silver(I) and carbene-copper(I) complexes. *Organometallics* **1993,** *12*, 3405-3409. https://doi.org/10.1021/om00033a009

681. Bildstein, B.; Malaun, M.; Kopacka, H.; Wurst, K.; Mitterböck, M.; Ongania, K.-H.; Opromolla, G.; Zanello, P., N,N'-Diferrocenyl-N-heterocyclic Carbenes and Their Derivatives. *Organometallics* **1999,** *18*, 4325-4336. https://doi.org/10.1021/om990377h

682. Tate, B. K.; Wyss, C. M.; Bacsa, J.; Kluge, K.; Gelbaum, L.; Sadighi, J. P., A dinuclear silver hydride and an umpolung reaction of CO2. *Chem. Sci.* **2013,** *4*, 3068-3074. http://dx.doi.org/10.1039/C3SC50896J

683. Weske, S.; Li, Y.; Wiegmann, S.; John, M., H(C)Ag: a triple resonance NMR experiment for 109Ag detection in labile silver-carbene complexes. *Magn. Reson. Chem.* **2015,** *53*, 291-294. https://doi.org/10.1002/mrc.4196

684. O'Beirne, C.; Althani, H. T.; Dada, O.; Cassidy, J.; Kavanagh, K.; Müller-Bunz, H.; Ortin, Y.; Zhu, X.; Tacke, M., Novel derivatives of the antibiotic NHC–Ag(I) drug candidate SBC3: Synthesis, biological evaluation and 109Ag NMR studies. *Polyhedron* **2018,** *149*, 95-103. https://doi.org/10.1016/j.poly.2018.04.017

685. Dias, H. V. R.; Ayers, A. E., Reactions of divalent group 14 compounds containing an azide functionality: synthesis and characterization of [HB(3,5-(CF3)2Pz)3]AgGe(N3)[(n-Pr)2ATI] and [HB(3,5-(CF3)2Pz)3]AgSn(N3)[(n-Pr)2ATI]. *Polyhedron* **2002,** *21*, 611-618. https://doi.org/10.1016/S0277-5387(01)01022-1

686. Hitchcock, P. B.; Lappert, M. F.; Pierssens, L. J. M., Novel SnII−AgI Reactions from Sn[CH(SiMe3)2]2 and AgX (X = NCS, CN, NCO, or I): SnII−AgI or SnIVX2 Complexes. *Organometallics* **1998,** *17*, 2686-2688. https://doi.org/10.1021/om980086t

687. Johannsen, S.; Megger, N.; Böhme, D.; Sigel, R. K. O.; Müller, J., Solution structure of a DNA double helix with consecutive metal-mediated base pairs. *Nat. Chem.* **2010,** *2*, 229-234. https://doi.org/10.1038/nchem.512

688. Sekabunga, E. J.; Smith, M. L.; Hill, W. E., A variable temperature 31P NMR study of 9-30 atom macrocylic rings of silver(I) with long chain diphosphines. *J. Coord. Chem.* **2005,** *58*, 1187-1198. https://doi.org/10.1080/00958970500095548

689. Seliman, A. A. A.; Altaf, M.; Kawde, A.-N.; Wazeer, M. I. M.; Isab, A. A., NMR and kinetic studies of the interactions of [Au(cis-DACH)Cl2]Cl and [Au(cis-DACH)2]Cl3 with potassium cyanide in aqueous solution. *J. Coord. Chem.* **2014,** *67*, 3431-3443. https://doi.org/10.1080/00958972.2014.971020

690. Joost, M.; Gualco, P.; Coppel, Y.; Miqueu, K.; Kefalidis, C. E.; Maron, L.; Amgoune, A.; Bourissou, D., Direct Evidence for Intermolecular Oxidative Addition of σ(Si□Si) Bonds to Gold. *Angew. Chem. Int. Ed,* **2014,** *53*, 747-751. https://doi.org/10.1002/anie.201307613

691. Joost, M.; Gualco, P.; Coppel, Y.; Miqueu, K.; Kefalidis, C. E.; Maron, L.; Amgoune, A.; Bourissou, D., Direct Evidence for Intermolecular Oxidative Addition of σ(Si□Si) Bonds to Gold. *Angewandte Chemie International Edition* **2014,** *53*, 747-751. https://onlinelibrary.wiley.com/doi/abs/10.1002/anie.201307613

692. Anseau, M. R.; Leung, J. P.; Sahai, N.; Swaddle, T. W., Interactions of Silicate Ions with Zinc(II) and Aluminum(III) in Alkaline Aqueous Solution. *Inorg. Chem.* **2005,** *44*, 8023-8032. https://doi.org/10.1021/ic050594c

693. Li, B.; Nie, Z.; Vijayakumar, M.; Li, G.; Liu, J.; Sprenkle, V.; Wang, W., Ambipolar zinc-polyiodide electrolyte for a high-energy density aqueous redox flow battery. *Nat. Commun.* **2015,** *6*, 6303. https://doi.org/10.1038/ncomms7303

694. Zhang, Y.; Mukherjee, S.; Oldfield, E., 67Zn NMR Chemical Shifts and Electric Field Gradients in Zinc Complexes: A Quantum Chemical Investigation. *J. Am. Chem. Soc.* **2005,** *127*, 2370-2371. https://doi.org/10.1021/ja040242p

695. Lutz, M.; Findeis, B.; Haukka, M.; Graff, R.; Pakkanen, T. A.; Gade, L. H., Metal-metal bonds between group 12 metals and tin: structural characterization of the complete series of Sn-M-Sn (M = Zn, Cd, Hg) heterodimetallic complexes. *Chem. Eur. J.* **2002,** *8*, 3269-3276. http://doi.org/10.1002/1521-3765(20020715)8:14<3269::AID-CHEM3269>3.0.CO;2-W

696. Vinje, J.; Sletten, E., Internal versus terminal metalation of double-helical oligodeoxyribonucleotides. *Chem. Eur. J.* **2006,** *12*, 676-688. http://doi.org/10.1002/chem.200500731

697. Gombler, W.; Lange, H.; Naumann, D., A 113Cd, 19F, and 13C NMR study on perfluoroorganocadmium-diglyme adducts. *J. Magn. Reson.* **1990,** *89*, 10-20. https://doi.org/10.1016/0022-2364(90)90157-5

698. Munakata, M.; Kitagawa, S., Coordination power series of solvents: 2. The solvent effects on complex formations, half-wave potentials, 113Cd NMR resonances and Gibbs free energy changes of transfer. *Inorg. Chim. Acta* **1990,** *169*, 225-234. https://doi.org/10.1016/S0020-1693(00)80522-8

699. Fratiello, A.; Kubo-Anderson, V.; Lee, D. J.; Mao, T.; Ng, K.; Nickolaisen, S.; Perrigan, R. D.; Lucas, V. S.; Tikkanen, W.; Wong, A.; Wong, K., Multinuclear Magnetic Resonance Study of Zinc(II) and Cadmium(II) Complexing with Isothiocyanate. *J. Solution Chem.* **1998,** *27*, 331-359. https://doi.org/10.1023/A:1022675615486

700. Janiak, C.; Deblon, S.; Wu, H.-P.; Kolm, M. J.; Klüfers, P.; Piotrowski, H.; Mayer, P., Modified Bipyridines: 5,5′-Diamino-2,2′-bipyridine Metal Complexes Assembled into Multidimensional Networks via Hydrogen Bonding and π–π Stacking Interactions. *Eur. .J. Inorg. Chem.* **1999,** *1999*, 1507-1521. https://doi.org/10.1002/(SICI)1099-0682(199909)1999:9<1507::AID-EJIC1507>3.0.CO;2-I

701. Dakers, M. A. R.; Hill, M. N. S.; Lockhart, J. C.; Rushton, D. J., Exchange in mixtures of cadmium with bis(benzimidazoles). *J. Chem. Soc., Dalton Trans.* **1994**, 209-213. http://dx.doi.org/10.1039/DT9940000209

702. Darensbourg, D. J.; Billodeaux, D. R.; Perez, L. M., 113Cd NMR Determination of the Binding Parameters of Alicyclic Epoxides to [Hydrotris(3-phenylpyrazol-1-yl)borate]Cd(II) Acetate. *Organometallics* **2004,** *23*, 5286-5290. https://doi.org/10.1021/om049761r

703. Reger, D. L.; Pascui, A. E.; Smith, M. D.; Jezierska, J.; Ozarowski, A., Dinuclear Complexes Containing Linear M–F–M [M = Mn(II), Fe(II), Co(II), Ni(II), Cu(II), Zn(II), Cd(II)] Bridges: Trends in Structures, Antiferromagnetic Superexchange Interactions, and Spectroscopic Properties. *Inorg. Chem.* **2012,** *51*, 11820-11836. https://doi.org/10.1021/ic301757g

704. Chung, K. H.; Moon, C. H., Cadmium-113 nuclear magnetic resonance studies of cadmium(II)—carboxylate complexes in aqueous solution. *J. Chem. Soc., Dalton Trans.* **1996**, 75-78. http://dx.doi.org/10.1039/DT9960000075

705. Dołęga, A.; Walewski, M., Reaction of bis[bis(tri-tert-butoxysilanethiolato) cadmium(II)] with 3,5-dimethylpyridine - 113Cd NMR solution study. *Magn. Reson. Chem.* **2007,** *45*, 410-415. https://doi.org/10.1002/mrc.1983

706. Reger, D. L.; Mason, S. S., Solution state 113Cd NMR investigation of an extensive series of [HB(3,5-Me2pz)3]Cd(alkyl) complexes. *Polyhedron* **1994,** *13*, 3059-3061. https://doi.org/10.1016/S0277-5387(00)83671-2

707. Goodfellow, B. J.; Lima, M. J.; Ascenso, C.; Kennedy, M.; Sikkink, R.; Rusnak, F.; Moura, I.; Moura, J. J. G., The use of 113Cd NMR chemical shifts as a structural probe in tetrathiolate metalloproteins. *Inorg. Chim. Acta* **1998,** *273*, 279-287. https://doi.org/10.1016/S0020-1693(97)06074-X

708. Kordel, J.; Johansson, C.; Drakenberg, T., 113Cd NMR relaxation study of the protein calbindin D9K. *J. Magn. Reson.* **1992,** *100*, 581-587. https://doi.org/10.1016/0022-2364(92)90063-D

709. Narula, S. S.; Armitage, I. M.; Brouwer, M.; Enghild, J. J., Establishment of two distinct protein domains in blue crab Callinectes sapidus metallothionein-I through heteronuclear (1H□113Cd) and homonuclear 1H□1H) correlation NMR experiments. *Magn. Reson. Chem.* **1993,** *31*, S96-S103. https://doi.org/10.1002/mrc.1260311319

710. Scheller, J. S.; Irvine, G. W.; Stillman, M. J., Unravelling the mechanistic details of metal binding to mammalian metallothioneins from stoichiometric, kinetic, and binding affinity data. *Dalton Trans.* **2018,** *47*, 3613-3637. http://dx.doi.org/10.1039/C7DT03319B

711. Shaw Iii, C. F.; He, L.; Muñoz, A.; Savas, M. M.; Chi, S.; Fink, C. L.; Gan, T.; Petering, D. H., Kinetics of reversible N-ethylmaleimide alkylation of metallothionein and the subsequent metal release. *J. Biol. Inorg. Chem.* **1997,** *2*, 65-73. https://doi.org/10.1007/s007750050107

712. Stachura, M.; Chakraborty, S.; Gottberg, A.; Ruckthong, L.; Pecoraro, V. L.; Hemmingsen, L., Direct Observation of Nanosecond Water Exchange Dynamics at a Protein Metal Site. *J. Am. Chem. Soc.* **2017,** *139*, 79-82. https://doi.org/10.1021/jacs.6b11525

713. van Roon, A.-M. M.; Yang, J.-C.; Mathieu, D.; Bermel, W.; Nagai, K.; Neuhaus, D., 113Cd NMR Experiments Reveal an Unusual Metal Cluster in the Solution Structure of the Yeast Splicing Protein Bud31p. *Angew. Chem. Int. Ed.* **2015,** *54*, 4861-4864. https://doi.org/10.1002/anie.201412210

714. Malandrinos, G.; Louloudi, M.; Mitsopoulou, C. A.; Butler, I. S.; Bau, R.; Hadjiliadis, N., On the mechanism of action of thiamin enzymes, Crystal structure of 2-(α-hydroxyethyl)thiamin pyrophosphate (HETPP). Complexes of HETPP with zinc(II) and cadmium(II). *J. Biol. Inorg. Chem.* **1998,** *3*, 437-448. https://doi.org/10.1007/s007750050253

715. Omburo, G. A.; Mullins, L. S.; Raushel, F. M., Structural characterization of the divalent cation sites of bacterial phosphotriesterase by cadmium-113 NMR spectroscopy. *Biochemistry* **1993,** *32*, 9148-9155. https://doi.org/10.1021/bi00086a021

716. Dodi, K.; Louloudi, M.; Malandrinos, G.; Hadjiliadis, N., Metal complexes with 2-(α-hydroxy-benzyl) thiamin pyrophosphate (HBTPP). Models for metal binding of thiamin enzymes. *J. Inorg. Biochem.* **1999,** *73*, 41-47. https://doi.org/10.1016/S0162-0134(98)10089-2

717. Iranzo, O.; Khalili, H.; Epstein, D. M.; Morrow, J. R., Recruitment of divalent metal ions by incorporation of 4-thio-2′-deoxythymidine or 4-thio-2′-deoxyuridine into DNA. *J. Biol. Inorg. Chem.* **2004,** *9*, 462-470. https://doi.org/10.1007/s00775-004-0545-0

718. Jalilehvand, F.; Amini, Z.; Parmar, K.; Kang, E. Y., Cadmium(ii) N-acetylcysteine complex formation in aqueous solution. *Dalton Trans.* **2011,** *40*, 12771-12778. http://dx.doi.org/10.1039/C1DT11705J

719. Sola, M., Cadmium-113 and carbon-13 NMR of cadmium(II) transferrins. *Inorg. Chem.* **1990,** *29*, 1113-1116. https://doi.org/10.1021/ic00331a002

720. Hemmingsen, L.; Olsen, L.; Antony, J.; Sauer, S. P. A., First principle calculations of 113Cd chemical shifts for proteins and model systems. *J. Biol. Inorg. Chem.* **2004,** *9*, 591-599. https://doi.org/10.1007/s00775-004-0553-0

721. Kidambi, S.; Ramamoorthy, A., Quantum Chemical Calculations of Cadmium Chemical Shifts in Inorganic Complexes. *J. Phys. Chem. A* **2002,** *106*, 10363-10369. https://doi.org/10.1021/jp0265891

722. Kirchmann, M.; Eichele, K.; Wesemann, L., Homoleptic Cadmium and Mercury Compounds of Stanna-closo-dodecaborate. *Inorg. Chem.* **2008,** *47*, 5988-5991. https://doi.org/10.1021/ic800357z

723. Wrackmeyer, B.; Contreras, R., 199Hg NMR Parameters. *Annu. Rep. NMR Spectrosc.* **1992,** *24*, 267-329. https://doi.org/10.1016/S0066-4103(08)60200-8

724. Bebout, D. C.; Berry, S. M., Probing Mercury Complex Speciation with Multinuclear NMR. *Struct. Bond.* **2006,** *120*, 81-105. https://doi.org/10.1007/430_017

725. Maliarik, M.; Persson, I., The solvation of the mercury(II) ion—a 199Hg NMR study. *Magn. Reson. Chem.* **2005,** *43*, 835-842. https://doi.org/10.1002/mrc.1625

726. Nilsson, K. B.; Maliarik, M.; Persson, I.; Fischer, A.; Ullström, A.-S.; Eriksson, L.; Sandström, M., Coordination Chemistry of Mercury(II) in Liquid and Aqueous Ammonia Solution and the Crystal Structure of Tetraamminemercury(II) Perchlorate. *Inorg. Chem.* **2008,** *47*, 1953-1964. https://doi.org/10.1021/ic7013489

727. Nilsson, K. B.; Maliarik, M.; Persson, I.; Sandström, M., Structure of solvated mercury(ii) halides in liquid ammonia, triethyl phosphite and tri-n-butylphosphine solution. *Dalton Trans.* **2008**, 2303-2313. http://dx.doi.org/10.1039/B716134D

728. Klose, G.; Volke, F.; Peinel, G.; Knobloch, G., 199Hg NMR of aqueous solutions of inorganic mercury salts. Chemical shifts of HgCl2 − n with n = 0–4. *Magn. Reson. Chem.* **1993,** *31*, 548-551. https://doi.org/10.1002/mrc.1260310606

729. Karhu, A. J.; Rautiainen, J. M.; Oilunkaniemi, R.; Chivers, T.; Laitinen, R. S., Mercury- and Cadmium-Assisted [2 + 2] Cyclodimerization of tert-Butylselenium Diimide. *Inorg. Chem.* **2015,** *54*, 9499-9508. https://doi.org/10.1021/acs.inorgchem.5b01434

730. Bernatowicz, P.; Szymański, S.; Wrackmeyer, B., Cross-Correlation of Nuclear Quadrupolar Interactions as a Probe in Structure Elucidation: Liquid-Phase Nuclear Magnetic Resonance Studies on Bis(hexamethyldisilylamido)mercury(II). *J. Phys. Chem. A* **2001,** *105*, 6414-6419. https://doi.org/10.1021/jp010707n

731. Wilker, J. J.; Wetterhahn, K. E.; Lippard, S. J., Methyl Transfer to Mercury Thiolates: Effects of Coordination Number and Ligand Dissociation. *Inorg. Chem.* **1997,** *36*, 2079-2083. https://doi.org/10.1021/ic961178i

732. Helm, M. L.; Helton, G. P.; VanDerveer, D. G.; Grant, G. J., Mercury-199 NMR Studies of Thiacrown and Related Macrocyclic Complexes: The Crystal Structures of [Hg(18S6)](PF6)2 and [Hg(9N3)2](ClO4)2. *Inorg. Chem.* **2005,** *44*, 5696-5705. https://doi.org/10.1021/ic050500z

733. Bardin, V. V., The dependence of ^{199}Hg NMR spectra of polyfluoroarylmercurials ArFHgR on solvent, concentration, temperature, and ligands. *Magn. Reson. Chem.* **2018,** *56*, 1124-1130. https://doi.org/10.1002/mrc.4755

734. Vieco, F. S. H.; Hiramatsu, N. M.; Tedeschi, E.; Rezende, D. d. B.; de Arruda Campos, I. P., The γ-cis Effect in the Mercury-199 NMR Spectroscopy of Substituted Vinylmercury Halides. *J. Chem. Res.* **2002,** *2002*, 25-27. https://doi.org/10.3184/030823402103170358

735. Gryff-Keller, A.; Kraska-Dziadecka, A.; Molchanov, S.; Wodyński, A., Shielding and Indirect Spin–Spin Coupling Tensors in the Presence of a Heavy Atom: An Experimental and Theoretical Study of Bis(phenylethynyl)mercury. *J. Phys. Chem. A* **2012,** *116*, 10615-10620. https://doi.org/10.1021/jp307828e

736. Gryff-Keller, A.; Molchanov, S., Carbon-13 and mercury-199 nuclear spin relaxation study on solution dynamics of the bis(phenylethynyl)mercury molecule and shielding anisotropy of its acetyleniccarbon and mercury nuclei. *Magn. Reson. Chem.* **2000,** *38*, 17-22. https://doi.org/10.1002/(SICI)1097-458X(200001)38:1<17::AID-MRC603>3.0.CO;2-V

737. Breitinger, D. K.; Krumphanzl, U.; Moll, M., Vibrational and multinuclear NMR spectra of anionic mercuriomethanes $[CH_{4-n}(HgX)_n]_n$. *J. Mol. Struct.* **1990,** *218*, 27-32. https://doi.org/10.1016/0022-2860(90)80239-G

738. Cano, M.; Campo, J. A.; Le Gall, J. Y.; Pichon, R.; Salaun, J. Y.; Kubicki, M. M., Molybdenum-mercury bond. NMR (^{199}Hg, ^{31}P, ^{1}H) and IR study on[$(C_5H_5)(CO)_2$LMoHgZ] (L · P(4-X-$C_6H_4)_3$ (X · F, Cl, Me, OMe), $P(CH_2CH_3)_3$, $P(CH_2CH_2CN)_3$; Z · Cl, I, $(C_5H_5)(CO)_2$LMo) complexes. *Inorg. Chim. Acta* **1992,** *193*, 207-212. https://doi.org/10.1016/S0020-1693(00)80354-0

739. Cotton, J. D.; Miles, E. A., Steric effects of tertiary phosphines on 199Hg chemical shifts in [{(η5-C5H5)(CO)2(L)Mo}2Hg] complexes. *Inorg. Chim. Acta* **1990,** *173*, 129-130. https://doi.org/10.1016/S0020-1693(00)80201-7

740. Cano, M.; Campo, J. A.; Pinilla, E.; Monge, A.; Pichon, R.; Salaün, J.-Y.; L'Haridon, P.; Szymoniak, J.; Kubicki, M. M., Effects of substitutions on cyclopentadienyl rings in complexes with molybdenum-mercury bonds. ^{95}Mo and ^{199}Hg NMR studies. *Inorg. Chim. Acta* **1995,** *228*, 251-254. https://doi.org/10.1016/0020-1693(94)04172-R

741. Jalilehvand, F.; Leung, B. O.; Izadifard, M.; Damian, E., Mercury(II) Cysteine Complexes in Alkaline Aqueous Solution. *Inorg. Chem.* **2006,** *45*, 66-73. https://doi.org/10.1021/ic0508932

742. Mah, V.; Jalilehvand, F., Mercury(II) complex formation with glutathione in alkaline aqueous solution. *J. Biol. Inorg. Chem.* **2008,** *13*, 541-553. https://doi.org/10.1007/s00775-008-0342-2

743. Dairaku, T.; Furuita, K.; Sato, H.; Šebera, J.; Yamanaka, D.; Otaki, H.; Kikkawa, S.; Kondo, Y.; Katahira, R.; Matthias Bickelhaupt, F.; Fonseca Guerra, C.; Ono, A.; Sychrovský, V.; Kojima, C.; Tanaka, Y., Direct detection of the mercury–nitrogen bond in the thymine–HgII–thymine base-pair with 199Hg NMR spectroscopy. *Chem. Commun.* **2015,** *51*, 8488-8491. http://dx.doi.org/10.1039/C5CC02423D

744. Utschig, L. M.; Wright, J. G.; Dieckmann, G.; Pecoraro, V.; O'Halloran, T. V., The 199Hg Chemical Shift as a Probe of Coordination Environments in Blue Copper Proteins. *Inorg. Chem.* **1995,** *34*, 2497-2498. https://doi.org/10.1021/ic00114a004

745. Utschig, L.; Bryson, J.; O'Halloran, T., Mercury-199 NMR of the metal receptor site in MerR and its protein-DNA complex. *Science* **1995,** *268*, 380-385. https://doi.org/10.1126/science.7716541

746. Flórez, E.; Maldonado, A. F.; Aucar, G. A.; David, J.; Restrepo, A., Microsolvation of methylmercury: structures, energies, bonding and NMR constants (199Hg, 13C and 17O). *Phys. Chem. Chem. Phys.* **2016,** *18*, 1537-1550. http://dx.doi.org/10.1039/C5CP04826E

747. Froeystein, N. A.; Sletten, E., Interaction of Mercury(II) with the DNA Dodecamer CGCGAATTCGCG. A 1H and 15N NMR Study. *J. Am. Chem. Soc.* **1994,** *116*, 3240-3250. https://doi.org/10.1021/ja00087a009

748. Tanaka, Y.; Oda, S.; Yamaguchi, H.; Kondo, Y.; Kojima, C.; Ono, A., 15N-15N J-Coupling Across HgII: Direct Observation of HgII-Mediated T-T Base Pairs in a DNA Duplex. *J. Am. Chem. Soc.* **2007,** *129*, 244-245. https://doi.org/10.1021/ja065552h

749. Egorochkin, A. N.; Kuznetsova, O. V.; Khamaletdinova, N. M.; Kurskii, Y. A.; Domratcheva-Lvova, L. G.; Domrachev, G. A., Transition metal NMR chemical shifts and polarizability effect in organometallic complexes. *Magn. Reson. Chem.* **2009,** *47*, 782-790. https://doi.org/10.1002/mrc.2465

750. Egorochkin, A. N.; Kuznetsova, O. V.; Khamaletdinova, N. M.; Kurskii, Y. A., NMR spectroscopy on heavy nuclei of transition metal complexes. The role of polarization effect. *Rus. J. Gen. Chem.* **2011,** *81*, 2450-2458. https://doi.org/10.1134/S1070363211120061

751. Egorochkin, A. N.; Kuznetsova, O. V.; Khamaletdinova, N. M.; Domratcheva-Lvova, L. G.; Domrachev, G. A., Polarizability effect in transition metal carbonyl complexes. *J. Organomet. Chem.* **2009,** *694*, 1447-1452. https://doi.org/10.1016/j.jorganchem.2008.12.035

752. Thakur, A.; Sao, S.; Ramkumar, V.; Ghosh, S., Novel Class of Heterometallic Cubane and Boride Clusters Containing Heavier Group 16 Elements. *Inorg. Chem.* **2012,** *51*, 8322-8330. https://doi.org/10.1021/ic3008602

753. Agustin, D.; Ehses, M., ^{119}Sn NMR spectroscopic and structural properties of transition metal complexes with terminal stannylene ligands. *C. R. Chim.* **2009,** *12*, 1189-1227. https://doi.org/10.1016/j.crci.2009.04.004

754. Eichler, B. E.; Phillips, A. D.; Haubrich, S. T.; Mork, B. V.; Power, P. P., Synthesis, Structures, and Spectroscopy of the Metallostannylenes (η5-C5H5)(CO)3M−S̈n−C6H3-2,6-Ar2 (M = Cr, Mo, W; Ar = C6H2-2,4,6-Me3, C6H2-2,4,6-Pri3). *Organometallics* **2002,** *21*, 5622-5627. https://doi.org/10.1021/om020583g

755. Pazderski, L., 15N and 31P NMR Coordination Shifts in Transition Metal Complexes with Nitrogen- and Phosphorus-Containing Heterocycles. *Annu. Rep. NMR Spectrosc.* **2013,** *80*, 33-179. https://doi.org/10.1016/B978-0-12-408097-3.00002-0

756. Bradley, D. C.; Hodge, S. R.; Runnacles, J. D.; Hughes, M.; Mason, J.; Richards, R. L., Nitrogen nuclear magnetic resonance spectroscopy as a probe of bonding, bending and fluxionality of the imido ligand. *J. Chem. Soc., Dalton Trans.* **1992**, 1663-1668. http://dx.doi.org/10.1039/DT9920001663

757. Pazderski, L., 15N NMR coordination shifts in Pd(II), Pt(II), Au(III), Co(III), Rh(III), Ir(III), Pd(IV), and Pt(IV) complexes with pyridine, 2,2′-bipyridine, 1,10-phenanthroline, quinoline, isoquinoline, 2,2′-biquinoline, 2,2′:6′, 2′-terpyridine and their alkyl or aryl derivatives. *Magn. Reson. Chem.* **2008,** *46*, S3-S15. https://doi.org/10.1002/mrc.2301

758. Pazderski, L., 15N and 31P NMR Coordination Shifts in Transition Metal Complexes with Nitrogen- and Phosphorus-Containing Heterocycles. In *Annu. Rep. NMR Spectrosc.*, Webb, G. A., Ed. Academic Press: 2013; pp 33-179. https://doi.org/10.1016/B978-0-12-408097-3.00002-0

759. Aizawa, S.-i.; Matsuda, K.; Tajima, T.; Maeda, M.; Sugata, T.; Funahashi, S., Variable-Temperature and -Pressure Multinuclear Magnetic Resonance Studies on Solvent Exchange of Cobalt(II), Iron(II), and Manganese(II) Ions in Ethylenediamine. Kinetic Chelate Effect and Chelate Strain Effect. *Inorg. Chem.* **1995,** *34*, 2042-2047. https://doi.org/10.1021/ic00112a015

760. Sen-ichi, A.; Shigeo, I.; Kayoko, M.; Shigenobu, F., Variable-Temperature and -Pressure Nitrogen-14 Magnetic Resonance Studies on Solvent Exchange of Nickel(II), Iron(II), and Manganese(II) Ions in Neat 1,3-Propanediamine and n-Propylamine. *Bull. Chem. Soc. Jpn.* **1997,** *70*, 1593-1597. https://doi.org/10.1246/bcsj.70.1593

761. Hannan, J. P.; Whittaker, S. B. M.; Hemmings, A. M.; James, R.; Kleanthous, C.; Moore, G. R., NMR studies of metal ion binding to the Zn-finger-like HNH motif of colicin E9. *J. Inorg. Biochem.* **2000,** *79*, 365-370. https://doi.org/10.1016/S0162-0134(99)00235-4

762. Jørgensen, L. E.; Ubbink, M.; Danielsen, E., Amicyanin metal-site structure and interaction with MADH: PAC and NMR spectroscopy of Ag-, Cd-, and Cu-amicyanin. *J. Biol. Inorg. Chem.* **2004,** *9*, 27-38. https://doi.org/10.1007/s00775-003-0493-0

763. Trujillo, L. D. C.; Jios, J. L.; Franca, C. A.; Güida, J. A., New NMR investigation of [RuF5NO]2− anion. *Inorg. Chim. Acta* **2018,** *477*, 130-134. https://doi.org/10.1016/j.ica.2018.03.010

764. Roodt, A.; Leipoldt, J. G.; Helm, L.; Merbach, A. E., Equilibrium behavior and proton transfer kinetics of the dioxotetracyanometalate complexes of molybdenum(IV), tungsten(IV), technetium(V), and rhenium(V): carbon-13 and oxygen-17 NMR study. *Inorg. Chem.* **1994,** *33*, 140-147. https://doi.org/10.1021/ic00079a026

765. Roodt, A.; Leipoldt, J. G.; Helm, L.; Abou-Hamdan, A.; Merbach, A. E., Kinetics and Mechanism of Oxygen Exchange and Inversion along the M:O Axis in the Diprotonated and Monoprotonated Dioxotetracyanometalate Complexes of Re(V), Tc(V), W(IV), and Mo(IV). *Inorg. Chem.* **1995,** *34*, 560-568. https://doi.org/10.1021/ic00107a007

766. Gonzalez, G.; Moullet, B.; Martinez, M.; Merbach, A. E., Steric Effects on Water-Exchange Mechanisms of Aquapentakis(amine)metal(III) Complexes (Metal = Chromium, Cobalt, Rhodium). A Variable-Pressure Oxygen-17 NMR Study. *Inorg. Chem.* **1994,** *33*, 2330-2333. https://doi.org/10.1021/ic00089a005

767. Maigut, J.; Meier, R.; Zahl, A.; van Eldik, R., Effect of Chelate Dynamics on Water Exchange Reactions of Paramagnetic Aminopolycarboxylate Complexes. *Inorganic Chemistry* **2008,** *47*, 5702-5719. https://doi.org/10.1021/ic702421z

768. Helm, L.; Nicolle, G. M.; Merbach, R. E., WATER AND PROTON EXCHANGE PROCESSES ON METAL IONS. *Adv. Inorg. Chem.* **2005,** *57*, 327-379. https://doi.org/10.1016/S0898-8838(05)57007-7

769. O'Halloran, K. P.; Zhao, C.; Ando, N. S.; Schultz, A. J.; Koetzle, T. F.; Piccoli, P. M. B.; Hedman, B.; Hodgson, K. O.; Bobyr, E.; Kirk, M. L.; Knottenbelt, S.; Depperman, E. C.; Stein,

B.; Anderson, T. M.; Cao, R.; Geletii, Y. V.; Hardcastle, K. I.; Musaev, D. G.; Neiwert, W. A.; Fang, X.; Morokuma, K.; Wu, S.; Kögerler, P.; Hill, C. L., Revisiting the Polyoxometalate-Based Late-Transition-Metal-Oxo Complexes: The "Oxo Wall" Stands. *Inorg. Chem.* **2012,** *51*, 7025-7031. https://doi.org/10.1021/ic2008914

770. Winkler, J. R.; Gray, H. B., Electronic Structures of Oxo-Metal Ions. *Struct. Bond.* **2012,** *142*, 17-28. https://doi.org/10.1007/430_2011_55

771. Abe, M.; Isobe, K.; Kida, K.; Nagasawa, A.; Yagasaki, A., Intramolecular rearrangements of cyclooctadienerhodium(I) fragments supported on a vanadium oxide cluster as evidenced by dynamic 17O NMR spectroscopy. *J. Clust. Sci.* **1994,** *5*, 565-571. https://doi.org/10.1007/BF01171386

772. Kolehmainen, E.; Laihia, K.; Rybinskaya, M. I.; Kaganovich, V. S.; Kerzina, Z. A., Comparative multinuclear magnetic resonance spectroscopic study of transition metal (Cr, W and Mn) mesitylene tricarbonyls and transition metal (Ru and Co) carbonyl clusters. *J. Organomet. Chem.* **1993,** *453*, 273-278. https://doi.org/10.1016/0022-328X(93)83122-C

773. Kony, M.; Brownlee, R. T. C.; Wedd, A. G., Complexes of tetrathiomolybdate and -tungstate with copper(I) and silver(I): sulfur-33 NMR properties. *Inorg. Chem.* **1992,** *31*, 2281-2282. https://doi.org/10.1021/ic00037a052

774. Schreckenbach, G.; Ziegler, T., Density functional calculations of NMR chemical shifts and ESR g-tensors. *Theor. Chem. Acc.* **1998,** *99*, 71-82. https://doi.org/10.1007/s002140050306

775. Bühl, M.; Kaupp, M.; Malkina, O. L.; Malkin, V. G., The DFT route to NMR chemical shifts. *J. Comput. Chem.* **1999,** *20*, 91-105. https://doi.org/10.1002/(SICI)1096-987X(19990115)20:1<91::AID-JCC10>3.0.CO;2-C

776. Autschbach, J., The Calculation of NMR Parameters in Transition Metal Complexes in *Principles and Applications of Density Functional Theory in Inorganic Chemistry I*. *Struct. Chem.* **2004,** *112*, 1-48. https://doi.org/10.1007/b97936

777. Bühl, M., NMR of Transition Metal Compounds. In *Calculation of NMR and EPR Parameters*, Kaupp, M.; Bühl, M.; Malkin, V. G., Eds. 2004; pp 421-431. https://doi.org/10.1002/3527601678.ch26

778. Barquera-Lozada, J. E.; Obenhuber, A.; Hauf, C.; Scherer, W., On the Chemical Shifts of Agostic Protons. *J. Phys. Chem. A* **2013,** *117*, 4304-4315. https://doi.org/10.1021/jp4013174

779. Weller, A. S.; Fehlner, T. P., Molecular Orbital Analysis of the Trend in 11B NMR Chemical Shifts for (Cp*M)2B5H9 (M = Cr, Mo, W; Cp* = η5-C5Me5). *Organometallics* **1999,** *18*, 447-450. https://doi.org/10.1021/om980808g

780. Bühl, M.; Holub, J.; Hnyk, D.; Macháček, J., Computational Studies of Structures and Properties of Metallaboranes. 2. Transition-Metal Dicarbollide Complexes. *Organometallics* **2006,** *25*, 2173-2181. https://doi.org/10.1021/om051025f

781. Grigoleit, S.; Bühl, M., Thermal Effects and Vibrational Corrections to Transition Metal NMR Chemical Shifts. *Chem. Eur. J.* **2004,** *10*, 5541-5552. https://doi.org/10.1002/chem.200400256

782. Pastor, A.; Martínez-Viviente, E., NMR spectroscopy in coordination supramolecular chemistry: A unique and powerful methodology. *Coord. Chem. Rev.* **2008,** *252*, 2314-2345. https://doi.org/10.1016/j.ccr.2008.01.025

783. Lu, T.; Liu, Z.; Steren, C. A.; Fei, F.; Cook, T. M.; Chen, X.-T.; Xue, Z.-L., Synthesis, structural characterization and NMR studies of group 10 metal complexes with macrocyclic amine N-heterocyclic carbene ligands. *Dalton Trans.* **2018,** *47*, 4282-4292. http://dx.doi.org/10.1039/C7DT04666A

784. Chen, S.-J.; Li, J.; Dougan, B. A.; Steren, C. A.; Wang, X.; Chen, X.-T.; Lin, Z.; Xue, Z.-L., Unexpected formation of a trinuclear complex containing a Ta(IV)–Ta(IV) bond in the reactions of $Bu^tN{=}Ta(NMe_2)_3$ with silanes. *Chem. Commun.* **2011,** *47*, 8685-8687. http://dx.doi.org/10.1039/C1CC12837J

785. Chen, S.-J.; Abbott, J. K. C.; Steren, C. A.; Xue, Z.-L., Synthesis, Characterization, and Crystal Structures of Metal Amide Cage Complexes Containing a M_4O_4 (M = Nb, Ta) Core Unit. *J. Clust. Sci.* **2010,** *21*, 325-337. https://doi.org/10.1007/s10876-010-0297-7

786. Lu, T.; Yang, C.-F.; Steren, C. A.; Fei, F.; Chen, X.-T.; Xue, Z.-L., Synthesis and characterization of Ag(i) and Au(i) complexes with macrocyclic hybrid amine N-heterocyclic carbene ligands. *New J. Chem.* **2018,** *42*, 4700-4713. http://dx.doi.org/10.1039/C7NJ04020B

787. Nolis, P.; Parella, T., Practical aspects of the simultaneous collection of COSY and TOCSY spectra. *Magn. Reson. Chem.* **2019,** *57*, S85-S94. https://doi.org/10.1002/mrc.4835

788. Williamson, M. P., NOESY. In *eMagRes*, 2009. https://doi.org/10.1002/9780470034590.emrstm0347.pub2

789. Liu, X.; Li, L.; Diminnie, J. B.; Yap, G. P. A.; Rheingold, A. L.; Xue, Z., Reactivities of a Bis(alkylidene) Complex. Synthesis of a Silyl Bis(alkylidyne) Complex and a Reaction Cycle among Symmetric Bis(alkylidyne), Bis(alkylidene), and Nonsymmetric Bis(alkylidyne) Compounds. *Organometallics* **1998,** *17*, 4597-4606. https://doi.org/10.1021/om980652k

790. Macchioni, A., Elucidation of the Solution Structures of Transition Metal Complex Ion Pairs by NOE NMR Experiments. *Eur. .J. Inorg. Chem.* **2003,** *2003*, 195-205. https://doi.org/10.1002/ejic.200390026

791. Orrell, K. G., Two-Dimensional Methods of Monitoring Exchange. In *eMagRes*, 2007. https://doi.org/10.1002/9780470034590.emrstm0580

792. García, J.; Martins, L. G.; Pons, M., NMR Spectroscopy in Solution. In *Supramolecular Chemistry*, 2012. https://doi.org/10.1002/9780470661345.smc019

793. Chen, T.; Wu, Z.; Li, L.; Sorasaenee, K. R.; Diminnie, J. B.; Pan, H.; Guzei, I. A.; Rheingold, A. L.; Xue, Z., Direct Observation of an Equilibrium between $(Bu^tCH_2)_2W(CBu^t)(SiBu^tPh_2)$ and $(Bu^tCH_2)W(CHBu^t)_2(SiBu^tPh_2)$ and an Unusual Silyl Migration. *J. Am. Chem. Soc.* **1998,** *120*, 13519-13520. https://doi.org/10.1021/ja982571l

794. Chen, T.; Zhang, X.-H.; Wang, C.; Chen, S.; Wu, Z.; Li, L.; Sorasaenee, K. R.; Diminnie, J. B.; Pan, H.; Guzei, I. A.; Rheingold, A. L.; Wu, Y.-D.; Xue, Z.-L., A Tungsten Silyl Alkylidyne Complex and Its Bis(alkylidene) Tautomer. Their Interconversion and an Unusual Silyl Migration in Their Reaction with Dioxygen. *Organometallics* **2005,** *24*, 1214-1224. https://doi.org/10.1021/om049031j

795. Bertini, I.; Felli, I. C.; Kümmerle, R.; Moskau, D.; Pierattelli, R., $^{13}C-^{13}C$ NOESY: An Attractive Alternative for Studying Large Macromolecules. *J. Am. Chem. Soc.* **2004,** *126*, 464-465. https://doi.org/10.1021/ja0357036

796. Ghini, V.; Chevance, S.; Turano, P., About the use of 13C-13C NOESY in bioinorganic chemistry. *J. Inorg. Biochem.* **2019,** *192*, 25-32. https://doi.org/10.1016/j.jinorgbio.2018.12.006

797. Bax, A.; Grzesiek, S., ROESY In *eMagRes*, 2007. https://doi.org/10.1002/9780470034590.emrstm0473

798. Biasiolo, L.; Belpassi, L.; Ciancaleoni, G.; Macchioni, A.; Tarantelli, F.; Zuccaccia, D., Diffusion NMR measurements on cationic linear gold(I) complexes. *Polyhedron* **2015,** *92*, 52-59. https://doi.org/10.1016/j.poly.2015.03.007

799. Zuccaccia, D.; Belpassi, L.; Tarantelli, F.; Macchioni, A., Ion Pairing in Cationic Olefin−Gold(I) Complexes. *J. Am. Chem. Soc.* **2009,** *131*, 3170-3171. https://doi.org/10.1021/ja809998y

800. Biasiolo, L.; Ciancaleoni, G.; Belpassi, L.; Bistoni, G.; Macchioni, A.; Tarantelli, F.; Zuccaccia, D., Relationship between the anion/cation relative orientation and the catalytic activity of nitrogen acyclic carbene–gold catalysts. *Catal. Sci. Technol.* **2015,** *5*, 1558-1567. http://dx.doi.org/10.1039/C4CY01440E

801. Raya-Barón, Á.; Oña-Burgos, P.; Fernández, I., Chapter Three - Diffusion NMR spectroscopy applied to coordination and organometallic compounds. *Annu. Rep. NMR Spectrosc.* **2019,** *98*, 125-191. https://doi.org/10.1016/bs.arnmr.2019.04.004

802. Martínez-Viviente, E.; Rüegger, H.; Pregosin, P. S.; López-Serrano, J., 31P and 35Cl PGSE Diffusion Studies on Phosphine Ligands and Selected Organometallic Complexes. Solvent Dependence of Ion Pairing. *Organometallics* **2002,** *21*, 5841-5846. https://doi.org/10.1021/om020613f

803. Fernández, E. J.; Laguna, A.; Monge, M.; Montiel, M.; Olmos, M. E.; Pérez, J.; Sánchez-Forcada, E., Dendritic (phosphine)gold(i) thiolate complexes: assessment of the molecular size through PGSE NMR studies. *Dalton Trans.* **2009**, 474-480. http://dx.doi.org/10.1039/B812500G

804. Crockett, M. P.; Zhang, H.; Thomas, C. M.; Byers, J. A., Adding diffusion ordered NMR spectroscopy (DOSY) to the arsenal for characterizing paramagnetic complexes. *Chem. Commun.* **2019,** *55*, 14426-14429. http://dx.doi.org/10.1039/C9CC08229H

805. Cox, N.; Nalepa, A.; Lubitz, W.; Savitsky, A., ELDOR-detected NMR: A general and robust method for electron-nuclear hyperfine spectroscopy? *J. Magn. Reson.* **2017,** *280*, 63-78. https://doi.org/10.1016/j.jmr.2017.04.006

806. Dikanov, S. A.; Taguchi, A. T., Influence of Hyperfine Coupling Strain on Two-Dimensional ESEEM Spectra from I = 1/2 Nuclei. *Appl. Magn. Reson.* **2020,** *51*, 1177-1200. https://doi.org/10.1007/s00723-020-01246-6

807. Cutsail, G. E.; Telser, J.; Hoffman, B. M., Advanced paramagnetic resonance spectroscopies of iron–sulfur proteins: Electron nuclear double resonance (ENDOR) and electron spin echo envelope modulation (ESEEM). *Biochim. Biophys. Acta Mol. Cell Res.* **2015,** *1853*, 1370-1394. https://doi.org/10.1016/j.bbamcr.2015.01.025

808. Murphy, D. M.; Farley, R. D., Principles and applications of ENDOR spectroscopy for structure determination in solution and disordered matrices. *Chem. Soc. Rev.* **2006,** *35*, 249-268. http://dx.doi.org/10.1039/B500509B

809. Hoffman, B. M., ENDOR of Metalloenzymes. *Acc. Chem. Res.* **2003,** *36*, 522-529. https://doi.org/10.1021/ar0202565

810. Nietlispach, D.; Bakhmutov, V. I.; Berke, H., Deuterium quadrupole coupling constants and ionic bond character in transition metal hydride complexes from 2H NMR T1 relaxation data in solution. *J. Am. Chem. Soc.* **1993,** *115*, 9191-9195. https://doi.org/10.1021/ja00073a038

811. Wang, S. P.; Yuan, P.; Schwartz, M., NMR relaxation and π bonding in group 6 transition-metal hexacarbonyls. *Inorg. Chem.* **1990,** *29*, 484-487. https://doi.org/10.1021/ic00328a029

812. Wang, K. S.; Wang, D.; Yang, K.; Richmond, M. G.; Schwartz, M., Directional Effects of CO .pi. Bonding in Group VIB Pentacarbonyl Amines. *Inorg. Chem.* **1995,** *34*, 3241-3244. https://doi.org/10.1021/ic00116a016

813. Robertson, G. P.; Odell, B.; Kuprov, I.; Dixon, D. J.; Claridge, T. D. W., Measuring Spin Relaxation Rates Using Satellite Exchange NMR Spectroscopy. *Angew. Chem. Int. Ed.* **2018,** *57*, 7498-7502. https://doi.org/10.1002/anie.201801322

814. Jackman, L. M.; Cotton, F. A., *Dynamic Nuclear Magnetic Resonance Spectroscopy*. 1975; Academic Press: New York.

815. Sandstrom, J., *Dynamic NMR Spectroscopy*. 1982; Academic Press: London.

816. Macomber, R. S., *A Complete Introduction to Modern NMR Spectroscopy*. 1998; Wiley: New York.

817. Fernández, I.; Pregosin, P. S.; Albinati, A.; Rizzato, S., X-ray Diffraction, PGSE Diffusion, and Related NMR Studies on a Series of Cp*-Based Ru(IV)(Cp*)(η3-CH2−CH−CHPh) Allyl Complexes. *Organometallics* **2006,** *25*, 4520-4529. https://doi.org/10.1021/om060448u

818. Morton, L. A.; Wang, R.; Yu, X.; Campana, C. F.; Guzei, I. A.; Yap, G. P. A.; Xue, Z.-L., Tungsten Alkyl Alkylidyne and Bis-alkylidene Complexes. Preparation and Kinetic and Thermodynamic Studies of Their Unusual Exchanges. *Organometallics* **2006,** *25*, 427-434. https://doi.org/10.1021/om050745j

819. Sharma, B.; Callaway, T. M.; Lamb, A. C.; Steren, C. A.; Chen, S.-J.; Xue, Z.-L., Reactions of Group 4 Amide Guanidinates with Dioxygen or Water. Studies of the Formation of Oxo Products. *Inorg. Chem.* **2013,** *52*, 11409-11421. https://doi.org/10.1021/ic4016965

820. Lamb, A. C.; Wang, Z.; Cook, T. M.; Sharma, B.; Chen, S.-J.; Lu, Z.; Steren, C. A.; Lin, Z.; Xue, Z.-L., Preparation of all N-coordinated zirconium amide amidinates and studies of their reactions with dioxygen and water. *Polyhedron* **2016,** *103*, 2-14. https://doi.org/10.1016/j.poly.2015.07.045

821. Morton, L. A.; Zhang, X.-H.; Wang, R.; Lin, Z.; Wu, Y.-D.; Xue, Z.-L., An Unusual Exchange between Alkylidyne Alkyl and Bis(alkylidene) Tungsten Complexes Promoted by Phosphine Coordination: Kinetic, Thermodynamic, and Theoretical Studies. *J. Am. Chem. Soc.* **2004,** *126*, 10208-10209. https://doi.org/10.1021/ja0467263

822. Abbott, J. K. C.; Li, L.; Xue, Z.-L., Preparation and Use of $Ta(CD_2Bu^t)_5$ To Probe the Formation of $(Bu^tCD_2)_3Ta{=}CDBu^t$. Kinetic and Mechanistic Studies of the Conversion of Pentaneopentyltantalum to the Archetypical Alkylidene Complex. *J. Am. Chem. Soc.* **2009,** *131*, 8246-8251. https://doi.org/10.1021/ja901251c

823. Morton, L. A.; Chen, S.; Qiu, H.; Xue, Z.-L., Preparation of Tungsten Alkyl Alkylidene Alkylidyne Complexes and Kinetic Studies of Their Formation. *J. Am. Chem. Soc.* **2007,** *129*, 7277-7283. https://doi.org/10.1021/ja067914r

824. Li, L.; Hung, M.; Xue, Z., Direct Observation of (Me3ECH2)5Ta (E = C, Si) as the Precursors to (Me3ECH2)3Ta:CHEMe3 and (Me3SiCH2)2Ta(.mu.-CSiMe3)2Ta(CH2SiMe3)2. Kinetic and Mechanistic Studies of the Formation of Alkylidene and Alkylidyne Ligands. *J. Am. Chem. Soc.* **1995,** *117*, 12746-12750. https://doi.org/10.1021/ja00156a011

825. Bowers, C. R.; Jones, D. H.; Kurur, N. D.; Labinger, J. A.; Pravica, M. G.; Weitekamp, D. P., Symmetrization Postulate and Nuclear Magnetic Resonance of Reacting Systems. *Adv. Magn. Opt. Reson.* **1990,** *14*, 269-291. https://doi.org/10.1016/B978-0-12-025514-6.50018-6

826. Eisenberg, R., Parahydrogen-induced polarization: a new spin on reactions with molecular hydrogen. *Acc. Chem. Res.* **1991,** *24*, 110-116. https://doi.org/10.1021/ar00004a004

827. Duckett, S. B.; Mewis, R. E., Improving NMR and MRI Sensitivity with Parahydrogen (in Hyperpolarization Methods in NMR Spectroscopy edited by Lars T. Kuhn). *Top. Curr. Chem.* **2013,** *338*, 75–104. https://doi.org/10.1007/128_2012_388

828. Köckenberger, W.; Matysik, J., Hyperpolarization Methods and Applications in NMR. In *Encyclopedia of Spectroscopy and Spectrometry, 2nd Ed.*, 2 ed.; Lindon, J. C., Ed. Academic Press: Oxford, 2010; pp 963-970. https://doi.org/10.1016/B978-0-12-374413-5.00054-3

829. Duckett, S. B.; Wood, N. J., Parahydrogen-based NMR methods as a mechanistic probe in inorganic chemistry. *Coord. Chem. Rev.* **2008,** *252*, 2278-2291. https://doi.org/10.1016/j.ccr.2008.01.028

830. Duckett, Simon B.; Blazina, D., The Study of Inorganic Systems by NMR Spectroscopy in Conjunction with Parahydrogen-Induced Polarisation. *Eur. .J. Inorg. Chem.* **2003,** *2003*, 2901-2912. https://doi.org/10.1002/ejic.200300119

831. Godard, C.; López-Serrano, J.; Gálvez-López, M.-D.; Roselló-Merino, M.; Duckett, S. B.; Khazal, I.; Lledós, A.; Whitwood, A. C., Detection of platinum dihydride bisphosphine complexes and studies of their reactivity through para-hydrogen-enhanced NMR methods. *Magn. Reson. Chem.* **2008,** *46*, S107-S114. https://doi.org/10.1002/mrc.2342

832. López-Serrano, J.; Duckett, S. B.; Dunne, J. P.; Godard, C.; Whitwood, A. C., Palladium catalysed alkyne hydrogenation and oligomerisation: a parahydrogen based NMR investigation. *Dalton Trans.* **2008**, 4270-4281. http://dx.doi.org/10.1039/B804162H

833. Eshuis, N.; van Weerdenburg, B. J. A.; Feiters, M. C.; Rutjes, F. P. J. T.; Wijmenga, S. S.; Tessari, M., Quantitative Trace Analysis of Complex Mixtures Using SABRE Hyperpolarization. *Angew. Chem. Int. Ed.* **2015,** *54*, 1481-1484. https://doi.org/10.1002/anie.201409795

834. van Weerdenburg, B. J. A.; Engwerda, A. H. J.; Eshuis, N.; Longo, A.; Banerjee, D.; Tessari, M.; Guerra, C. F.; Rutjes, F. P. J. T.; Bickelhaupt, F. M.; Feiters, M. C., Computational (DFT) and Experimental (EXAFS) Study of the Interaction of [Ir(IMes)(H)2(L)3] with Substrates and Co-substrates Relevant for SABRE in Dilute Systems. *Chem. Eur. J.* **2015,** *21*, 10482-10489. https://doi.org/10.1002/chem.201500714

835. Fekete, M.; Rayner, P. J.; Green, G. G. R.; Duckett, S. B., Harnessing polarisation transfer to indazole and imidazole through signal amplification by reversible exchange to improve their NMR detectability. *Magn. Reson. Chem.* **2017,** *55*, 944-957. https://doi.org/10.1002/mrc.4607

836. Roy, S. S.; Appleby, K. M.; Fear, E. J.; Duckett, S. B., SABRE-Relay: A Versatile Route to Hyperpolarization. *J. Phys. Chem. Lett.* **2018,** *9*, 1112-1117. https://doi.org/10.1021/acs.jpclett.7b03026

837. Frey, U.; Helm, L.; Merbach, A. E.; Roulet, R., High Pressure NMR in Organometallic Chemistry. In *Advanced Applications of NMR to Organometallic Chemistry*, Gielen, M.; Willem, R.; Wrackmeyer, B., Eds. Wiley: New York, 1996; pp 193-225.

838. Iggo, J. A.; Shirley, D.; Tong, N. C., High pressure NMR flow cell for the insitu study of homogeneous catalysis. *New J. Chem.* **1998,** *22*, 1043-1045. http://dx.doi.org/10.1039/A806311G

839. Kégl, T.; Kollár, L.; Radics, L., High-pressure NMR investigation of the intermediates of platinum-phosphine hydroformylation catalysts. *Inorg. Chim. Acta* **1997,** *265*, 249-254. https://doi.org/10.1016/S0020-1693(97)05745-9

840. Nozaki, K.; Hiyama, T.; Kacker, S.; Horváth, I. T., High-Pressure NMR Studies on the Alternating Copolymerization of Propene with Carbon Monoxide Catalyzed by a Palladium(II) Complex of an Unsymmetrical Phosphine−Phosphite Ligand. *Organometallics* **2000,** *19*, 2031-2035. https://doi.org/10.1021/om990985x

841. Leone, A.; Gischig, S.; Elsevier, C. J.; Consiglio, G., High-pressure NMR study of migratory CO-insertion in palladium–methyl complexes modified with Cs-symmetrical 1,4-diphosphines. *J. Organomet. Chem.* **2007,** *692*, 2056-2063. https://doi.org/10.1016/j.jorganchem.2007.01.020

842. Balogh, E.; Casey, W. H., High-pressure ^{17}O NMR studies on some aqueous polyoxoions in water. *Prog. NMR Spec.* **2008,** *53*, 193-207. https://doi.org/10.1016/j.pnmrs.2008.01.001

843. Denmark, S. E.; Williams, B. J.; Eklov, B. M.; Pham, S. M.; Beutner, G. L., Design, Validation, and Implementation of a Rapid-Injection NMR System. *J. Org. Chem.* **2010,** *75*, 5558-5572. https://doi.org/10.1021/jo100837a

844. Ji, Y.; DiRocco, D. A.; Kind, J.; Thiele, C. M.; Gschwind, R. M.; Reibarkh, M., LED-Illuminated NMR Spectroscopy: A Practical Tool for Mechanistic Studies of Photochemical Reactions. *ChemPhotoChem* **2019,** *3*, 984-992. https://doi.org/10.1002/cptc.201900109

845. Bertini, I.; Luchinat, C.; Mincione, G.; Parigi, G.; Gassner, G. T.; Ballou, D. P., NMRD studies on phthalate dioxygenase: evidence for displacement of water on binding substrate. *J. Biol. Inorg. Chem.* **1996,** *1*, 468-475. https://doi.org/10.1007/s007750050080

846. Chen, Y.; Liu, G.; Tang, W., ^{1}H NMR Saturation Transfer Studies of Exogenous Ligands Binding to Metmyoglobin. *Spectrosc. Lett.* **1996,** *29*, 1381-1396. https://doi.org/10.1080/00387019608007130